

Karl Hoffmann

An Introduction to Stress Analysis and Transducer Design using Strain Gauges

The definitive work
on strain gauge
measurement



Contents	Page
1. Introduction	1
1.0.1 Metal strain gages	2
1.0.2 Semiconductor strain gages	7
1.0.3 Vapor-deposited (thin-film) strain gages	8
1.0.4 Capacitive strain gages	9
1.0.5 Piezoelectric strain gages	10
1.0.6 Photoelastic strain gages	11
1.0.7 Mechanical strain gages	11
1.0.8 Other systems	11
1.1 The operating principle of the strain gage	12
1.1.1 Metal strain gages	12
1.1.2 Semiconductor strain gages	14
1.2 The measurement system	15
2 Terms and units of measurement used in strain gage technology	17
2.1 Strain: Definition and unit of measurement	17
2.1.1 Absolute change of length	17
2.1.2 Relative change of length or strain	18
2.1.3 Unit of measurement for strain [2-1]	19
2.2 Mechanical stress: Definition and unit of measurement	21
2.2.1 Normal stress	21
2.2.2 Shear stress	22
2.2.3 Residual stress, thermal stress	24
2.2.4 Stress states	25
2.3 Material parameters	26
2.3.1 Modulus of elasticity, definition and units	26
2.3.2 Shear modulus	28
2.3.3 Poisson's ratio	29
2.3.4 Thermal expansion	31
2.4 Strain gage loading	32
2.4.1 Static measurements (zero referenced)	32
2.4.2 Quasi-static measurements	33
2.4.3 Dynamic measurements (non-zero referenced)	33
3 Selection criteria for strain gages	34
3.1 Range of application	36
3.1.1 Stress analysis, model measurement techniques, biomechanics	36
3.1.2 Transducer construction	36
3.2 Types of strain gages	37
3.2.1 Length of measuring grid	37
3.2.1.1 Homogeneous field of strain	38
3.2.1.2 Inhomogeneous strain field	40
3.2.1.3 Dynamic strain conditions	42
3.2.2 Multiple strain gages, their advantages and fields of application	42
3.2.2.1 Strain gage chains for the determination of stress gradients	42
3.2.2.2 Strain gage rosettes for the determination of stress conditions	44
3.2.2.3 Strain gage rosettes for the investigation of residual stress	46
3.2.3 Special strain gages	48

3.2.3.1	Weldable strain gages.....	49
3.2.3.2	Free-grid strain gages, high-temperature strain gages.....	49
3.2.3.3	Weldable high-temperature strain gages.....	50
3.2.4	Electrical resistance.....	50
3.2.5	Useful temperature range.....	51
3.3	Technical data.....	52
3.3.1	Strain gage sensitivity (gage factor) for metal strain gages.....	53
3.3.2	Gage factor for semiconductor strain gages.....	54
3.3.3	Transverse sensitivity.....	56
3.3.4	Temperature response of a mounted strain gage.....	59
3.3.4.1	Temperature compensated strain gages.....	61
3.3.4.2	Thermal drift.....	67
3.3.5	The dependence of sensitivity on temperature.....	67
3.3.6	Static elongation.....	69
3.3.7	Dynamic strain measurement.....	70
3.3.7.1	Continuous vibration characteristics.....	71
3.3.7.2	The cut-off frequency.....	74
3.3.8	Electrical loading.....	79
3.3.9	Creep.....	80
3.3.10	Mechanical hysteresis.....	87
3.4	Environmental influences.....	90
3.4.1	Temperature.....	90
3.4.2	Humidity.....	90
3.4.3	Hydrostatic pressure.....	91
3.4.4	Vacuum.....	96
3.4.5	Ionizing radiation.....	99
3.4.5.1	The effects of ionizing radiation on strain gage measuring points.....	100
3.4.6	Magnetic fields.....	104
3.4.7	Storage.....	107
4	Materials used for mounting strain gages.....	108
4.1	Strain gage bonding materials.....	108
4.2	Mounting materials.....	112
4.2.1	Cleaning agents.....	112
4.2.2	Soldering agents.....	113
4.2.2.1	Soldering devices.....	113
4.2.2.2	Solders and fluxing agents.....	114
4.2.3	Connection methods.....	115
4.2.3.1	Solder terminals.....	115
4.2.3.2	Lead material.....	116
4.2.4	Methods of testing.....	118
4.2.4.1	Visual inspection.....	118
4.2.4.2	Electrical continuity.....	118
4.2.4.3	Insulation resistance.....	119
4.3	Protection of the measuring point.....	120
5	The Wheatstone bridge circuit.....	126
5.1	The circuit diagram of the Wheatstone bridge.....	126
5.2	The principle of the Wheatstone bridge circuit.....	127
5.3	Bridge excitation and amplification of the bridge output voltage.....	133

6	Calibrating measurement equipment	135
6.1	The operating principle of the compensation and calibration devices on a measuring amplifier.....	137
6.2	Calibration using the calibration signal from the measuring amplifier.....	140
6.3	Shunt calibration.....	141
6.4	Calibration with a calibration unit.....	144
6.5	Taking account of gage factors with a value other than 2.....	146
7	The reduction and elimination of measurement errors	149
7.1	Compensation of thermal output	151
7.1.1	Compensation for thermal output using a simple quarter bridge circuit.....	152
7.1.2	Thermal output of a quarter bridge in a three-wire configuration.....	154
7.1.3	Temperature compensation of a quarter bridge with compensating strain gages.....	155
7.1.4	Compensation of thermal output with the double quarter or diagonal bridge.....	157
7.1.5	Compensation for thermal output using the half bridge circuit.....	158
7.1.6	Compensation for thermal output with the full bridge circuit.....	159
7.2	The influence of lead resistances.....	160
7.2.1	Simple quarter bridge circuit.....	161
7.2.2	Quarter bridge in a three-wire circuit.....	163
7.2.3	Quarter bridge with compensating strain gage.....	164
7.2.4	Double quarter or diagonal bridge.....	164
7.2.5	Half bridge circuit.....	165
7.2.6	Full bridge circuit.....	166
7.2.7	Error correction using the gage factor selector.....	167
7.3	Eliminating cable effects with special circuits in the measuring amplifier....	168
7.3.1	HBM bridge (citation from [5-2])	168
7.3.2	The six-wire circuit.....	171
7.4	The influence of cable capacitances	172
7.4.1	Capacitive unsymmetry	173
7.4.2	Phase rotation	177
7.5	Correction of the transverse sensitivity of a strain gage.....	179
7.5.1	Corrections for individual measuring grids.....	180
7.5.2	Correction for strain gage rosettes.....	186
7.5.2.1	X rosettes 0°/90°	186
7.5.2.2	Rosettes.....	187
8.	Hooke's Law for the Determination of Material Stresses from Strain Measurements	189
8.1	The uniaxial stress state.....	189
8.2	The biaxial stress state.....	192
8.2.1	The biaxial stress state with known principal directions.....	192
8.2.2	The biaxial stress state with unknown principal directions.....	195
8.2.2.1	Measurements with the 0°/45°/90° rosette	196
8.2.2.2	Measurements with the 0°/60°/120° rosette	196
8.2.2.3	The determination of the principal directions.....	197
8.2.2.4	Other ways of determining the principal normal stresses and their directions	199
8.2.3	Mohr's Stress Circle.....	199
8.3	Determination of residual stresses according to the drill-hole method	202

8.4	Strain measurements and stress analysis for various loading cases	205
8.4.1	Measurement on a tension/compression bar	206
8.4.2	Measurements on a bending beam	209
8.4.3	Symmetrical and asymmetrical cross-sectional beams loaded with both an axial force and a bending moment	212
8.4.4	Measurements on a shaft under torsion (twisted shaft)	218
8.4.4.1	Transferring the measuring signal from rotating shafts	222
8.4.5	Measurement on a twisted shaft with superimposed axial force and bending moment	226
8.4.6	Measurements on a shear beam	227
8.4.7	Measurement of thermal stresses	230
8.4.7.1	Comparison of measurements on a free and on a restrained object	231
8.4.7.2	Measurement with a compensating piece	232
8.4.7.3	Separate or later determination of the thermal output	232
9	Measurement accuracy	234
9.1	Causes of measurement errors	235
9.2	Calculating the degree of random deviation in a measurement series	236
9.2.1	Test requirements	236
9.2.1.1	The Gaussian distribution	237
9.2.2	Arithmetical mean	239
9.2.3	(Empirical) standard deviation s and coefficient of variance v	239
9.2.4	Confidence limits and confidence range for the expected value μ	240
9.2.5	Measurement uncertainty u	241
9.2.6	Measurement result	242
10	Literature	243
11	Index	251
	List of Tables	257

1. Introduction

The usual way of assessing structural parts of machines, buildings, vehicles, aircraft, etc. is based on strength of material calculations.

This method is satisfactory provided the component loads are known both qualitatively and quantitatively. Problems arise particularly where the loads are unknown or where they can only be roughly approximated. Formerly the risk of overloading was countered by using safety margins, i.e. through overdimensioning. However, modern design strategies demand savings in material, partly for reasons of cost and partly to save weight; this is clearly illustrated, for example in aeronautics. In order to satisfy the safety requirements and to provide an adequate component service life, the material stresses must be known. Therefore measurements under operational conditions are necessary.

The quantity employed in the evaluation of structural parts is the mechanical stress to which the material is subjected. Mechanical stresses are virtually impossible to determine under operational conditions. The X-ray process, which might be suitable, is subject to restrictions in its application. A practical method for the experimental determination of material stresses is based on a discovery made in 1678 by the English scientist *Robert Hooke* (1635 - 1703) [1-1]. He found a relationship between the material stress and the resulting deformation. This deformation, called “strain”, also occurs on the surface of objects and is therefore accessible for measurement.

An important branch of experimental stress analysis is based on the principle of strain measurement.

At first cumbersome mechanical devices were used for strain measurement, which displayed the strain using a lever ratio of one thousand or more. An example is shown in Fig. 1.0-1.

Devices of this type or similar were for a long time the only method of carrying out measurements that were so essential for stress analysis. Despite their often ingenious design and precise construction, they possessed intrinsic disadvantages which severely restricted their range of application and reduced their significance:

- only static processes can be observed,
- strong clamping forces are needed to prevent the devices from slipping under vibration,
- the test sample must be fixed with respect to the observer,
- the size of the devices places restrictions on their use for small test samples and in some cases such measurements are impossible,

- the relatively long measurement base only gives correct results for uniform conditions of strain and so closely situated stress concentrations cannot be measured,
- the local conditions may be untenable for the observer,
- automatic recording of the measurements is not possible.

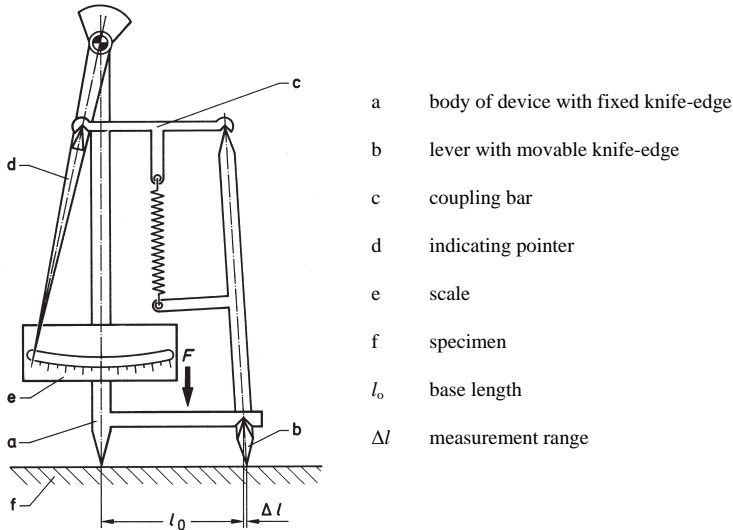


Fig. 1.0-1: The Huggenberger tensometer with its double lever mechanism.

As a result of these shortcomings, the restriction of making only static measurements was regarded as a severe disadvantage. Electrical measurement techniques were to provide the solution.

1.0.1 Metal strain gages

In the latter half of the 1930s attention was given to an effect which *Charles Wheatstone* had mentioned as long ago as 1843 in his first publication on the bridge circuit that he had invented [1-2]. This effect is the change of resistance in an electrical conductor due to the effects of mechanical stress. *William Thomson* (1824-1905, *Lord Kelvin* after 1892) went further with some work published in 1856 [1-3].

There are a number of reasons why more than 80 years passed before the technical application of the phenomenon occurred.

The change of resistance of a wire under tension is very small. For his measurements Thomson used highly sensitive galvanometers which are unsuitable for general technical applications or for use in industry. They are also only suitable for the measurement of static processes. It was only with the advent of the electronic amplifier that these requirements were fulfilled.

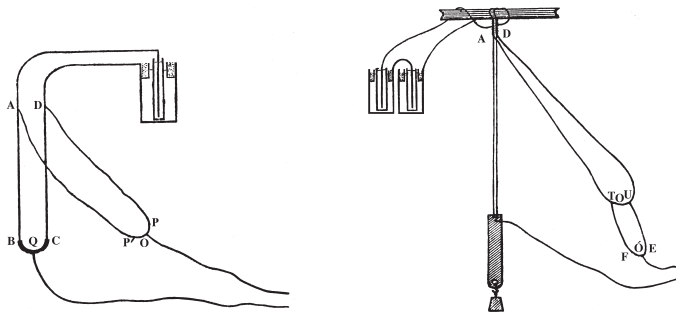


Fig. 1.0-2: William Thomson's test rig for the investigation into the change of resistance of electrical conductors under mechanical stress. (Taken from [1-3].)

In Germany the first investigations to explain the effect were undertaken at the Research Institute for Aviation, but they were not followed up. Carbon film strips for strain measurement developed by AEG proved to be of little use.

During 1938 in the USA, two people were working almost simultaneously but independently, on the idea of using the "Thomson effect" for measurement purposes. The development, which led to the strain gage and its subsequent widespread application, is described in detail in [1-4].

One of the two people, *Edward E. Simmons*, worked in California. With silk thread as warp and thin resistance wire as weft, he made a woven material which he stuck onto a steel cylinder and made an electrical device for measuring the force impulses exerted on a specimen by a pendulum ram impact testing machine, Fig. 1.0-3.

Arthur Claude Ruge was working in the Faculty of Seismology at the Massachusetts Institute of Technology and wanted to measure the stress due to simulated earthquake vibrations on a model of an earthquake-resistant water tank.

The strain measuring equipment available at that time could not be used on the very thin-walled model. From the numerous different devices none of them was suitable. In a last attempt Ruge took a very thin resistance wire, stuck it in a meander shape on to some thin tissue paper and terminated the ends with thicker connections. In order to investigate the properties of this prototype device, he glued it to a bending beam and compared the measurements with a traditional strain measuring device. He found good correlation with a linear relationship between strain and the displayed values over the complete measurement

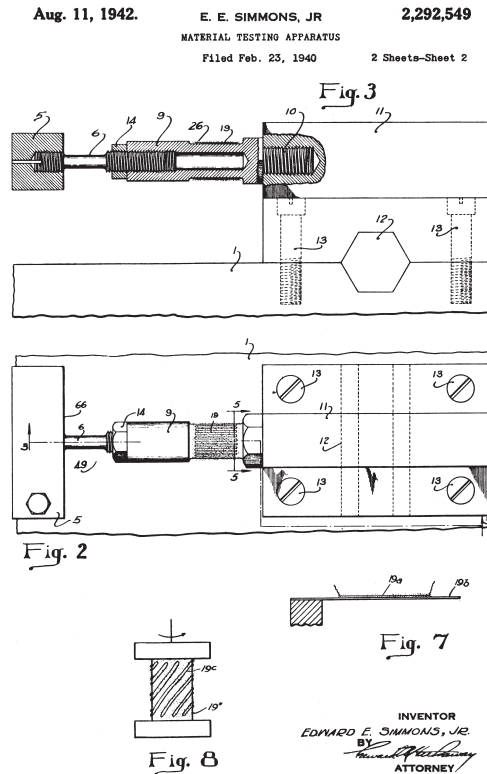


Fig. 1.0-3: E.E. Simmons's force measuring device as reproduced in [1-5]. The force impulse to be measured acts in the axial direction.

range, both with positive and with negative, i.e. compressive, strain, including good zero point stability. So the “electrical resistance strain gage with bonded grid” was invented. The shape used in those very first tests was the same as that normally used today.

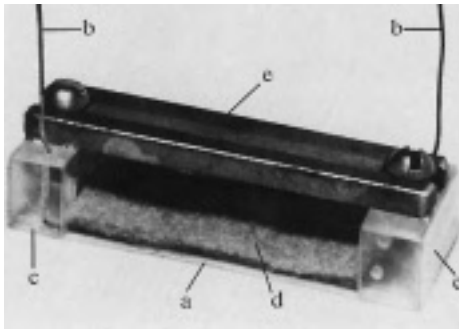


Fig. 1.0-4: *Arthur Claude Ruge*, the inventor of the strain gage, working on his measurements.

The main difference between Ruge's idea and that of Simmons was that Ruge fixed the measuring wire onto a carrier material, giving an independent measuring instrument which was easy to handle and could be glued to any surface. It was very thin and light, required no clamping force and produced practically no feedback effects, enabling measurements on very thin objects. Even the first prototypes of the strain gage appeared to be superior to previous strain measuring devices in every respect.

The second of Ruge's accomplishments was to take the development of the strain gage further to the production stage and it was this final step which heralded the supremacy of the strain gage. It is therefore only proper to name Ruge as the father of the strain gage. He had not only the idea, but was also able to see the wide possibilities of its application and he had the determination necessary to turn the strain gage into a reliable instrument in stress analysis.

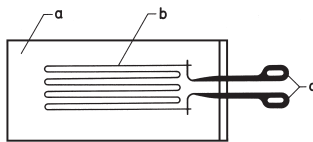
It was first thought that the slender structure had to be fixed on a firm support and that the fine wires, which were only 25 μm thick, had to be protected by a felt covering. Fig. 1.0-5 shows an example of the first production strain gage.



- a measuring grid bonded to paper with cellulose lacquer
- b connecting wires
- c insulating supports
- d felt cover for protecting the measuring grid
- e temporary bracket which is removed after application

Fig. 1.0-5: Ruge's first production strain gage design

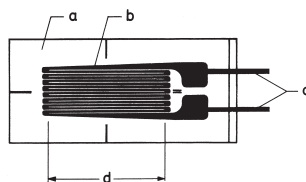
The demand, particularly from the American aviation industry, was so great that this construction had to be abandoned. (*Tatmall* mentions a turnover in 1941 of 50,000 strain gages in 2 months [1-4]). Eventually experience showed that the complicated supporting structure was unnecessary and the simplified model shown in Fig. 1.0-6 was introduced. This design was retained with only slight modification for a number of decades. Numerous patents are evidence of Ruge's continuing efforts in improving the measuring characteristics.



- a carrier material
- b measuring grid
- c connections

Fig. 1.0-6: The characteristic design of a sirain gage with its wire measuring grid.

In the following period various modifications were tried in order to rationalize production. Here should be mentioned *Paul Eisler's* "printed circuit" technique, which in its refined form led to the development of the "foil strain gage" from about 1952 [1-6].



- a carrier material
- b measuring grid
- c connections
- d effective grid length

Fig. 1.0-7: The characteristic design of a strain gage with etched metal foil measuring grid.

Compared with wound-wire techniques this method substantially extended the possibilities of design since all gage shapes that can be represented in one plane can be made without additional effort. Spiral shapes can be easily reproduced, as can complete networks, such

as those that are used in transducers for the measurement of force, pressure, torque and other mechanical variables.

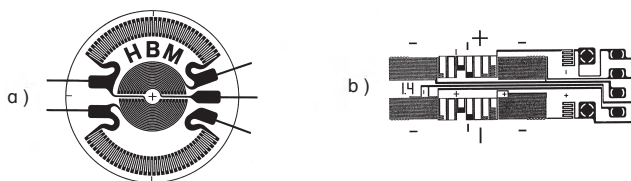


Fig. 1.0-8: Examples of strain gage design in etched foil technology:
 a) four-part diaphragm rosette in a bridge configuration for pressure transducers,
 b) complete strain gage bridge circuit including all connections and compensation elements.

Strain gages are manufactured in a multitude of different types, providing a method that can be matched to various measurement tasks, even under arduous conditions.

The main areas of application for strain gages are:

- experimental stress analysis, including model measurement techniques and biomechanics
- transducer manufacture.

Whereas the strain gage's adaptability contributed to its widespread use in the field of experimental stress analysis, it was the high degree of measurement accuracy that could be obtained which made the strain gage attractive for transducer manufacture. Both wound-wire and foil types produce strain gages which are known as *metal strain gages* due to their metal alloy measuring grids.

1.0.2 Semiconductor strain gages

Apart from metal strain gages there are other types of electrical resistive strain gages. *Semiconductor strain gages* belong to this group and they extend the range of applications in strain gage technology. The measurement principle is based on the semiconductor piezoresistive effect discovered by *C.S. Smith* in 1954. Initially germanium was used, which was later superseded by silicon.

In construction, semiconductor strain gages are substantially the same as metal strain gages. The measuring element consists of a strip a few tenths of a millimeter wide and a few hundredths of a millimeter thick which is fixed to an insulating carrier foil and is provided with connecting leads. Diode effects are prevented by using a thin gold wire as connection between the semiconductor element and the connecting strips.

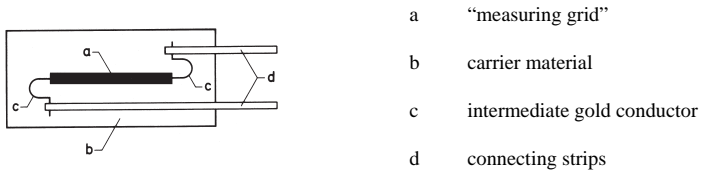


Fig. 1.0-9: Diagrammatic representation of a semiconductor strain gage.

The gage factor for normally available semiconductor strain gages, i.e. the ratio between the measured strain and the signal given by the strain gage, is about fifty to sixty times that of metal strain gages. They are therefore mainly used in transducer manufacture for the measurement of other physical quantities, being supplemented by simple electronic devices to form transmitters.

Semiconductor strain gages are not widely used in experimental stress analysis and there are a number of reasons for this:

- The non-linear characteristics of the semiconductor strain gage call for measurement correction demanding high accuracy.
- Semiconductor strain gages are substantially more expensive than metal types.
- Even when the greater sensitivity is taken into account, the adverse temperature dependent effects are more severe with semiconductor strain gages than with metal ones and these effects are more difficult to compensate.
- Handling is more difficult due to the semiconductor's brittle nature.

On the other hand the high sensitivity is a reason for using semiconductor strain gages for the measurement of very small strains. The large signal given by this type of strain gage is of particular advantage in the presence of strong interference fields.

Apart from conventional strain gages, there are other types which are only mentioned here for the sake of completeness and are not treated in great detail.

1.0.3 Vapor-deposited (thin-film) strain gages

A third type of electrical resistive strain gage is provided by vapor deposition techniques. Here the measuring element is directly deposited onto the measurement point under a vacuum by the vaporization of the alloy constituents.

The range of applications is restricted to the production of transducers [1-7].

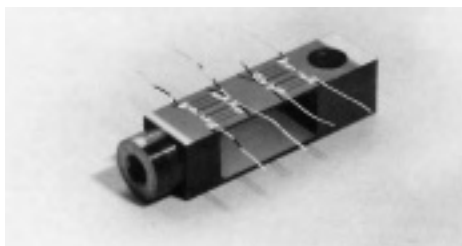


Fig. 1.0-10: Thin-film strain gage on the spring body of a transducer.

The manufacture of strain gages by vapor deposition techniques for wider application has been tried, but without any satisfactory results [1-8, 1-9] and the attempts were abandoned. Other efforts of manufacturing vapor-deposited semiconductor strain gages are described in [1-10]. During the last 20 years there- has not been any noticeable increase in the market acceptance for this type.

1.0.4 Capacitive strain gages

The capacitive strain gage is a new development, which is mainly regarded as an alternative to conventional strain gages for use at high temperatures beyond the limit of metal strain gages. At the present time there are three known versions:

1. A British development by the Central Electricity Research Laboratories (C.E.R.L.) in cooperation with the company Planer. Here a plate capacitor is used where the plate separation changes depending on the strain to be measured.



Fig. 1.0-11: Diagram of a capacitive strain gage from CERL-Planer.

2. An American development from Boeing Aircraft which is constructed as a differential capacitor.

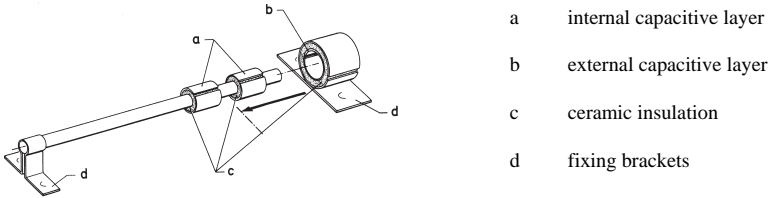


Fig. 1.0-12: Diagram of a capacitive strain gage from Boeing.

3. A German development from Interatom. This is also constructed as a plate capacitor.

Capacitive transducers are fixed to the test object using spot welding techniques.

Good results can be obtained with capacitive strain gages in the temperature range up to about 500°C. The results are still usable in the range up to 800°C.

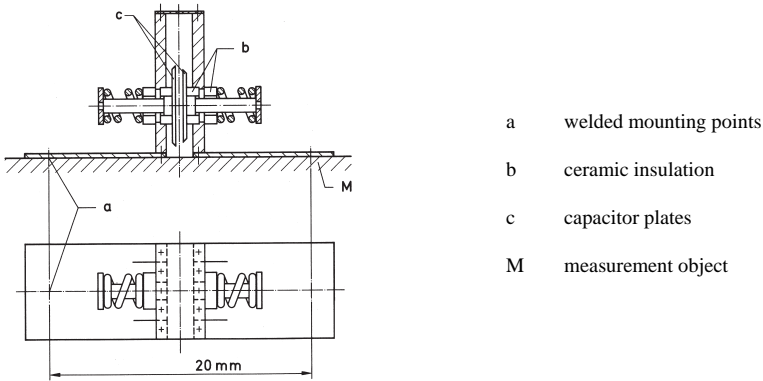


Fig. 1.0-13: Diagram of a capacitive strain gage from Interatom.

Capacitive strain gages are not discussed further here since their measurement technique is somewhat different to that of resistive strain gages. Those interested are referred to the literature [1-11 to 1-15].

1.0.5 Piezoelectric strain gages

Piezoelectric strain gages are active devices. Barium titanate is used as the strain sensing material. As with piezoelectric transducers using quartz as the sensing material, the strain gage provides an electrical charge on its surfaces which is proportional to strain and which can be measured with charge amplifiers. Static measurements are only possible under certain conditions.

Piezoelectric strain gages have only achieved limited recognition and, to the author's knowledge, appear to have disappeared from use entirely.

1.0.6 Photoelastic strain gages

A strip which is made from optically stressed active material exhibits an isochromatic field as a result of a “frozen”, continually increasing stress. The isochromatics become displaced as a result of the strain. The degree of displacement which is read off a scale is a measure of the strain. Strain gages of this type are made in the USA. They have achieved no practical significance and are no longer commercially available.

1.0.7 Mechanical strain gages

These devices occur relatively infrequently, but they have a long tradition. On account of their construction they can usually only be applied to larger objects. The measurement effect is shown by a trace scratched on a metal plate or on a glass cylinder, which however can only be evaluated at the end of the test under a microscope. This disadvantage is offset somewhat by the large temperature range. The recorded measurement can still be read for example, if the transducer is subject to a fire following an accident [1-16].

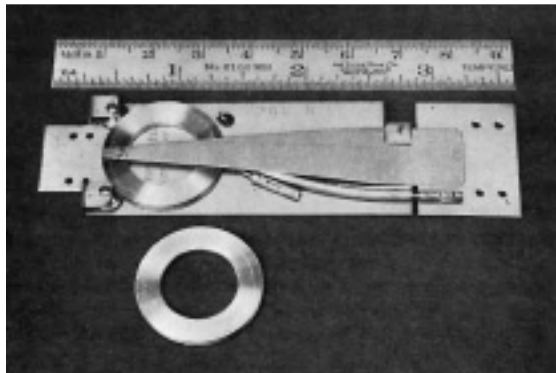


Fig. 1.0-14: Mechanical extensometer (from [1-16])

1.0.8 Other systems

Numerous other devices are available under the designation “strain transducer”. Strain gages based on resistive systems, inductive systems (differential inductance and differential transformer types) and the vibrating wire method all belong to this group, which also includes a few devices operating on optical and mechanical principles. Huggenberger's tensometer shown in Fig. 1.0-1 also falls into the last category.

In most cases the signal given by these devices is not proportional to the strain, i.e. the relative change of length, but is proportional to the absolute change in length. The strain must be calculated by dividing the measurement by the base length. These devices are not strain gages and are therefore not dealt with here.

1.1 The operating principle of the strain gage

The measurement of strain using strain gages assumes that the strain on the object under investigation is transferred without loss to the strain gage. This requires a close bond between the strain gage and the object. In almost all cases only the open surface of the measurement object is accessible for measurement, although this may be in an internal cavity as well as on the outside of the object. The very close bonding which is needed between the measurement object and the strain gage is best provided by an adhesive. Internal measurements on the object, i.e. measurements within the mass of the object itself, are only possible with strain gages under special conditions. These might occur, for example, when using plastic measurement objects in modeling techniques, where the strain gage is molded in during the part's manufacture or with concrete structures where the strain gage can be embedded in the concrete during pouring. In the latter case encapsulated strain transducers are necessary.

Other bonding materials and methods are mainly restricted to special applications, such as for example ceramic bonding for high temperature ranges and spot welding for steel construction, etc. Both of these processes require special strain gages.

The various bonding methods are described in section 4.

With electrically resistive strain gages, which are the only type dealt with here, the strain transferred to the strain gage from the measurement object causes a change in its electrical resistance.

In the introduction reference was made to two types of resistive strain gage, i.e. metal strain gages and semiconductor strain gages.

The operational principle is based on two different physical processes which are briefly explained below.

1.1.1 Metal strain gages

The working principle of the metal strain gage is based on the strain/resistance relationship of electrical conductors which was discovered by Wheatstone and Thomson (see section 1.0.1).

Any electrical conductor changes its resistance with mechanical stress, e.g. through tension or compression forces. The resistance change is partially due to the conductor's deformation and partially due to the change in the resistivity Q of the conductor material as a result of microstructural changes. This process is described by the relationship

$$\frac{dR}{R_0} = \underbrace{\epsilon (1 + 2\nu)}_{\text{geometrical portion}} + \underbrace{\frac{dQ}{Q}}_{\text{micro-structural portion}} \quad (1.1-1)$$

R = electrical resistance

ϵ = strain

ν = Poisson's ratio

Q = resistivity

The results of an investigation into various materials have been published in [1-17]. The diagram in Fig. 1.1-1 is an extract from this publication, the numbers labeling the curves indicating the slope S , which is the quotient of the relative change of resistance $\Delta R/R_0$ and the strain ϵ :

$$S = \frac{\Delta R/R_0}{\Delta l/l} = \frac{\Delta R/R_0}{\epsilon} \quad (1.1-2)$$

The measurements were carried out on freely tensioned wires.

The diagram highlights two characteristics:

1. There are significant differences in the initial slopes of the curves. They extend from +6.5 for platinum-iridium 95/5 up to -10 for nickel. These differences can be explained by the marked variations in the change of resistance due to the microstructure.
2. At certain levels of strain the slopes of those curves change whose initial slope deviates from the value of 2. This change occurs for different levels of strain and always at the transition from the elastic to the plastic deformation condition. If it is assumed that in the plastic deformation region Poisson's ratio has the value $\nu = 0.5$ at constant volume, then just from the geometrical part of equation (1.1-1) is

$$\frac{\Delta R}{R_0} = \epsilon (1 + 2\nu) = \epsilon (1 + 2 \cdot 0.5) = 2\epsilon.$$

The microstructural portion becomes zero.

Therefore materials which are particularly attractive are those with an initial characteristic slope of

$$S = \frac{\Delta R/R}{\Delta l/l} = 2 \frac{\Omega/\Omega}{m/m}$$

and which retain this figure through the whole elastic region. This is found with some alloys and so these are preferred for the manufacture of strain gages.

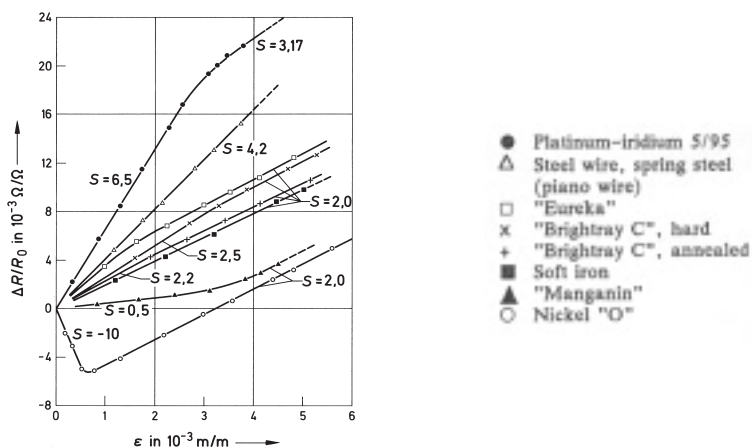


Fig. 1.1-1: Resistance/strain characteristics for freely tensioned wires (from [1-17]).

1.1.2 Semiconductor strain gages

As with metal strain gages, the measuring effect of semiconductor strain gages is based on the change of electrical resistance, but in contrast to metal strain gages, the strain/resistance relationship is mainly due to the change in electron mobility. The geometric part of the resistance change is however small and is less than 2%.

Only silicon is currently used for the manufacture of semiconductor strain gages and a monocrystal is pulled from this material using the Czochralsky process [1-18]. In order to achieve the required purity, any impurity atoms still remaining are extracted using the zone refining process until a purity of about 1 impurity atom to 10^{10} silicon atoms is achieved. Then certain impurity atoms are added to the crystal lattice by diffusion. This process is known as "doping". Trivalent atoms, acceptors, are used to dope the quadrivalent silicon, e.g. boron or gallium, giving p conductivity by electron depletion. If atoms are used having a valence of five, e.g. donors such as phosphorus or arsenic, then there is an excess of electrons and n conductivity is obtained. The degree of doping determines the electrical conductivity.

A characteristic of monocrystals prepared in this way is that their electrical resistance changes under the influence of strain and the strength of this effect varies in the three axes of the crystal lattice. The effect is anisotropic. For a positive strain in p silicon a positive change of resistance occurs on the $\langle 111 \rangle$ axis and with n silicon a negative change occurs on the $\langle 100 \rangle$ axis. With negative strain the effect is reversed. Whereas the effects are quite noticeable in the directions just mentioned, they are much weaker in the other axial directions.

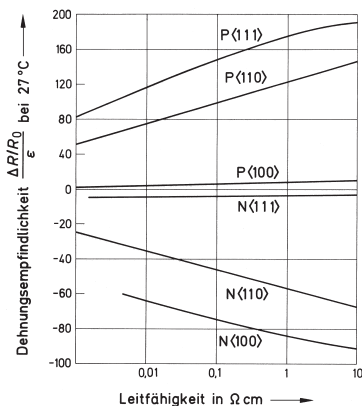


Fig. 1.1-2: Gage factor for p and n monocrystalline silicon in the three crystal lattice axes in relationship to conductivity (from [1-19]).

It can be seen from Fig. 1.1-2 that the gage factor, the change of resistance in relationship to strain, depends on the silicon's conductivity and hence on the degree of doping.

For the manufacture of strain gages the monocrystal is doped in strips, whose longitudinal direction corresponds to the lattice axis having the highest gage factor.

Semiconductor strain gages obey the relationship

$$\frac{\Delta R}{R_0} = k \epsilon \frac{T_0}{T} + C \epsilon^3 \left(\frac{T_0}{T} \right)^2 \dots \tag{1.1-3}$$

The parameters k , ϵ , T and C determine the characteristic.

1.2 The measurement system

The strains measured with strain gages are normally very small. Consequently the changes of resistance are also very small and cannot be measured directly, say with an ohmmeter. The strain gage must therefore be included in a measurement system where precise determination of the strain gage's change of resistance is possible.

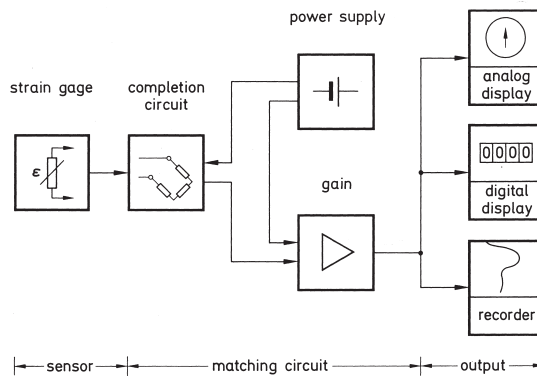


Fig. 1.2-1: Diagram of a measurement system for measuring strains with a strain gage.

The first component in the system is formed by the strain gage itself. It converts the mechanical strain into a change in the electrical resistance.

The second component in the system is a measuring circuit, shown here as a Wheatstone bridge having the strain gage as one arm. Both the strain gage and the measuring circuit are in the physical sense passive components. Energy must be passed to them to obtain a useful signal. This auxiliary energy is taken from a separate source. Usually a constant electrical voltage is used, but a constant current can also be used.

When the strain gage's resistance changes due to a strain, the bridge circuit loses its symmetry and becomes unbalanced. A bridge output voltage is obtained which is proportional to the bridge's unbalance (see section 5).

An amplifier is included in the measuring system as the third component which amplifies the bridge output voltage to a level suitable for indicating instruments. Sometimes amplifiers are designed to give an output current proportional to the bridge output voltage, but some models can provide either voltage or current outputs. With a linear amplifier the output voltage or output current is proportional to the amplifier input voltage which is also the bridge output voltage and this is in turn proportional to the measured strain.

The fourth component in the measuring system is the display. It converts the amplifier's output signal into a form which can be observed by the human being. In the simplest case the measurement is displayed by the indicating scale of a voltmeter or ammeter or the figures on a digital measuring device. If the change of strain with time is needed as in a dynamic process, recording instruments are better suited than purely indicating ones. Many amplifiers enable the connection of both types of instrument, either as an alternative or in parallel as shown in Fig. 1.2-1.

The above description of the measurement system only outlines the essential elements. In practice the system is often extended through the use of additional equipment, e.g. scanners, filters, peak value storage, limit switches, transient recorders, etc. Electronic data processing systems can also be connected to the system instead of the indicating instruments and this significantly increases the versatility.

2 Terms and units of measurement used in strain gage technology

2.1 Strain: Definition and unit of measurement

The term “strain” is usually used to describe the elongation of a section. Strain can be caused by the effect of a force. A rubber band for example is strained when it is pulled. Strain can arise however without the effect of an applied force, i.e. if an object is heated.

In the 1st case *mechanical strain* occurs,

in the 2nd case *thermal strain* results.

The opposite process is known as “compressive strain”, which also occurs as a result of a force, i.e. a compressive force. A compressive force also occurs when a body cools resulting in “contraction”.

Misunderstandings can arise due to the common use of the term “strain”, including the use of “strain” to mean the “absolute change of length” as well as the “relative change of length”. There are historical reasons for the mixing of these terms. The following explanation should clarify the different meanings.

2.1.1 Absolute change of length

The early methods, some of which are still used today, measured the absolute change in the length of an object. The term “strain measurement” was used to describe the method and even today the devices are called “strain gages”.

The absolute change of length Δl is the difference between a section's length l at the time of the measurement and its original length, i.e. the base length or the reference length l_0 :

$$\Delta l = l - l_0 \quad (2.1-1)$$

Absolute changes in length are measured with devices which measure length or the change in length.

The change in length Δl can be positive or negative as shown in Fig. 2.1-1.

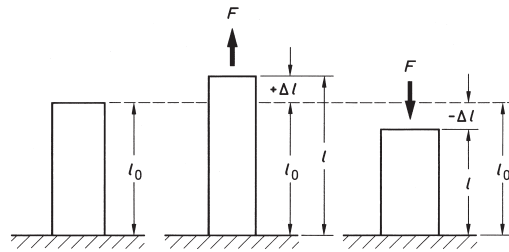


Fig. 2.1-1: Positive and negative absolute changes of length Δl .

Equation 2.1-1 shows that the absolute change of length and the result of the measurement depends on the reference length selected. In Fig. 2.1-2 a test is illustrated that clarifies this fact.

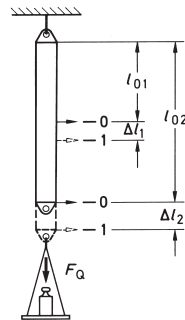


Fig. 2.1-2: Model test for "absolute change of length".

The length l_{01} and the length l_{02} , which is twice as large as l_{01} , are marked as base lengths on a freely suspended, bar-shaped object. Then the bar is loaded with force F . A measurement shows that the increase in length Δl_2 is twice as great as Δl_1 . Therefore the change of length is a function of the base length:

$$\Delta l = f(l_0) \quad (2.1-2)$$

However, if the change of length is expressed as a ratio of the base length, the same figure is obtained in each case.

$$\frac{\Delta l_2}{l_{02}} = \frac{2 \Delta l_1}{2 l_{01}} = \frac{\Delta l_1}{l_{01}}$$

2.1.2 Relative change of length or strain

In the previous section it was shown that the length ratios $\Delta l_1:l_{01}$ and $\Delta l_2:l_{02}$ are the same, assuming equivalent strain conditions. For this reason the length ratio for relative change

of length is used as the measurement variable in the theory of strength of materials and in strain gage technology. The symbol ϵ is used for the relative change of length.

$$\epsilon = \frac{\Delta l}{l_0} \quad (2.1-3)$$

The designation “strain” is a technical term which is laid down in the international standard ISO 31. “Strain” is used as a general term for the elongation process as well as for the shortening process; the former is known as “positive strain”, the latter as “negative strain”.

ϵ is positive if Δl is positive,

ϵ is negative if Δl is negative.

2.1.3 Unit of measurement for strain [2-1]

Length is measured with the unit of length, the meter [m]. Strain ϵ is defined as the quotient of a change in length Δl and a reference length l_0 (see section 2.1.2). Consequently the unit [m/m] is obtained for strain:

$$(\epsilon) = \left\{ \frac{\Delta l}{l_0} \right\} \left[\frac{\text{m}}{\text{m}} \right].$$

This is known as a dimensional ratio.

Since the changes in length considered here are usually very small, the standard subdivisions of the meter are used with the units:

$$10^{-6} \text{ m} = \mu\text{m}$$

$$10^{-3} \text{ m} = \text{mm}$$

$$10^{-2} \text{ m} = \text{cm}$$

The above subdivisions are used depending on the value for the change of length. This gives figures that are easy to handle. The figures may be written in the scientific exponential form or with one of the prefix symbols standardized in DIN 1301. Both methods are equivalent (see example).

Example: the dimensional unit for strain may be written using the following methods:

$$\epsilon_1 = 180 \cdot 10^{-6} \frac{\text{m}}{\text{m}} = 180 \frac{\mu\text{m}}{\text{m}};$$

$$\epsilon_2 = 2.5 \cdot 10^{-3} \frac{\text{m}}{\text{m}} = 2.5 \frac{\text{mm}}{\text{m}};$$

$$\epsilon_3 = 3 \cdot 10^{-2} \frac{\text{m}}{\text{m}} = 3 \frac{\text{cm}}{\text{m}}.$$

Often the following designations are used

% instead of 10^{-2} m/m = cm/m

‰ instead of 10^{-3} m/m = mm/m.

Percent and per mil figures ought to be exclusively reserved for tolerance figures. They should be avoided for strain figures since they may be misinterpreted as tolerance or measurement error figures as shown in the example below.

Example: The significance of percentage figures in conjunction with strain values.

a) $\varepsilon = 2.72 \text{ cm/m} \pm 0.5\%$ means:
27200 $\mu\text{m/m} \pm 136$

b) $\varepsilon = 2.72\% \pm 0.5\%$ however means that if percent is used as a measure of the strain:
27200 $\mu\text{m/m} \pm 5000 \mu\text{m/m}$!

Pseudo-units, such as “microstrain”, “ μD ” or “ $\mu\varepsilon$ ” have no mathematical basis and do not conform to dimensional calculations. In particular the designation $\mu\varepsilon$, which originates in America, gives misleading results, as shown by the example “ $\varepsilon = 250 \mu\varepsilon$ ”. It is poor mathematical practice to use *formula symbols* (ε for strain) as *dimensional units*.

Note:

Dimensional ratios possess the same unit in the numerator as in the denominator of the ratio, e.g. m/m. The ratio could be abbreviated mathematically, giving an undimensioned figure. The physical information regarding its origin is then lost unless $\varepsilon = \dots 10^{-6}$ is always written, the significance of the dimensioned figure being shown by the formula symbol. In strain gage technology various dimensional relationships are brought together, such as the strain gage's relative change of resistance or the Wheatstone bridge's relative Output voltage (see example). To prevent mistakes it is advisable to show the dimensional unit designation when presenting measurement figures.

Example: Various dimensional relationships used.

A strain of $\varepsilon = \frac{\Delta l}{l_o} = 0.001 \frac{m}{m}$

produces in a strain gage (k factor = 2)

a relative change of resistance $\frac{\Delta R}{R_o} = 0.002 \frac{\Omega}{\Omega}$

Hence a voltage of V_o occurs on the output of the Wheatstone bridge when configured as a quarter bridge.

$$\frac{V_o}{V_B} = 0.0005 \frac{V}{V}$$

2.2 Mechanical stress: Definition and unit of measurement

“Mechanical stress” is defined as the stress in materials due to force. It usually occurs as a result of an applied force, but is also often due to the effects of force within a material or within a larger system. Stresses are subdivided as follows:

- a) type: normal stresses and shear stresses;
- b) origin: tension, compression, bending, torsion, residual and thermal stresses.

The stresses mentioned under b) are categorized within the type of stress mentioned under a). When considering strength of materials, the type of stress is of interest irrespective of its cause.

In addition subdivisions are made between uniaxial, biaxial, triaxial and spatial stress conditions.

Mechanical stresses are not accessible for direct measurement. X-ray techniques form an exception to this where the material stresses in the microscopic range can be determined from distortions in the crystal lattice structure, i.e. from the relative changes in the inter-atomic separation. The process is restricted to layers near the surface of about 5 to 15 μm depth [2-2].

Stresses are calculated either according to the theory of the strength of materials or from strain gage measurements. The latter method is based on Hooke's Law (see section 8).

2.2.1 Normal stress

Tensile and compressive stresses both come under this heading. Normal stresses arise when tensile or compressive forces act against one another. Fig. 2.2-1 explains how tensile and compressive stresses arise. The symbol for normal stress is σ .

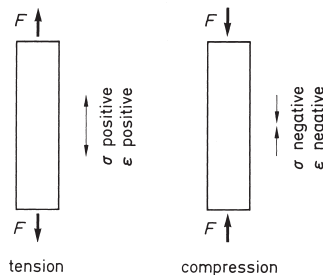


Fig. 2.2-1: Positive and negative normal stresses.

For the same cross-sectional area the stress in the material is greater the stronger the force.

For the same force the stress changes in inverse proportion to the cross-sectional area:

large cross-sectional area → low stress,
 small cross-sectional area → high stress.

An equally large force working in the opposite direction must be present to stop the bar shown in Fig. 2.2-1 from being pushed away. The opposing force is often not recognizable, because it is applied by the fastenings or supporting parts. Normal stresses can also occur in moving objects, e.g. in the hawser between a tug and a ship. Here the tug's tensile force is counteracted by the force from the water current.

The mechanical stress is expressed by the quotient of the force F and the cross-sectional area A of the stressed material:

$$\sigma = \frac{F}{A}. \quad (2.2-1)$$

Tensile stresses are positive.
 Compressive stresses are negative.

Earlier units of mechanical stress were

kp/mm² in mechanical engineering and
 kp/cm² in civil engineering.

According to the SI System (Système International d'Unités) [2-3 to 2-5] the unit for force is the "Newton" [N] and for area the "square meter" [m²]. This gives the unit [N/m²] for mechanical stress, which is also known by the special name "Pascal" [Pa].

$$1 \text{ N/m}^2 = 1 \text{ Pa.}$$

This unit leads to very large numbers. Hence force is often stated in decimal multiples, e.g. daN or kN and the area in decimal subdivisions, e.g. cm² or mm².

$$1 \text{ N/mm}^2 = 100 \text{ N/cm}^2$$

$$1 \text{ N/mm}^2 = 10^6 \text{ Pa}$$

$$1 \text{ N/cm}^2 = 10^4 \text{ Pa}$$

Sometimes one comes across the designation daN/mm². This gives numbers similar to kp/mm², which was previously very common.

$$1 \text{ daN/mm}^2 = 10 \text{ N/mm}^2 \approx 1 \text{ kp/mm}^2$$

This designation is only given as a concession to earlier practice. Hopefully, a universal notation will prevail. In this book only the designation N/mm² will be used for numbers denoting stress.

2.2.2 Shear stress

With normal stress the tensile and compressive forces, which occur in opposite directions, always act on the same axis. They try to pull the material apart or to press it together, depending on whether they are oriented going away from one another or towards one

another. Shear stresses are principally a different type of stress. To imagine their formation, one must think of two forces F_1 and F_2 which act in opposite directions, but with a small distance between them, as they would be produced by the cutting edges of a pair of scissors. Fig. 2.2-2 shows two examples.

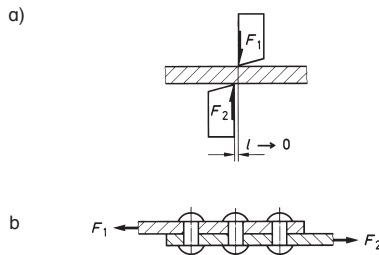


Fig. 2.2-2: Formation of shear stress.

- a) panel cutters
- b) riveted joint

If the forces are so large that the strength of the material is exceeded, the neighboring parts of the material move relative to one another over the whole cross-section and the part is “sheared”.

The forces are identified with half arrows in Fig. 2.2-2a. Half arrows are used, because the distance l is very small and close to zero. Even when the distance l is larger, the term shear stress is used (see sections 8.4.4 to 8.4.6). Shear stresses are designated with the symbol τ .

The example in Fig. 2.2-2b illustrates a similar situation with a riveted joint.

Shear stresses act inside the stressed object and cannot be detected externally. However, shear stresses, which occur for example with the torsion stressing of a shaft, are apparent from surface distortions, i.e. on the cylindrical surface. An example is shown in Fig. 2.2-3.

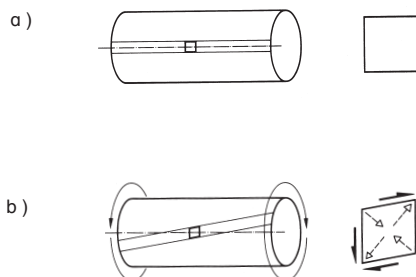


Fig. 2.2-3: Surface distortion as a result of shear stress due to torsion.

- a) Unloaded shaft. Lines on the cylindrical surface run parallel to the axis; the surface element is square
- b) Shaft stressed by torsion. Lines on the surface run at an angle to the axis; the surface element has become a rhombus.

A square section marked on the surface of the unstressed cylindrical shaft, bounded by lines running parallel to the shaft, is distorted to a rhombus after the shaft is loaded with a torque. The lines drawn on the surface are still parallel to one another, but they now have a steep helical shape. The process can be represented in the following manner.

The shaft can be regarded as being made up of a large number of round slices arranged parallel to the cross-sectional plane, the thickness of each slice being one molecule. The counteracting torques try to rotate the slices against one another as with a slipping clutch. However, since the slices are held together by their elastic cohesive forces, only a tiny angular displacement occurs between adjacent slices.

The shear stresses occurring between the individual slices cannot be measured. The shear stress τ can be calculated from the two main normal stresses σ_1 and σ_2 :

$$\tau = \frac{\sigma_1 - \sigma_2}{2}. \quad (2.2-2)$$

Shear stresses always occur with normal stresses (see section 8.2-3).

The main normal stresses in the planar stress state are two stresses resolved at an angle of 90° to one another within a plane, e.g. in the surface of an object. In the example in Fig. 2.2-3 a maximum positive normal stress occurs in the direction of the surface element's major rhombus diagonal and a negative normal stress occurs in the direction of the minor diagonal.

The same units are used for shear stress as for normal stress.

2.2.3 Residual stress, thermal stress

The causes of these stresses are apparent from their names. They comprise normal and shear stresses. The difference between these and other stresses named after their origin, e.g. bending stress, torsion stress, is that they occur without any external forces being involved.

“Residual” or “inherent” stresses can arise in material due to the internal effects of force, e.g. from non-uniform changes in volume in heat-treated parts during the hardening of steel, by non-uniform cooling of cast or injection molded metal or plastic objects, with welded or forged parts, through mechanical processing or, with larger objects, simply from the effect of their own weight [2-6]. “Thermal stresses” are a type of residual stress. They occur in systems, in which parts with different thermal expansions are joined together such that free thermal expansion is prevented or they occur as a result of non-uniform heating. Residual and thermal stresses affect the material similarly to loading stresses. They reduce the load-bearing capacity of the material by externally applied forces. Questions regarding the operational safety of structural parts can therefore only be answered adequately if the residual stresses are known quantitatively and qualitatively. The determination of these stresses is only possible with normal practical methods when they are “released” and the degree of resilient relaxation exhibited by the material in the non-stressed state is measured. The release of these stresses can take place in different ways.

Scientific investigations sometimes go so far as to break the test object up into small parts to measure the resilience [2-7]. A complete picture of the stress distribution is obtained, but the measurement object is lost. Therefore, such destructive methods are not suited to normal problems in stress analysis. Instead methods are needed which require only minor interference with the test object. The hole drilling method ([3-6 and 3-7] and section 8.3) and the ring core method [3-5] are among these. Rosettes for the measurement of residual stress are described in section 3.2.2.3.

2.2.4 Stress states

These are subdivided as follows:

- a) the uniaxial stress state,
- b) the biaxial or planar stress state,
- c) the triaxial or three-dimensional stress state.

The *uniaxial stress state* is the simplest case. It occurs in tension and compression bars, see Fig. 2.2-1.

A biaxial or planar stress condition is said to occur if the forces producing the stresses occur on two axes that are perpendicular to one another. Resolving of the effective directions of the forces into two main axes at 90° to one another is made on theoretical grounds. The effective directions of different forces acting in the same plane, but at different angles, can be very different. However, they can always be resolved into the two main directions.

A triaxial or three-dimensional stress state is present if the forces can act in any direction. Similar to the planar stress state, three main axes are defined which are all situated perpendicular to one another.

Strain measurements are restricted by necessity to the accessible surfaces of the structural parts and consequently they can only give information on the stress state at the component surface. Whereas uniaxial and planar stress states can be analyzed relatively simply with strain measurement techniques, in particular using strain gages, three-dimensional stress states present problems since the required measurements along the third axis, i.e. inside the object, are usually not possible. However, in a three dimensional body, which is stressed by external forces, the maximum stresses occur at the surface! (Exception: Hertz effect problems). For the designer, who is usually only interested in the maximum stresses, the determination of the stresses at the surface is sufficient. The internal processes are of lesser importance.

Three-dimensional stress states can only be analyzed from strain measurements if the strain can be measured along the third axis, i.e. in the object's depth. This is found for example in model measuring techniques where strain gages can be cast into plastic models. This is also possible in civil engineering where strain measuring equipment can be embedded in concrete during pouring.

2.3 Material parameters

2.3.1 Modulus of elasticity, definition and units

A fundamental parameter for denoting the mechanical load-bearing capacity of materials is tensile strength. It is determined in the test laboratory on specimens with standardized dimensions [2-8]. Fig. 2.3-1 shows a schematic representation of the method used.

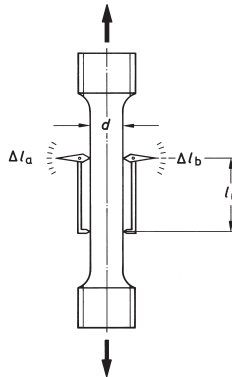


Fig. 2.3-1: Schematic diagram for the determination of tensile strength and static modulus of elasticity of materials.

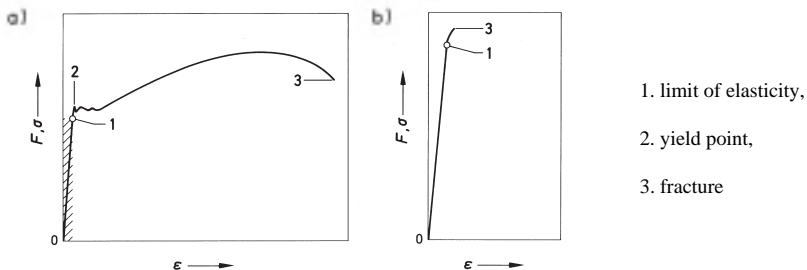


Fig. 2.3-2: Examples of force/strain and stress/strain curves.
a) Characteristic of a ductile material with large yield range
b) Characteristic of a brittle material

The material specimen is clamped in a testing machine and subjected to tensile loading. The strain ε of the material is measured in relationship to the applied force. The result is drawn in the form of a graph. The nominal stress σ can also be recorded instead of the force F ; this is calculated according to equation (2.2-1) from the specimen's cross-sectional area A_0 present at the start of the test. Fig. 2.3-2 illustrates an example of F/ε and σ/ε diagrams. The shape of the σ/ε curve is dependent on the material. Hence, ductile, i.e. plastically deformable materials exhibit a large post-yield range, Fig. 2.3-2a, whereas brittle materials and high-strength steels do not yield very much at all, Fig. 2.3-2b.

With “linearly elastic” materials there is a linear rise in the σ/ϵ curve in the region of elastic deformation. The slope in this section of the diagram characterizes the material's rigidity. This is expressed as the ratio between σ and ϵ is termed the modulus of elasticity or Young's modulus having the symbol E .

$$E = \frac{\sigma}{\epsilon} \tag{2.3-1}$$

Young's modulus is the value of the ratio σ/ϵ and has the units [Pa] or [N/cm²] or [N/mm²].

$$1 \text{ Pa} = 1 \text{ N/m}^2 = 10^{-4} \text{ N/cm}^2 = 10^{-6} \text{ N/mm}^2$$

$$\text{or } 1 \text{ N/mm}^2 = 102 \text{ N/cm}^2 = 106 \text{ N/m}^2 = 10^6 \text{ Pa.}$$

This designation can present problems for the “uninitiated”, particularly if the requirements for correct dimensional calculation must be satisfied. Strictly speaking the designation should be:

$$(E) = \left\{ \frac{\sigma}{\epsilon} \right\} \left[\frac{\text{N/mm}^2}{\text{m/m}} \right] \text{ or } \left[\frac{\text{N/cm}^2}{\text{mm}} \right] \text{ or } \left[\dots \right].$$

As is usual in mathematics the dimensions for the ratio ϵ [m/m] are canceled out and therefore disappear. Then the same dimensions remain for Young's modulus as for the material stress σ , although two completely different quantities are involved.

Example:

$$E = \frac{70 \text{ N/mm}^2}{1000 \text{ } \mu\text{m/m}} = \frac{70 \text{ N/mm}^2}{10^{-3} \text{ m/m}} = 70000 \frac{\text{N/mm}^2}{\text{m/m}} = 70000 \text{ N/mm}^2$$

Every material has a certain value of Young's modulus. The different figures result from different slopes on the σ/ϵ diagrams. Some examples are illustrated in Fig. 2.3-3 where only the linear sections of the curves are shown.

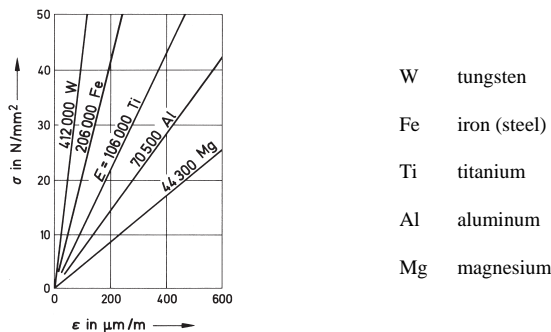


Fig. 2.3-3: Examples of Young's modulus

Lists of Young's moduli can be found in tables. It should be noted that table values are always mean values taken from a large number of measurements.

Material	E[kN/mm ²] (0...100°C)	Material	E[kN/mm ²] (0...100°C)
Aluminum	66	molybdenum	330
AlCuMg	70	Monel	156
AlMgSi	69	nickel	193
AlMgS	68	gunmetal Gm5	93
AlCuNi	70	steel C15	204
G-AlSi	78	C35	202
G-AlSiMg	75	C60	200
bronze SnBz6	109	41Cr4	203
G-SnBz12	79	X10Cr13	216
AlBz5	123	X12CrNi 18 8	191
AlBz8	122	36% Ni-steel	142
FeAlBz10	123	titanium	103
Copper	123	TiA16V4	108
CuBe (copper-beryllium)	131	strain gage adhesives	E[kN/mm ²] (0...50°C)
CuNi55/45 (constantan)	161		
magnesium	44	X 60 (acrylic resin, filled)	4.5...6
MgAl7	43	Z 70 (cyano acrylate)	3
brass Br58	88	H (polyester)	3.5
Br60	88	EP 250, EP 310 (epoxy resin)	2.8
Br72	88	CR 760 (ceramic putty)	20..21

Table 2.3-1: Young's modulus for some materials

As a result of alloy modifications, etc. a few percent deviation must be expected from the table values. If higher accuracy is required, a measurement should be carried out following the basic method described.

Consideration should also be given to the fact that Young's modulus is dependent on temperature.

Table 2.3-1 gives some figures for common materials.

2.3.2 Shear modulus

The shear modulus G simplifies the calculation of shear stress. It is not an independent material parameter such as Young's modulus E (section 2.3.1) and Poisson's ratio ν (section 2.3.3), but is derived from these.

$$G = \frac{E}{2} \cdot \frac{1}{1+\nu} = \frac{E}{2(1+\nu)} = 0.385 E \text{ for } \nu = 0.3 \quad (2.3-2)$$

The unit for the shear modulus is N/mm², i.e. the same as for Young's modulus (section 2.3.1). It describes the ratio of the shear stress τ to the shear deformation angle γ measured in radians:

$$G = \frac{\tau}{\gamma} \quad (2.3-3)$$

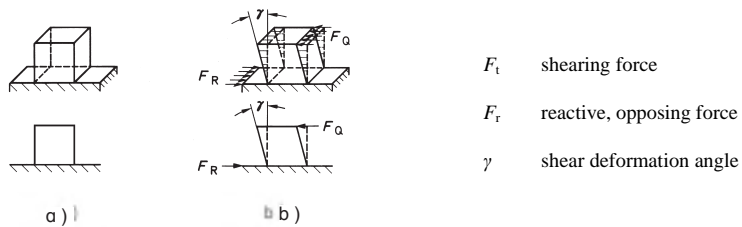


Fig. 2.3-4: The shear deformation angle γ on a material under shear stress
 a) without load
 b) with load applied

2.3.3 Poisson's ratio

If a rubber band is pulled, it becomes longer but at the same time thinner; if a rubber object is compressed, it becomes shorter but thicker.

The French scientist *Siméon Denis Poisson* (1781-1840) discovered the following effects in his investigations:

If a bar is loaded with a tensile force F_T , then it extends by $\Delta l/l_0 = \epsilon_l$ (longitudinal strain); its thickness is also reduced by $\Delta b/b_0 = \epsilon_t$ (transverse contraction). ϵ_l is positive, ϵ_t is negative, see Fig. 2.3-5a.

If a rod is loaded with a compressive force F_C , then it shortens by $\Delta l/l_0 = \epsilon_l$ (“negative longitudinal strain”); it also becomes thicker by $\Delta b/b_0 = \epsilon_t$ (transverse elongation or transverse dilatation). ϵ_l is negative, ϵ_t is positive, see Fig. 2.3-5b.

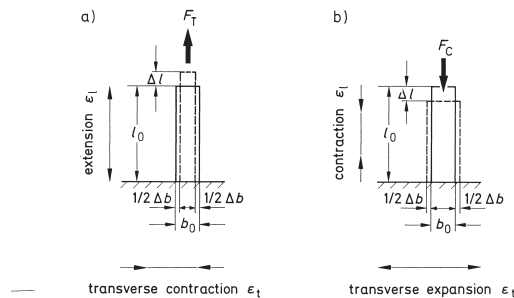


Fig. 2.3-5: Transverse contraction and transverse expansion.

The following relationship is defined:

$$\left| \frac{\epsilon_r}{\epsilon_l} \right| = \nu \text{ (Poisson's ratio)} \quad (2.3-4)$$

In the theory of mechanical stability Poisson's ratio is often allocated the Greek letter μ (mu) as its symbol. However, since the letter μ is used very much in engineering and has other meanings, the letter ν (nu) is being increasingly used. Both symbols are currently found in publications. The letter ν will be used throughout this book.

Poisson's ratio is dependent on the material and is valid in the material's elastic deformation region. It has a value of around 0.3 for metals, but it can deviate substantially from this approximate value, as shown in Table 2.3-2. Poisson's ratio ν is about 0.4 for plastics; with incompressible materials, e.g. rubber and water, and in the plastic deformation region of metals it is $\nu = 0.5$.

Material	ν	Material	ν
Aluminum alloys	0.33	Silver, annealed	0.37
Niobium	0.38	hard	0.39
Glass	0.22	Steel	0.28
Rubber	0.5	construction steel, hot-rolled	0.26
Cast iron, gray	0.25	17-7PH	0.28
Inconel	0.29	15-7PHMo	0.28
Copper	0.33	invar, 36% Ni	0.29
Magnesium	0.35	XCrNi18.9(SS304)	0.305
Brass	0.33	XcrNiMol8.12(SS316)	0.33
Molybdenum	0.32	Titanium	0.34
Monel	0.32	Vanadium	0.36
Nickel	0.31	Tungsten	0.284
Platinum	0.39	Zircaloy 2	0.39
Rhenium	0.49		

Table 2.3-2: Poisson's ratio for some materials

Note:

Table 2.3-2 contains figures for Poisson's ratio from different sources. On account of the wide spread of values it is advisable to determine Poisson's ratio in a test if high accuracy is needed, e.g. measurement of the longitudinal strain and the transverse contraction under identical conditions using strain gages. The measurements obtained should then be corrected according to the method described in section 7.5 for errors resulting from the strain gages' transverse sensitivity.

Important: Poisson's ratio ν is always stated purely as a value, i.e. without its sign, even in books of tables. This is due to historical reasons. It also applies to Table 2.3-2 and must be taken into account when writing formulae.

2.3.4 Thermal expansion

Every object alters its dimensions when its temperature changes.

Heating produces expansion, cooling produces contraction.

Elongation caused by temperature does not produce any mechanical stress in the material if

- free expansion or contraction of the object is not prevented, e.g. by clamping,
- the object has a completely uniform temperature over its full extent

Material	ϑ [°C]							
	-196	100	200	300	400	500	600	800
Metals								
aluminum (99.5%)	-22.6	23.8	24.5	25.5	26.5	27.4	28.3	
AlZnMgCu 1.5	-17.8	23.4	24.4	22.5				
Duralumin (95Al ;0.04Cu ;		23.5	24.5	26.0	26.7	27.3		
lead	-26.8	29.0	29.6	31.1				
bronze(85Cu; 9Mn; 6Sn)	-14.9	17.5	17.9	18.3	18.8	19.2		
cast iron	-8.4	10.4	11.1	11.6	12.3	12.9	13.5	14.7
constantan (60Cu; 40Ni)	-11.9	15.2	15.6	16.0	16.4	16.7		
copper	-13.9	16.5	16.9	17.2	17.7	18.1	18.5	
magnesium	-21.1	26.0	27.1	27.9	28.8	29.8		
brass(62Cu; 38Zn)	-16.4	18.4	19.3	20.1	21.0			
molybdenum	-4.2	5.2	5.4	5.5	5.6			
nickel	-10.0	13.0	13.6	14.3	14.9	15.2	15.5	16.1
steel								
mild steel	-8.8	12.0	12.6	13.1	13.6	14.1	14.7	
Invar (64Fe; 36Ni)		1.5	3.8	5.3	7.8	9.4	10.8	13.1
1.4301 (XCrNi18.9)		16.1	17.1					
titanium (Ti6 A14V)		8.4	8.6	8.9	9.0	9.2		
tungsten	-3.8	4.5	4.5	4.7	4.7	4.5	4.5	4.5
Glass								
Jenaer 16 III	-5.9	8.1	8.4	8.7	9.0	9.3		
Jenaer 1565 III		3.5	3.6	3.7	3.9	4.1		
silica glass	+0.16	0.50	0.60	0.63	0.62	0.62	0.6	0.56
Zerodur®	-0.18	0.02	0.02					
Plastics	$\vartheta = 50^{\circ}\text{C}$						$\vartheta = 50^{\circ}\text{C}$	
acetyl cellulose	80-90		polyamide				90-100	
acrylic resin	70-80		polyester				100-150	
epoxy resin	60		polystyrene				60-80	
phenolic resin	50-80		impact resistant polystyrene				80-100	
polyacetal	90		polyurethane				190	
high density polyethylene	160-180		polyvinyl chloride (PVC)				70	
low density polyethylene	230		impact resistant PVC				80-100	

Table 2.3-3: Average thermal expansion coefficients for various materials for different temperature ranges between 20° and ϑ °C in $10^{-6} \frac{m}{m} \cdot \frac{1}{K}$

If the thermal expansion is restricted, thermal stresses occur in the material, see sections 2.2.3 and 8.4.7.

There are definitions for longitudinal expansion, surface expansion and volume expansion. Thermal longitudinal expansion is of interest in strain measurement.

The longitudinal expansion coefficient α , also called the linear thermal expansion coefficient, states the relative change in length in 10^{-6} m/m per K:

$$\alpha = \frac{l_2 - l_1}{l_1} \cdot \frac{1}{\Delta\theta} = \frac{\Delta l}{l_0 \cdot \Delta\theta} \text{ in } \left[\frac{\text{m/m}}{\text{K}} \right] = \left[\frac{1}{\text{K}} \right] \quad (2.3-5)$$

$l_1 = l_0$ = initial length before temperature change, i.e. reference length

l_2 = final length after temperature change

Δl = change in length due to change in temperature

$\Delta\theta$ = temperature change, positive for heating, negative for cooling

The ratio m/m is also canceled here so that the unit is dimensioned only with 1/K.

Note: The longitudinal expansion coefficient α is dependent on the material and the temperature. Therefore, different figures are found in tables for different temperature ranges. The difference in the figures should not be taken to indicate a step-change in the material's expansion characteristics.

2.4 Strain gage loading

The method of loading a strain gage during a measurement has effects on its characteristics. Therefore various limits are stated for some characteristics, e.g. different temperature limits, different elongation limits, etc. The following shows how the terms “static measurement”, “quasi-static measurement” and “dynamic measurement” should be interpreted when encountered in strain gage literature and data sheets.

2.4.1 Static measurements (zero referenced)

“The term 'static measurement' in strain gage techniques includes all measurements of strain or strain components which are constant in time. It is therefore also used, for example, for a process which is constant in time, but which has a varying process superimposed upon it.” (Quotation from [2-1]) With regard to the strain gage this means that errors in the measuring signal due to disturbance conditions within the strain gage during a time period do not exceed an acceptable level. The measuring signal can be referred to the zero point present at the start of the measurement.

2.4.2 Quasi-static measurements

“Quasi-static measurements” is the term used to denote slowly changing processes whose rate of change with time is so small that an indicating instrument can be read with sufficient accuracy without any special measures being taken.

2.4.3 Dynamic measurements (non-zero referenced)

“All measurements of changing strain processes are defined as dynamic measurements where only the dynamic component is determined, e.g. the amplitude of an oscillation.” (Quotation from [2-1])

This definition needs closer consideration. If for technical strain gage data, details are given for “dynamic measurements” which are different to those for static measurements, then these figures only apply to rapidly altering processes where time-dependent changes in the strain gage are not able to have an effect. If a static basic value or mean value is allocated to an oscillating process, then the limits for static, i.e. “zero referenced” measurements apply if this basic value or mean value must also be determined. It would be more practical to speak of “non-zero referenced measurements” rather than “dynamic measurements”.

3 Selection criteria for strain gages

The questions that should be considered during the selection of a type of strain gage from the ranges available from the manufacturers arise due to the variety of strain gage applications and due to the conditions affecting the strain gages during service. There is no strain gage that fulfils *all* requirements. For this reason numerous different strain gages are available and are supplemented with special types when required. It is a question of the manufacturer's business strategy of whether he maintains a range which is kept within bounds or of whether he allows it to grow to mammoth proportions. Most problems can be solved with a carefully conceived range of defined limits without needing to resort to special manufacture. Selection is then easier for the user. This is particularly important for users with only average or slight experience. It has been shown that half of all measurement problems can be solved with a collection of about two dozen types of strain gages.

From the following it should be possible to select a suitable type of strain gage using a logical procedure. It is possible, however, that conflicting arguments may arise that force a compromise, but this is common in engineering and is not restricted to strain gage techniques.

The author has found that the user very often only has a vague impression of what takes place at the point of measurement. A little more thought before starting the measurement could help to prevent expensive mistakes and might lead to better results. The selection system presented here requires the user to analyze his measurement problem. To use the system two requirements must be fulfilled:

- 1st requirement: The measurement task must have a clear objective and the details of the process and its boundary conditions must be known.
- 2nd requirement: The strain gage characteristics must be known.

Table 3.0-1 is intended to provide help in fulfilling the *1st requirement*. Here the most important factors affecting the selection of a type of strain gage are listed as headings in five groups. The table can be used as a checklist so that the user does not overlook an important point.

1.	Measurement problem Primary: strain measurement Secondary: experimental analysis - transducer design - plant monitoring - safety systems.
2.	Mechanical conditions at the point of measurement
2.1	Stress state uniaxial - biaxial - principal direction known - unknown
2.2	Stress field topography homogeneous - inhomogeneous - steep variations (stress around notches) determination of average or peak value
2.3	Type of loading static: amplitude - direction (positive, negative) - number of loadings dynamic: impulse - stochastic - cyclic - changing load - expansion loading (positive, negative) - amplitude - number of load cycles - measurements referred to zero - non-zero referenced
2.4	Ratio of the useful portion of the measurement to the disturbance portion e.g. normal force as the useful portion with superimposed bending moment as disturbance
3.	Environmental conditions
3.1	Duration of the measurement once only - short term - repeated short term - long term - required operational duration - required service life of the bonding system
3.2	Temperature level - range (before, during and between measurements) - rate of change - one-sided radiation - thermal expansion coefficient of the component material
3.3	Disturbance effects intensity - effective duration
3.3.1	humidity - water - pressurized water - steam - ice
3.3.2	oil (transformer oil, paraffin, machine oil, hydraulic oil)
3.3.3	chemicals (solid, liquid, gaseous, reactive, inert)
3.3.4	pressure - vacuum
3.3.5	electrical fields - magnetic fields - energy transfer (e.g. welding current, lightning strike)
3.3.6	high energy radiation
3.3.7	external forces (shock, impact, soil pressure)
4.	Electrical conditions at the point of measurement
4.1	Measurement circuit Quarter bridge - three-wire circuit - half bridge - double quarter bridge - full bridge
4.2	Strain gage supply direct voltage - alternating voltage (carrier frequency) - voltage with respect to ground - continuous/pulse supply (time - duty ratio)
4.3	Cable length - resistance - insulation - capacitance - resistance to environment effects (mechanical, thermal, chemical) - connecting elements (plugs, cable entry)
5.	Application conditions
5.1	Component material machinability - bonding and welding properties
5.2	Application access Access - use of sand blasting or other surface treatments - resistance to solvent and temperature
5.3	Cable routing
5.4	Spatial conditions strain gage - cable - covering agent - protective caps

Table 3.0-1: Chart for the analysis of conditions which must be fulfilled by a strain gage measurement point.

If as much as possible is known about the conditions affecting the measurement, then the required cost and effort can be more easily assessed and the chance of success is also greater. Unpredictable results can never be completely eliminated, but they can be reduced to a minimum.

Knowledge of strain gage characteristics is needed to fulfill the *2nd requirement* for the selection of the optimum gage.

The determination of strain gage parameters is not always carried out using the same method, so that the results may be interpreted differently. The purpose of Guideline 2635, which was prepared and published by the VDI/VDE Gesellschaft Mess- und Regelungstechnik, was to ease this situation and encourage a universal measurement method [2-1]. Work on international adaptation is in progress. An explanation of the aim and the content of the guideline is given in [3-1]. Data in the form of data sheets is enclosed in the package with every strain gage. Further details and empirical values can be found in section 3.3 (Technical Data).

Since interference effects do not all occur simultaneously, one does not need to assess all the characteristics, but rather only those relating to the application conditions. These are defined beforehand, if necessary using Table 3.0-1. This also applies to the bonding method and to the covering agent used for the protection of the measurement point against adverse mechanical or chemical effects.

3.1 Range of application

In principle all strain gages can be used both for the solution of problems in experimental stress analysis and for the construction of transducers. There are however certain differences between types of strain gage, making them suitable for particular applications.

3.1.1 Stress analysis, model measurement techniques, biomechanics

For *experimental stress analysis*, including model measurement techniques and biomechanics, robust and flexible strain gages, which can be used under arduous conditions, have distinct advantages. Strain gages having the synthetic, polyimide, as carrier material for the measuring grid and with the series identification “Y” are in this category. This series contains a large number of different types of strain gages used for a variety of tasks in stress analysis.

There are also numerous special types, e.g. hole-drilling and ring core rosettes for the determination of residual stresses in structural parts; strain gage chains for the investigation of stress distribution on complex structures; strain gages with metal carriers which are fixed to the measuring point by spot welding and there are many others. The appropriate brochures on strain gages provide details.

3.1.2 Transducer construction

In *transducer design* such a large number of types is not necessary. Instead, higher demands are placed on measurement accuracy. Strain gages which also fulfill the extreme demands of accuracy for calibrated load cells are of the same type as the strain gages in the

“G” series. The carrier for the measuring grid consists of glass-fiber reinforced phenolic resin.

Special types of strain gages can also be manufactured if the demand is high enough. Negotiations with the manufacturer are then required.

The “K” series was developed specially for use in transducer construction. A specialized publication provides details of their characteristics and applications.

If there is sufficient requirement, HBM also supplies *special types* which are optimally designed for certain tasks. The most modern equipment is available within the company for the production of negatives [3-51]. It enables full use to be made of the various design options presented by photo-etching techniques for the manufacture of foil strain gages. However, the user should not be misled into unnecessarily having a special strain gage made, since this belies the previously mentioned fact that in most cases a small range of strain gage types is sufficient. Special strain gages should only be applied if certain features are needed or if certain conditions are to be fulfilled. In these cases it is best to make an inquiry giving exact details of the application. Sometimes, a suitable shape can be found from the range of existing special negatives.

3.2 Types of strain gages

Strain gages are available in various shapes and sizes. Apart from different lengths of the measuring grid there are various designs and positions for the connections. There is also a difference between linear strain gages in single and double (parallel) arrangements, X rosettes with measurement grid axes at 90° to one another, R rosettes with 3 measuring grid axes arranged at certain angles to one another, strain gage chains and numerous other special shapes.

The large number of shapes and sizes is the result of adaptation to different application problems. Criteria for the selection of a suitable type of strain gage are dealt with in the following sections.

3.2.1 Length of measuring grid

Fig. 3.2-1 is a schematic representation of a selection of strain gages having different lengths. Some also have different connections.

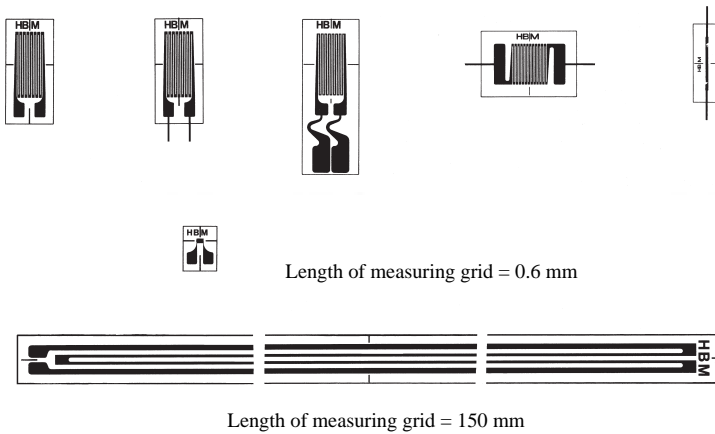


Fig. 3.2-1: Typical shapes of measuring grid for linear strain gages.

3.2.1.1 Homogeneous field of strain

The first criterion is the space available on the measurement object. If the object is sufficiently large, strain gages with 3 to 6 mm length of measuring grid are optimum, both with regard to quality and their ease of application.

The arrangement of the connections to the side of the measuring grid and an extremely narrow grid design take account of space restrictions at the bonding point.

The idea, often encountered, that a strain gage's sensitivity is dependent on its length is incorrect. A metal strain gage's sensitivity is proportional to the relative elongation, i.e. strain, and not to the absolute elongation. In this respect the absolute length of the strain gage has no effect on its sensitivity. However, extremely small strain gages should only be used where necessary for technical reasons, e.g. for investigations into stresses in notches. It is then better to consider cutting a large strain gage to adapt it to the available space. This naturally leads to the question of whether some of the strain gage can be cut off. The answer is "yes", but one must know where and one must also be acquainted with the possible consequences.

Here a short digression is needed into the mechanics of the transfer of strain to the strain gage's measuring grid (see Fig. 3.2-2).

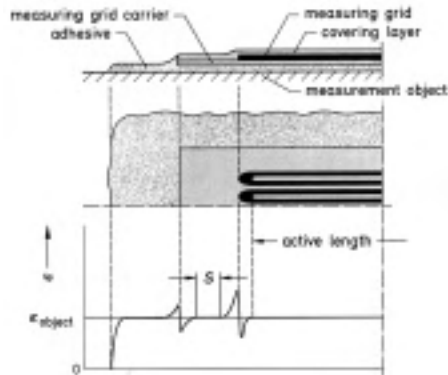


Fig. 3.2-2: Schematic illustration of the transfer of strain to the strain gage's measuring grid.

It is assumed that the measurement object is uniformly strained by the amount ϵ_{object} . This strain must be transferred through the adhesive layer and the measuring grid carrier to the measuring grid itself. For measurement objects which are not too thin the forces needed to do this are negligible in comparison to the forces acting on the object.

Transition sections exist for the transfer of the strain in the measurement object through the individual bonding layers up to the strain gage's measuring grid. A transition section occurs at the junction of one layer and the next, i.e.

- from the measurement object to the adhesive layer
- from the adhesive layer to the measuring grid carrier
- from the measuring grid carrier to the measuring grid.

The length of the transition section depends on the thickness of the individual layers and on the rigidity, i.e. the Young's modulus, of the layer materials. The diagram shows a section's transition phase where the strain in the measurement object is equal to the partial strain in the strain gage parts. At each transition point from one strain gage part to the next, an increase in strain occurs which compensates for the slack in the following part.

The measuring grid carrier can if necessary be shortened by the amount identified by the letter "S" in the diagram without affecting the strain gage characteristics. If it is shortened further then the strain transition section would stretch into the region of the "active" grid length. This leads to an apparent reduction in the strain sensitivity, which is expressed by the gage factor (see section 3.3.1). This effect is only slight for strain gages with a long measuring grid, but for very short strain gages reductions in sensitivity of a few percent can occur. If the strain transition sections of the measuring grid carrier are shortened too much, it can also have adverse effects on strain gage creep, see section 3.3.9.

Young's modulus is temperature dependent for synthetics, including adhesives and grid carrier materials. This means that for higher temperatures the transition sections become longer and vice versa. This fact should be considered where applicable. A minimum of 1 to 2 mm should be maintained for the extension of the carrier foil beyond the measuring grid.

Cutting the strain gage carrier parallel to the measurement direction has only a very slight effect on the strain gage's transverse sensitivity, see section 3.3.3. Since the transverse sensitivity of modern strain gages is in any case very small, this effect can be ignored and the strain gage carrier cut almost up to the edge of the measuring grid.

3.2.1.2 Inhomogeneous strain field

The strain gage forms an arithmetic mean of the strain conditions existing under its measuring grid. This fact is taken into account when considering the most appropriate length of measuring grid.

If the mean value is required, then a long measuring grid is used.

Here is a typical example concerning measurements on concrete (could also be on wood, fiber-reinforced plastics, etc.). With short strain gages partial strains would be obtained which would be smaller than the average figure in the region of the aggregate and larger than this figure in the region of the cement mixture [3-2], see Fig. 3.2-3.

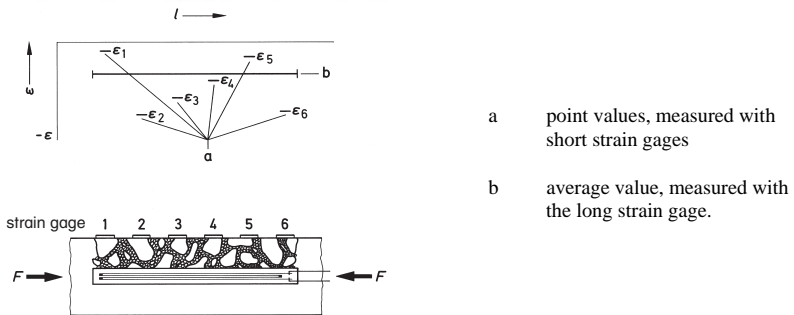


Fig. 3.2-3: Application example for a strain gage with a long measuring grid, giving an average value with inhomogeneous material, e.g. concrete.

The ratio between the minimum and maximum values of strain may be between 1:3 and 1:15 for concrete, depending on the aggregate. An adequately averaged value is obtained when the length of measuring grid is at least four times, or preferably five times, the largest aggregate core size. The diagram in Fig. 3.2-4 shows the expected measurement error against the ratio of strain gage length/particle size.

The opposite applies if the peak value or local strain condition is required in an inhomogeneous stress field, e.g. the maximum value of stress in a notch. Short strain gages are of advantage here, since a long strain gage would give an undesired mean value.

The interdependence between the measured value and the length of measuring grid is shown schematically in Fig. 3.2-5. The curve should indicate the actual change in strain along the notched specimen. The ordinate values $\varepsilon_1 \dots \varepsilon_4$ show the measurements that are obtained if the measuring grid of the applied strain gage has the respective lengths $l_1 \dots l_4$. The peak value is only correctly obtained with the short strain gage of length l_4 .

On this basis it could be assumed that a length of measuring grid equal to zero would be ideal, but of course limits must be set. Technically it is quite possible to produce strain

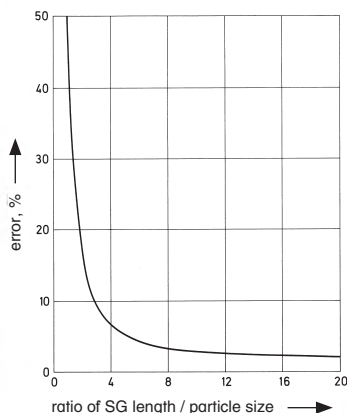


Fig. 3.2-4: Measurement error with measurements on inhomogeneous materials, e.g. concrete, in relationship to the ratio strain-gage length/particle size (from)

gages with a grid length of 0.2 mm. The shorter the measuring grid, the more significant are the problems of transferring the strain to the measuring grid.

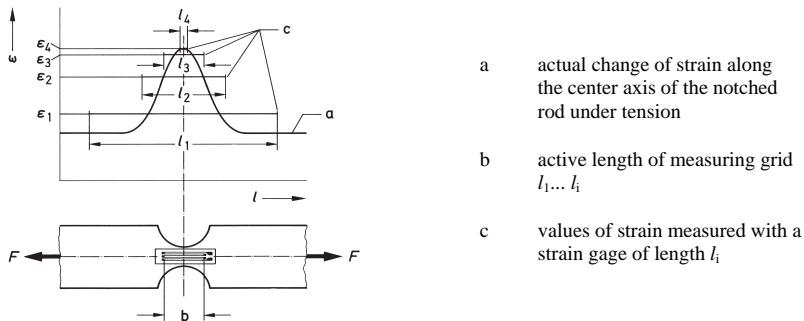


Fig. 3.2-5: The effect of the measuring grid length l on the measurement due to averaging when measuring stress peaks.

These problems arise mainly when bonding the strain gage to the object. This is particularly difficult in notches and leads to large measurement errors. Consideration should also be given to the fact that with small areas of measuring grid the thermal dissipation through the measurement object is very low. This means that the supply current, which causes heating due to the Joule effect, must be kept to a minimum and must be taken into account during the selection and adjustment of the supply source. The strain gage must therefore be chosen to be no shorter than is necessary. As a rough guide the length of measuring grid $\leq \frac{1}{2}$ the notch's radius.

3.2.1.3 Dynamic strain conditions

Strain gages are also well suited to the measurement of dynamic strain conditions. If these are time-varying strains, which are however uniform over the length of the measurement section, then the arguments dealt with in section 3.2.1.1 apply for the selection of the strain gage. With shock or high frequency oscillating processes attention should be paid to the length of the measuring grid. This is treated further in section 3.3.7.

3.2.2 Multiple strain gages, their advantages and fields of application

Multiple strain gages have a number of measuring grids on a common carrier. Typical shapes for multiple strain gages are double strain gages, chains and rosettes. Their particular advantage is that the separation between the measuring grids and their orientation to one another are maintained with a high degree of accuracy. A further advantage is that less bonding work is required, since a number of measuring grids can be bonded in one process. Also some mounting problems with closely arranged measuring grids can only be solved with the use of multiple strain gages, because the mounting of individual strain gages is not technically possible.

3.2.2.1 Strain gage chains for the determination of stress gradients

In the section on stresses in notches the influence of the length of measuring grid on the measurement result was explained. In practice the relationships are often not so clearly visible and the point of maximum loading cannot be determined with certainty. Perhaps not only the peak value is required, but also the variation of loading over a certain section or the displacement of the peak value under the influence of a variable point of loading. Strain gage chains were developed for the solution of such problems.

Strain gage chains are a combination of measuring grids which are of the same type or which alternate at regular intervals, but all are on one common carrier.

Some of the most important types are shown in Fig. 3.2-6.

The chains each contain 10 individual measuring grids or 5 groups each with 3 measuring grids. At the end of each chain an additional grid is located, which can be applied separately to a suitable point and used as a compensating or supplementary strain gage.

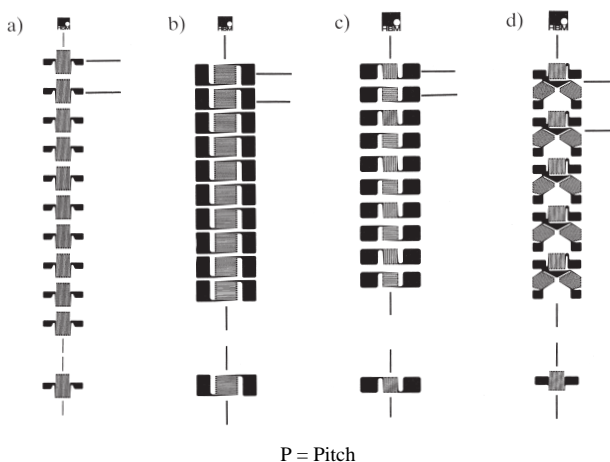


Fig. 3.2-6: Shapes of strain gage chains

- measuring grids in a direction parallel to the chain's longitudinal axis
- measuring grids in a direction perpendicular to the chain's longitudinal axis
- measuring grids in a direction alternately parallel and perpendicular to the chain's longitudinal axis
- measuring grids in groups of 3 at $0^\circ/60^\circ/120^\circ$ to the chain's longitudinal axis (rosette chain)

Strain gage chains are manufactured in various sizes. The dimension P, the pitch, gives the distance between the center axes of two neighboring measuring grids; with the rosette chain this is the distance between two groups of grids. Chains of the types a) and b) are manufactured with pitches of 1 mm, 2 mm and 4 mm, the type c) 2 mm and 4 mm and the rosette chain d) is produced with a 4 mm pitch.

Fig. 3.2-7 illustrates an example of the application of strain gage chains for the determination of the stress distribution in the rounded section at the root of a gearwheel tooth [3-4]. Here, the tangential and transverse strains were measured with 5 chains at 50 points on the root of the tooth.

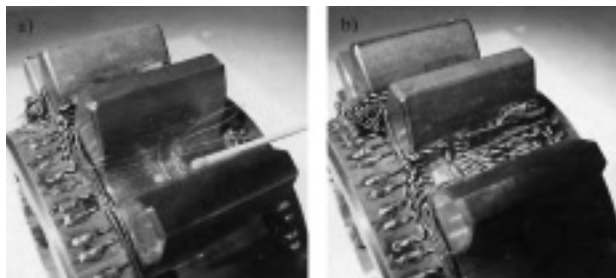


Fig. 3.2-7: Strain measurement with strain gage chains in the tooth root of a gearwheel, from 3-4.

- mounted strain gage with matchstick to give a comparison of size
- completed gage installation, ready for measurement

The left-hand picture illustrates a bonded strain gage chain and a matchstick to give a comparison of size; the right-hand picture shows the finished, wired measuring point.

The tangential stresses found on a test gearwheel are shown in the diagram in Fig. 3.2-8 (left: compression stresses, right: tensile stresses) under three different points of loading. The tests were carried out by the Research Establishment for Gearwheels and Transmission

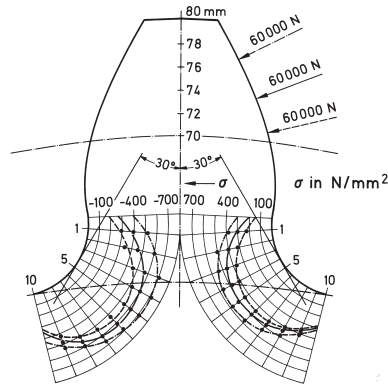


Fig. 3.2-8: Tangential stresses in the rounded section of the root of a gearwheel tooth.

Drives at the Technical University in Munich. With this example the position of maximum stress was not predictable; in addition a certain measure of dependence on the point of loading can be recognized. This type of measurement problem can only be resolved satisfactorily with strain gage chains.

3.2.2.2 Strain gage rosettes for the determination of stress conditions

The designation “rosette” is derived from the original shape of multiple strain gages which bore a number of star-shaped, crossed measuring grids on a common carrier; it is now used to describe all other multiple strain gages with crossing grid axes. The crossed arrangement of the measuring grids was originally necessary due to the large lengths of grid; they are also still occasionally used. Modern production techniques, particularly those involving foil etching techniques, give rosette shapes with measuring grids arranged close together, see Fig. 3.2-9. Both types have their advantages and disadvantages.

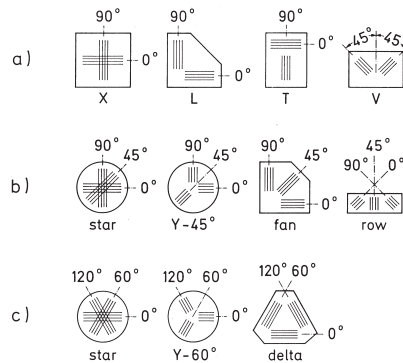


Fig. 3.2-9: Strain gage rosettes

- a) X rosettes with axes crossed at 90° . For applications involving biaxial stress conditions with known principal directions (see section 8.2.1)
 - b) R rosettes with axes crossed at $0^\circ/45^\circ/90^\circ$ (also called right-angled rosettes.)
 - c) R rosettes with axes crossed at $0^\circ/60^\circ/120^\circ$ (also called delta rosettes.)
- b) and c) are used in applications with biaxial stress conditions with unknown principal directions (see section 8.2.2.)

With star or cross-shaped rosettes the measuring grids are arranged over one another. This has the advantage that the strain components can be measured close together at the same position. However, there are disadvantages owing to the different distances of the measuring grids from the surface of the measurement object. This is particularly noticeable where bending stresses are present on thin objects or on curved surfaces. The high strain rigidity (spring rate) due to the thicker build-up of rosette shapes must be considered with a regard to strain reinforcement for thin objects and also for materials, mainly synthetics, having a low Young's modulus [3-52]. The build-up of heat resulting from unfavorable thermal dissipation in the upper and center measuring grids can be offset with reduced supply voltage. In this respect rosette shapes having the measuring grids situated close together on the same plane are better. However, the large amount of area required can lead to problems with small measurement objects or with steep stress gradients in the region of the rosette. Rosettes are therefore manufactured in various shapes and sizes.

The letter “X” is used as the coding symbol for rosettes with 2 measuring grids whose axes intersect at 90° (see Fig. 3.2-9a). The letter X is also used as the identification symbol for the crossed axes of the measuring grids even if they form a T, L or V shape.

In stress analysis X rosettes are used for the investigation of biaxial stress conditions with known principal directions. They are used to obtain positive and negative strains for cumulative calculation (see section 8.4) in the design of simple transducers and in related applications, e.g. machine monitoring.

The coding symbol for rosettes with three measuring grids is the letter “R”. There are two basic shapes which differ due to the angular interval between their measuring grids: $0^\circ/45^\circ/90^\circ$ and $0^\circ/60^\circ/120^\circ$ (see Figs. 3.2-9b and c). The angular values always refer to the *directions* of the measuring grids, irrespective of whether the grids are arranged as a star, Y, delta, fan or some other shape. R rosettes are used for the analysis of biaxial stress

conditions where the main directions are unknown, both qualitatively and quantitatively. Application examples and evaluation formulae for measurements with rosettes are given in section 8.2.

3.2.2.3 Strain gage rosettes for the investigation of residual stress

The method of measuring residual stress in structural parts is best explained using an example. A plate is to be examined for its residual stress condition, see Fig. 3.2-10. Uniaxial or biaxial normal stresses with unknown principal directions may be involved and bending stresses may also be superimposed.

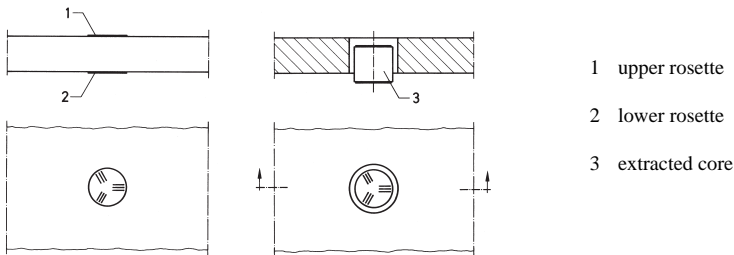


Fig. 3.2-10: Example illustrating the measurement method for the determination of residual stresses

- a) initial condition
- b) condition after a "core" has been removed.

A strain gage rosette is bonded to the point of interest and the direction of its measuring grid is set with reference to the measurement object. Then the measurements from the individual measuring grids are recorded in this initial state. If superimposed bending stresses are involved, another rosette is applied exactly opposite the first rosette on the other side using the same procedure. Then the section of material bearing the rosette is extracted using an annular milling tool or some other suitable method. The extracted core is now free of forces from the surrounding material which were previously acting on it. Consequently, it springs back to its natural, unstressed state.

Further measurements from the each of the measuring grids show the changed situation. The evaluation is made according to the formulae for rosette measurements given in section 8.2. The only point to note is that the *release* of stress is measured, i.e. the residual stress has the opposite sign.

It has been found that it is unnecessary to completely mill out a core from the object under investigation, particularly if compact structural parts are involved and where access from both sides, which is only available with plates, is not possible. It is sufficient to establish a relatively shallow, ring-shaped groove that adequately releases the stress on the core's surface, see Fig. 3.2-11.

With the "ring-core method", as this is known, the restrictions of the method regarding the part's thickness no longer apply. The depth of the ringed groove influences the degree of stress release obtained which must be considered when evaluating the results. The theoretical principles and the evaluation of the measurement results are described in [3-5].

A special ring-core rosette, which is optimally designed for this process, is illustrated in Fig. 3.2-12.

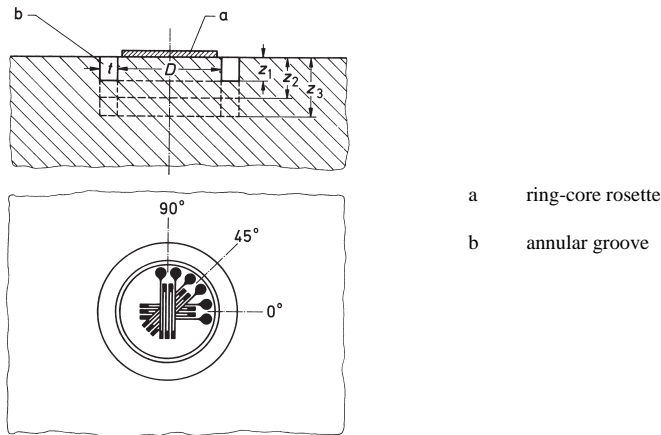


Fig. 3.2-11: The ring-core method of Böhm and Wolf.

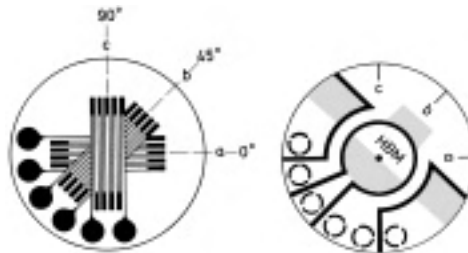


Fig. 3.2-12: Special strain gage rosette for the ring-core method devised by Böhm and Wolf
a) measuring grid arrangement
b) outward appearance

An older method for measuring residual stress is the “hole-drilling method”. A small hole is drilled which disturbs the existing stress condition. The force flow lines are modified and the drilled hole is deformed at its edges, see Fig. 3.2-13.

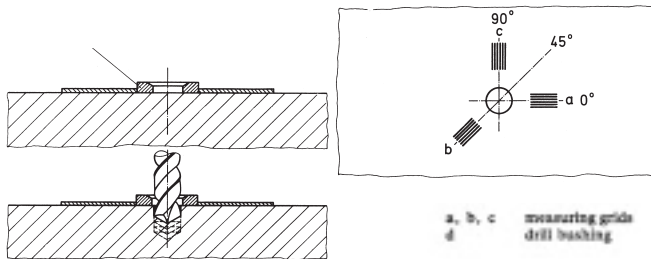


Fig. 3.2-13: The hole drilling method.

It is sufficient to drill a hole with a depth equal to its diameter. A special hole drilling rosette has three measuring grids arranged at $0^\circ/45^\circ/90^\circ$, so that stress analysis can be carried out, both quantitatively and qualitatively. A small drill bushing ensures that the drill hole is positioned centrally, which is an important requirement for accurate results. Fig. 3.2-14 illustrates a type of hole drilling rosette.

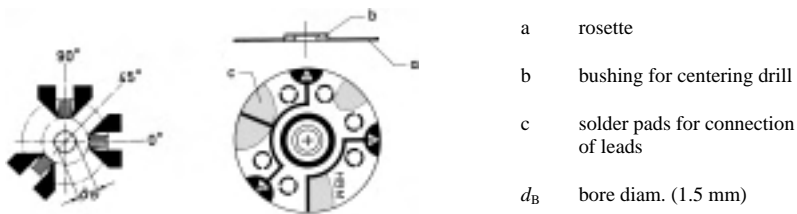


Fig. 3.2-14: Special strain gage rosette RY 61 for the hole drilling method
 a) arrangement of measuring grids
 b) complete rosette

The increase in stress at the edges of the drilled hole due to notch effects places restrictions on the method. Here the material can be deformed right into the yield region, although the residual stresses are still below this limit.

The principle of the method and the evaluation procedures are dealt with in [3-6, 3-7] and in section 8.3.

3.2.3 Special strain gages

Apart from various shapes of measuring grid, produced for specific applications, there are other special strain gages, which differ from standard strain gages, for example, in their method of attachment to the measurement object. Three examples are mentioned here. There are other special versions which cannot be discussed here and the reader is referred to the product information.

3.2.3.1 Weldable strain gages

These have a metal base, e.g. stainless steel, and attachment is by spot welding. Fig. 3.2-15 shows some examples. Because of the steel base, these strain gages have a very high strain rigidity. Therefore, they can only be used on thick-walled, strong objects, e.g. in steel construction.



Fig. 3.2-15: Examples of weldable strain gages
a) strain gage with steel base, connecting leads and protective cover
b) strain gage with steel base
c) metal encapsulated strain gage

3.2.3.2 Free-grid strain gages, high-temperature strain gages

Free-grid (strippable carrier) strain gages are mainly used in extremely high or low temperature ranges. The measuring grid is fixed to an auxiliary carrier, which is removed during bonding, see Fig. 3.2-16. Ceramic adhesive is used for bonding; with the platinum-tungsten alloy measuring grid, this enables non-zero referenced measurements to be carried out in the high temperature region up to 800°C.

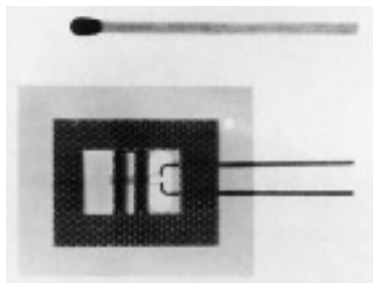


Fig. 3.2-16: High-temperature, strippable-carrier strain gage suitable for bonding with ceramic adhesives

3.2.3.3 Weldable high-temperature strain gages

In contrast to the previously mentioned strippable-carrier strain gages, whose application is very difficult, the Ailtech strain gage system using spot welding has distinct advantages. They are manufactured in quarter and half-bridge versions.

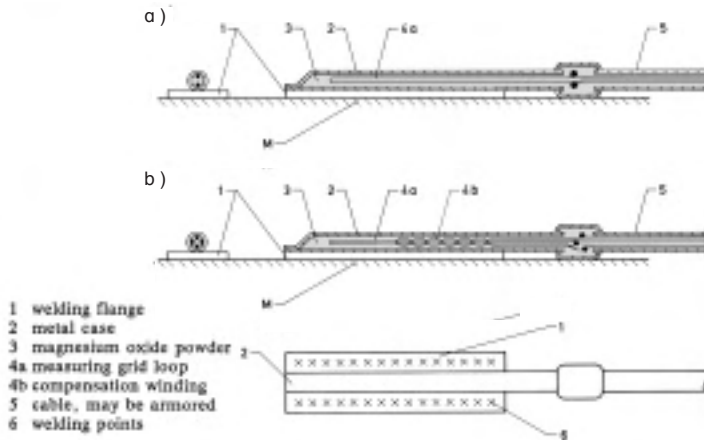


Fig. 3.2-17: Ailtech/Eaton weldable, encapsulated, high-temperature strain gage system
 a) quarter bridge version
 b) half-bridge version (measuring wire loop and passive wire winding for temperature compensation)

The metal wire is embedded in compacted MgO powder and enclosed in a metal protective tube (see fig. 3.2-17). Versions with metal sheathed cable are also available. The useful temperature range of strain gages with PtW measuring grids extends from about -200°C up to $+550^{\circ}\text{C}$ and up to about 700°C for non-zero referenced measurements. Further information can be obtained from [3-8 to 3-10, 3-14, 3-18, 3-19, 3-23, 3-50].

3.2.4 Electrical resistance

Strain gages are produced with various resistances. The values have an historical origin, but they have proven useful and so they have been retained. The value of 120Ω is the most popular. The widest selection of different types of strain gages are found in this resistance group. They are preferred for stress analysis, monitoring systems, etc. Among other resistance values, 350Ω strain gages are produced in large quantity and these are used to a large extent in transducers.

There is no clear answer to the question of which value is the best. Three points are important in the selection of the strain gage resistance value:

- matching to the instrumentation to which the strain gage is connected
- effects of the interconnecting wiring between the strain gage and the instrumentation
- the strain gage's permissible electrical loading.

Occasionally conflicting requirements occur and compromises must be made.

HBM measurement amplifiers have such a wide matching range that there are no problems with regard to the electrical resistance.

If a dc amplifier is connected to the strain gage, high resistance strain gages operated with a high supply voltage improve zero drift due to the amplifier. On the other hand, high resistance measurement circuits are more likely than those of low resistance to form antennas for receiving interference. With dc amplifiers this can easily lead to measurement errors if less than perfect shielding is used.

With long measurement cables there is an attenuation effect, which not only occurs with carrier frequency supplies, but also - and this is often overlooked - with high frequency dynamic measurement signals. This effect is less pronounced with low resistance cables than with those of high resistance (see section 7.4).

Electrical resistances in the connection paths, e.g. in the cables, terminals, slip-rings, etc., have less effect with high resistance strain gages. However, variations in the insulation resistance have a lesser effect with low resistance strain gages (see section 7.2). The 120Ω strain gage is in most cases the optimum choice.

3.2.5 Useful temperature range

The question of temperature limits in the application of strain gages is extremely difficult to answer. The reasons for this are the different influences of strain gage parameters at the relevant level, the duration of the temperature and also the tolerable measurement error. Therefore, in [2-1] the following appears under the heading "Resistance to temperature":

"This guideline's recommendation is that all significant strain gage parameters must be stated in relationship to the temperature. The user himself can then estimate the upper and lower permissible temperature limits."

With regard to the effects of temperature and the quality of a measurement, two factors must be considered:

- the temperature level
- the variation in temperature during the measurement.

At high temperature levels it is important to know how long the strain gage bonding can withstand the temperature and what possible effects may occur. Here, the temperature is not an independent variable. It is always related to time, perhaps the rise time or the dwell time of the temperature; it is accompanied by external influences, such as atmospheric conditions that may have a physical effect, e.g. pressure, or a chemical effect, e.g. oxidation. Conversion processes in the measuring grid's alloys, which may occur at increased temperatures, are also included here.

When considering the upper temperature limit for reliable operation of a particular strain gage bond, the boundary conditions must also be included and here there are problems. Only answers of a general nature can be given which refer to common applications. Usually temperature effects do not give rise to sudden changes from which realistic limits

could be derived; there is a gradual transition from good to still useable to unusable measurements. The classification of the measurements depends on the desired accuracy.

It can be generally stated that low temperatures present fewer problems than high temperatures. Whether the measurements are required as “zero referenced” or “non-zero referenced” is also an important point (see section 2.4); in the former case the upper temperature limits should be set substantially lower than in the latter case, also taking into account the time factor. In addition it should be noted that it is not only the strain gage data itself that is relevant to a measurement, but that the data on the bonding agent, the protective covering, the cabling, etc. is also important. The following temperature figures give an idea of the range of application for metal strain gages:

The range for non-zero referenced measurements extends from -269°C to over 800°C . For zero referenced, short-term measurements the upper limit is around 500°C if all the options for error compensation and correction are exploited. For strain gages with a constantan measuring grid the range is restricted to about -200°C to $+200^{\circ}\text{C}$, for “transducer quality” from -20°C to $+70^{\circ}\text{C}$ and for the highest accuracy requirements, e.g. load cells, down to -10°C to $+40^{\circ}\text{C}$ with a time restriction of 20 minutes.

The wealth of literature, in particular relating to high temperatures, is an indication of the special problems that exist; it is also apparent that development in this sector is still in progress [3-8 to 3-23].

Temperature variations mainly affect the zero point, i.e. the measurement's reference point. Errors can be maintained within reasonable bounds by the selection of self-compensating strain gages (see section 3.3.4) and/or the use of suitable compensation methods, see section 7.1.

Measurements in the temperature range above 200°C to 300°C give problems both with regard to zero-point stability and the service life [3-23]. Capacitive strain gages (see section 1.0.4) appear to fill a gap here [1-11 to 1-15].

3.3 Technical data

The characteristics and parameters described in this section are significant for strain gage measurements and they also give useful information for the selection of strain gages with regard to special requirements. The figures have been determined using the guidelines given in [2-1]. It should also be noted that most of the strain gage parameters can only be determined using gages that are already bonded. Hence the characteristics of the adhesive used can also influence the parameters, e.g. an adhesive can restrict a strain gage's thermal application range.

It must also be clearly stated that limits can only be given within certain margins of measurement. Sharply defined limits hardly ever occur and time, temperature and other influencing parameters can displace acceptable limits. Therefore in [2-1] graphical representation is used instead of a single parameter value and this shows the variation of the parameters under the influence of important variables.

3.3.1 Strain gage sensitivity (gage factor) for metal strain gages

The physical relationship between strain and the change of resistance in a metal conductor was discussed in section 1.1.1. It was also pointed out that some metals exhibit a linear relationship between the relative change of resistance and the strain. If these metals, which are various types of alloys, also exhibit a low or negligible temperature coefficient of electrical resistance, then they may be selected for the manufacture of strain gages. Other alloys are used if there are special requirements relating to temperature stability or to the resistance against fatigue during dynamic loading.

A strain gage's sensitivity is expressed by the ratio of the relative change of resistance to the strain and it is represented by the symbol k :

$$k = \frac{\Delta R/R_0}{\Delta l/l_0} = \frac{\Delta R/R_0}{\epsilon} \quad (3.3-1)$$

The relevant dimensional units are

$$(k) = \left\{ \frac{\Delta R/R_0}{\Delta l/l_0} \right\} \text{ in } \left[\frac{\Omega/\Omega}{\text{m/m}} \right].$$

The units are only significant in dimensional calculations; in practice they are canceled so that the gage factor k appears as an dimensionless quantity.

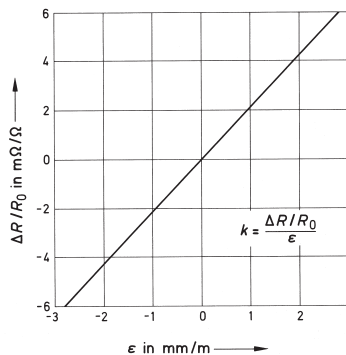


Fig. 3.3-1: Characteristic for a metal strain gage and the definition of the gage factor

In the resistance vs. strain diagram the slope of the strain gage characteristic represents the k factor, see Fig. 3.3-1.

In contrast to the parameter S of the stretched conductor, which is defined in section 1.1.1 (see equation 1.1-2), the k factor is a parameter, a proportionality factor, for the complete strain gage. Influences of the configuration of the measuring grid and the strain transfer conditions into the measuring grid cause a difference between S and k , although this is usually slight. For this reason the gage factor k is determined by the manufacturer using as

test sample for each production lot according to the rules in [2-1]. The statistical methods of quality assurance are followed and the figure is noted on the data sheet enclosed in the strain gage package.

It is not possible to adjust the gage factor during manufacture in order to achieve a specific value. Average gage factor values are shown in Table 3.3-1 for normal measuring grid alloys.

Measuring grid material (trade name)	Guide values for composition [%]	Average approx. gage factor, k
Constantan	57 Cu, 43 Ni	2.05
Karma	73 Ni, 20 Cr, res. Fe + Al	2.1
Nichrome V	80 Ni, 20 Cr	2.2
Platinum-tungsten	92 Pt, 8 W	4.0

Table 3.3-1: Average gage factors for strain gages with various measuring grid alloys.

The fact that metal strain gages have a linear characteristic needs qualification. For strain gages with a constantan measuring grid a non-linear characteristic was found in the region of large strains up to $150,000 \mu\text{m} = 15 \text{ cm/m}$. The relationship is parabolic and can be approximated quite well with a polynomial of the form $\epsilon^* = \epsilon + \epsilon^2$. It can be assumed that other measuring grid alloys have similar behavior. For further information, see section 3.3.6.

If the strain gage is operated in the region of high strain, as is usual in quarter bridge circuits, compensation for the strain gage's non-linearity is provided automatically (see section 5.2 and [3-29]).

3.3.2 Gage factor for semiconductor strain gages

In section 1.1.2 it was stated that with semiconductor strain gages the characteristic is parabolic. Fig. 3.3-2 shows the characteristics for semiconductor strain gages in p and n type silicon.

The characteristics are dependent on temperature, as may be seen from equation (1.1-3).

The temperature dependence can be restricted by heavy doping of the silicon; however, this also reduces the sensitivity. A satisfactory compromise must be found.

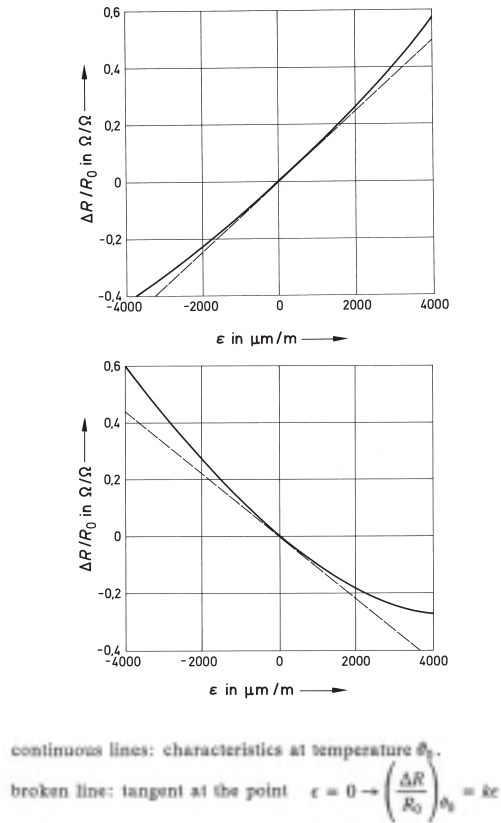


Fig. 3.3-2: Characteristics of semiconductor strain gages for
 a) p silicon 0.020 Ωcm

$$\left(\frac{\Delta R}{R_0}\right)_{\theta_0} = k\epsilon + c\epsilon^2 = 119.5 \cdot \epsilon + 4000 \cdot \epsilon^2,$$

b) n silicon 0.031 Ωcm

$$\left(\frac{\Delta R}{R_0}\right)_{\theta_0} = k\epsilon + c\epsilon^2 = 110 \cdot \epsilon + 10000 \cdot \epsilon^2.$$

It is not possible to describe the characteristic curve by a parameter similar to the gage factor for metal strain gages. This is only possible for the tangential slope as in Fig. 3.3-2 at the reference temperature θ_0 . For normally available p-conducting semiconductor strain gages approximate gage factors have values between +110 and +130 and for n-conducting semiconductor strain gages between -80 and -100.

Provided the strains to be measured do not exceed $\pm 1000 \mu\text{m/m}$ and a measurement error of $\pm 5\%$ is acceptable, measurements can be carried out in a simplified manner by taking a constant gage factor.

If more accurate results are required, the measurement must be corrected. Many manufacturers enclose individually compiled correction tables with their semiconductor strain gages and this makes the evaluation of the results much easier for the user.

It is not the intention in this book to describe in more detail semiconductor strain gage characteristics which arise due to temperature changes and due to deviations at the measurement temperature υ with respect to the reference temperature υ_0 . There are comprehensive details in [3-24].

3.3.3 Transverse sensitivity

Strain gages should really only give a change of resistance to a strain in their “active” direction and this should be in the ratio designated by the gage factor. The “active” direction is set by the direction of the wires or conducting parts of the measuring grid, see Fig. 3.3-3.

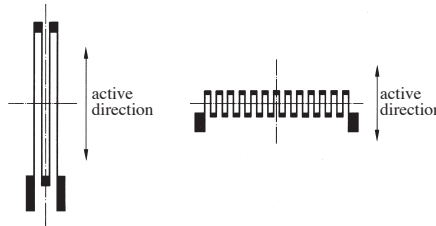


Fig. 3.3-3: A strain gage's “active” direction.

Note

With resistive strain gages, the terms “active direction” or “active strain gage” always mean the “direction of measurement” or “measuring strain gage” (in contrast to compensating strain gages). They are generally used with this meaning and should not be confused with the physical term “active transducer”. In the physical sense an active strain gage is mentioned in section 1.0.5 “Piezoelectric strain gages”.

Sometimes a change of resistance, which is usually slight, is observed when the strain gage is subject to strains transverse to the “active” direction. The strain gage is then said to have “transverse sensitivity”.

The definition of transverse sensitivity is based on the following assumptions:

- a) If a strain gage is loaded in its “active” direction with a *unidirectional* strain, see Fig.3.3-4a, then it exhibits a gage factor k_1 , which is described with the expression:

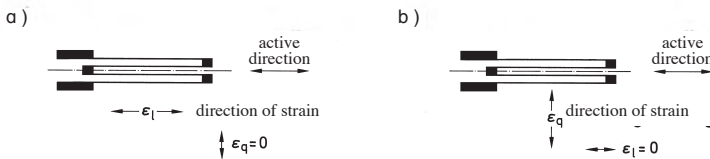
$$k_1 = \frac{\Delta R/R_0}{\epsilon_1} \quad (3.3-2)$$

- b) If the strain gage is loaded with a unidirectional strain transverse to its “active” direction, see Fig. 3.3-4b, then similarly a gage factor k_1 is found, which is usually slight and can be described by:

$$k_t = \frac{\Delta R/R_0}{\epsilon_t} \quad (3.3-3)$$

The transverse sensitivity q is defined as the ratio of the gage factor k_t , transverse to the direction of measurement and the gage factor k_l , in the measurement direction:

$$q = \frac{k_t}{k_l} \quad (3.3-4)$$



ϵ_l strain in the strain gage's longitudinal direction

ϵ_t strain in the strain gage's transverse direction

Fig. 3.3-4: Definition of transverse sensitivity

- "active" strain gage direction and direction of strain are the same
- "active" strain gage direction and direction of strain are 90° to one another.

The cause of lateral sensitivity in strain gages was earlier thought to be due to the parts of the measurement grid that are located transverse to the active direction. This was substantially true for the original strain gage designs which used wire grids with large intervening distances, see Fig. 3.3-5a. Improvements in design therefore concentrated on this point and with refined winding methods intervening wire distances down to 0.1 mm could be produced, see Fig. 3.3-5b.



Fig. 3.3-5: Various shapes of strain gage measurement grid and methods of reducing the transverse sensitivity.

- original shape
- tighter winding
- thicker transverse links
- wide transverse connections

In another idea an attempt was made to counter the transverse sensitivity by connecting the individual longitudinal sections of the measuring grid with thick transverse links, see Fig.

3.3-5c. This method, which was difficult to use in production, gave a significant reduction in the transverse sensitivity, although it did not eliminate it entirely.

With modern foil strain gages, see Fig. 3.3-5d, the latter principle of the cross-link grid is used, in that transverse connections are made at the ends of the longitudinal grid sections. This is however much easier to achieve with foil strain gages than with wire strain gages.

An experimental investigation into foil strain gages gave the following results:

In the region of the widened transverse connections a slight positive change of resistance is obtained for positive strains, see Fig. 3.3-6b and c. This process is restricted to a small area at the end of the measuring grid. It therefore has a more pronounced effect with short measuring grids than with long ones, because the proportion of the measuring grid that is distorted is greater. This is confirmed with measurements whose results are illustrated in Fig. 3.3-7.

A second, superimposed effect arises due to the forces which act sideways along the longitudinal sections of the measurement grid and pull it in the transverse direction, see Fig. 3.3-6d. The effect which the forces have on the conductor depends on its dimensions and on the forces that are transferred. A conductor completely embedded in the measuring

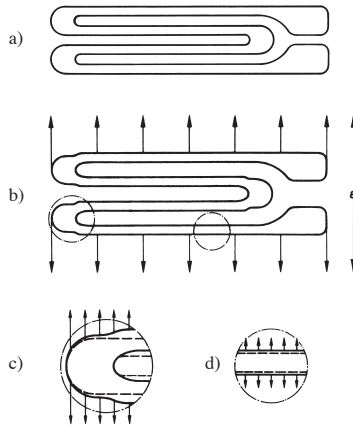


Fig. 3.3-6: The causes of transverse sensitivity in strain gages
 a) initial condition
 b) under transverse strain
 c) deformation in the region of the transverse connections
 d) deformation in the other regions of the measuring grid

grid carrier will be loaded more than one which is bonded on top. On foil strain gages with constantan or Karma measuring grids this effect causes a slight negative change of resistance for positive strains. This explains a negative transverse strain gage sensitivity that is occasionally observed.

When designing a strain gage the geometry of the measuring grid is selected where possible such that a low figure is obtained for transverse sensitivity. However, since other considerations must be taken into account during the design this cannot always be achieved.

Whereas the gage factor k_1 is measured in the unidirectional *strain field*, the measurement of the gage factor k is made in the unidirectional *stress field*, see section 3.3.1. Hence there is a difference between k_1 and k which depends on the strain gage's transverse sensitivity.

This is not a disadvantage in transducer applications, since transducers are always calibrated in the finished state. This is also true for all other applications, where the relationship between the measurement signal and the measured variable is determined by calibration.

Corrections are required for stress analysis in the bidirectional stress field, see section 7.5, but these can be waived for small transverse sensitivities of $q \leq 0.01$ [7-3].

The diagram in Fig. 3.3-7 shows the results of an investigation carried out on different series of strain gages according to the method specified in [2-1].

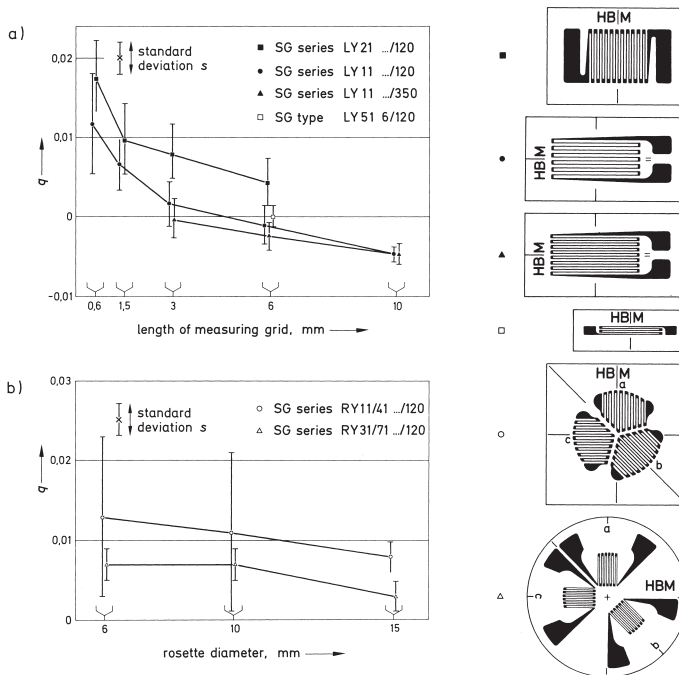


Fig. 3.3-7: Transverse sensitivity q in relationship to the length of measuring grid for some types of strain gage and rosette

- a) linear strain gages
 b) strain gage rosettes

3.3.4 Temperature response of a mounted strain gage

This heading refers to the change in the measurement signal due to temperature under conditions where the mechanical loading of the measurement object is zero or constant. A response to temperature can occur if during the observation period, i.e. between zeroing or

recording of the reference value and the taking of the measurement itself, the measurement object's temperature or that of its environment changes. The response to temperature is reversible and the temperature effects disappear when the original temperature conditions at the measuring point return. In the literature the response to temperature is often called “apparent strain”, which is a term giving no indication as to its cause.

There are many factors affecting the temperature response ϵ_θ :

- the component material's thermal expansion, α_C ,
- the thermal expansion of the material of the strain gage's measuring grid, α_M ,
- the temperature coefficient of the grid material's electrical resistance, α_R
- the temperature change $\Delta\vartheta$ as the variable causing the effects.

In addition the temperature response of the electrical resistance of the wiring, which is connected in series with the strain gage, can also contribute to the overall temperature response. This is discussed further in section 7.1.

The temperature response should not be confused with thermal drift, which is a non-reversible process, but which is also superimposed on the temperature response, see section 3.3.4.2.

An approximate calculation of a strain gage's temperature response can be made using the equation

$$\epsilon_\theta = \left(\frac{\alpha_R}{k} + \alpha_C - \alpha_M \right) \Delta\vartheta \tag{3.3-5}$$

The figure obtained can only be used as a guideline value for a limited temperature range, because the parameters α_R , α_C , α_M and k are temperature dependent. Therefore

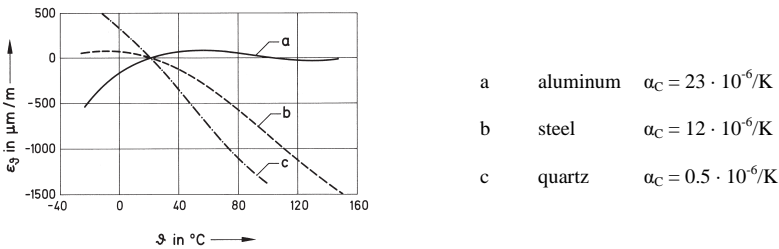


Fig. 3.3-8: Examples of temperature responses of strain gage measuring points for the mounting of the same types of strain gage on different component materials.

representation of the temperature response is more correct in diagrammatic form. If strain gages with identical parameters are bonded to component materials having different values for α_C , then different curves of ϵ_θ are obtained. Examples are shown in Fig. 3.3-8.

Sufficient rigidity in the measurement object is assumed for the validity of the diagram, so that the forces originating from the strain gage and the adhesive have no effect. This assumption is always valid for metal objects apart from extremely thin components.

A measurement, during which the measurement object experiences both a temperature change and mechanical loading, gives as a result the sum of the mechanical strain and the thermal strain. The thermal portion of the indicated strain is therefore an error. This unsatisfactory result can be remedied by the use of self-temperature compensating strain gages, see section 3.3.4.1 or compensation techniques, see section 7.1, [3-25, 3-26].

3.3.4.1 Temperature compensated strain gages

Through the adoption of certain production methods, it is possible to influence the strain gage such that its temperature response within a limited temperature range is minimized. Here, the advantage is taken of being able to change the temperature coefficient of electrical resistance of the measuring grid's material. This can be achieved by adding corrective alloying ingredients to the constantan which is the main alloy used and also by heat treatment. Fig. 3.3-9 shows the positive and negative values that can be obtained.

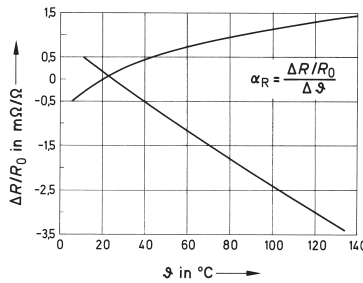


Fig. 3.3-9: Temperature coefficients α_R , for various constantan compositions.

α_R must be adjusted such that

$$\alpha_R = (\alpha_M - \alpha_C)k \tag{3.3-6}$$

Complete compensation is not possible in this equation due to the non-linear terms which have been ignored. It can be seen from Fig. 3.3-10 how effective this is, if the ordinate scale is compared with the extended ordinate scale in Fig. 3.3-8.

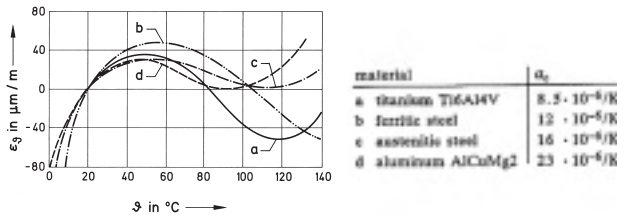


Fig. 3.3-10: Residual temperature responses of temperature compensated strain gages with optimum matching to the thermal expansion coefficients of various component materials in the temperature range 10 to 130° C.

Strain gages of this type are termed “strain gages with matched temperature coefficient” or “self-temperature compensated strain gages”. Temperature response curves, as shown in Fig. 3.3-10 are included on a data sheet enclosed with the strain gages. They are only applicable for component materials having the same thermal expansion characteristic as the material sample on which the curve is measured. This cannot be assumed in every case, as shown in Fig. 3.3-11. The diagram shows differential thermal expansion coefficients for various materials; this is the value for the slope of the expansion curve at each point. It can be seen that even the treatment of a material, e.g. whether it is rolled or annealed, causes a change. The curve for rolled X5CrNi18 9 exhibits an anomaly which can be explained by the effect of residual stresses in the test specimen. Occasionally anisotropic conditions are also observed.

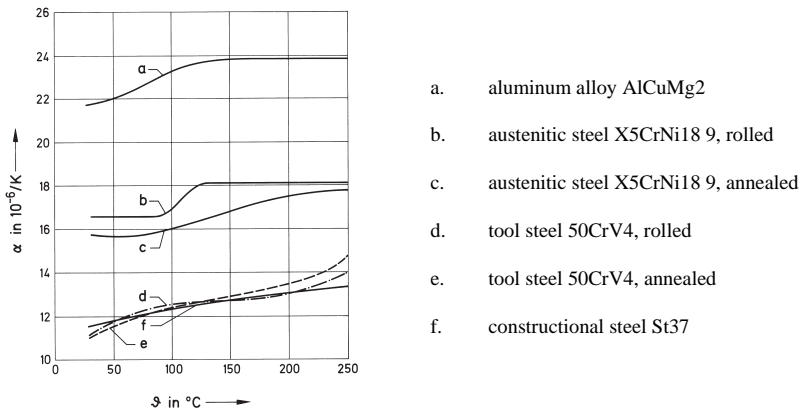
A temperature compensated strain gage cannot of course compensate for such anomalies. The deviations in the component material's temperature characteristic from the temperature curves enclosed with the strain gage should not be attributed to the strain gage. Compensation of this remaining error is possible using the methods described in section 7.1. A citation from [3-27] is relevant here:

“It is imperative to note that the thermal expansion coefficient for a material depends on:

1. its composition
2. heat treatment
3. past history of cold work
4. temperature level
5. past history of temperature excursions
6. time at temperature (at elevated temperature)

Thus it is quite possible for a material to exhibit three completely different thermal expansions coefficients as a result of three different heat treatments even though these heat treatments result in comparable strength characteristics! Furthermore, the thermal expansion coefficients can vary differentially with temperature in all three cases,

It is almost always possible to tailor a strain gage to “fit” the thermal expansion coefficient of any particular structural material over any given temperature range, provided the thermal expansion characteristics of this material remain repeatable from test run to test run, from temperature cycle to temperature cycle. Most strain gages are far more repeatable and stable in this respect than the materials on which strain measurements are to be made.”



- a. aluminum alloy AlCuMg2
- b. austenitic steel X5CrNi18 9, rolled
- c. austenitic steel X5CrNi18 9, annealed
- d. tool steel 50CrV4, rolled
- e. tool steel 50CrV4, annealed
- f. constructional steel St37

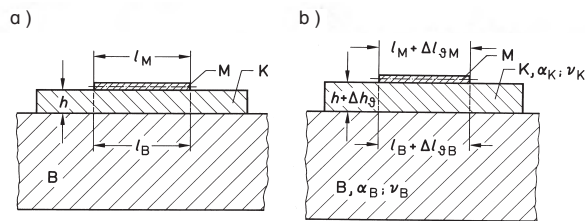
Fig. 3.3-11: The temperature dependence of various linear thermal expansion coefficients.

Matching of temperature compensated strain gages to the component material's thermal expansion is optimum for flat mounting surfaces; deviations occur with curved surfaces of small radius.

The following requirements must be fulfilled for the correct mounting of strain gages:

On flat application surfaces the strain gage closely follows the component's thermal expansion, i.e. the component's strain and that of the strain gage are identical; equation (3.3-5) describes this case and Fig. 3.3-12, exaggerated for clarity, illustrates the conditions.

For the sake of simplicity the measuring grid and the adhesive are taken to be one material.



- C component
- M measuring grid
- A intervening layer made up of adhesive and measuring grid carrier
- H thickness of the layer A

Fig. 3.3-12: Influence of a temperature change on the bonding of a strain gage mounted to a flat surface.

- a) initial condition at temperature ϑ_0
- b) condition at temperature $\vartheta_0 + \Delta\vartheta$

As a result of the change in temperature $\Delta\vartheta$, the component's original length l_C alters by the amount Δl_{0C} . The strain gage is compelled to follow this change in length. The length of the measuring grid l_M , which was equal to the component section l_C under consideration, has altered by the amount Δl_{0M} . Thus:

$$\text{if } l_C = l_M, \quad \Delta l_{0C} = \Delta l_{0M}.$$

Consequently the strains are also the same:

$$\frac{\Delta l_{0C}}{l_C} = \epsilon_{0C}; \quad \frac{\Delta l_{0M}}{l_M} = \epsilon_{0M}; \quad \epsilon_{0C} = \epsilon_{0M}.$$

The increase in the thickness of the layer h by Δh_ϑ has no influence on the strain conditions, because a correctly mounted strain gage closely follows the longitudinal strain on a flat surface.

Now the relationships on a curved surface will be examined. A section of a roller is considered as an example, see Fig. 3.3-13. The thermal expansion in the axial direction along a

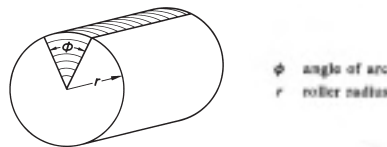


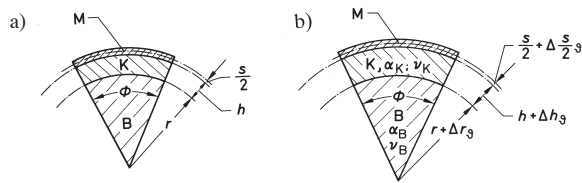
Fig. 3.3-13: Section of roller

surface layer is the same as with a flat section, i.e. $\epsilon_{0C} = a_C \cdot \Delta\vartheta$. In the circumferential direction the thermal expansion is

$$\epsilon_{0C} = \frac{r\phi a_C \Delta\vartheta}{r\phi} = a_C \Delta\vartheta.$$

As expected the thermal expansion is the same as for a flat surface.

The section of the roller under consideration is shown in cross-section in Fig. 3.3-14 including the bonding layers; the thicknesses are again markedly exaggerated for clarity.



s thickness of the measuring grid
 A, C, M, h , see Fig. 3.3-12

Fig. 3.3-14 Section of a roller with a strain gage bonded to the surface layer.

- a) initial condition at temperature \mathcal{T}_0
 b) condition at temperature $\mathcal{T}_0 + \Delta\mathcal{T}$

The layers A and M have the same significance as for the flat, layered plate (see Fig. 3.3-12). On heating, the sections r , h and s do not expand with the same relationship as the component material owing to different thermal expansion coefficients. Also in the A and M layers there is an additional superimposed change in thickness due to the Poisson contraction. Consequently, the measuring grid's thermal expansion ϵ_{0M} on the curved surface is different from that on the flat surface.

The thermal expansion of the measuring grid in the region of its neutral plane i.e. on the line $s/2$, is described by the expression

$$\epsilon_{0M} = \frac{[ra_C + h [a_A 2\nu_A (\alpha_A - \alpha_C)]] + s/2 [a_M + 2\nu_M (\alpha_M - \alpha_C)]}{r + h + s/2} \Delta\theta. \quad (3.3-8)$$

Whereas the strains $\epsilon_{\theta C}$ and $\epsilon_{\theta M}$ were equal for the flat plate, here there is a difference. Therefore the temperature responses of the measuring points are different.

Two examples have been calculated to give some idea of the extent of the variation in temperature response.

Example 1:

r	=	shaft radius: 5 mm
h	=	thickness of adhesive plus measuring grid carrier: 100 μm
s	=	thickness of the measuring grid: 5 μm
α_c	=	thermal expansion coefficient for component material: $12 \cdot 10^{-6}/\text{K}$
α_A	=	thermal expansion coefficient for the adhesive: $70 \cdot 10^{-6}/\text{K}$
α_M	=	thermal expansion coefficient for the measuring grid material: $15 \cdot 10^{-6}/\text{K}$
ν_A	=	Poisson's ratio for the adhesive and measuring grid carrier: 0.4
ν_M	=	Poisson's ratio for the measuring grid material: 0.3

Result: $\varepsilon_{gM} = 14.05 \cdot 10^{-6}/\text{K}$

compared with $\varepsilon_{gC} = 12.00 \cdot 10^{-6}/\text{K}$

Difference $\varepsilon^*(g) = + 2.05 \cdot 10^{-6}/\text{K}$

Example 2:

For a radius $r = 10$ mm (all other data is the same) $\varepsilon_{gM} = 13.04 \cdot 10^{-6}/\text{K}$

The difference $\varepsilon^*(g)$ is only $+ 1.04 \cdot 10^{-6}/\text{K}$.

Conclusions:

- The temperature response of a strain gage measuring point is dependent on the contours of the bonding surface. Applications in which the strain gage measuring grid is curved in its active direction, i.e. where it tangentially follows the curve, have temperature responses which are different to those in which the measuring grid's active direction is straight.
- The difference between the two conditions decreases with increasing radius of curvature.
- The curvature's influence becomes less if the component material's thermal expansion coefficient is similar to those of the measuring grid carrier and of the adhesive.
- The sign of the change in temperature response for a concave surface is opposite that for a convex surface.
- For metal component materials the change in temperature response increases with increasing adhesive thickness.
- Temperature compensated strain gages are designed for mounting on flat surfaces. The effective compensation as described is reduced on curved surfaces.
- The Wheatstone bridge's temperature compensating effect is also reduced if the "active" strain gage and the "compensating" strain gage are applied to surfaces having different contours.

Measurement errors can therefore only arise if the test object's temperature changes during the measurement.

The errors due to temperature response, which are outlined above, may be insignificant in experimental stress analysis, but not for transducer construction where high measurement accuracy is required. If the cause of the error is known, a remedy can be found. In practice two main methods are applied:

- The cylindrical surface is provided with small flat sections in the region of the strain gage installation to correct erroneous effects. This is a method which is easily adopted in transducer construction.
- The adhesive layer should be made as thin as possible.

3.3.4.2 Thermal drift

Thermal drift is mainly caused by microstructural changes and oxidation or corrosion of the measuring grid or it may also be due to stress relief processes in the strain gage or adhesive as a result of thermal influences. It is dependent on temperature and time. Thermal drift causes non-reversible zero point changes in the applied strain gage.

A significant contribution to drift is made by the alloying ingredients and the state of mechanical and thermal treatment of the measuring grid material. Hence, drawn or cold-rolled grid materials exhibit a more pronounced drift which is apparent at relatively low temperatures, e.g. 100°C, whereas soft tempered alloys have less drift. As with the temperature response, the “mechanical history” of the gage also has an effect. Therefore, a soft tempered material can be cold worked by strains into the plastic deformation region or by dynamic loading, leading to changes in its characteristics.

Plastic deformation can under some circumstances arise as a result of different thermal expansion in the measuring grid and the component. Similarly improper handling of the strain gage during application may also add to drift.

Adhesives also contribute to drift. Hence, similar types of strain gage may exhibit different drift properties, depending if they are bonded, for example, with cold or hot curing adhesive.

At high temperature ranges metallurgical effects have a substantial influence on the drift characteristics of strain gages. Comprehensive details in this respect are given in [3-23].

Thermal drift only produces errors in zero referenced measurements. The error can be eliminated by the compensating effects of the Wheatstone bridge circuit using half-bridge or full-bridge circuits and also with quarter and double quarter bridges if compensating gages are used. The same requirements must be satisfied as for temperature response compensation, see section 7.1. The effectiveness of the compensation is however less than with the temperature response owing to large variations from sample to sample.

3.3.5 The dependence of sensitivity on temperature

A strain gage's sensitivity is expressed by the gage factor, see section 3.3.1. The gage factor value enclosed in the strain gage packing applies at room temperature. It changes at other temperatures and varies depending on the material used for the measuring grid. Fig. 3.3-15 shows relative gage factor changes in relationship to temperature for four normal measuring grid alloys.

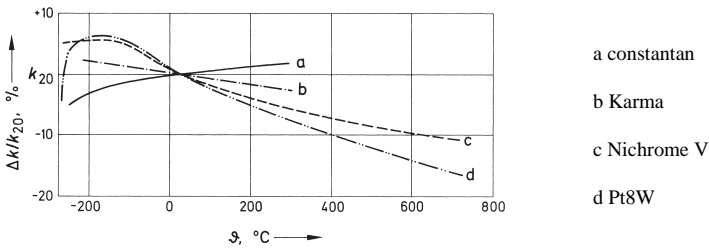


Fig. 3.3-15: The dependence of the gage factor on temperature for four normal measuring grid alloys

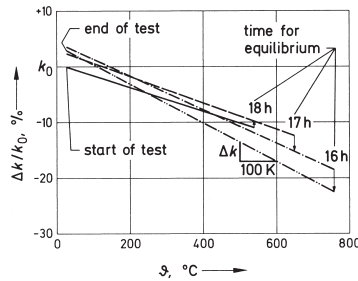


Fig. 3.3-16: The dependence of the gage factor on the temperature and the dwell period for platinum-tungsten strain gages.

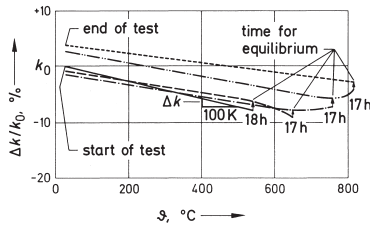


Fig. 3.3-17: The dependence of the gage factor on the temperature and the dwell period for Nichrome V strain gages.

Details on the gage factor's temperature dependence can be found on the data sheet enclosed in the strain gage packing. For the high temperature platinum-tungsten and Nichrome V alloys an additional change in the gage factor occurs in dependence of the temperature level and its dwell period; this can be seen in Figs. 3.3-16 and 3.3-17.

3.3.6 Static elongation

The use of strain gages is generally restricted to strains in the range of $\leq \pm 3000 \mu\text{m/m}$. However, for measurements on synthetics or for investigations in the plastic deformation region of metals, this range may be far exceeded. The question remains of the extent to which strain gages can be used for measuring large strains.

In this respect it is perhaps relevant to consider here the behavior of strain gages with large strains, see also [3-28, 3-29].

A strain gage's maximum elongation depends on its construction and on its material. There are ranges of strain gages that can only be used up to a maximum strain of $\pm 2 \text{ cm/m}$, while other ranges of gages may be loaded up to 20 cm/m ($1 \text{ cm/m} = 10,000 \mu\text{m/m}$). Further details can be taken from the product literature. Recommendations are given in [2-1] for strain gages with a length of measuring grid of 6 mm . Experience has shown that long strain gages withstand large strains better than short ones.

The measuring grid material work hardens due to the enormous plastic deformation and it loses its original ductile properties. Therefore, repetitive measurements are not possible, or only possible in a limited manner, unless the maximum extensibility of the strain gage has not been exceeded. There are no known investigations on the repeatability of large strains by only using part of the strain gage's possible elongation. They would be difficult to carry out with the device in [2-1], because no reliable statement could be made regarding the reproducibility of the surface strain in the plastically deformed test beam.

The use of high-strain strain gages on rubber or similar materials is not practical, not only because of the once-only extensibility, but also because of the restriction of extension with soft materials. Other strain measuring devices with a smaller restraining force are more practical. Apart from commercially available strain transducers which are suitable for this purpose, auxiliary equipment is described in [3-30] for the measurement of strain in rubber using strain gages.

With large strains the strain gage and the Wheatstone bridge circuit (see section 5.2) exhibit non-linearities which cannot be regarded as negligible. Whereas the Wheatstone bridge's non-linearity problems are adequately covered in the literature, there is no information on the linearity characteristics of strain gages in the high strain region. Sometimes the linearity error in the quarter bridge circuit, which is the circuit used almost exclusively in the high strain region, is taken as being the only error. An investigation carried out to the rules in [2-1] in the strain region of $\pm 15 \text{ cm/m} = \pm 150,000 \mu\text{m/m}$ led to the fact that the characteristic for metal strain gages with a constant measuring grid is curved, see Fig. 3.3-18. In the diagram the actual strain ϵ is recorded on the abscissa and the strain value ϵ^* , calculated from the relative change in resistance in equation (3.3-9), is recorded on the ordinate.

$$\epsilon^* = \frac{\Delta R/R_0}{k} \quad (3.3-9)$$

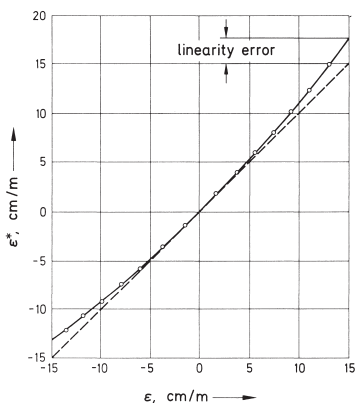


Fig. 3.3-18: Values of ϵ^* as a function of the actual strain ϵ for a strain gage in the high strain region (strain gage characteristic) .

The ordinate distance between the characteristic and the broken tangential line with slope $\epsilon^* = \epsilon$ indicates the strain gage's linearity deviation.

The results presented here strictly apply only to the type of strain gage investigated on account of possible edge effects. However, it can be assumed that strain gages having measuring grids of different shape or alloy composition behave in a similar manner, provided they are suitable for high strain measurements.

It should be noted at this point that the linear deviations of strain gages and the quarter bridge circuit largely compensate one another, see section 5.2 and [3-29].

The microstructural changes in the measuring grid material which accompany the strain gage's plastic deformation alter the grid's temperature coefficient of electrical resistance. Therefore high-elongation strain gages cannot be produced as temperature compensated types. Other temperature compensated strain gages forfeit this parameter if they are subject to strong plastic deformations. With a constant measuring grid material the change is in the direction of a positive temperature response.

The maximum elongation for a strain gage can therefore only be achieved with proper bonding. This assumes adequate elongation and bonding strength for the adhesive as well as correct application. The special demands placed on the bonding agent are dealt with in section 4.1.

3.3.7 Dynamic strain measurement

Strain gages are excellent for the measurement of dynamic strain processes. On account of their very low mass there is no noticeable influence on the vibration characteristics of the test object. Various points must be observed with regard to the strain gage:

- the strain gage's continuous vibration and fatigue characteristics,
- the upper frequency that can be reliably measured with strain gages.

Here bonding agents have only a slight influence. One aspect not to be overlooked is that under some circumstances with spot welding the test object's vibration characteristics may be modified. In contrast, with adhesive joints at the highest frequencies a lowering of the upper limit is observed with increasing temperature. The cause is related to the reduction in the adhesive's modulus of elasticity together with that of the strain gage carrier material, giving detrimental effects on the transfer rate. On the other hand the measurable frequency limit for strain gages is so high that it can only be acquired and investigated using special test apparatus [3-31, 3-32]. Under normal test conditions, including shock loading, the vibration frequencies to be measured are significantly lower than this limit.

3.3.7.1 Continuous vibration characteristics

If a strain gage is continuously dynamically loaded, then non-uniformities in the indication of strain can occur depending on the amplitude and the variation of the load. These are mainly due to problems with the measuring grid and the connections. The fatigue strength of the measuring grid's carrier material and of the adhesive is generally so large that they are not susceptible to damage.

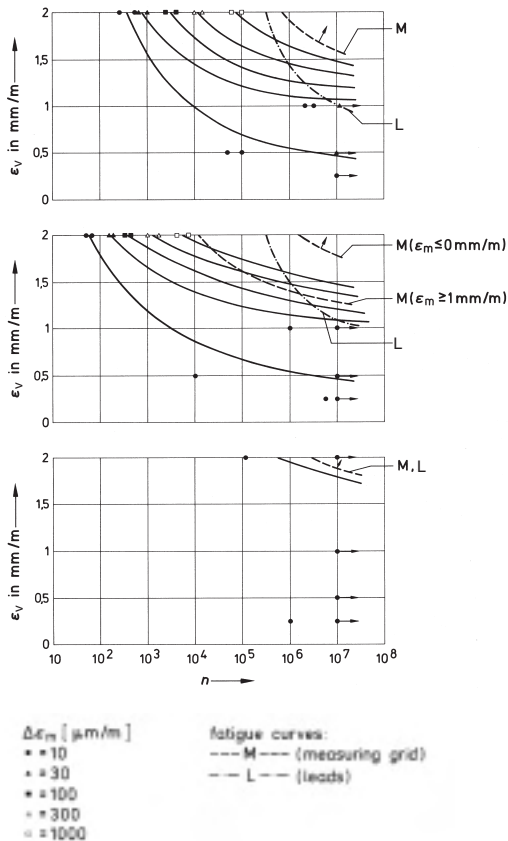
For strain gages with a metal measuring grid fatigue occurs as a result of the continuous vibration loading and this is exhibited in two ways:

- an increase in electrical resistance occurs depending on the amplitude and variation in the load which is apparent as dynamic zero point drift.
- with increasing disintegration of the material, microscopic cracks occur on the grain boundaries in the metal of the measuring grid. These slowly enlarge, eventually resulting in permanent fracture.

One method for determining the continuous vibration characteristics of strain gages is described in [3-33] ; the method was used in [2-1]. The diagrams for continuous vibration shown in Figs. 3.3-19 a to c were obtained using this method. The continuous lines show the zero drift in $\mu\text{m/m}$ which arises from the combination of the vibrational strain amplitude ε_v and the number of loading cycles n , corresponding to the accompanying figures. The broken lines show the permanent fracture of the measuring grid (M) and the leads (L). In Fig. 3.3-19b a damage line (M) is indicated for a positive static mean strain ε_m superimposed on the vibrational strain. The test was carried out up to a maximum number of loading cycles, $n = 10^7$.

The diagram in 3.3-19c differs substantially from the others. In the publication's text is stated: "A change in the zero point strain of $10 \cdot 10^{-6}$ occurs only with very large loadings. A change in the zero point of $30 \cdot 10^{-6}$ or more was not obtained in the loading range under investigation." Investigations by the author confirm good continuous vibration characteristics for this type of strain gage up to a vibrational strain amplitude of $\pm 3,000 \mu\text{m/m}$. A material was used for the measuring grid with a limit of elasticity which was higher than usual. Unfortunately, the elastic limit for the measuring grid material cannot be increased indefinitely. Therefore, continuous tests with large amplitudes are only possible on test objects using strain reducing auxiliary equipment, as described for example in [3-30] and with transducers as illustrated in Fig. 3.3-33.

There is also mutual dependence between the continuous vibration characteristics and the maximum static elongation. The maximum static elongation of strain gages capable of high



An arrow means that the relevant effect has not yet occurred at this number of load cycles.

Fig. 3.3-19: Curve for continuous vibration of various strain-gage types with wire measuring grids (extracts from [3-33]).

- a) HBM type 20/600 FB1
- b) HBM type 20/600 FB3
- c) HBM type 20/120 FB4S

sustained vibration is limited to about 1 ... 2 cm/m (10,000 ... 20,000 $\mu\text{m}/\text{m}$), whereas high-elongation strain gages possess only modest continuous vibration characteristics.

A measuring grid material encountered in America called “Isoelastic” exhibits very good continuous vibration characteristics, but it also has a very large temperature response. In addition it also reacts strongly to magnetic fields. To the author’s knowledge this material is not used by European strain gage manufacturers.

The foil strain gages shown in Fig. 3.3-20 give good results for an extended range of vibrational strain up to $\pm 3,000 \mu\text{m}/\text{m}$. This can be regarded as being typical for higher

quality strain gages. The following generally applies: The fatigue strength of a strain gage is greatest in the negative zone, less in the intermediate zone and lowest in the positive zone. Strain gages with long measuring grids have a slightly better fatigue strength than short strain gages.

A practical tip: If a measurement is to be made in the positive range then, if the circumstances permit it, the test object is loaded with half the peak load and the strain gage is applied in this state. During the test the strain gage experiences a vibrational strain with

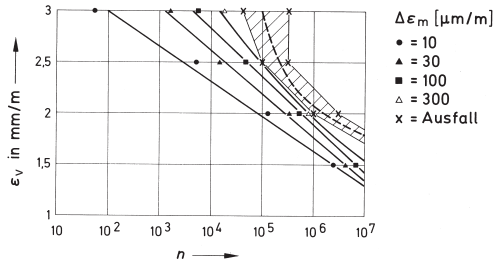


Fig. 3.3-20: Continuous vibration curves for a foil strain gage series.

The zero point drift in relation to the alternating strain amplitude ε_v and the number of load cycles n

only half the peak loading. Finally, it should be mentioned that problems are more likely to arise in the strain gage leads and connections than in the gage itself. This is borne out by practical experience. Therefore highly flexible lead material is used and the leads are routed to be as free of stress as possible.

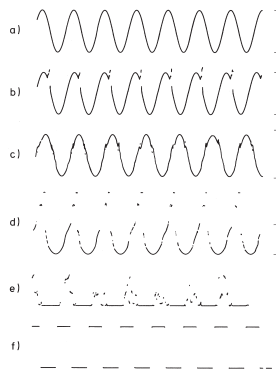


Fig. 3.3-21: Some oscillations typically occurring during vibrational loading (from [3-33]). The calibration marks on the right-hand edge of the diagrams indicate a vibration range of 4000 $\mu\text{m/m}$ which would be reproduced by an undamaged strain gage.

The start of the permanent fracture in the strain gage can be easily observed with an oscilloscope. The initial small cracks in the measuring grid can be recognized as spikes in the positive vibration diagram which can extend to a “spiky region” as the crack pro-

gresses. After the fracture is complete the conductor then only functions as a switch, see Fig. 3.3-21.

With semiconductor strain gages the monocrystalline silicon “measuring grid” possesses an ideal vibration strength over the complete strain range of about $\pm 5000 \mu\text{m/m}$, but unfortunately this does not apply to the connections, see Fig. 1. 0-9.

Cracks in the adhesive or in the measuring grid carrier as a result of continuous dynamic loading should not be expected due to the high resistance to alternating loads for the materials in question.

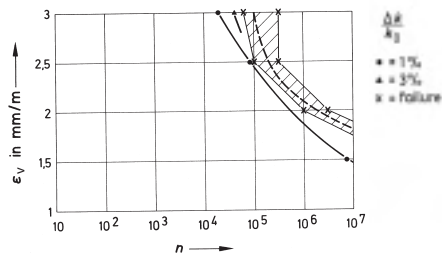


Fig. 3.3-22: Changes in the gage factor for continuous alternating loads in relationship to the alternating strain amplitude ϵ_v and the load cycles n .

Apart from the load variations obtained in continuous vibration tests and the accompanying zero point drift, the influence on the strain gage's sensitivity, i.e. on the gage factor, is also of interest. It can be seen from the diagram in Fig. 3.3-32 that an increase in the gage factor of 1% is the first symptom of an impending total failure. The previously determined differences in sensitivity are within the test apparatus's range of measurement error.

3.3.7.2 The cut-off frequency

The work carried out by Oi [3-31] and Bagaria/Sharpe [3-32] is useful in assessing the capability of strain gages with regard to the repeatability of dynamic strain processes. Oi examined the step change in strain that occurred with the fracturing of a notched, hardened steel bar. Bagaria and Sharpe investigated the repetition of a shock wave which was produced by a pendulum ram impact test machine when the hammer hit the face of a steel bar. The contact surfaces were flat to within a tolerance of 325 nm and had a roughness of between 72 and 127 nm ($1 \text{ nm} = 10^{-9} \text{ m}$). These figures are interesting in that they indicate the enormous effort required to come as near as possible to obtaining a rectangular step change. I am mentioning this because these conditions never occur in routine measurement problems. This will be apparent later from the description of a test.

The following is relevant when considering a strain gage's capability to reproduce a rectangular step change:

The sudden change of strain penetrates the length of the strain gage in the time t . As a result of averaging by the strain gage, the signal which it produces rises linearly to the maximum value with the propagation speed of the strain pulse depending on the length of

the measuring grid. The propagation speed corresponds to the speed of sound v . The theoretical time period t_{th} required to reach the full measurement value is

$$t_{th} = \frac{l_{sg}}{v}. \quad (3.3-10)$$

Due to various influences, which are not fully explained, the actual reproduced signal is of the shape shown in Fig. 3.3-23c.

For step functions the time period between 10% and 90% of the measurement value is taken as the rise time t_r .

Oi derived the equation

$$t_r = t_a + 0.8 \frac{l_{gs}}{v}, \quad (3.3-11)$$

where the term t_a is a time period dependent on the test rig and which is stated by Oi as being $0.5 \mu\text{s}$, but is reduced to $0.2 \mu\text{s}$ by Bagaria/Sharpe.

With sinusoidal vibration processes, the relationship of the strain gage length l_{sg} to the wavelength λ has a significant effect on the accuracy with which the process is reproduced. If it is assumed that the strain gage length is equal to the wavelength of a standing or moving sinusoidal vibration then the strain gage produces the value of zero as an average of the positive and negative parts of the vibration, although the peak value may be quite large. Therefore the ratio $l_{sg} : \lambda$ must be made as small as possible in order to obtain sufficiently accurate results. In the diagram in Fig. 3.3-24 the vibration process is assumed to be sinusoidal and the ratio of the strain's actual peak value is given as a percentage of the indicated peak value in relationship to the ratio $l_{sg} : \lambda$. The diagram is calculated for the condition where the center of the measuring grid is located at the point of maximum strain.

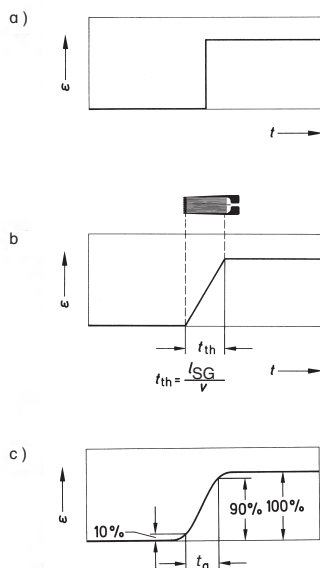


Fig. 3.3-23: Indication of a step change in strain by a strain gage

- a) rectangular step change
- b) theoretical signal wave-shape
- c) actual signal wave-shape

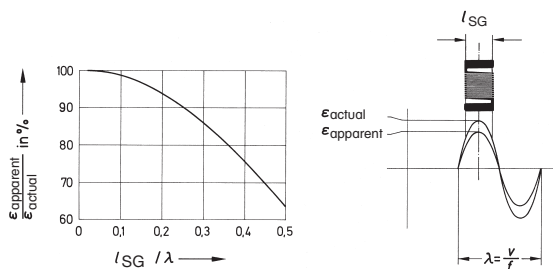


Fig. 3.3-24: Reduction in sensitivity in relationship to the ratio $l_{SG} : \lambda$ for a sinusoidal process. The center of the measuring grid is located at the point of maximum strain.

In [3-49] Bickle shows how the influence of the $0.8/v$ term in equation (3.3-11) can be significantly reduced using an analytical compensation technique. The validity of the method has been substantiated by a test. Here a detonator in an aluminum rod produces a shock wave whose rise time is about $10 \mu\text{s}$. The measurement is carried out with various lengths of strain gage. The shortest gage was 0.38 mm long; its signal was taken as being the “true measured value”. The longest strain gage was 48 mm long. It is shown how its deviating signal can be brought into agreement with the “true measured value” using the compensation calculation.

The investigations which have been quoted have attempted to find the limits of strain gage response to dynamic processes, but here a more common process is shown using an example.

Example:

Two strain gages, located opposite to one another, were mounted diametrically opposed on a 3050 mm long steel bar of 20 mm diameter at a distance of 1565 mm from the end surface. One strain gage had a measuring grid length of 6 mm, the other 1.5 mm, see Fig. 3.3-25. The strain gages were connected in a quarter bridge circuit (see section 5), each

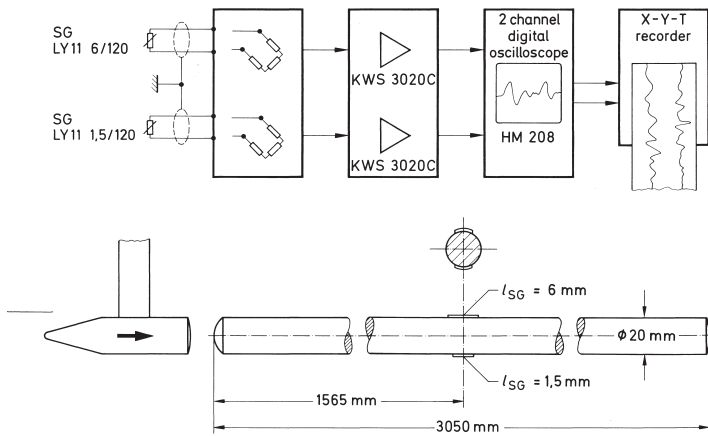


Fig. 3.3-25: Experimental arrangement for a shock test.

connected to a KWS 3020 DC Measuring Amplifier, The frequency range of both amplifiers was set to 25 kHz (-1 dB). Their output signals were passed to a two channel digital storage oscilloscope with pretriggering. The output signals could be observed on the screen and could be plotted out synchronously on a two-channel recorder. The recording is shown in Fig. 3.3-26.

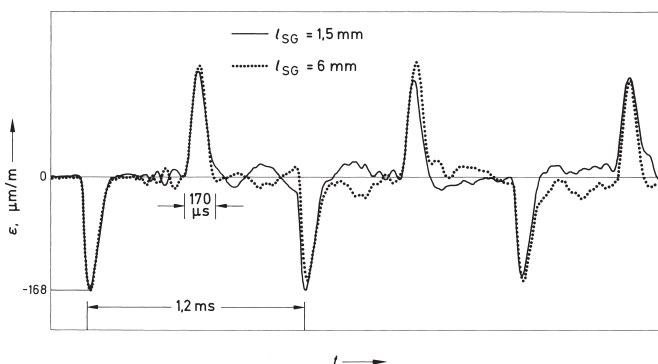


Fig. 3.3-26: Trace of a shock test on a steel bar of approx. length 3 m.

Result:

The distance between the negative Signal peaks corresponds to a time of 1.2 ms for the shock wave's travel in both directions, i.e. a run of $2 \times 3050 = 6100$ mm.

The positive signal peaks indicate the reflected wave.

The shock signal itself is applied for 170 μ s.

The amplitudes of the Signals are 168 μ m/m.

A vibration in the opposite direction is superimposed on the signal peaks which can be taken to be bending (lateral) vibration.

Evaluation:

From the time period of 1.2 ms for the shock wave's travel in both directions over a distance $2 \times 3050 = 6100$ mm the propagation speed v can be calculated to be 5083 m/s; it is the same as the speed of sound in steel.

The speed of sound in solid bodies can be calculated from the modulus of elasticity E and the material density ρ according to the following relationship:

$$v = \sqrt{\frac{E}{\rho}} \quad (3.3-12)$$

$$v_{\text{steel}} = \sqrt{\frac{E}{\rho}} = \sqrt{\frac{206 \cdot 10^9 \text{ kg} \cdot \text{m} \cdot \text{m}^3}{7.8 \cdot 10^3 \text{ s}^2 \cdot \text{m}^2 \cdot \text{kg}}} = \sqrt{\frac{206 \cdot 10^6 \text{ m}^2}{7.8 \text{ s}^2}} = 5140 \frac{\text{m}}{\text{s}}$$

The difference between the measured and calculated speed of sound is only 0.7%, which, considering the table values used for E and ρ and the possible inaccuracies in the recording, can be regarded as being very small.

The length of the shock wave can be calculated from the duration of the shock signal of 170 μ s and the speed of sound v

$$l = v \cdot t \quad (3.3-13)$$

$$= 5083 \frac{\text{m}}{\text{s}} \cdot 170 \cdot 10^{-6} \text{s} = 0.864 \text{ m.}$$

The strain amplitude is $\epsilon = -168 \mu\text{m/m}$. Hence the material stress can be calculated as

$$\sigma = \epsilon E = -168 \cdot 10^{-6} \frac{\text{m}}{\text{m}} \cdot 206000 \frac{\text{N}}{\text{mm}^2} = -34.6 \frac{\text{N}}{\text{mm}^2}$$

and the force impulse

$$F = \sigma A = -34.6 \frac{\text{N}}{\text{mm}^2} \cdot 314 \text{mm}^2 = -10864 \text{ N.}$$

If the recorded shock wave in Fig. 3.3-26 is regarded as a rough approximation to a half sinewave oscillation with $\lambda/2 = 864 \text{ mm}$ and if this is compared with the error in the ratio $l_{\text{sg}} : \lambda$ taken from the diagram in Fig. 3.3-24, then it will be realized that no discernable difference can occur between the signals of the two strain gages with 6 mm and 1.5 mm length of measuring grid. However, the differences occurring alternately on each side can be explained as a superimposed lateral vibration of the rod.

Conclusion:

Shock processes which approximate a rectangular waveform can only be produced with sophisticated test equipment. In normal practical conditions shock impulses are less sudden.

Dynamic measurement problems can be overcome without difficulty with the commonly used lengths of strain gage of 3 mm and 6 mm. Even vibrations in the ultrasonic region can be measured with sufficient accuracy. Also, the frequency response of the measurement equipment used must always be considered.

3.3.8 Electrical loading

If a strain gage with a grid length of 6 mm and a grid resistance of 120 Ω , e.g. the type LY11 6/120, is connected in a symmetrical bridge circuit fed with a voltage of 5 V, a current of 20.8 mA flows through the strain gage. At a glance this is not very much. However, if the current is considered in conjunction with the extremely small cross-section of the measuring grid's elements, then it is found that a current density of 46 A/mm² arises, which is extremely high, even in the field of power engineering. With small conductor cross-sectional areas, it is only possible to dissipate the electrical heat energy to the ambient if there is a favorable relationship between the cross-sectional and the surface areas. In order to achieve this the power transferred to the gage and the dissipated power must be matched so that the rise in temperature on the strain gage is kept within reasonable bounds. Here there are a few requirements to be met and the parameters which have the most influence are:

- the bridge excitation voltage level,
- the electrical resistance of the measuring grid
- the size and geometry of the strain gage's measuring grid,

- the ambient temperature,
- the thermal conductance of the component material,
- the component's thermal capacity and its radiation and cooling characteristics.

If the electrical loading on the measuring grid is too severe, similar effects are obtained as when the ambient temperature is too high, e.g. overheating of the measuring grid, the carrier material and the bonding layer, which results in hysteresis, creep, an unstable zero point and worsening of the temperature compensation.

In the technical data for each type of strain gage HBM states the maximum permissible bridge excitation voltage. This value is a guide value and applies for an average range of accuracy for continuous operation at room temperature and for strain gages mounted on objects having good thermal conducting properties. A higher ambient temperature, worse thermal conductance (bonding layers too thick) and low component thermal capacity (small objects) all require a reduction in the bridge excitation voltage.

For measurements on synthetic components [3-34] the supply voltage should be reduced to about 10% of the table value. Pulse supplies are a suitable method of overcoming problems due to high self-heating with strain gages. Modern scanners for multipoint measurements provide both options, but the reduction of the excitation voltage is the more effective method, because the excitation voltage V and the power P have a quadratic relationship.

$$P = \frac{V^2}{R} \quad (3.3-14)$$

With cyclic scanning of the measurement points or with a pulse supply, the power passed to the strain gage depends on the duty cycle and the repetition frequency.

If high accuracy is required and for the construction of transducers, it is recommended that a reduction in the excitation voltage be made to approximately half the stated maximum value.

If a reduction in the bridge excitation voltage is not possible, perhaps due to the equipment involved, then the selection of a high strain gage resistance may be helpful. However, the power and resistance only have a linear relationship to one another, as can be seen from equation (3.3-14).

Lowering of the excitation voltage with series resistances is in principle possible, but it is always accompanied with a loss of measuring signal, see section 7.2. Additional errors due to temperature dependence or instability of the series resistor must be expected.

3.3.9 Creep

In almost all publications on strain gages creep is shown as a detrimental parameter. Thirty years ago this was certainly correct, but this impression now needs correction. For precise measurements a certain amount of creep is essential. With modern methods of producing foil strain gages it is possible to match the strain gage's creep characteristics to the measurement application. For example, without this technique it would not be possible to satisfy the demands of extreme accuracy for load cells subject to official calibration.

What is meant by creep?

If a strain gage is subject to a static strain, its resistance changes with time despite constant strain in the test component. This change in the measurement signal of an extended or shortened strain gage takes place very slowly and is said to “creep” in the direction of “strain relief”.

The cause lies in the rheological characteristics of the bonding layers and measuring grid material which transfer the strain [3-35]. The extended measuring grid behaves similar to a tensioned spring. The force of the spring produces shear stress mainly in the region of the measuring grid's end loops on the contact surfaces between the measuring grid and the carrier. This shear stress is in addition to the normal stress due to the extension. The synthetics in the strain gage and the bonding material relax, i.e. the reactive force slackens, the measuring grid draws in and a negative error occurs. This process is shown in Fig. 3.3-27.

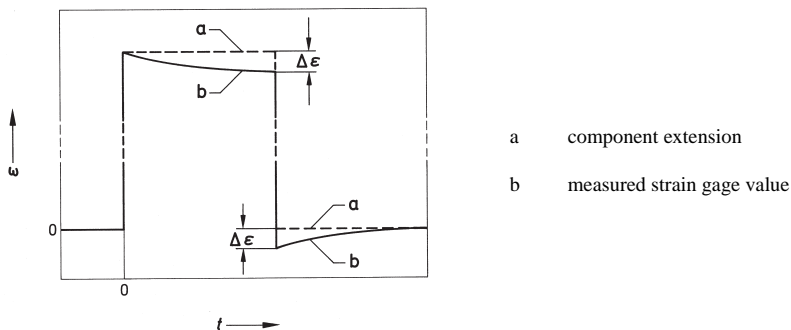


Fig. 3.3-27: Change in the measured value of a strain gage with time after instantaneous loading of the component and after its instantaneous release.

Since this process takes place in a relatively tightly bounded region of the measuring grid, it has greater influence on short measuring grids than on long ones, see Fig. 3.3-28.

Foil strain gages have an advantage over the wire gages which were previously more common, because the widened end loops distribute the forces over a larger area and thus reduce the shear stress.

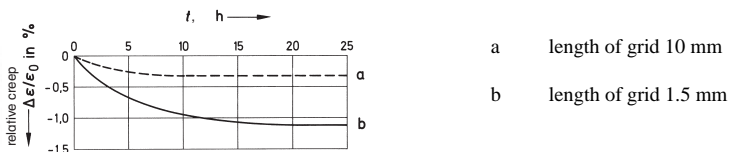


Fig. 3.3-28: Examples of creep curves for two strain gages of different length.

The parameters which determine creep characteristics are numerous and complicated. These include the cross-sectional area of the measuring grid's elements, the number of ele-

ments, the carrier material, the type of adhesive and its thickness, as well as time, temperature and humidity. High temperatures encourage creep and low temperatures restrict it. Therefore details given here can only show the trends. Figures should not be taken as absolute values and should not be transferred to other strain gages.

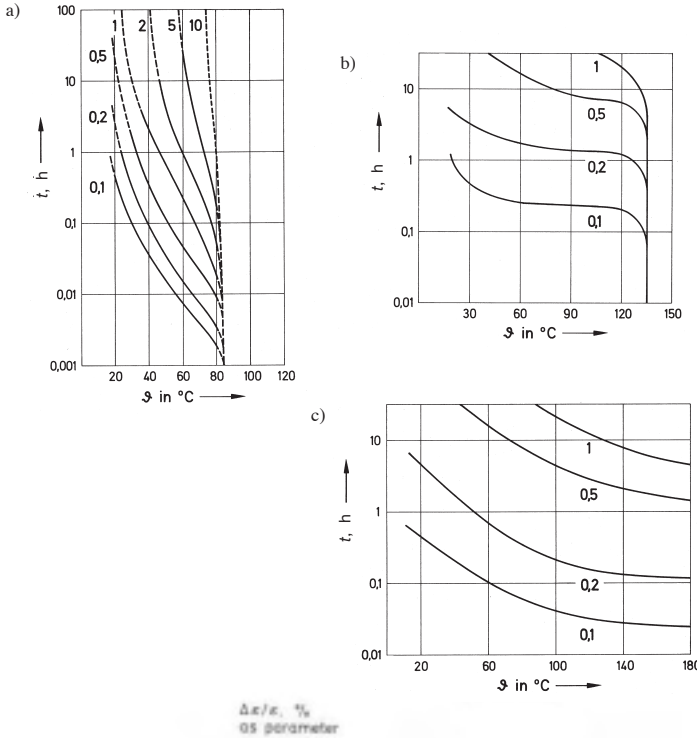


Fig. 3.3-29: Time/temperature creep diagram (TTC) from [2-1].
 Relative creep in % of $\Delta \varepsilon / \varepsilon_0$, measured at $\varepsilon_0 = 2000 \mu\text{m/m}$.
 Strain gage type: LY11 6/120.
 Adhesive:
 a) Rapid adhesive X 60, cold curing
 b) Rapid adhesive Z 70, cold curing
 c) EP 250 adhesive, hot cured for 2 h at 180°C + 2 h at 200°C.

In [2-1] strain gage creep was measured with a device giving a strain which was constant with time. Fig. 3.3-29 shows the results of a series of measurements for determining creep using a different method of representation. Here the relative creep $\Delta \varepsilon / \varepsilon_0$ is plotted as a function of time t and temperature ϑ . The strain on the strain gage ε_0 at the Start of the measurement was + respectively - 2000 $\mu\text{m/m}$.

In principle such time/temperature/creep diagrams (TTC diagrams) can only be determined for strain gage/adhesive combinations and never for the strain gage on its own. The TTC diagrams illustrated in 3.3-29 were obtained using strain gages of the same type but with

different adhesive. It can be seen that the rapid adhesive X 60 is to be preferred for measurements at room temperature. At 50°C and with load cycles of up to 1 hour duration good measurement can still be obtained. In contrast the rapid adhesive Z 70 exhibits significantly better stability and a larger useful temperature range. An interesting feature that cannot be seen in the diagram are the X 60's advantages in the low temperature region, including temperatures around the freezing point.

What effects does creep have on the results of a measurement?

It has already been stated that the production of high precision load cells would not be possible without a certain amount of strain gage creep. Why is this?

The relationships are best explained using a simple tensioned beam as an example; it also applies for other load applications, but only in the elastic deformation region. A basic requirement for transducers is that the loading of the spring element material should be kept low, so that non-reversible plastic deformation is eliminated. The material must be chosen suitable for the intended application.

If the beam is loaded with a tensile force, then it extends by an amount according to Hooke's Law. As a result of material relaxation this spontaneous extension is followed by a time dependent, asymptotic additional extension. If the beam is released, then it springs back by an amount equal to the spontaneous extension obtained under load. A small residual extension remains which is equal to the time dependent additional extension and this decays slowly until the original condition is established. This is termed "elastic after-effect" to differentiate it from non-reversible material creep. Fig. 3.3-30 illustrates the elastic after-effect.

For stress analysis and for the measurement of other physical quantities accompanied by force effects (force, weight, bending moment, torque, pressure, etc.), the instantaneous material strain is a measure of the loading.

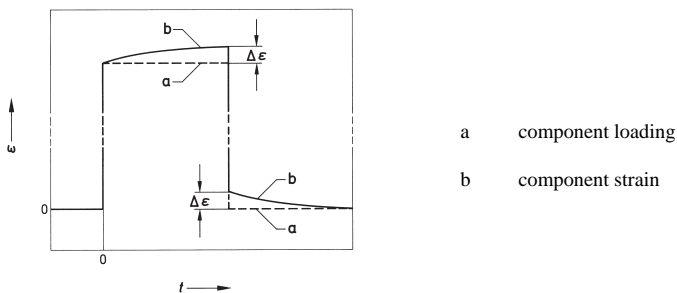
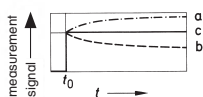


Fig. 3.3-30: Variation of component strain with time during constant loading and after complete release (elastic after-effect).

The elastic after-effect gives a time dependent, positive error. Strain gage creep and elastic after-effect have opposite signs and reduce one another, see Fig. 3.3-31. In the most favorable cases quite good compensation can be obtained.



- a elastic after-effects for a spring element/component material
- b strain gage creep
- c measurement signal

Fig. 3.3-31: Schematic diagram for creep compensation.

Whereas the principle of creep compensation is quite simple, it is difficult to put into practice, depending on the required measurement accuracy. Optimum matching under realistic conditions should always be determined by testing. It is now possible to manufacture transducers whose creep error is less than 0.005% of the measurement range referred to a time period of 30 minutes. This time period is sufficient for many load cell applications.

The influence of temperature on creep is shown in the result of a laboratory test in Fig. 3.3-32. The specimen was loaded at room temperature, at 60°C and at 100°C, each for 24 hours and then released for 24 hours. Measurements were recorded during this period.

At room temperature the matching is better than + 0.05% of the reference value .

At 60°C the positive error, which mainly indicates an elastic after-effect, reaches about +0.15% in the time period of 24 hours. After release the original zero point returns again, also after 24 hours.

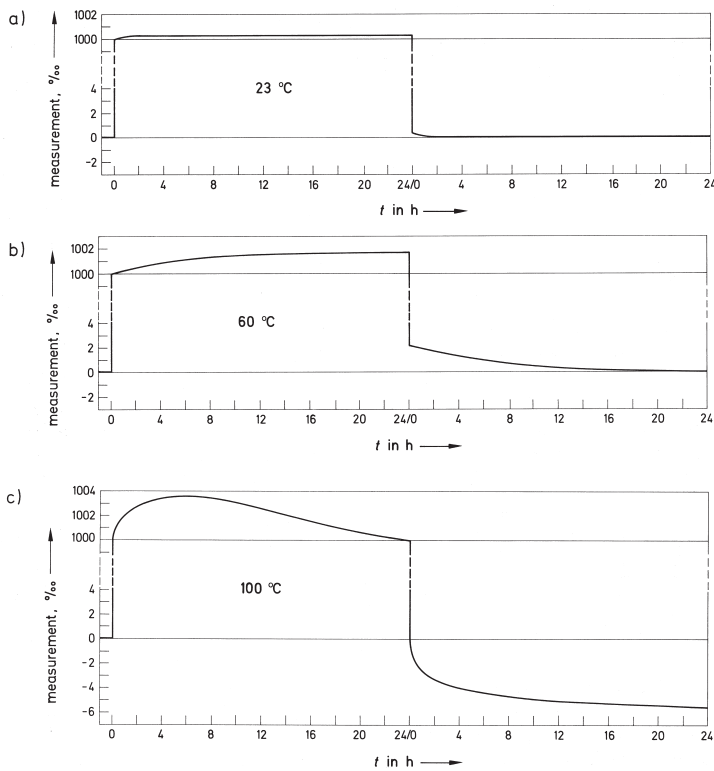


Fig. 3.3-32: Time dependent and temperature dependent creep of a test object fitted with strain gauges during a 24 hour period at different temperatures.

At 100°C there is initially a positive slope to the signal which reverses direction after a few hours. This reverse indicates a non-reversible yield in the strain gage and the adhesive. The amount of yield can be seen in the remaining displacement of the zero point when the reversible creep has decayed after the load is released.

This example shows that similar effects can arise from different influences and that creep compensation can only be carried out within a limited time/temperature/accuracy range.

It should be mentioned in this respect that creep in modern foil strain gauges is so slight that it must sometimes be artificially increased to obtain sufficient compensation of the elastic after-effects in the spring element material.

The problem must be considered differently for measurements dependent on *displacement* controlled conditions in contrast to the measurements dependent on *force* controlled conditions, which have just been described.

Example: A change in length is to be measured with a bending element. The strain close to the element's clamping point is the measure of the change in length. The principle is illustrated in Fig. 3.3-33. Relaxation in the bending element material only causes a reduction in the reactive force. It has no influence on the strain, which in this case only depends on the element's deflection and not on the reactive force. Here the strain gage creep does not have any compensating effect and it would only be a source of error which could be eliminated with creep-free strain gages, see Fig. 3.3-34. With this type of strain

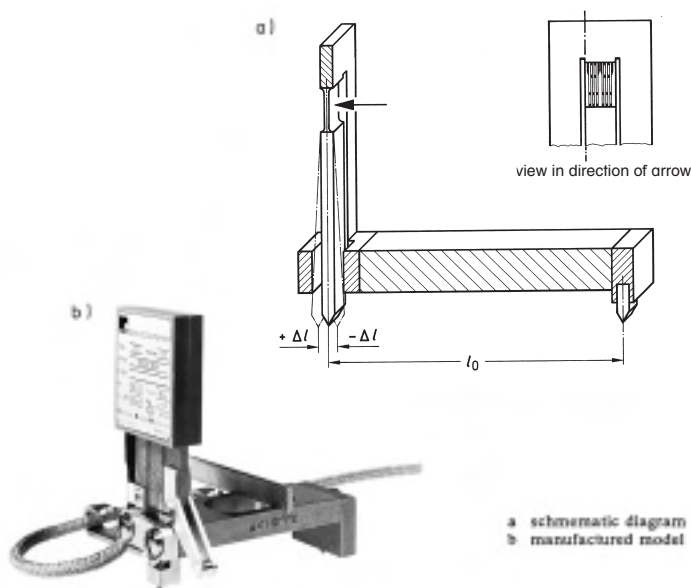
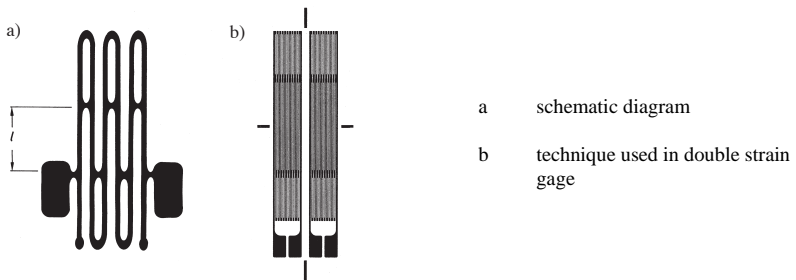


Fig. 3.3-33: Equipment for the measurement of the change in length using a bending element fitted with strain gages (DD1 Strain Transducer from HBM).

gages creep is reduced by providing an equivalent force on the transverse links which bound the active sections of the measuring grid at a distance l . This is also the function of the grid extensions which themselves do not contribute to the measurement. With correct design the creep occurring on the external ends has no effect on the measuring part of the grid.



l active, measuring length of the measuring grid

Fig. 3.3-34: Example of a creep-free strain gage.

3.3.10 Mechanical hysteresis

The mechanical hysteresis of a strain gage is the difference in the measured value for rising and falling strain loadings with the same strain value on the specimen. A more specific definition is given in [2-1] with regard to universal test conditions. Here mechanical hysteresis is given as the largest difference in the zero point on the abscissa of a curve for tension rising and falling through a complete cycle with the extreme values of $\pm 1000 \mu\text{m/m}$ and $\mp 1000 \mu\text{m/m}$.

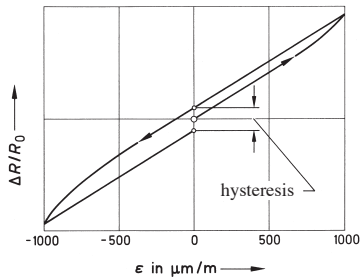


Fig. 3.3-35: Definition of mechanical hysteresis from [2-1]

As with a number of other parameters, the mechanical hysteresis does not just depend on the strain gage, but also on the bonding and other parts which form the measuring point. Experience shows that hysteresis becomes smaller after a number of load cycles. Therefore details on the first and third load cycles are required. Supplementary measurements in the strain ranges $\pm 2000 \mu\text{m/m}$ and $\pm 3000 \mu\text{m/m}$ are also shown.

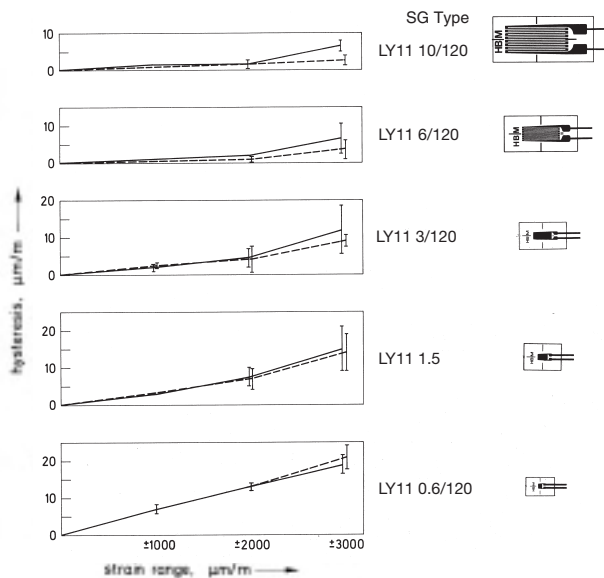


Fig. 3.3-36: Mechanical hysteresis for 6 different types of strain gages in the LY 11 series, bordered with Rapid Adhesive Z 70. In the type designation the number to the left of the slash gives the length of measuring grid.



The results of a test as shown in the diagrams go beyond the requirements in [2-1]. They should show how much type dependence there is within a strain gage family and the effects exhibited by various adhesives. The measurement results are shown according to the scheme

- 1st and 3rd cycle at $\pm 1000 \mu\text{m/m}$ and $\mp 1000 \mu\text{m/m}$
- 1st and 3rd cycle at $\pm 2000 \mu\text{m/m}$ and $\mp 2000 \mu\text{m/m}$
- 1st and 3rd cycle at $\pm 3000 \mu\text{m/m}$ and $\mp 3000 \mu\text{m/m}$

It can be seen from Fig. 3.3-36 that there is a dependence of the hysteresis on the length of the measurement grid, which is particularly pronounced with short measuring grids.

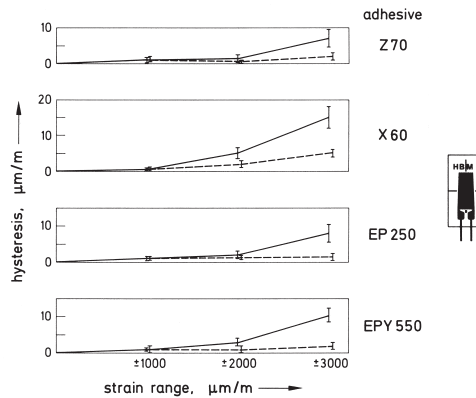


Fig. 3.3-37: Mechanical hysteresis for the strain gage type LY 11 6/120, bonded with 4 different adhesives



In Fig. 3.3-37 the parameters are formed by the adhesives used for the same type of strain gage. Z 70 is a cold curing rapid adhesive based on cyano acrylate, X 60 is also a cold curing rapid adhesive but based on polymethacrylate and the two adhesives EP 250 and EPY 550 are hot curing epoxy resin adhesives.

The test, the results of which are given in Fig. 3.3-38, differs from the previous test of Fig. 3.3-37 only in the type of strain gage used.

The significant reduction in hysteresis, in particular in the strain region $\pm 3000 \mu\text{m/m}$, indicates that the design of the strain gage has a marked influence.

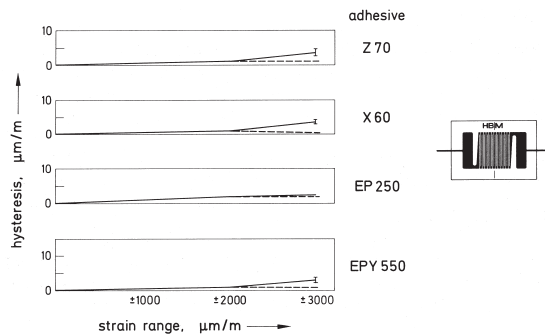


Fig. 3.3-38: Mechanical hysteresis of the strain gage type LY 21 6/120, bonded with four different adhesives



3.4 Environmental influences

Environmental influences affect not only just the strain gage but also the whole measurement point. It is therefore not sufficient to consider the strain gage alone.

The zero point stability of a strain gage measurement point depends on numerous factors. These begin with the proper mounting of the strain gage, including careful preparation of the measurement point and providing it with effective protection, see section 4 and [4.1] .

However, the strain gage's previous history and the history of the component to be tested can also have an effect. Mechanical and thermal loading of the mounted parts before the actual measurement have been shown by experience to provide better stability. (Here it must be mentioned that instability and errors are not always caused by the strain gage or its mounting; there are often other reasons, e.g. incorrect wiring, ineffective protection, interference from the power supply).

The strongest influences are due to external effects. These are most often temperature and humidity, but other effects can influence the strain gage measurement in undesired ways. Under this heading are for example pressure, vacuum, atomic radiation, together with electrical and magnetic fields.

It is possible to partially counteract such effects by a specific choice of material or they can be reduced or compensated by taking appropriate measures.

3.4.1 Temperature

The many effects of temperature on strain measuring points cannot be properly considered when viewed altogether. Therefore at this point reference only is made to the sections which give more detailed information.

- 2.3.4: Thermal expansion
- 3.2.3: Special strain gages (also high temperature versions)
- 3.2.5: Useful temperature range
- 3.3.4: The temperature response of a strain gage measuring point
- 3.3.5: The dependence of sensitivity on temperature
- 3.3.8: Electrical loading
- 3.3.9: Creep
- 7.1: Compensation for thermal output

3.4.2 Humidity

Along with temperature, humidity is a main cause of instability in strain gage measurements. Changes in humidity during a measurement give rise to uncontrollable changes in the zero point which, in particular with zero referenced measurements, show up as errors in the measurement result. Sometimes the sensitivity is also affected [3-36]. The degree of influence depends on the rate of change and current level of the relative humidity.

Humidity penetrating the measuring point changes the insulation resistance between the strain gage and the test object and between the elements of the measuring grid, acting as a varying shunt across the strain gage. Extreme effects are experienced with ceramic bonding agents (e.g. high temperature bonding) resulting from their high hygroscopicity. Changes in the humidity content also cause swelling or shrinking of the measuring grid carrier and adhesive. Even the adhesive's bonding can be destroyed and the strain gage may partially or completely free itself from the test object.

High levels of humidity can lead to corrosion damage in the strain gage. A direct voltage field between the measuring grid and the component can cause polarization to occur in the insulation layers, rendering the measuring point completely unusable. The presence of other reactive substances, e.g. sea air, industrial atmospheres, etc. reinforces the effects of humidity.

Problems due to humidity are not restricted to the strain gage. Insulation defects in the test cabling and in the following measurement instruments also lead to errors and must therefore also be considered when looking for their cause. Although it is important to detect the cause of problems, it is more efficient to prevent them in the first place. Where possible during the manufacture of the strain gage only those materials are used which take up very small amounts of moisture. Unfortunately, there are no suitable insulating and adhesive materials which do not absorb any moisture at all. It is therefore essential that suitable protective measures are taken. These depend on the medium in question (not only moisture or water, but other substances must be considered), the degree of accuracy required and the duration of the measurement and the service life of the measuring point. For short term measurements in dry rooms little action is required, whereas continuous measurements in the open air or under water require comprehensive protective measures. Details on the methods of protecting measuring points can be found in section 4.3 and [4-1].

3.4.3 Hydrostatic pressure

It is apparent from the literature that strain gages can withstand hydrostatic pressures of over 10,000 bar without any decrease in their functional capability. The published results show that in principle a certain change of resistance occurs depending on pressure, which is superimposed as an error on the strain measurement signal. However, the results cannot be universally applied, which may be due to the variation in test conditions, but which is more likely to be due to the different designs of strain gages. Different bonding methods also contribute to the variation. In contrast to most papers that only describe empirical results and which are difficult to transfer to other applications, the various contributing parameters are treated theoretically in [3-37] and their effects are validated with test results.

The quality of the bonding has a more pronounced effect on validity of the measurement than with other environmental influences. Therefore some important features are discussed below.

The main requirement for good test results is careful bonding. The quality of the bonding for measurements under hydrostatic pressure or under hydrostatic vacuum, affects the accuracy of the test result more than with any other field of application.

The two diagrams shown in Fig. 3.4-1, which are taken from [3-38], clearly illustrate this fact. The diagram 3.4-1a shows the result of improper bonding, whereas the results used for diagram 3.4-1b are from measurements where all the necessary additional measures were taken.

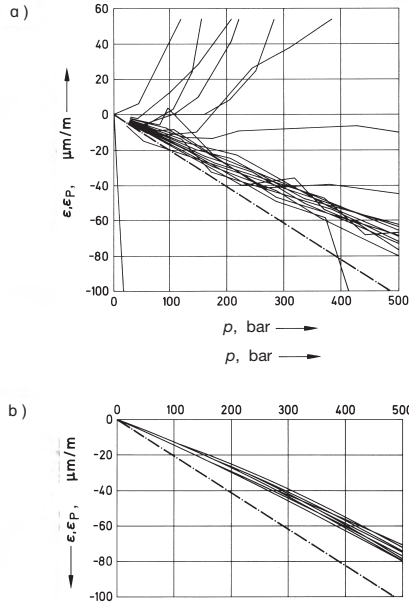


Fig. 3.4-1: The influence of hydrostatic pressure on the strain gage measurement
a) with improper bonding
b) with the necessary additional measures taken for measurements made under pressure.

Adhesives can only be used which do not contain any solvent, which do not release any gaseous substances during curing and which produce a bonding layer as thin as possible but having uniform thickness. The adhesive layer must be absolutely free from air bubbles; even small air inclusions can lead to uncontrollable zero point changes, hysteresis or even fracture of the measuring grid. Therefore care must be taken that no air is mixed in when mixing multicomponent adhesives. This is achieved by mixing under a vacuum or evacuating the mixture afterwards.

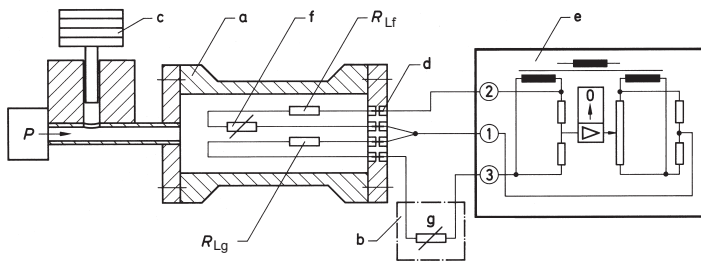
Adhesive layers of non-uniform thickness are squeezed together by varying amounts, giving rise to distortions of the measuring grid, which are reflected in the measured value. A high compressive force during the adhesive's curing phase produces a uniform layer thickness. With the types of bonding, the results of which are shown in the diagram 3.4-1b, compression forces of 15 bar = 1.5 MPa were used. In diagram 3.4-1a only 1 bar = 0.1 MPa was used. The difference is apparent.

Whereas bonding problems can be avoided by careful preparation, physical effects result in other difficulties. These are:

- the piezo-resistive effect (pressure coefficient) of the measuring grid,
- the compressibility of the measuring grid carrier material and of the adhesive, As well As the uniformity of the layer thicknesses,
- the test object's surface structure and contours (porous or fine grained, flat or curved),
- Young's modulus and Poisson's ratio for the component material, the value $(2\nu-1)/E$.

The following can occur as parasitic effects:

- the piezo-resistive effect of the connecting cable laid in the pressurized zone,
- influences of the thermal output due to the adiabatic heating during the increase in pressure or cooling during a fall in pressure.



- a pressure vessel
- b oil reservoir (open)
- c piston and cylinder with pump P
- d pressure tight cable glands
- e indicating Instrument
- f measuring (active) strain gage
- g compensating strain gage
- R_{L_f} cable resistance in series with strain gage f
- R_{L_g} cable resistance in series with strain gage g

Fig. 3.4-2: Test-rig and circuit for investigating the pressure sensitivity of strain gages.

The usual method of investigating the pressure sensitivity of strain gages is described in detail in [3-38]. A schematic diagram of the test equipment is shown in Fig. 3.4-2.

Fig. 3.4-3 illustrates a test probe with bonded strain gages and the open pressure cylinder of the test-rig.

As a result of the hydrostatic pressure p which acts on all sides of the strain gage and the compressibility of its isotropic material, a negative strain occurs on its surface. The magnitude of this strain is

$$\epsilon_p = \frac{2\nu-1}{E} \cdot p. \quad (3.4-1)$$

This strain which is impressed on the strain gage by the test probe is shown in the diagrams in Fig. 3.4-1 as a broken reference line. The difference between the reference line and the measurements arises due to the pressure sensitivity of the strain gage bond. The effect is

positive. Disturbing influences can be compensated or corrected, depending on the type of effect.

The investigations in [3-38] apply in various combinations to the strain gages and adhesives listed in Table 3.4-1.

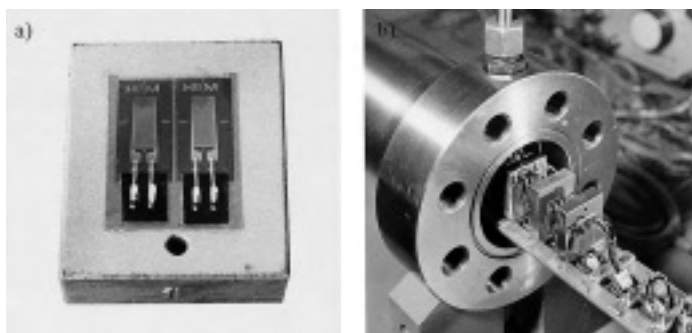


Fig. 3.4-3: Test probe for the measurement of pressure sensitivity of strain gages.

- a) steel test probe fitted with strain gages
b) open pressure cylinder with test probes.

Two characteristic strain gage families were selected from the types with foil measuring grids and with wire grids and, in turn, from these were selected the strain gage types which were the most popular. These were then combined with three different adhesives, producing 17 different combinations of adhesive and strain gage. Eight tests were carried out on each combination, giving a total of 136 tests.

Type of strain gage	Adhesive			
	Family	Acrylic resin rapid adhesive X 60	Cyano-acrylate rapid adhesive Z 70	Epoxy resin adhesive (hot curing) EP 250
Constantan foil measuring grid	Polyamide resin, LY 11 series	3/120* 6/120	3/120 6/120	3/120 6/120
	Phenolic resin with glassfiber, LG 11 series	- -	3/120 6/120	3/120 6/120
Constantan wire measuring grid	Acrylic resin with cellulose fiber, LA 11 ser.	6/120 10/120	6/120 10/120	- -
	Phenolic resin with cellulose fiber, LP 11 ser.		6/120	6/120
all types of strain gages are temperature compensating types when used on steel				
* 3/120 means: 3 mm length of measuring grid/ 120 Ω resistance				

Table 3.4-1: The strain gage/adhesive combinations which were investigated for pressure sensitivity.

The ground steel test probes were roughened by sand blasting just prior to bonding the strain gage, then carefully cleaned and degreased. The following details apply to the adhesives:

The two-component room temperature curing rapid adhesive X 60 is reduced by finger pressure to a layer thickness of $65 \pm 15 \mu\text{m}$ and it cures chemically within 1 hour at room temperature.

The single component rapid adhesive Z 70 is applied with a layer thickness of $8 \pm 2 \mu\text{m}$ and chemically cures under finger pressure within 30 seconds and is ready for measurements after about 30 minutes.

The two component adhesive EP 250 was cured according to the following method: 1 hour at 180°C under mechanical pressure of 15 bar plus 1 hour at 180°C without mechanical pressure. The resulting layer thickness was $20 \pm 5 \mu\text{m}$.

Stranded copper wire with a cross-sectional area of 0.25 mm^2 was used for connecting the strain gage. All connections were soldered.

The insulation oil used as a pressure medium rendered the use of additional strain gage protection unnecessary.

Manual instruments of the MK type, operating on the carrier frequency principle, were used for strain measurement. The supply voltage was 1 V/225 Hz and the resolution was $1 \mu\text{m}/\text{m}$.

The results are summarized in Table 3.4-2. The mean values are $+7.4 \mu\text{m}/\text{m}$ per 100 bar for the foil strain gages and $+5.5 \mu\text{m}/\text{m}$ per 100 bar for the wire strain gages. The measuring grid lengths and the adhesives have relatively little influence. These amount to only $\pm 0.8 \mu\text{m}/\text{m}$ per 100 bar for the foil strain gages and about $\pm 1.3 \mu\text{m}/\text{m}$ per 100 bar for the wire strain gages and therefore they correspond to the standard deviation s of the individual series of tests.

Strain gage			ε_p in $\frac{\mu\text{m}/\text{m}}{100\text{mbar}} \pm s$ when bonded with		
			X 60	Z 70	EP 250
Type	Family	Version			
Foil measuring grid	LY 11	3/120	6.6 ± 1.2	7.9 ± 1.0	8.1 ± 1.0
		6/120	7.3 ± 1.0	8.1 ± 1.0	8.2 ± 0.4
	LG 11	3/120 6/120	-	7.0 ± 1.5 7.9 ± 1.0	5.7 ± 1.0 6.8 ± 0.6
Wire measuring grid	LA 11	6/120	5.7 ± 0.8	6.5 ± 1.1	-
		10/120	74.0 ± 0.8	5.1 ± 1.6	
	LP 11	6/120	5.6 ± 0.7	5.3 ± 1.0	5.9 ± 0.6

Table 3.4-2: The influence of hydrostatic pressure on the tested strain gage bonds in $\mu\text{m}/\text{m}$ per 100 bar, also showing the standard deviation s . Valid for the pressure range under investigation, i.e. 0 to 500 bar.

With curved bonding surfaces an additional strain, $\Delta\varepsilon_p$, on the measuring grid occurs which is not present on flat surfaces and which is the result of the greater compressibility of the adhesive/measuring grid layers. The effect is similar to the temperature response effect on curved surfaces described in section 3.3-4.

In the diagram in Fig. 3.4-4, which is taken from [3-37], the pressure dependent change of strain $\Delta\varepsilon_p$ is recorded for the two layer thicknesses of $d = 0.05$ and 0.1 mm for the adhesive plus the measuring grid carrier. The calculation is based on the following data:

Young's modulus for adhesive and measuring grid carrier $\approx 10000 \text{ N/mm}^2$;
 Poisson's ratio $\nu = 0.32$;
 pressure $p = 100 \text{ bar (10 MPa)}$;
 change in the component radius $\Delta r = 0$.

The sign is negative for convex curvatures and positive for concave curvatures.

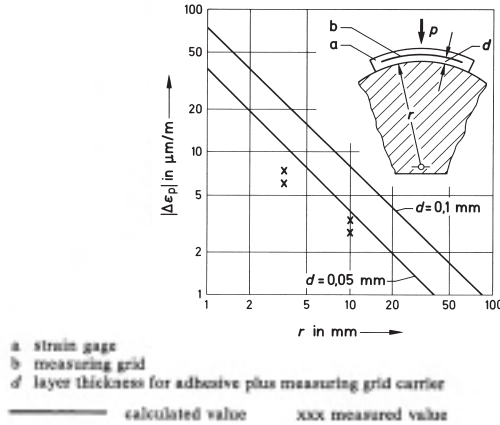


Fig. 3.4-4: Zero point displacement $\Delta \epsilon_p$ caused by hydrostatic pressure p for the bonding of a strain gage to a curved surface (from [3-37])

An effect of hydrostatic pressure on the sensitivity of the strain gage, i.e. on the gage factor, could not be found. The distribution of the measurements lay within the measurement error of $\pm 0.5\%$ for the test equipment used.

3.4.4 Vacuum

The ability of strain gages to operate in a vacuum was spectacularly demonstrated by their application on the American moon probe “Surveyor I” for measuring the landing impact, see Fig. 3.4-5. The fact that successful measurements were obtained proves in principle the applicability of strain gages under extreme vacuum conditions [3-39]. Other examples of measurements in extreme vacuums are described in [3-40, 3-41].

With the unrestricted pump capacity of space, gaseous release from substances (strain gages, adhesives, covering agent, insulating material, etc.) presents no problems. This is not the case in an enclosed system, where the release of gas from the materials has a detrimental effect on the vacuum. Vacuums down to 10^{-7} mbar can be maintained without difficulty. Harder vacuums present problems, where gaseous release and desorption not only destroy the vacuum but also contaminate the test apparatus and can impair its correct operation. Vacuum specialists are familiar with these problems; they also realize that a single fingerprint inside the apparatus can lead to disastrous results.

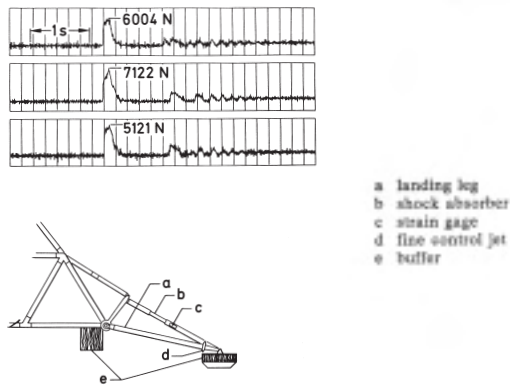


Fig. 3.4-5: Measurement record of the landing impact of the lunar probe "Surveyor I" on the moon (1966).

The following should be observed when bonding strain gages: gages with carriers of pure polyimide or pure epoxy resin are preferred, even those having an open measuring grid. Phenolic resin carriers have proven suitable under conditions in outer space. The measuring grid carrier is cut to the minimum permissible dimensions.

Similarly, adhesives of pure resin have advantages. Hot curing adhesives are used wherever possible. The adhesives must be fully cured; the maximum curing method is used, followed by a number of hours at about 200°C if possible. Solid wire leads are preferred for connecting the strain gage. The insulation must be thoroughly cleaned. Gloves and tweezers are used to avoid fingerprints. Thorough cleaning of the solder joint is essential.

The adsorption of moisture, which is unavoidable during these procedures, is eliminated by heating or storage in a drying agent, e.g. silica gel or in a desiccator above phosphorus pentoxide. Gaseous release in the vacuum is therefore reduced and the measuring point's zero stability improved. Table 3.4-3, which is compiled from extracts from [3-41], contains gaseous release rates for numerous materials, including some after pre-treatment and for different time periods.

Material	Condition	Degassing rate in mbar • l/(s • cm ²) after		
		1 hour	10 hours	100 hours
Aluminum		$1.7 \cdot 10^{-7}$	$2.7 \cdot 10^{-8}$	$4.0 \cdot 10^{-9}$
“	450°C	$1.3 \cdot 10^{-6}$		
“	anodized		$1 \cdot 10^{-7}$	
Al-6061-T6			$2.5 \cdot 10^{-9}$	
“	200°C		$4.5 \cdot 10^{-9}$	
“	13.5h heated to 200°C		$3.7 \cdot 10^{-10}$	
“	300°C		$1.4 \cdot 10^{-8}$	
“	15 h heated to 300°C		$1.6 \cdot 10^{-10}$	
Copper		$2.3 \cdot 10^{-6}$		
“	450°C	$1.6 \cdot 10^{-6}$		
“	450°C, degreased	$1.4 \cdot 10^{-6}$		
Molybdenum		$7 \cdot 10^{-7}$		
Nickel		$6 \cdot 10^{-7}$		
Silver		$6 \cdot 10^{-7}$		
Steel		$5 \cdot 10^{-7}$	$5 \cdot 10^{-8}$	
“	Shot-blasted		$6 \cdot 10^{-6}$	
“	200°C		$8.6 \cdot 10^{-9}$	
“	400°C		$8.4 \cdot 10^{-9}$	
“	15 h heated to 200°C			$4.3 \cdot 10^{-11}$
“	15 h heated to 400°C		$1.2 \cdot 10^{-11}$	
“	450°C	$4.2 \cdot 10^{-7}$		
“	450°C, degreased	$3.6 \cdot 10^{-7}$		
Stainless steel		$2 \cdot 10^{-7}$	$2 \cdot 10^{-8}$	
“	degreased	$3 \cdot 10^{-10}$	$2 \cdot 10^{-10}$	$9 \cdot 10^{-11}$
“	polished, vapor-degreased		$1.4 \cdot 10^{-9}$	
“	400°C	$7.6 \cdot 10^{-10}$		$1.1 \cdot 10^{-10}$
“	after 3.5 h			after 167 h
“	400°C, 24 h heated to 200°C		$1.5 \cdot 10^{-10}$	
“			after 22 h	
“	400°C, 12 h heated to 400°C		$9.3 \cdot 10^{-13}$	
Steel chrome-plated	polished, vapor-degreased	$1 \cdot 10^{-8}$	$9 \cdot 10^{-10}$	
Steel nickel-plated	polished, vapor-degreased	$5 \cdot 10^{-7}$	$1 \cdot 10^{-9}$	
Tantalum		$9 \cdot 10^{-7}$		
Wolfram		$2 \cdot 10^{-7}$		
Zircon		$1.3 \cdot 10^{-6}$		
Araldite D			$1 \cdot 10^{-6}$	$3 \cdot 10^{-7}$
KEL-F (PTFE grease)		$4 \cdot 10^{-8}$		
Teflon (PTFE)	as supplied	$5 \cdot 10^{-6}$		
“		$4.6 \cdot 10^{-7}$	$2.1 \cdot 10^{-7}$	$9 \cdot 10^{-8}$
Mylar	degassed	$2 \cdot 10^{-7}$		
“	as supplied	$3 \cdot 10^{-6}$		
Nylon		$1.2 \cdot 10^{-5}$		
Plexiglas	degassed	$1 \cdot 10^{-6}$		
Polyethylene		$2.6 \cdot 10^{-7}$		
Polyvinylchloride			$8 \cdot 10^{-7}$	$1.3 \cdot 10^{-7}$
“	as supplied	$9 \cdot 10^{-7}$		
Butyl rubber		$1.5 \cdot 10^{-6}$		
Neoprene		$3 \cdot 10^{-5}$	$1.5 \cdot 10^{-5}$	
“	as supplied	$2 \cdot 10^{-4}$		
Silicon rubber	as supplied	$3 \cdot 10^{-5}$		
Porcelain	glazed	$6.5 \cdot 10^{-7}$		
Steatite		$9 \cdot 10^{-8}$		

Table 3.4-3: Gas release rates for various materials in a vacuum (from [3-41]).

3.4.5 Ionizing radiation

The term “ionizing radiation” includes corpuscular and electromagnetic wave radiations. On account of the energy that they contain, they are able to split off electrons from the materials in which they are absorbed. The original electrically neutral atoms therefore become positively charged ions. The number of ion pairs that are produced increases with the intensity, i.e. the dose rate, of the radiation.

The atomic structure and the thickness of the absorbing medium are the main factors determining the absorption of ionizing radiation.

Ionizing radiation includes α -, β - γ - and X radiation as well as proton and neutron radiation.

The radiated energy is usually given in millions of electron volts (MeV). An electron volt (eV) is the energy achieved by one electron when it passes through a potential difference of 1 volt.

$$1\text{MeV} = 10^6\text{eV} = 1.6 \cdot 10^{-13}\text{Nm} = 1.6 \cdot 10^{-13}\text{Ws} = 1.6 \cdot 10^{-13}\text{J}$$

α radiation is corpuscular radiation consisting of rapidly moving helium nuclei. It is produced by natural nuclear disintegration. The penetration through solids for α particles is of the order of a few μm . It then comes to rest and emits secondary γ radiation. The retarded α particle captures two electrons from the medium and becomes a stable helium atom.

β radiation is also corpuscular radiation, but consists of electrons. It penetrates solids up to a depth of a few mm and emits secondary γ radiation on coming to rest.

γ and X radiation have the characteristics of electromagnetic waves. They differ in their wavelengths; γ radiation has a short wavelength, X radiation has a long wavelength. γ radiation occurs both during atomic fission in the reactor and during the atomic disintegration of radioactive substances. It can penetrate deep into materials. Due to the low ranges of α and β particles, γ radiation is the principle radiation which is encountered outside of reactors. As with α and β radiation, it does not lead to artificial radioactivity of the irradiated material.

Neutron radiation is corpuscular radiation without an electrical charge; it consists of neutral atomic particles. It occurs during atomic fission in the reactor and produces artificial radioactivity in the irradiated material. Fast and thermal neutrons can be captured by any atomic nucleus owing to their lack of electrical charge. The atomic mass is thus increased and an isotope of the originally stable element is produced which may be unstable and which may disintegrate through emission of radioactive α , β or γ radiation.

Protons are hydrogen nuclei, having a positive charge. Protons and alpha particles have much higher ionizing densities than electrons due to their mass which is greater by a factor of 10^3 . Therefore they have a correspondingly reduced range for the same kinetic energy.

From the various types of atomic radiation only neutrons and gamma radiation can penetrate deeper than a few centimeters in solid bodies. These types of radiation therefore form the main radiation field in and around an atomic reactor. However, all other types of

radiation are released in the irradiated material by these two types. It is mainly this secondary low range radiation which causes damage.

The mechanism of radiation damage can be explained in the following manner: On penetrating a material, corpuscular radiation transfers energy to the electrons and nuclei of individual atoms which is large enough to break the interatomic bonds within the molecular structure. The broken sections then react chemically with one another, forming bonds which are different to the original ones. The concentration of these impurity bonds rises with the radiation energy and dosage, leading to changes in the material parameters of varying intensity.

Particles which collide with atomic nuclei cause permanent damage. If the collision involves electrons, this leads to

- a. heating effects in metals without serious damage. Work hardening of the material takes place resulting in reduced ductility.
- b. irreversible chemical changes in synthetics, producing permanent damage.

During the irradiation of strain gage measuring points corrosion has also been observed, caused by nitrogen oxide, ozone and water vapor. Also the effect of other gases formed as a result of the radiation of air should also be considered. If the vessel containing the samples is purged with dry helium, the corrosion on electrical connections caused by nitrogen oxide could be avoided.

Very significant differences in the insulation resistance of the strain gage bond and the connecting leads were apparent in a follow-on test when the helium purging was switched off. The initial resistance of 2000 M Ω dropped in the course of 30 days to 3 k Ω . After the helium purging was restarted, the insulation resistance rose to 1000 M Ω within 12 hours [3-27].

3.4.5.1 The effects of ionizing radiation on strain gage measuring points

It is difficult to give firm facts on this subject. The sources available to the author give mainly information relating to individual observations which are applicable to specific cases, but whose results cannot be transferred easily to other situations. The following information should be considered with this in mind.

The effects of ionizing radiation can be divided into four groups:

1. the effects on the measuring grid material
 2. the effects on the measuring grid carrier
 3. the effects on the bonding agent (adhesive)
 4. the effects on the connections (solder pads, cables, etc.)
- A) The following factors determine the degree of influence of radiation:
- a) for the radiation: dosage, flux density, energy (and the energy spectrum), type of radiation.
 - b) for the material: molecular structure, geometry, molecular size, molecular weight, dimensions, volume, thickness and density.

- B) The resistance to radiation can be ranked from good to bad as follows: metals, ceramics, semiconductors, plastics.

The effects of nuclear radiation on the materials forming a strain gage measuring point produce damage in the materials. Here, radiation damage is taken to mean changes in the physical material characteristics as well as the chemical composition.

- a) Metals exhibit a change in their electrical resistance following irradiation. Among the metals used in strain gages the alloys Cu/Ni 45/55 (“constantan”) and Pt/W 90/10 have been found to be relatively stable, whereas the alloy Cr/Ni 80/20 (“Nichrome V”) changes its resistance by a few percent.
- b) Among the semiconductor materials silicon, which is normally used in semiconductor strain gages, exhibits a relatively large change of resistance.

Example:

The resistance change after having received a radiation dose of

$3.5 \cdot 10^{15} \text{ n/cm}^2$ ($E \geq 4.8 \cdot 10^{13} \text{ J} = 3 \text{ MeV}$): +25%,

$4 \cdot 10^{16} \text{ n/cm}^2$ ($E \geq 4.8 \cdot 10^{13} \text{ J} = 3 \text{ MeV}$): +86%.

- c) Strain gage carrier materials and adhesives consist of organic materials. They degenerate to various degrees on being irradiated.

For synthetic materials there is the following ranking for radiation resistance: polyimide, phenolic resin, polyester resin, glass-fiber reinforced silicon resin, epoxy resin, polyethylene, cellulose, silicon, Teflon.

Sometimes after the irradiation has finished, a time dependent partial recovery of the material is observed. Damage occurs through the ionization of the insulating materials, which accompanies the radiation. Therefore, the insulating properties of these materials are lost to some extent and the measurement is affected. The ionization disappears after the irradiation has finished and when the recombination of the molecular structure is concluded.

High radiation resistance is exhibited by high purity bonding agents, e.g. Al_2O_3 , which are applied by flame spray techniques; ceramic putty can also be used. Therefore, free grid strain gages, i.e. strain gages without a measuring grid carrier, which are bonded with ceramic bonding agents are better suited for use in radiation fields than normal strain gages.

Example:

A strain gage bonded with ceramic putty and having a constantan measuring grid exhibits an average drift of $2 \mu\text{m/m}\cdot\text{n}^{-1}$ over a period of 150 hours in neutron radiation of $10^{13} \text{ n}/(\text{cm}^2\cdot\text{s})$.

- C) Results of irradiation of a measuring point
- a) The bond between the strain gage is damaged or destroyed. The following ranking applies for the radiation resistance of bonding agents: ceramic bonding agents, hot curing organic adhesives, room temperature curing adhesives.

- b) The insulation resistance of the measuring grid carrier, the adhesive and the cable sleeving falls. Resistance changes in the strain gage can be compensated in part by half or full bridge circuits. Weldable strain gages in a full bridge circuit have proved satisfactory where ceramic bonding is used between the measuring grid and the weldable carrier.
- c) Particularly strong ionization occurs in the region of solder pads. Other damaging effects can be expected due to flux residues. Welded connections should be used exclusively.
- d) Stray currents flow in the circuit as a result of ionization.
- e) The resistance and gage factor of the strain gage change.

Summary

The following is recommended for strain gage measurements made under the effects of radiation:

- a) free-grid strain gages with measuring grids of constantan or the PtW alloy 1200 (e.g. series LF 30);
- b) attachment with Rokide ceramic using the flame spray method or with ceramic putty, e.g. CR 760, or use weldable strain gages;
- c) spot welded lead connections;
- d) ceramic cable insulation;
- e) use full or half-bridge circuits if possible.

See [3-42].

D) Some information on the effects of ionizing radiation.

- a) The radiation resistance of synthetic materials.

The critical dose for synthetics is about $10^4 \dots 10^5$ J/kg. The radiation resistance of synthetics can be increased by filling materials such as metal oxides and minerals.

Synthetic material	Critical dose [J/kg]
PVC	$10^5 \dots 10^6$
Vinyl	$10^5 \dots 10^6$
phenolic resin cement (BC 6035 adhesive)	10^3
Teflon	10^2
cellulose adhesive (Duco)	10
silicone resin with asbestos	$1 \dots 2 \cdot 10^6$
epoxy resin with metal oxide	$10^5 \dots 10^6$

Table 3.4-4: Critical radiation dose for some synthetic materials.

Note:

There is a large variation of terms used for radiation energy doses. The following are approximately equivalent with regard to their effects:

1 J/kg	joule per kilogram) (SI unit)
$1 \cdot 10^2$ rad	(radiation absorbed dose) (gray)
$1 \cdot 10^4$ erg/g	(erg per gram)
$1.2 \cdot 10^2$ r	(roentgen)
$1 \cdot 10^{12}$	(thermal neutrons/cm ²)
$2.8 \cdot 10^{10}$	(fast neutrons/cm ²)
$1.4 \cdot 10^{11}$	(gamma photons/cm ²)
$5.2 \cdot 10^9$	(electrons/cm ²)

- b) For the effects of gamma radiation on the various components of a strain gage measurement point see Table 3.4-5.

Designation	Radiation dose y [J/kg]
1. Strain gage	
1.1 Open strain gage with constantan measuring grid	1·10 ⁶ is regarded as a safe operating limit 4·10 ⁶ possible strain gage failure
1.2 Strain gage with encapsulated constantan measuring grid	2 to 4·10 ⁶ safe operating range 6·10 ⁶ possible strain gage failure
2. Measuring grid carrier material	
2.1 Epoxy resin, open measuring grid	4·10 ⁶ maximum limit for safe operation
2.2 Polyimide	10 ⁹ without reduction of insulation or physical damage
2.3 Glass-fiber reinforced epoxy resin, encapsulated measuring grid	5·10 ⁴ safe operating range
2.4 Glass-fiber reinforced phenolic resin, encapsulated measuring grid	3 to 4·10 ⁵ maximum dose 6·10 ⁶ maximum dose
3. Measuring grid alloys	
3.1 Constantan, open measuring grid	1·10 ⁶ safe operating range 4·10 ⁶ possible strain gage failure
3.2 Constantan, encapsulated	2 to 4·10 ⁶ safe operating range 6·10 ⁶ maximum dose
3.3 Karma, encapsulated	5·10 ⁴ safe operating range 4·10 ⁵ possible failure
4. Adhesive	
4.1 Epoxy resin adhesive	6·10 ⁶ maximum dose
5. Strain gage covering material	
5.1 Silicone rubber	4·10 ⁶ beginning of hardening 6·10 ⁶ completely hard, bonding to the object may loosen
6. Insulation	
6.1 Teflon (PTFE)	1·10 ⁴ safe range 1·10 ⁵ upper limit 2·10 ⁵ formation of cracks
6.2 Polyvinyl Chloride	8·10 ⁵ safe range 1·10 ⁶ white PVC darkens 6·10 ⁶ maximum dose
6.3 Glass-fiber mesh	5·10 ⁴ safe range 4·10 ⁵ upper limit
7. Solder	
7.1 Tin-lead solder	2·10 ⁵ upper limit
7.2 Silver-solder paste	5·10 ⁴ normal range
7.3 Spot or gas welding	3 to 4·10 ⁵ upper limit 6·10 ⁶ approx. upper limit

Table: 3.4-5: Resistance of parts of a strain gage measuring point to gamma radiation.

3.4.6 Magnetic fields

Four effects appear during strain gage measurements in magnetic fields:

- the magnetostriction of the test object to which the strain gage is bonded,
- the magnetostriction of the gage's measuring grid material,
- the magnetoresistive effect of the measuring grid material,
- induced electrical voltages in the strain gage and its circuit due to pulsing or changing magnetic fields.

With ferromagnetic materials exposed to magnetic fields magnetostriction leads to changes in dimensions which are transferred to the bonded strain gage .

If the strain gage itself is subject to the magnetostriction, then it gives incorrect measurement indications. This effect occurs only with paramagnetic measuring grid materials.

The magnetoresistive effect is the change in resistance of an electrical conductor caused by the influence of a magnetic field. This effect is seen with almost all ferromagnetic conducting materials. It was the subject of various investigations on strain gages. The ferromagnetic alloy “isoelastic”, which is still used in America, exhibits strong effects.

The copper-nickel alloy “constantan”, which is widely used in Germany for the manufacture of strain gages, has been found by various authors to be insensitive or only very slightly sensitive. The differences in this assessment may be caused by differences in the alloy composition of the “constantan” material supplied by various manufacturers and by the strength of the magnetic field in which the strain gage is tested. In [3-43] information is given on the investigations in the magnetic field of the Berkeley “Bevatron” proton accelerator with flux densities up to 2 Tesla (= 20000 Gauss).

No effects due to the magnetic field were observed on strain gages with measuring grids of constantan or the alloy Pt/W 90/10.

It is difficult to draw clear conclusions from the available information, because the results do not provide a unified picture. This may be due to different test conditions, the lack of adequate information regarding measurement equipment or also to the inability to separate the effects described at the beginning of this section.

In [3-44] information is provided on the strain gage investigations in the field of the Saturn synchrotron. The magnetic field with a flux density of 1.5 T (15000 Gauss) builds up in 0.8 seconds and decays in the same time. The cycle is repeated every 3.2 seconds. The strain gages under investigation originated from two unnamed sources, In order to eliminate the magnetostriction of the component, the strain gages were fixed to non-magnetic materials (copper, plexiglas, etc.). The direction of the strain gages' measuring grids was oriented in part parallel and in part perpendicular to the direction of the magnetic flux. The strain gages were at times connected in quarter bridge arrangements and sometimes in half bridge arrangements; the latter arrangement was used to ascertain the degree of compensation. A dc supply was used; the polarity was changed during the investigation to isolate the signal caused by the magnetic field from the other effects. The interference level did not exceed 7 $\mu\text{m/m}$. Table 3.4-6 shows the measurements obtained.

Strain gage supplier	Strain gage arrangement and alignment of measuring grid to flow direction	Magnetic flux density, Tesla					
		0.26	0.6	1	1.4	1.6	2
		Zero-point displacement, $\mu\text{m/m}$					
1	1 strain gage \perp	8	70	95	110	130	185
	1 strain gage \parallel	4	12	18	22	28	35
	2 strain gage \perp	Compensation					5
	2 strain gage \parallel						5
2	1 strain gage \perp	2	8	10	12	16	20
	1 strain gage \parallel	5	8	10	12	15	20
	2 strain gage \perp	Compensation					3
	2 strain gage \parallel						3

Table 3.4-6: Zero-point displacement of strain gages in a static magnetic field (from 3-44).

Details of further relevant literature are given in [3-45 to 3-48].

With semiconductor strain gages the size of the magnetoresistive effect depends on the mobility of the charge carriers. It is given by the following equation

$$R = R_0 (1 + \beta^2 B^2) \tag{3.4-2}$$

- R electrical resistance
- R_0 resistance without magnetic effects
- β mobility of the charge carriers
- B magnetic flux density

Pulsing or varying magnetic fields induce voltages in electrical conductors and these are then transferred as errors in the measurement signal. To prevent this, non-inductive strain gages are sometimes used where two halves of the measuring grid are wound in opposite directions or the strain gage is magnetically screened in mumetal foil or by a cover. Non-inductive twisted or magnetically screened cable is used for wiring. Carrier frequency measuring amplifiers present particular advantages in such cases. In contrast to direct voltage amplifiers they eliminate all voltages whose frequencies are located outside of their bandwidth, see section 5.3.

The measurement engineer is seldom confronted with such large magnetic fields. Table 3.4-7 enables a rough estimation of the intensity of magnetic fields to be made (from [3-48]).

The magnetic field strength H in the region of a conductor can be calculated according to the equation

$$H = \frac{I}{2\pi r} \tag{3.4-3}$$

- I = current
- r = radius

Flux density B in millitesla [mT]	Emanating source
low (≤ 2)	power transformers, fluorescent lights and power cables at about 1 m distance; soldering irons at 2...4 m distance; electric motors.
medium (2... 50)	all previously mentioned objects nearer than 1 m; soldering irons at 15 cm...2 m; busbars, cables, connections etc. carrying a current of ≥ 5000 A at 3...15 m distance or 1000 A up to 2 m distance
high (50... 3200)	vibration table within 3 m; electric motors and generators in immediate vicinity

Table 3:4-7: Flux density, i.e. intensity, of magnetic fields (from [3-48]).

The magnetic flux density B is

$$B = \mu \cdot \mu_0 \cdot H. \quad (3.4-4)$$

- μ = permeability of the test object's material ,
 μ_0 = permeability of free space
 H = magnetic field strength

The magnetic flux is situated in a circumferential direction for a straight conductor.

3.4.7 Storage

Under normal conditions strain gages can be stored indefinitely. For protection against mechanical damage they should be left in their original packing until required for use. Temperature variations due to the weather cannot affect strain gages. Strain gages should be protected from moisture; they are manufactured in standard conditions of 23°C and 50% relative humidity according to DIN 50014. Deviations from the relative humidity value of 50% may lead to insignificant changes in the electrical resistance. High values of humidity are more critical, because they may lead to corrosion damage if they are continuous. Similarly, the direct effects of water, acids, bases, reactive gases, contaminant materials and nuclear radiation are potentially damaging.

The following restrictions for some special strain gages are exceptions to the above:

Free-grid strain gages have a self-adhesive strippable carrier and the adhesive layer dries out in the course of time, losing its adhesive properties. Therefore,

- a) for flame deposition bondings (Rokide) a maximum storage period of 6 months is specified.
- b) for putty bondings (CR 760) a storage period of at least 1 year is stated.

The strain gage itself is not subject to ageing.

Encapsulated strain gages with metal or rubber-type encapsulation can be stored indefinitely. Weldable strain gages should be stored as normal strain gages.

4 Materials used for mounting strain gages

Mounting materials include the materials used for fixing the strain gage to the measurement object, for connecting up the strain gage and material used for the protection of the measuring point. The mounting of the strain gage itself is a task that requires extreme care. Only correctly mounted strain gages can operate properly.

It is therefore essential that the instructions for mounting the strain gage and those for using the mounting materials are followed. It must be borne in mind that the results of a measurement may possibly affect the lives and health of many people.

Training in mounting techniques is recommended in the form of special courses arranged by HBM and the Institutes of Engineer and Technician Training. Details on application techniques are not dealt with in this publication. The reader is referred to the publication [4-1] which gives comprehensive instructions on the mounting of strain gages; certain passages from it are cited here.

4.1 Strain gage bonding materials

The bonding materials have the task of holding the strain gage firmly to the surface of the test object and of transferring its deformation without loss to the strain gage. Various fringe conditions and influencing variables together with widely different fields of use require various fixing materials and methods of application. The use of adhesive is the most significant method employed but spot welding and fixing with ceramic materials is also used.

The particular advantages of adhesives with regard to their use in strain gage bonding are:

- The possibility of bonding different materials. Depending on the adhesive, the bonding is carried out at room temperature or at a higher temperature.
- There is no effect on the materials to be bonded, although there may be restrictions with synthetics.
- Chemically curing adhesives (it is only these which have a role to play in strain gage techniques) exhibit low absorption of moisture.
- Control of the rate of curing by selection of different types of adhesives or different curing conditions, e.g. hot or cold curing.
- High resistivity contributes to high insulation resistance between the strain gage and the component.

The particular suitability of adhesives for strain gage mounting is also an advantage, i.e. they must be able to correctly transfer the strain in the test object to the strain gage. The

transfer process is illustrated schematically in section 3.2.1.1, Fig. 3.2-2. The force needed to strain the strain gage is taken from the test object and transferred to the strain gage by the adhesive layer. Hence, shear stresses arise in this layer, the size of the stresses being dependent on the force to be transferred and the transfer area. Due to the elasticity of the adhesives distortion of the layer occurs which is greatest at the edges in the strain direction and which decreases towards the center. This distortion determines the length of the transition sections in Fig. 3.2-2. With soft adhesives and thick layers this results in the strain on the strain gage side of the layer being smaller than that on the side in contact with the test object. An attempt has been made to illustrate this in Fig. 4.1-1a. In the left half of the illustration the vertical lines in the adhesive layer indicate the direction of the cross-sectional planes in the unstrained state. The right halves of the illustration show the same object in the strained condition. The cross-sectional planes now lean progressively more towards the edges. This indicates that the adhesive does not fully transfer the strain in the test object to the strain gage.

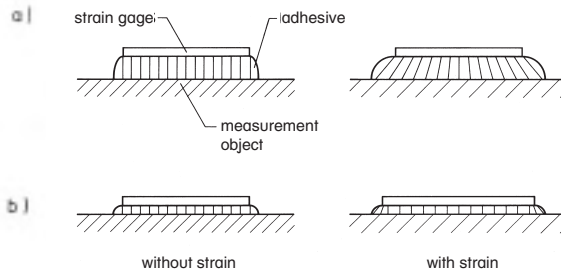


Fig. 4.1-1: Transfer of strain from the component to the strain gage through the adhesive.
 a) unsuitable (too soft) adhesive with a layer that is too thick
 b) suitable adhesive with a thin layer.

However, if hard adhesives are used, i.e. adhesives with a high Young's modulus, together with a thin adhesive layer then the distortions within the layer are much smaller and are mainly restricted to the outside sections. This situation is shown in Fig. 4.1-1b. In this case the transition distances are small and the strain transfer is correct.

The bonding between components depends on the adhesion between the adhesive and the surfaces wetted by the adhesive. Adhesion arises chiefly due to attraction forces between neighboring molecules. The amount by which the adhesive clings to the pores of the roughened surfaces of the joint or responds to capillary action is only slight. The increase in bonding strength which can be observed with moderate roughening of the joint's surfaces is due to the increase in contact area thus produced and not due to "mechanical adhesion".

The cause of the adhesion is complex and only partially understood [4-2, 4-3]. A significant contribution to the bonding forces is made by adsorption, sometimes referred to as "partial valency formation", together with slight chemical bonding, i.e. through primary valency bonding and other sources of energy.

Under the term “*Van der Waals forces*” different types of bonding mechanisms in the adsorption region are summarized which can be subdivided into mainly three types of effect:

- The dipole moment (Keesom forces). If the positive and negative charges in a molecule are asymmetrically distributed, then although the molecules are in total neutral, they possess an electrical dipole moment and are polar. Neighboring molecules attempt to align their dipole moments so that the positively charged side of one molecule is turned to the negatively charged side of the neighboring molecule and vice versa. The average range of Keesom forces is 0.4 to 0.5 nm ($1 \text{ nm} = 10^{-9} \text{ m}$).
- The induction effect (Debye forces). If the charge center of the electric field of a molecule is displaced by the inductive effect of an external field, e.g. of another molecule, then similar interactive effects are produced. In contrast to Keesom forces, with Debye forces one particle has a permanent dipole and the other an induced dipole moment. The average range of Debye forces is 0.35 to 0.45 nm.
- The dispersion effect (London forces). This effect has been indicated by the theory of wave mechanics, where, due to the continuously changing surface probability of the centers of electrical charge, an “in phase” oscillating system of two particles arises, which continuously and mutually induce a dipole. The average range of London forces is 0.35 to 0.45 nm.
- “Hydrogen bonding” has a special place within Van der Waals forces. This also involves the interactive effects of dipoles, but has the feature that the positive pole of at least one dipole is formed by a hydrogen atom. The range of hydrogen bonding is 0.26 nm to 0.3 nm. The portion due to chemical bonding forces, i.e. primary valency bonds, is still not clear. It would appear from what is known that the contribution to adhesive forces is slight.

The working conditions at the mounting point and different requirements on the performance of the bonding agent, above all with regard to service temperature, form the reason for the wide range of fixing materials available. The same applies to the strain gage itself. There are therefore combinations of certain ranges of strain gage and certain types of adhesive having optimum characteristics within a limited area of application. For other combinations with different performance capabilities the application limits are decided by the component with the narrower range of performance. There are of course strain gages and fixing materials whose combination is not possible due to technical reasons. Therefore the recommendations in the product literature and technical data sheets should always be followed.

A special warning is given against the use of an adhesive other than the one which is recommended. Strain gage adhesives must fulfill requirements above those of normal joining adhesives. They are therefore usually produced as a result of special development or are at the least modifications of normally available adhesives. That a strain gage is firmly bonded is itself not an adequate criterion for assessing the suitability of an adhesive for measurement purposes.

The following mounting techniques are used:

- cold curing adhesives
- hot curing adhesives

- ceramic putty
- flame deposited ceramics
- spot welded joints.

- Cold curing adhesives can be used easily and with little effort. There are one part adhesives, which, for example begin to react by the elimination of air (“anaerobic”) and two part adhesives which must be mixed before being applied. “Rapid adhesives” are those having short reaction times. They are preferred in experimental analysis and allied fields.

- Hot curing adhesives are only used where the test object can be subjected to the required hardening temperature. This is usually possible in the manufacture of transducers and is very often the case where machine parts, etc. can be fitted with strain gages before being assembled or can be taken out to have them fitted. In contrast to cold curing adhesives those for hot curing give a wider range of application at higher temperatures and are suitable, when used with precision strain gages, for satisfying the demands for high accuracy that are usual in transducer construction. Both one and two part versions of hot curing adhesives are used.

- Ceramic putty is only used in conjunction with special strain gages, i.e. open-grid strain gages. Its preferred field of use is at high temperature ranges and sometimes in the cryogenic temperature range. Ceramic putty requires somewhat high baking temperatures and this restricts its area of application. High hygroscopicity leads to zero point stability problems in the range between freezing point and the water vaporization point, requiring effective protective measures.

- Flame sprayed ceramics are intended for the same special strain gages as ceramic putty and they also need special equipment. The field of application is similar to that of ceramic putty. A particular advantage of this method is that the test object is only moderately heated during the bonding process. The hygroscopic properties of flame sprayed bondings are the same as for ceramic putty. This type of bond has favorable properties against nuclear radiation.

- Spot welding is one of the simplest fixing methods. It requires the minimum of equipment, i.e. a small welding unit, only a slight amount of preparation and little practice. Despite this the method is seldom used and for the following reasons:

Special strain gages are required which are only produced in a limited number of types.

Weld-on strain gages cannot be used on curved surfaces, nor can they be made very small, which restricts their field of application still further.

The test object must consist of a weldable material. On some weldable test objects this type of fixing is rejected due to the risk of microcorrosion, e.g. with highly stressed sections of steam cylinders, with austenitic steels, etc. The test object must be strong enough, i.e. sufficiently thick, so that the stress distribution in it is not modified due to the relatively large restraining force of the strain gage. There should not be any noticeable restriction of strain.

4.2 Mounting materials

4.2.1 Cleaning agents

Various actions are necessary for the preparation of the mounting point.

Mechanical cleaning methods and commercially available household cleaning agents are suitable for *rough cleaning*.

For *fine cleaning* organic solvents are preferred. Table 4.1-1 lists some usual agents along with the MAK number which indicates the maximum concentration permitted at the place of work. The remarks “highly flammable” and “dangerous to health” have been taken from

General designation or commercial name	Other chemical designation	Chem. formula [total formula]	Max. conc.: at work place		Remarks
			ppm	$\frac{\text{mg}}{\text{m}^3}$	
Frigen 113 Cr® Freon TF®	1,1,2-trichloro-1,2,2-trifluoroethane	$\text{CCl}_2\text{F} \cdot \text{CClF}_2$ [$\text{C}_2\text{Cl}_3\text{F}_3$]	1000	7800	non-flammable; does not attack plastics or only a little; vapors should not be allowed to become heated above 300°C!
Methyl ethyl Ketone		$\text{CH}_3 \cdot \text{CH}_2 \cdot \text{CO} \cdot \text{CH}_3$ · [$\text{C}_4\text{H}_8\text{O}$]	200	590	highly flammable
Acetone Ketone	Acetone	$\text{CH}_3 \cdot \text{CO} \cdot \text{CH}_3$ · [$\text{C}_4\text{H}_8\text{O}$]	200	590	highly flammable
Isopropyl alcohol	Isopropanol	$\text{CH}_3 \cdot \text{CH}(\text{OH}) \cdot \text{CH}_3$ · [$\text{C}_3\text{H}_8\text{O}$]	400	980	highly flammable
Ethyl alcohol	ethanol	$\text{CH}_3 \cdot \text{CH}_2 \cdot \text{OH}$ · [$\text{C}_2\text{H}_6\text{O}$]	1000	1900	highly flammable
Ethyl acetate	Ethyl ester of acetic acid	$\text{CH}_3 \cdot \text{CO}_2\text{C}_2\text{H}_5$ · [$\text{C}_4\text{H}_8\text{O}_2$]	400	1400	highly flammable
Perchloro-ethyl.	1,1,2,2-tetrachloro-ethylene	$\text{CCl}_2 \cdot \text{CCl}_2$ · [C_2Cl_4]	100	670	health risk; gas-air mixture explosive
Methylene chloride	Dichloromethane	$\text{CH}_2 \cdot \text{Cl}_2$ · [CH_2Cl_2]	200	720	health risk; gas-air mixture explosive
Toluol	Methyl benzol	$\text{C}_6 \cdot \text{H}_5 \cdot \text{CH}_3$ · [C_7H_8]	200	750	health risk; highly flammable
pure benzene	-	-	*	*	highly flammable * official figures are not available
Chlorothene NU®	1,1,1-trichloroethane	$\text{CCl}_3 \cdot \text{CH}_3$ · [$\text{C}_2\text{H}_3\text{Cl}_3$]	200	1080	health risk

Table 4.2-1: Solvents used for cleaning and degreasing strain-gage measuring points

the “Regulation on dangerous materials at the place of work”, Federal Law Document I, page 2493 of 8th September, 1975 and should indicate the safety measures to be adopted.

Some of these solvents are available as being “technically pure” and “chemically pure”. Technically pure means free from solid impurities. Chemically pure, also identified by the phrases “pro analysi” or “p. a.” or “high grade”, means that it is free from soluble impurities within the scope of the techniques available. In spite of the high price of chemically

pure solvents, it is only these that should be used for cleaning strain gage measurement points. When using them, extreme care should be taken to ensure that they do not become impure due to negligence, rendering them unusable.

4.2.2 Soldering agents

4.2.2.1 Soldering devices

The best and by far the most popular type of electrical connection between strain gages and measurement leads is soldering. Similar excellent results can be obtained with crimp techniques, i.e. pressed connections. Screw terminal connections can cause changes in zero stability due to varying joint resistances. Plug connections are more critical still; here high quality gold-plated contact elements have proved satisfactory, provided their proper functioning is not impaired through contamination. In principle normal power connections are not adequate on account of the low voltage and current of the measuring signal.

The demands of the electronic industry have led to excellent designs of soldering iron of which the strain gage user should take advantage. Temperature controlled, low voltage soldering irons, which are supplied from the line through a control unit, are recommended. Models with a fine, continuous electronic control and a high heating capacity of about 50 W are preferred, because heat extracted from the point of the soldering iron is replaced immediately. The temperature control region for normally available soldering stations is between 120°C and 400°C; this is sufficient for the soft solders employed in strain gage techniques.

The selection of the correct soldering iron bit for the appropriate field of application is an important factor in the production of reliable soldered joints. The bit should not be too pointed since the heat flow from the iron to the joint is not sufficient and because the solder is withdrawn upwards away from the joint, leaving insufficient solder at the joint. A small area at the tip, appropriate to the size of the object to be soldered, is correct. Whether straight or bent soldering iron bits are more convenient depends purely on the accessibility of the solder joint.



Fig. 4.2-1: Controllable soldering station

Tempered soldering iron bits only take up solder at certain points and the solder remains on the part of the bit used for soldering. The treatment also prevents the bit from oxidizing.

4.2.2.2 Solders and fluxing agents

There are numerous soft solders available. They are optimum for certain requirements depending on their alloying components and composition. In strain gage techniques good wetting and flow properties are, needed as well as a melting temperature appropriate to the application conditions. The service temperature should not be higher than about 30 K below the melting point of the solder on account of the mechanical strength of the soldered joint which has a eutectic solder alloy composition.

Low concentrations of copper additive prevent excessive degradation of the solder tip ("copper protective solder"). For continuous dynamic loading solders with a high resistance to fatigue are of advantage. Some normal soft solders are listed in Table 4.2-2. Further information is given in DIN 1707 and in the lists from solder manufacturers. Welded joints are used if possible in the high temperature range. Hard solders should be used with care due to their reactive nature.

Fluxing agents have the task of freeing solder joints of oxide and of preventing re-oxidation during the solder process. They therefore provide the conditions for a perfect joint between the solder and the parts to be soldered. The choice of fluxing agent must be made depending on the type of solder (e.g. soft solder), the type of materials to be soldered, (heavy metals) and the type of object to be soldered, (electrical circuits) .

Solder designation	Alloy constituents %					Melting range °C	Recommended soldering temp. °C	Remarks
	Sn	Pb	Cu	Ag	In			
Flux-cored solder L-Sn 60 Pb Cu2/F-SW 32 (C3) 3.5; dia 1mm	60	38	2			183...190	230	order no.: 8-8403.0004 resin core of pure colophony, corrosion-proof
Doduco-Ceramin soft solder CN 306 0.8 mm dia., solid	1	97.5		1.5		304...310	360	Dr. E. Duerrwächter Doduco-KG P.Box 480, 7530 Pforzheim; heat-resistant solder
Lead-indium solder 50/50 dia. 0.5 mm, solid		50			50	190...210	250	good fatigue resistance; with continuous dyn. loads recommended for use with LY41, LY43 ranges of strain gages. Contained in WL521 Solder Set, order no.: 214.04-2009

Table 4.2-2: Examples of soft solders

Strongly corrosive fluxing agents are convenient, because they enable soldering to be carried out on poorly cleaned surfaces, but the disadvantage is that residues cause inevitable corrosion and the insulating properties of insulation sections are reduced. They are therefore unsuitable for soldering electrical circuits. Solder-paste should never be used.

The manufacture of non-corrosive fluxing agents is based on natural or modified natural resins. The best known is colophony. It is used as the flux core in tubular solder or is dissolved in spirit as a liquid. These “soft” fluxing agents demand thorough cleaning and smoothing of the solder joint immediately before soldering. They are very suitable for strain gage techniques.

Note:

The flux core in many tubular solders can comprise corrosive as well as non-corrosive fluxing agents. The type of fluxing agent should be ascertained before use. The standard document “DIN 8511: Fluxing agents for soldering metallic materials” gives information on the various fluxing agents. Page 2 deals with fluxing agents for the soft soldering of heavy metals.

Fluxing agents with the type abbreviation F-SW 31 and F-SW 32 do not leave any corrosive residues. The designation “acid-free fluxing agent” is unclear and leads to confusion. Therefore, according to DIN 8511 the term should not be used.

4.2.3 Connection methods

4.2.3.1 Solder terminals

Solder terminals have the task of providing a firm anchor point between the strain gage and the cable. They are manufactured in various versions and sizes. Fig. 4.2-2 illustrates examples of a few typical versions.

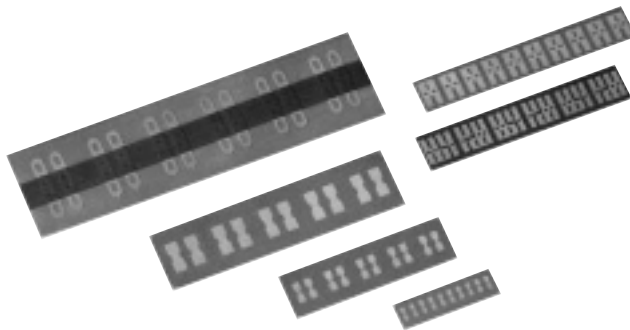


Fig. 4.2-2: Some types of solder terminals

The solder terminals are fixed immediately adjacent to the strain gage, usually using adhesive and the operation is most practically carried out during the mounting of the strain gage. For special types used at high temperatures spot welding is used. Details on shapes, technical data and fields of application can be obtained from the manufacturers' literature and [4-1].

4.2.3.2 Lead material

The success of the measurement also depends on the choice of the correct connecting leads and test cable, i.e. ones suitable for the specific application. They should not only transfer the measuring signals between the links in the measurement system, i.e. transducer - amplifier - output, but they should also restrict interference signals to a minimum and resist operational stresses and the effects of environmental conditions.

Short connections, e.g. the internal wiring within a transducer, can be made with jumper wire or stranded hook-up wire with a relatively thin cross-section. The core insulation must be adequate and able to withstand the temperatures that are likely to occur. In addition good solderability of the cores is needed. For extreme dynamic loading of the test object vibration resistant wire can be of advantage. This wire consists of one core of many very thin strands surrounded by flexible insulation.

Longer leads and cables must fulfill additional requirements. Here, the resistance must be kept in acceptable bounds through the correct choice of the conductor cross-section. Low capacitance cable is recommended for carrier frequency operation and also for direct voltage operation if high frequency signals must be transferred. A copper braid screen surrounding the core assists in maintaining the capacitance of the cores symmetrical to one another and provides protection by electrical screening against the interference effects of electric fields. For screening against magnetic fields the cable is laid in steel armored conduit or similar, see sections 7.2 and 7.4.

Electrostatic influences arise if the electric field from a voltage source has a capacitive effect on the measuring circuit. The best protection against this is to surround the cable or lead with an enclosed screen. Copper wire braiding usually gives sufficient screening. Special measurement cable has this type of screen. Grounding of the screen is important, because a screen with a floating potential has no effect.

Electromagnetic influences occur if cables in the measuring circuit are laid in the vicinity of current carrying conductors or electrical equipment, e.g. generators, welding units, transformers, motors, etc. Electrical interference voltages are induced in the measurement cable due to the transformer principle. Twisted cores provide effective protection and cable is manufactured with the cores already twisted. Where this is not sufficient, additional screening with steel armored conduit or gas/water conduit gives improvements.

The carrier frequency method (see section 5.3) is much less sensitive to stray interference effects than the direct voltage method, because the former method eliminates all interference frequencies outside the transmission band.

Material name	PVC polyvinyl chloride	PE polyethy- lene (low density)	PTFE polytetra- fluoro- ethylene (Teflon [®])	PUR poly- urethane	SIR silicone rubber	PA polyamide	Pi polyimide	Glass-fiber braiding	Glass-fiber tube	Seatite beads
Criterion										
heat resistance °C continuous short-term	-50...80 ...90	-80...80 ...100	-100...260 -269...300	-60...90 ...100	-80...180 ...250	-55...105 ...125	-269...275 ...400	-269...280 ...480	-269...400 ...600	>600
spec. volume resistance at 20°C Ωcm	10 ¹⁴ ...10 ¹⁵	10 ¹⁶	>10 ¹⁸	10 ¹¹ ...10 ¹⁴	10 ¹⁴ ...10 ¹⁵	10 ¹² ...10 ¹³	10 ¹⁴ ...10 ¹⁶	-	-	-
abrasion resistance	average	average	poor	very good	poor	very good	very good	poor	poor	very good
flammability ¹⁾	se	fl	nfl	se	se	sfl	se	nfl	nfl	nfl
resistance to diluted acids and alkalis	good	very good	²⁾ very good	partly resist	³⁾ good	non-resist good	very good poor	good	good	very good
oil solvents	poor most non-resist	good non-resist	very good very good	good non-resist	non-resist partly resist	good good	good most resist	very good very good	very good very good	very good very good
Water absorption %	1...2	0	0	1.4	0.1...0.4	2...10	1...3	-	-	-

1) se = self-extinguishing
 fl = flammable
 sfl = slightly flammable
 nfl = non-flammable
 2) non-resistant to molten alkalis and fluorine
 3) non-resistant in vapor above 130°C

Table 4.2-3: The most important cable and lead insulating materials and some of their technical data

It is important that the core insulation has a high value which should not change significantly due to temperature, moisture, etc. When half and full bridge circuits are connected, much depends on the symmetry of neighboring arms of the bridge with regard both to the resistance and also the cable capacitance between the cores, see sections 7.2 to 7.4. The cable covering should protect against external effects and should be resistant against moisture, water, oil, chemicals, both high and low temperatures and mechanical loading. Commercially available measurement cable meets many of these requirements, but unfortunately there is no cable that satisfies all of them.

The most important insulation materials with some information on their characteristics are listed in Table 4.2-3.

4.2.4 Methods of testing

Every strain gage measurement should be checked for correct mounting and other important features before measurements are made. Visual and electrical tests should be carried out.

4.2.4.1 Visual inspection

As an aid for checking purposes, a magnifying glass giving about 6x enlargements is sufficient. Faults in the strain gage bonding can be found in this way, such as for example:

- air bubbles under the strain gage,
- badly bonded edges,
- unreliable solder connections,
- flux residues and
- positioning errors.

This inspection can be supplemented with the “Eraser Test” [4-1].

4.2.4.2 Electrical continuity

Here a good ohmmeter is sufficient with which the strain gage resistance can be measured with an error of $< 1/4\%$. The test should show whether the gage resistance has altered as a result of improper mounting. Ohmmeters with a resolution down to 0.1Ω are also suitable for use prior to mounting for finding a strain gage with the correct resistance; this method is recommended in the construction of transducers in order to obtain good symmetry in the bridge circuit.

The resistance of the cable connecting the strain gage results in an apparent reduction in the gage's sensitivity using normal measurement systems with constant voltage supply. It should therefore be measured and the value used for the correction of the strain measurement, see section 7.2. The cable resistance is automatically compensated by equipment which operates on the principle of the “Kreuzer Circuit” for full or half bridge circuits or on the principle of the “extended Kreuzer circuit” for quarter, half and full bridge circuits. These circuits render a correction unnecessary, see section 7.3.

4.2.4.3 Insulation resistance

For the measurement of the insulation resistance between the strain gage and the test object and between the cores of the cable and the screening, instruments with a test voltage below 50 V and with a measurement range up to 20,000 M Ω or more are suitable. Hand-cranked generators are unsuitable.



Fig. 4.2-3: TO3 Pocket Ohmmeter for the measurement of the electrical continuity and insulation resistance of applied strain gages.

Under certain conditions there is a dependence of the insulation resistance on the type of test voltage, i.e. whether it is a direct or alternating voltage and the frequency where alternating voltage is used. The level of the applied voltage and the temperature of the insulator being measured also have an influence. Therefore, particularly at high temperatures in ceramic bonding agents, ion migrations occur, leading to incorrect measurements [4-4]. However, this also affects other insulating materials. There is a simple method of determining the insulation resistance of the strain gage under the conditions of the strain measurement. The measurement amplifier itself is used for this purpose. The method is in a way the reverse of the shunt calibration described in section 6.3. A separate bridge or half bridge circuit is wired in parallel to the insulation resistance to be measured and the strain indication is observed; it is a measure of the insulation resistance.

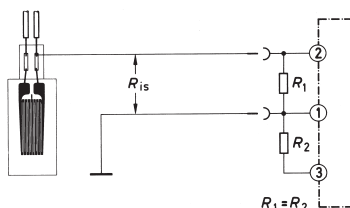


Fig. 4.2-4: Circuit for measuring the insulation resistance of strain gages with a measurement amplifier. The auxiliary circuit R_1 , R_2 can also be formed as a full bridge.

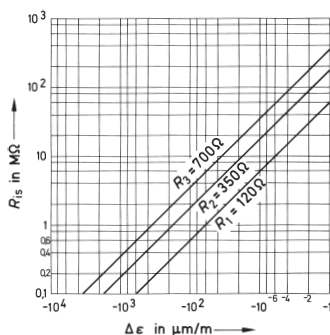


Fig. 4.2-5: Diagram for determination of the insulation resistance of a strain gage application.

Fig. 4.2-4 shows the circuit. The auxiliary circuit which is unbalanced by the insulation resistance R_{ins} (here a half-bridge circuit, R_1 , R_2) may consist of strain gages or stable resistors.

The diagram in Fig. 4.2-5 is used for the simple determination of the insulation resistance R_{ins} . Here, the resistance values of commercially available strain gages are recorded as parameters. The diagram is based on the equation (6.3-9a) and a gage factor of $k = 2$. The measured strain value is found on the $\Delta\epsilon$ scale, the point where the vertical line cuts the relevant parameter is identified and the insulation resistance is read off at this level on the R_{ins} scale.

4.3 Protection of the measuring point

Strain gage measuring points must be protected against mechanical or chemical damage. Even under ideal conditions, e.g. in the laboratory, the characteristics of the measuring point would be influenced in the course of time if suitable countermeasures were not taken. The measures used to protect measuring points are as widely varied as the different influences on the strain gage. In the laboratory where there is uniform dry air, light protection against contact, i.e. moisture of the hand, is sufficient, whereas in a rough rolling mill the protection must cover steam, water, oil, heat and mechanical effects. In the former case a

simple coating of varnish is sufficient, but in the latter case a number of layers of different protective materials are used to form a barrier.

However, it should be clear that absolute protection for an unlimited period of time is only possible using hermetically sealed encapsulation. This method of protection is therefore used in commercially available transducers where operation permits it. All other covering methods, even the best, only guarantee temporary protection. The period of protection provided depends on the type of covering employed and its thickness as well as the type of medium from which protection is required. The period of protection may be hours up to a number of years depending on circumstances. The length of protection period required does not only depend on the service life needed for the measurement point, but also on the duration of the individual measurements, the possibility of making intermediate checks on the zero point and insulation resistance and finally on the degree of accuracy desired.

Slight adverse effects on the measuring point, e.g. through the ingress of moisture due to diffusion, mainly result in changes to the zero point. If these can be checked, e.g. by releasing the load on the test object, and they are within acceptable limits of say 100 ... 200 $\mu\text{m/m}$, then measurements can still be made with sufficient accuracy for analytical stress investigations. The insulation resistance is a further indication of the condition of a measuring point. A fall in insulation resistance from 1,000 M Ω to 1 M Ω produces a zero point shift on a 120 Ω strain gage of -60 $\mu\text{m/m}$, -175 $\mu\text{m/m}$ on a 350 Ω gage and -350 $\mu\text{m/m}$ on a 700 Ω gage! This means that the lower limit for the insulation resistance also depends on the resistance of the strain gage's measuring grid.

More significant degradation of the measurement point can occur through the diffusion of corrosive and conducting substances. Corrosion is made much worse by the use of direct voltage for supplying the strain gage. It has been found that galvanic couples form and their voltage is superimposed on the measuring signal, causing large errors in the measurement. It is also important not to overlook the fact that leads and cables also need protecting to the same extent as the measuring point.

The method of protection must be effective, but it must not change the characteristics of the test object. Thin objects must not be made so rigid that deformation is restricted; synthetics must not be affected by substances containing solvent.

It is not possible to give advice for each individual case. However, the following information should enable decisions to be made regarding the correct method to be employed for most problems that occur.

The following should be considered during the **selection** of the protective material:

- the environmental conditions,
- the duration of the measurement and the required service life of the measuring point,
- the required accuracy,
- any impermissible stiffening of the test object,
- the substance coming into contact with the measuring point, including the connecting lead, must have a very high insulation resistance and must not initiate any chemical reactions or any corrosion.

During **use**, the following applies:

- The measuring point must be in perfect condition before being covered. Enclosed moisture, perspiration, flux residues from soldering, etc. are time-bombs which sooner or later lead to measurement errors or to the complete failure of the measuring point. The fact must be considered that an effective covering agent not only keeps out external moisture, but also traps internal moisture!
- The measuring point should be covered immediately after application.
- If the application of a strain gage in a humid environment is unavoidable, for example due to lack of time, bad weather or a humid room, then the test object should be heated in an oven if possible to about 110 ... 120°C or, if this method cannot be applied, the measuring point should be dried with a hot-air fan, e.g. hair dryer.
- The covering agent must form a good contact with the surrounding border area of the measuring point. Imperfections and capillaries formed by scratches and grooves provide entry points for the ingress of corrosive media. The bonding of the covering agent with the edge must remain unchanged throughout the measuring point's complete service life. Therefore the edge must be cleaned just as carefully as the bonding point and it should extend about 1 to 2 cm beyond the outside edges of the adhesive. Perspiration from fingerprints can lead to rust affecting the covering agent from underneath and despite good initial bonding this leaves the covering ineffective.
- Cable entries must be sealed with the greatest of care. The covering agent must enclose the end of the cable from all sides, i.e. also from underneath, so that no channels or capillaries are formed through which moisture can ingress into the inside of the covering. With multicored cable the cores should be embedded individually into the covering agent and a section of the cable sleeving should be enclosed in the covering. Fig. 4.3-1 shows an example.
- With commercially available covering agents for strain gage measuring points it is important that the instructions for use are followed.

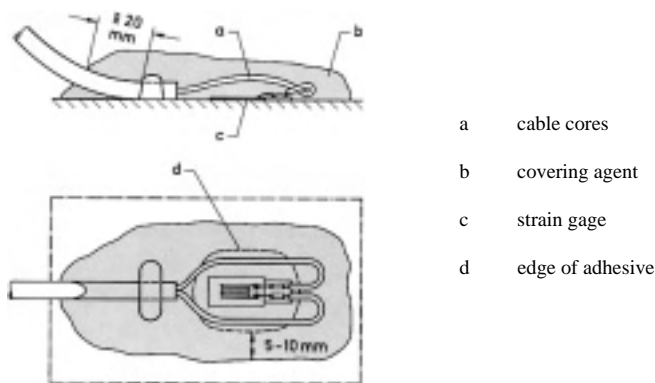


Fig. 4.3-1: Example of the protective covering of a strain gage measuring point.

Common covering agents

- Polyurethane varnish PU 100

Air drying varnish. Suitable for light protection of measuring points against contact (perspiration) and dust, for use at normal humidity levels with the usual variations in moderate zones, e.g. laboratory conditions. It is also suitable as an insulating layer under other covering agents. Resistant to oil. Good abrasion resistance. Temperature resistance -30 ... +100°C, short term to 120°C.

- Nitrile rubber varnish NG 150

Air drying varnish containing methyl ethyl ketone as solvent. Range of applications and characteristics are similar to PU 100. Resistant against oil and gasoline, preferred in applications involving contact with liquified gases, but not oxygen. Temperature range -269 ... +150°C.

- Silicone varnish SL 450

Air drying varnish. Preferred for the protection of ceramic putty against humidity absorption and contamination in high temperature applications. Temperature range -50 ... 450°C.

- AK 22, permanently plastic putty

Advantages:

Simple application by kneading on. Excellent bonding due to strong self-adhesion properties. Very good protection against moisture and water; may be used under water, protection in water at about 20°C approx. 1 year, 3 weeks in water at 75°C. Tested in pressurized water of 400 bar over a few days, limits not known. Very good resistance to weathering. Long term protection can be significantly improved by kneading on aluminum foil, e.g. household aluminum foil, as a diffusion barrier. Mechanical protection against shock and falling objects can be simply provided by pressing some sheet metal onto the self-adhesive putty. Temperature range in air -50 ... +170°C. Unlimited storage capability.

Disadvantages:

Non-resistant to oil and solvents. Cannot be used on the periphery of objects which are subject to high centrifugal forces.

- ABM 75, permanently plastic putty with aluminum foil

Range of applications and properties are similar to AK 22 with the following exceptions: The slab-shaped material is ready lined with a 50 µm covering of aluminum foil as a diffusion barrier. The temperature range is -200 ... +75°C, whereby the upper limit is set by the start of material flow.

- SG 250, transparent, solvent-free silicone rubber

Suitable for protection against moisture and the effects of the weather and against water at room temperature. Partially resistant to oil. The rubbery coating provides very good mechanical protection. Temperature range: -70... +180°C, short term up to 250°C; the material stays elastic within this range.

- Petroleum jelly, unbleached
Advantages:
Cheap, easy to apply; very good protection against moisture and water and it may be used under water.
Disadvantages:
Cannot be used in turbulent water, in rain or splashed water conditions; can easily be unintentionally wiped away in open positions; melts at about 50°C.
- Polychlorotrifluoroethylene grease (trade name: Halocarbon®)
Advantages:
Can be used at temperatures up to 200°C, otherwise it has the same advantages and disadvantages as petroleum jelly.
- Silicone grease
The use of silicone grease is not advised despite its good properties, because it is easily transferred to tools and from there to other objects. Due to its excellent adhesion characteristics silicone grease can only be completely removed with great difficulty. It is a very good separating agent and the slightest traces prevent proper bonding of the strain gage.
- Microcrystalline wax, beeswax
Good protection against moisture and general atmospheric effects. Must be applied in the melted state onto a heated object to obtain proper bonding. Low mechanical protection. Temperature range about -70 ... +100°C.
- Polysulfide rubber
Two part material producing a rubber-like compound which has excellent resistance against solvents and ageing. It also has good weathering properties. Temperature range -50 ... +120°C.
- Epoxy resin (trade names: Araldite®, UHU-plus®, etc.)
For strain gage coverings soft mixtures are the most suitable. The material available under the trade name UHU-plus, a two part resin, is suitable mainly for protection against oils, engine fuel, dilute acids, dilute alkalis, a number of solvents and it also provides good mechanical protection. Temperature limits are dependent on the curing conditions, i.e. cold or hot curing.
- Aluminum adhesive strips
Adhesive tape lined with aluminum foil forms a good water vapor barrier (diffusion barrier). It is suitable as additional covering for the measurement point to improve the characteristics of other covering agents, in particular their ageing characteristics. Aluminum foil is also a very good protective covering for measurement cables which in many cases are the weakest component of a measurement point.
- Liquids for protecting the applied strain gage.
Some problems in protecting the measuring point can be solved by the use of insulating liquids. One example would be the internal application on a small vessel which is

to be the subject of a pressure test. If a pressure medium can be used other than the usual one, water, then many problems can be solved in a simple manner. One requirement is that the selected pressure medium has good insulating properties and is free from additives which might attack the strain gage. The following are suitable:

oil which is free of water and acid,
kerosene,
pure gasoline.

This method of protecting the measurement point with liquids has also been used successfully for the protection of permanent measuring points where the surrounding capsule was filled with the protective medium. In this respect there is also another excellent medium:

polyisobutylene in low molar versions which flow like oil or are more viscous like honey (trade name: Oppanol® B 3, B 10 and B 15).

- Combined covering agents

Very often one covering agent alone does not provide sufficient protection for the measuring point. Examples of the use of combined agents have already been given with AK 22 and ABM 75 (plastic compound with aluminum foil). If the metal foil is to have additional protection, then, for example, silicone rubber SG 250 can be applied.

Often a number of different media affect a measuring point, e.g. oil and water. In these cases, for example, the oil-soluble ABM 75 can be applied directly to the strain gage, aluminum foil then used as a diffusion barrier for the second layer and then oil resistant epoxy resin is applied over that. With undefined media such as sea-water, multi-layer protection is essential. Other substances, e.g. asphalt, can be used for the upper layer which does not come into contact with the strain gage. They must not etch or chemically change the underlying layers, but no specific demands are made on their electrical insulation resistance.

The problem of protecting the measuring point is so wide ranging that only a general overview can be given. In critical applications it is recommended that a preliminary test is carried out under realistic conditions.

5 The Wheatstone bridge circuit

Sir Charles Wheatstone (1802 - 1875), an English scientist, reported in 1843 [1-2] on a circuit which made the accurate measurement of electrical resistances possible. This circuit has become known as the “Wheatstone bridge circuit”.

The Wheatstone bridge can be used in various ways to measure electrical resistances:

- for the determination of the absolute value of a resistance by comparison with a known resistance,
- for the determination of relative changes in resistance.

The latter method is used in strain gage techniques. It enables the relative changes of resistance in the strain gage, which are usually around the order of 10^{-4} to 10^{-2} Ω/Ω to be measured with great accuracy. The extraordinarily versatile Wheatstone bridge is dealt with below exclusively with regard to strain gage techniques.

5.1 The circuit diagram of the Wheatstone bridge

Fig. 5.1-1 shows two different illustrations of the Wheatstone bridge which are however electrically identical: Fig. 5.1-1a shows the usual rhombus type of representation which Wheatstone used; Fig. 5.1-1b is a representation of the same circuit which is more clear for the electrically untrained person.

The four arms or branches of the bridge circuit are formed by the resistances R_1 to R_4 . The corner points 2 and 3 of the bridge designate the connections for the bridge excitation voltage V_s ; the bridge output voltage V_o , the measurement signal, is available on the corner points 1 and 4:

The bridge excitation is usually an applied, stabilized direct or alternating voltage V_s . Sometimes a current supply is used, e.g. the double current method.

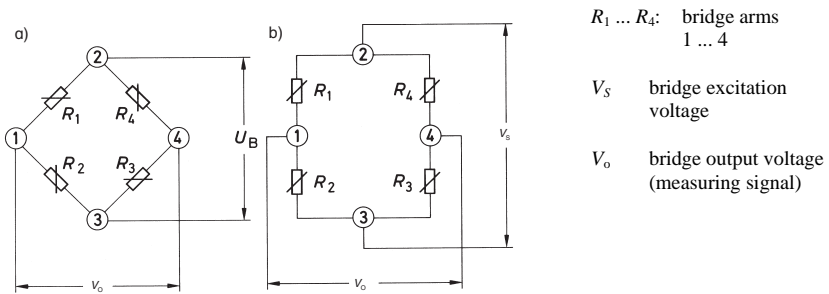


Fig. 5.1-1: Different representations of the Wheatstone bridge circuit.

The advantages of the voltage-fed bridge circuit with regard to its automatic correction of linearity deviations in the strain gage characteristic (see section 3.3-6) are shown in [5-1 to 5-4] and are proved with a test in [3-29]. A further advantage is the insensitivity to the strain gage resistance tolerances. The following is therefore restricted to the voltage-fed bridge circuit.

Note:

There is no generally accepted rule for the designation of the bridge components and connections. In the literature there are all kinds of designations and this is reflected in the bridge equations. Therefore, it is essential that the designations and indices used in the equations are considered together with their positions in the bridge networks in order to avoid misinterpretation. In this publication the designations in Fig. 5.1-1 are used exclusively.

5.2 The principle of the Wheatstone bridge circuit

If a supply voltage V_S is applied to the two bridge supply points 2 and 3 then this is divided up in the two halves of the bridge R_1, R_2 and R_4, R_3 as a ratio of the corresponding bridge resistances, i.e. each half of the bridge forms a voltage divider, see Fig. 5.2-1.

The following treatment of the bridge circuit assumes that the source resistance R_0 of the voltage supply is negligibly small and that the internal resistance of the instrument for measuring the bridge output voltage is very high and does not cause any load on the bridge circuit. This method of treatment is acceptable, because the instruments used in strain gage techniques fulfill these requirements to a large extent.

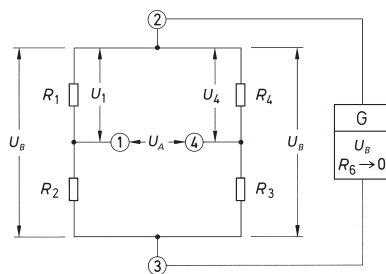


Fig. 5.2-1: Principle of the voltage-fed Wheatstone bridge circuit.

If the bridge is not balanced, this is caused by the difference in the voltages from the electrical resistances on R_1 , R_2 and R_3 , R_4 . This calculated as:

$$V_o = V_s \left(\frac{R_1}{R_1 + R_2} - \frac{R_4}{R_3 + R_4} \right) \quad (5.2-1)$$

If the bridge is balanced

$$\frac{R_1}{R_2} = \frac{R_3}{R_4} \quad (5.2-2)$$

the bridge output voltage is zero.

With a preset strain, the resistance of the strain gage changes by the amount ΔR . This gives:

$$V_o = V_s \left(\frac{R_1 + \Delta R_1}{R_1 + \Delta R_1 + R_2 + \Delta R_2} - \frac{R_4 + \Delta R_4}{R_3 + \Delta R_3 + R_4 + \Delta R_4} \right) \quad (5.2-3)$$

For strain measurements, the resistances R_1 and R_2 must be equal in the Wheatstone bridge. The same applies to R_3 and R_4 . Therefore:

$$R_1 = R_2 = R_1 \quad (5.2-4)$$

And correspondingly

$$R_3 = R_4 = R_3 \quad (5.2-5)$$

This gives:

$$V_o = V_s \left(\frac{(R_1 + \Delta R_1) \cdot (2R_3 + \Delta R_3 + \Delta R_4) - (R_3 + \Delta R_4) \cdot (2R_1 + \Delta R_1 + \Delta R_2)}{(2R_1 + \Delta R_1 + \Delta R_2) \cdot (2R_1 + \Delta R_3 + \Delta R_4)} \right) \quad (5.2-6)$$

When the results are expanded this gives many terms of $\Delta R_X \cdot \Delta R_Y$ that are very small when compared to the other terms. These can therefore be disregarded. Thus:

$$V_o = V_s \left(\frac{R_1(\Delta R_3 + \Delta R_4) - R_1(\Delta R_1 + \Delta R_2) + 2R_3\Delta R_1 - 2R_1\Delta R_4}{4R_1R_3 + 2R_1\Delta R_3 + 2R_1\Delta R_4 + 2R_3\Delta R_1 + 2R_3\Delta R_2} \right) \quad (5.2-7)$$

This can be further simplified when the nominator ($4R_1R_2 + \dots$) is examined more precisely. For example, take a full bridge from 120 Ω strain gage with a strain of 10,000 μm . Thus:

$$4R_1R_3 = 57600\Omega^2 \quad (5.2-8)$$

whereas the other terms are very small:

$$2R_1\Delta R_3 = 0.48^2 \quad (5.2-9)$$

The difference will be even greater, if the strain gage resistance is larger or the strain smaller. For this reason, we may disregard all terms under the horizontal line with the exception of $4R_1R_3$.

This results in:

$$\frac{V_o}{V_s} = \frac{R_1\Delta R_3}{4R_1R_3} + \frac{R_1\Delta R_4}{4R_1R_3} - \frac{R_3\Delta R_1}{4R_1R_3} - \frac{R_3\Delta R_2}{4R_1R_3} + \frac{2R_3\Delta R_1}{4R_1R_3} - \frac{2R_1\Delta R_4}{4R_1R_3} \quad (5.2-10)$$

Shortened to:

$$\frac{V_o}{V_s} = \frac{\Delta R_3}{4R_3} + \frac{\Delta R_4}{4R_3} - \frac{\Delta R_1}{4R_3} + \frac{\Delta R_2}{4R_1} + \frac{\Delta R_1}{2R_1} - \frac{\Delta R_4}{2R_3} \quad (5.2-11)$$

Equation (11) is summarized in the next step. It should be noted that the resistances R_1 , R_2 and R_3 , R_4 must be equal.

$$\frac{V_o}{V_s} = \frac{1}{4} \left(\frac{\Delta R_1}{R_1} - \frac{\Delta R_2}{R_2} + \frac{\Delta R_3}{R_3} - \frac{\Delta R_4}{R_4} \right) \quad (5.2-12)$$

In the last calculation step, the term $\Delta R/R$ must be replaced by the following:

$$\frac{\Delta R}{R} = k \cdot \varepsilon \quad (5.2-13)$$

Here k is the k-factor of the strain gage, ε is the strain. This gives:

$$\frac{V_o}{V_s} = \frac{k}{4} (\varepsilon_1 - \varepsilon_2 + \varepsilon_3 - \varepsilon_4) \quad (5.2-14)$$

It should be noted that it is sufficient for strain gage measurements if the inline switched strain gages are equal. A 120 Ω half bridge can also be extended with a 350 Ω half bridge.

The equations (5.2-3) and (5.2-14) assume that all the resistances in the bridge change. This situation occurs for example in transducers or with test objects performing a similar function. In experimental stress analysis this is hardly ever the case and usually only some of the arms of the bridge contain active strain gages, the remainder being made up of bridge completion resistors. Designations for the various forms such as quarter bridge, half bridge, double quarter or diagonal bridge and full bridge are commonplace. Fig. 5.2-2 illustrates the different forms.

High demands are made on the bridge completion resistors with regard to long-term stability and non-dependence on temperature. Very stable metal film resistances have proven useful. Some measurement amplifiers contain this type of bridge completion circuit. Instead of these completely passive resistances, compensation strain gages can also be used as bridge completion resistances. The requirements which a compensation strain gage must fulfill are described in section 7.1.3.

Section 8 explains how the various forms of bridges are used.

From equations (5.2-5 and 5.2-7) it can be seen that the resistance changes and the strains which cause them contribute to the unbalance in the bridge, and hence to the measurement signal, with different signs. On connecting a measuring instrument designed for taking strain measurements the following effects take place:

positive indication if $\varepsilon_1 > \varepsilon_2$ and/or $\varepsilon_3 > \varepsilon_4$
negative indication if $\varepsilon_1 < \varepsilon_2$ and/or $\varepsilon_3 < \varepsilon_4$

Note:

The signs “greater than” (>) and “smaller than” (<) apply in the algebraic sense and not to the magnitudes!

The following should also be noted:

The magnitudes of changes to strain gages which are located in *adjacent* bridge arms in the circuit are *subtracted* if they have *like signs*; (Application example: Temperature compensation, section 7.1); they are *added* if they have *unlike signs*; (Application example: Signal amplification, e.g. with transducers, etc., section 8.4).

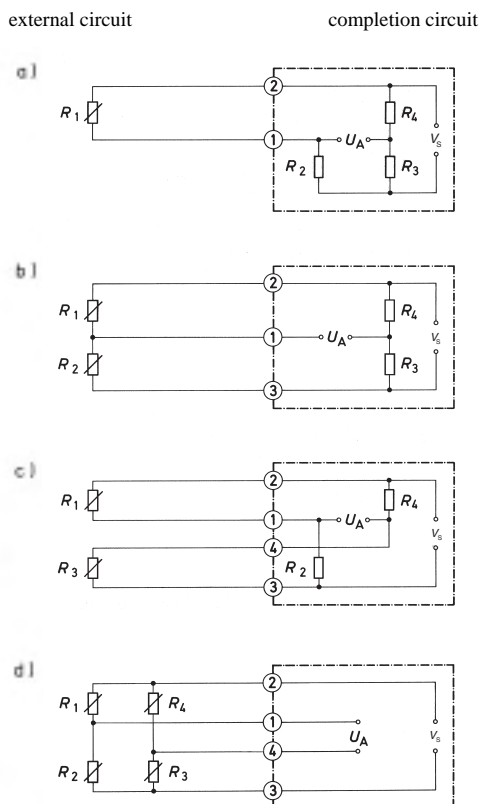


Fig. 5.2-2: Forms of the Wheatstone bridge circuit used in strain gage techniques

- a) quarter bridge
- b) half bridge
- c) double quarter or diagonal bridge
- d) full bridge

Depending on whether the changes of resistance occur in one or more arms of the bridge and depending on their amount and sign, a linear deviation in the bridge unbalance occurs.

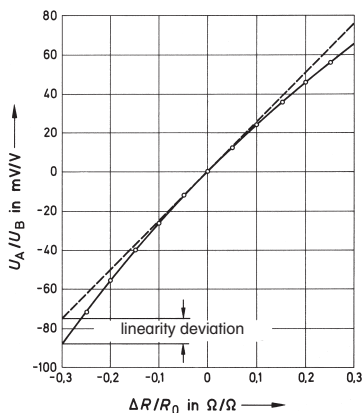


Fig. 5.2-3: Characteristic of the Wheatstone bridge circuit in the “quarter bridge” operating mode according to equation (5.2-15) and the comparison characteristic based on the approximation formula (5.2-16).

A markedly linear characteristic arises if the sum of the resistance changes in both halves of the bridge $\Delta R_1 + \Delta R_2$ and $\Delta R_4 + \Delta R_3$ is zero.

Maximum linear deviation occurs with the quarter bridge circuit and to the same extent with the double or diagonal bridge circuit. Fig. 5.2-3 shows the dependence of the bridge unbalance V_o/V_s to the relative change of resistance $\Delta R/R$ in bridge arm 1, calculated according to the equation

$$\frac{V_o}{V_s} = \frac{\Delta R}{2(R_0 + \Delta R)} \quad (5.2-15)$$

Assuming $R_1 = R_2 = R_3 = R_4 = R = R_0$. For comparison the linear characteristic

$$\frac{V_o}{V_s} = \frac{\Delta R}{4R_0} \quad (5.2-16)$$

which is calculated from the approximate formula is shown as a broken line.

The linear deviation of the quarter bridge circuit is often depicted in the literature as a big disadvantage of the constant voltage-fed Wheatstone bridge compared to the constant current-fed bridge. However, what is not considered is that for large strains the strain gage itself exhibits an almost equally large but opposing linear deviation, see section 3.3.6. Comparison with Fig. 3.3-18 shows that both linear deviations are almost fully compensating [3-29], but the constant current supply is not capable of this self-compensation [5-1, 5-4].

5.3 Bridge excitation and amplification of the bridge output voltage

The Wheatstone bridge circuit can be supplied from direct or alternating voltage. The type of bridge excitation must be considered in conjunction with the amplifier system that is used for amplifying the bridge output voltage.

Commercially available measuring amplifiers contain a constant voltage source for supply of the bridge circuit. The supply voltage is usually switchable to fixed values between 1 and 10 V, thus matching the permissible electrical loading on the strain gage, see section 3.3.8.

Amplifiers also have means of adjustment for compensation of the zero point and for setting the amplifier to the desired values. With a.c. or carrier frequency measurement amplifiers there is often, where required, means for compensating the phase.

The measuring amplifier's primary task is to raise the level of the bridge circuit's output signal from the millivolt region to a number of volts. The amplified signal voltage should if possible be a perfect reproduction of the measured variable. Interference, such as thermal voltages and line interference should not have any influence.

The types and variations of measurement amplifier are so numerous that they are beyond the scope of this book. Detailed information can be taken from the relevant product literature. The principal differences between the two systems are briefly mentioned below.

The direct voltage measuring amplifier contains a generator which provides a stabilized direct voltage for supplying the bridge circuit. The direct voltage amplifier, to which the bridge output voltage is passed, amplifies static signals and dynamic signals up to high frequencies. In most cases in the measurement of mechanical quantities an upper limit of 10 kHz is sufficient, because mechanical objects have a finite mass and this limit is only exceeded in extreme cases for which the direct voltage amplifier can be used if required. An example of a high frequency mechanical process is described in section 3.3.7.2.

Usually, higher frequencies are caused by interference pulses which should be kept well away from the measurement signal. The disadvantage of the direct voltage method is that interference due to electrical or magnetic fields together with thermal and galvanic voltages occurring in the measurement circuit are fully amplified and appear as errors in the measurement result. Electrical or magnetic screening is required to guard against stray interference effects. Errors due to thermal voltages can be detected by reversing the supply voltage; they must be corrected by calculation.

With the carrier frequency method the generator supplies an alternating voltage, stabilized in both frequency and voltage, for the supply of the bridge circuit. If the bridge circuit becomes unbalanced by the measured quantity, e.g. a strain on the strain gage, then it produces an output voltage in the same way as with the direct voltage method, but here it is an alternating voltage whose amplitude is proportional to the bridge unbalance (amplitude modulation). The amplifier is designed such that it only amplifies the frequency of the supply voltage and relatively narrow sidebands and does not accept frequencies above or below them. Hence, all direct voltage interference portions of the measurement signal, for example thermal voltages formed in the measurement circuit, are fully eliminated. The carrier frequency is selected such that the interfering alternating voltages, for example stray interference due to the line frequency and its harmonics as well as high frequency interfer-

ence pulses, also do not have any influence on the measurement signal. Common carrier frequencies are 225 Hz and 5 kHz. 225 Hz CF amplifiers are suitable for measurement of static and quasi-static processes, i.e. up to 9 Hz. 5 kHz CF amplifiers can accommodate static and dynamic frequencies up to 1 kHz with 1 dB attenuation of amplitude.

A comparison of the applications of the direct voltage and carrier frequency methods, which extends beyond the brief guide given here, is given in [5-5].

6 Calibrating measurement equipment

The measurement task comprises obtaining the value of a physical quantity and representing it as a number or in a converted form.

In order to acquire the measurement, equipment is used where the measured quantity is accepted at the input (transducer) and the measurement produced at the output (output stage). The component parts of the measurement equipment are joined together like the links of a chain and sometimes the measurement equipment is known as a “measuring chain”.

The user of the measurement equipment naturally expects that the figure obtained for the measured quantity and the measurement itself correspond with one another. This correspondence is achieved through “calibration” of the measurement equipment. In Germany the terms and designations that should be used are set down in [6-1], see also Fig. 6.0-1.

The calibration principle is explained using a simple example, the calibration of a spring balance, see Fig. 6.0-2.

The position of the pointer in the unloaded state is marked on the scale and identified with an “0”. Then various weights Q of known weight are suspended one after the other from the spring and the pointer position corresponding to each weight is marked and identified on the scale. It is then possible to determine the unknown weight of other objects provided the pointer is located within the calibrated range of the scale. Values between the markings can be read off by estimation.

The accuracy of the calibration depends on the accuracy of the calibrated weights used.

The correspondence of the indicated scale value with the value of the measured quantity must not necessarily consist of obtaining the same numerical values, since it is also sufficient if a relationship is produced through a known proportionality factor. This proportionality factor is determined by calibration in the same manner and must be considered when taking the measurement:

$$\text{measurement} = \text{scale reading} \times \text{factor.}$$

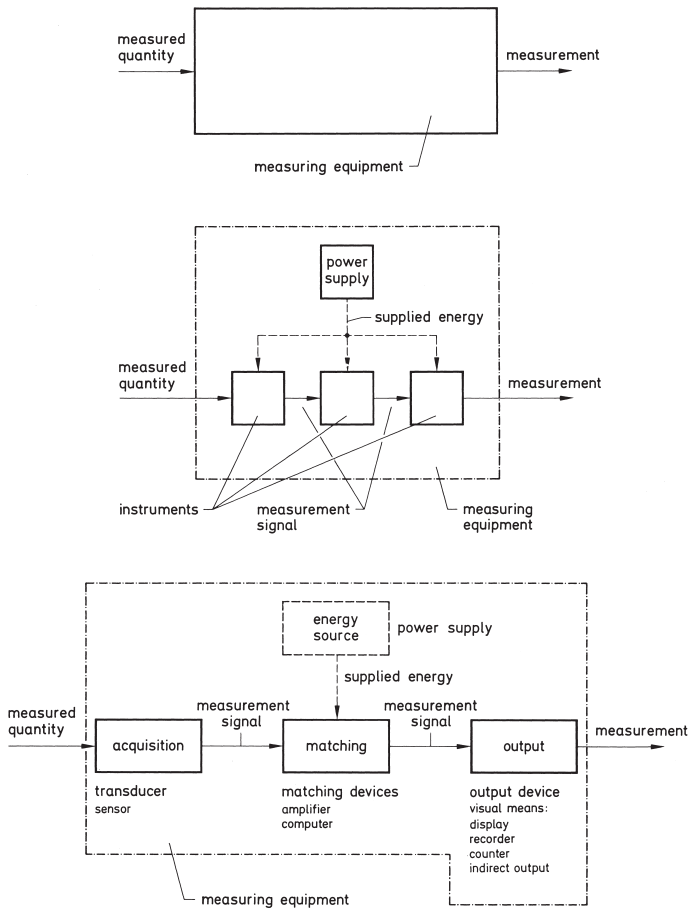


Fig. 6.0-1: Definition of the term “measurement equipment” and the designation of its components according to [6-1].

As this example shows, calibration requires that the measured quantity is transferred to the spring balance with a known value which is numerically as accurate as possible. Here care must be taken to correctly position the balance and to ensure that the effect of the measured variable, i.e. the weights, is not impaired. These conditions apply to any calibration.

With mechanical measuring equipment the transfer of the measured quantity for calibration purposes is usually carried out by direct methods, e.g. suspending weights, measuring a distance). With electrical methods of measurement the same procedure is used where possible. Problems occur if a calibration standard (calibrated weight, standard length, etc.) is not available or if there are other technical difficulties. This direct method of calibration cannot be used for strain measurements using strain gages. The reason for this is that a calibrated value for strain cannot be produced without a great amount of effort. Instead other methods used are:

- calibration with a calibration signal provided by a measuring amplifier, see section 6.2,
- direct shunt calibration, see section 6.3,
- calibration with a calibration unit, see section 6.4.

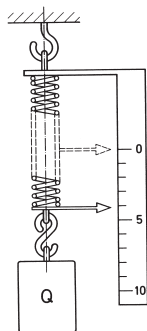


Fig. 6.0-2: Method of calibrating a spring balance.

6.1 The operating principle of the compensation and calibration devices on a measuring amplifier.

The equipment (see section 5.3) available under the description “measuring amplifier” which is intended for use with strain gages contains, apart from the actual amplifier, numerous auxiliary devices, such as for example the bridge completion circuit, the supply unit, range selector switches, calibration devices and various compensation or adjustment devices which are essential for practical work with strain gages. The term “measuring amplifier” therefore includes much more than just the amplifier. The actual amplifier section is designed to have a strictly linear characteristic, see Fig. 6.1-1a. This applies just the same to carrier frequency amplifiers as for direct voltage amplifiers. The output voltage V_Y is greater than the input V_X by a factor A , the gain of the amplifier. If a bridge circuit consisting of one or more strain gages is connected to the amplifier, then it is found that the bridge is already unbalanced by slight, unavoidable changes in the differences of the resistances forming the arms of the bridge. A bridge output voltage level is therefore passed to the amplifier, although the influence of the measured quantity, strain, weight, torque, etc., is not yet present. This signal is called the “tare signal” from the terms used in weighing techniques. (The term “zero signal” is also used instead of “tare signal”, because the measured quantity is “zero”.) The amplifier characteristic is displaced by tare signal T , see Fig. 6.1-1b; the displacement can be positive or negative.

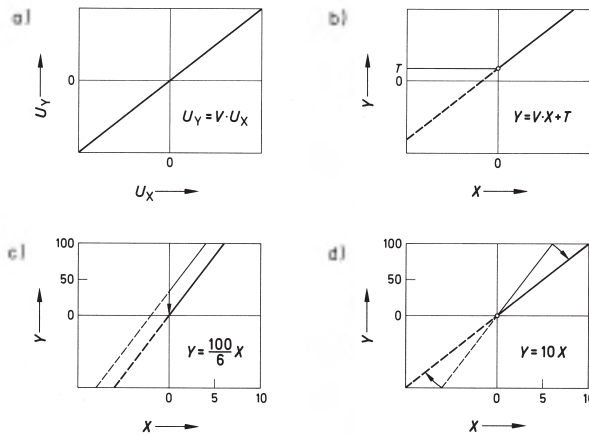
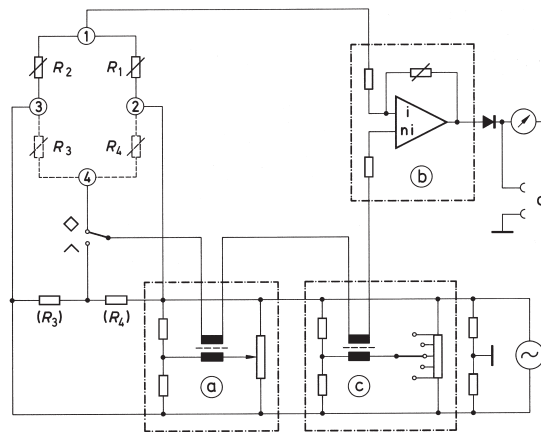


Fig. 6.1.1: The operating principle of balancing elements in the measuring amplifier.
 a) amplifier characteristic
 b) the effect of the tare signal T on the relationship of the measured quantity X to the reading Y (zero point displacement)
 c) correction of the tare reading with the aid of the zero point compensation device.
 d) adjustment to an integer ratio between the measured quantity and the reading by altering the gain setting

Using a compensating device called zero point or R compensation, the tare reading can be corrected so that the reading Y is now proportional to the signal X , see Fig. 6.1-1c. However, the ratio between the measured quantity and the indication, the amplifier gain A , is still arbitrary. Within certain limits adjustment of the gain can be made to obtain an integer ratio between the measured quantity and the reading. In the diagram in Fig. 6.1-1d the change in the gain appears as a rotation of the characteristic about the zero point.



- a additively coupled signal for zero point compensation
- b gain control for adjustment of the sensitivity
- c production of a signal with defined level for independent calibration of the measuring amplifier
- d signal output for external processing

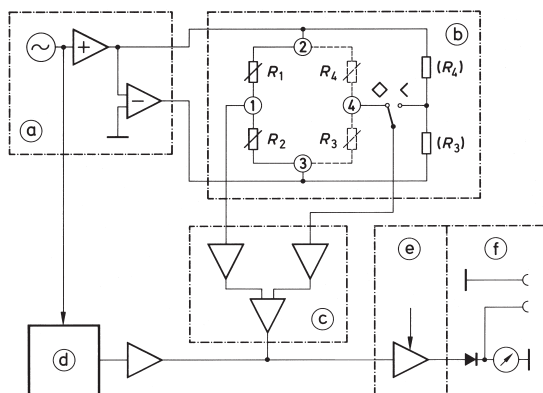
Fig. 6.1-2: Circuit for compensation and adjustment of a carrier frequency measuring amplifier (older version).

An example of a circuit which provides the compensation and adjustment features is shown in Fig. 6.1-2. This circuit is now obsolete, but it is suitable for explaining the principle.

An auxiliary voltage (a), which is adjustable using a potentiometer, is coupled additively in the signal circuit and provides compensation of signal voltages from the input circuit, the Wheatstone bridge, which may occur due to unsymmetry or a tare load. The compensation signal, which may be negative or positive as required, compensates for the difference between the zero value of the measured quantity and the zero value of the signal and hence further correction is then superfluous. In practice zero point compensation is usually set using stepwise switchable coarse and medium ranges and with a continuously adjustable fine range.

The gain control (b) is most practically implemented as a continuously adjustable control. Often the measurement range of the unit can also be switched in calibrated stages with a special switch and a “gage factor selector” set to the exact numerical value of the gage factor of the strain gage that is being used. The selector switches for the measurement range and the gage factor are also implemented as gain controls.

Signals having a defined level can also be additively coupled into the signal circuit with the calibration signal (c). This enables the measurement equipment to be calibrated from the signal input through to the output indicator independent of the connected transducer. This method of calibration is useful if direct calibration of the measurement equipment is not possible.



- a supply, symmetrical about ground
- b transducer circuit and bridge completion network for half bridges
- c pre-amplification
- d board for production of the compensation and calibration voltages
- e final stage amplifier with gain control and matching of gage factor
- f output indication and output signal for external processing

Fig. 6.1-3: Schematic circuit diagram of a bridge amplifier of a later type.

Fig. 6.1-3 illustrates the basic circuit diagram of a modern bridge amplifier. The functions are the same as previously, enabling the user to work with the unit in the accustomed manner; it is only the internal construction that is different and which gives advantages. The extremely low internal resistance of the supply generator ensures fully uniform supply conditions even with large differences in the internal resistance of the connected bridge circuit or transducer. The symmetrical pre-amplification raises the measurement signal to a higher level. High common mode suppression of interference ensures high accuracy of the measurement and of the compensation and calibration voltages which are produced by a board in the unit. These voltages are coupled into the measurement circuit with operational amplifiers. This has advantages over the formerly common transformer coupling, in particular when connected to inductive transducers, whose operation with carrier frequency bridge amplifiers from upwards of 5 kHz carrier frequency is a possible extension to applications involving resistive transducers and strain gages.

The gain control, including a range selector and gage factor matching, is implemented as previously in the amplifier final stage.

6.2 Calibration using the calibration signal from the measuring amplifier

The measuring amplifiers available for strain gage measurements contain either a switch or a pushbutton enabling a defined signal to be fed into the measurement circuit. The level of the calibration signal can either be given in the strain dimension of $\mu\text{m}/\text{m}$ or in terms of the bridge unbalance in mV/V .

Important!

Calibration using the calibration signal supplied by the measuring amplifier does not take into account the loss of sensitivity due to the resistance of long connection cables between the strain gage and the bridge amplifier. It is however sufficiently accurate for short cables, see also section 7.2.

If $\mu\text{m/m}$ are stated, the numerical value is only accurate if the gage factor for the strain gage has a value of 2.0. For other gage factors the procedure given in section 6.5 should be followed.

If the calibration signal is given in mV/V , then the following applies:

$$1 \text{ m V/V} \hat{=} 2000 \mu\text{m/m for } k = 2.0.$$

The derivation of this equivalence is simple. In section 6.3 (please refer to that section) the bridge unbalance V_o/V_s is given arising from the strain on the strain gage.

If substitutions are made in equation (6.3-8) for $k = 2$ and for $\epsilon = 2000 \cdot 10^{-6}$, then the following is obtained:

$$\frac{V_o}{V_s} = \frac{1}{4} k \cdot \epsilon = \frac{1}{4} \cdot 2 \cdot 2000 \cdot 10^{-6} = 1000 \cdot 10^{-6} \frac{\text{V}}{\text{V}} = 1 \frac{\text{mV}}{\text{V}}.$$

Here also the procedure described in section 6.5 must be followed if the gage factor is different.

6.3 Shunt calibration

In all cases where the measurement equipment cannot be calibrated with sufficient accuracy by the direct effect of the measured quantity on the transducer, i.e. here the strain gage, a substitution method is used. In this method an auxiliary device is used with which a comparable, defined effect on the measurement equipment can be exerted as produced by the transducer itself.

Using this technique, it is possible to unbalance the bridge circuit with a shunt resistance. Fig. 6.3-1 shows the principle of shunt calibration. The circuit is a good simulation of the real strain gage circuit.

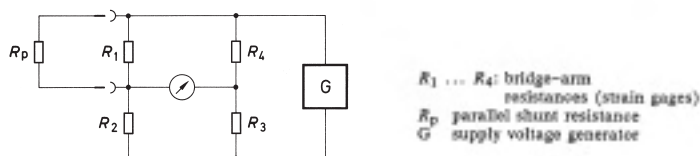


Fig. 6.3-1: Principle of shunt calibration

It is sufficient for the calculation of the bridge unbalance to use the approximate equation

$$\frac{V_o}{V_s} = \frac{1}{4} \left(\frac{\Delta R_1}{R_1} - \frac{\Delta R_2}{R_2} + \frac{\Delta R_3}{R_3} - \frac{\Delta R_4}{R_4} \right) \quad (6.3-1 \equiv 5.2-5)$$

For the quarter bridge circuit

$$\frac{\Delta R_2}{R_2} = \frac{\Delta R_3}{R_3} = \frac{\Delta R_4}{R_4} = 0$$

and this leaves

$$\frac{V_o}{V_s} = \frac{1}{4} \cdot \frac{\Delta R_1}{R_1} \quad (6.3-2)$$

Also

$$R_p \parallel R \rightarrow R_r \quad (6.3-3)$$

$$R_r = \frac{R \cdot R_p}{R + R_p} \quad (6.3-4)$$

$$\Delta R = R_r - R \quad (6.3-5)$$

R_p = parallel resistance (shunt)

R = strain gage resistance

R_r = resulting resistance

ΔR = change in resistance

This then gives

$$\begin{aligned} \frac{V_o}{V_s} &= \frac{1}{4} \cdot \frac{\Delta R}{R} = \frac{1}{4} \cdot \frac{R_r - R}{R} = \frac{1}{4} \cdot \frac{\frac{R \cdot R_p}{R + R_p} - R}{R} \\ &= \frac{1}{4} \left(\frac{R_p}{R + R_p} - 1 \right). \end{aligned} \quad (6.3-6)$$

For the strain gage, after rearranging equation (3.3-1) :

$$\frac{\Delta R}{R} = k \cdot \epsilon \quad (6.3-7)$$

$$\frac{V_o}{V_s} = \frac{1}{4} \cdot \frac{\Delta R}{R} = \frac{1}{4} \cdot k \cdot \epsilon. \quad (6.3-8)$$

If the calibration values are labeled ϵ^* , then

$$\epsilon^* = \frac{1}{k} \cdot \frac{\Delta R}{R} = \frac{1}{k} \left(\frac{R_p}{R + R_p} \right) - 1 \quad \text{in m/m} \quad (6.3-9)$$

or

$$\epsilon^* = \frac{1}{k} \left(\frac{R_p}{R + R_p} - 1 \right) \cdot 10^6 \quad \text{in } \mu\text{m/m}. \quad (6.3-9a)$$

If a resistance in parallel with the strain gage has a value one thousand times that of the strain gage and a gage factor $k = 2$ is assumed, then a calibration value $\epsilon^* = 499.5 \mu\text{m/m} \approx 500 \mu\text{m/m}$ is produced.

Example:

$$\begin{aligned} R_{SG} = R &= 120 \Omega \\ R_p &= 120 \text{ k}\Omega \\ k &= 2 \end{aligned} \quad \epsilon = \frac{1}{2} \left(\frac{120,000}{120,120} - 1 \right) \cdot 10^6 = -499.5 \mu\text{m/m} \\ \approx -500 \mu\text{m/m}$$

The sign of the calibrated value becomes negative if one of the bridge arms R_1 or R_3 is shunted and becomes positive if the arms R_2 or R_4 are shunted. With quarter bridge circuits the strain gage is always placed in the position of R_1 in the bridge circuit so that the signs of the strain and the indication agree. Therefore, calibration is only possible for the negative region. An indicating instrument with a negative range is hence required. The calibration is then also valid for the positive region. With half and full bridge circuits calibration is of course possible for both regions, depending on the position of the shunted resistance. The example which is given provides a rough guide for the checking of strain gage measurement points; for calibration the numerical values for R_{SG} , R_p and k must be known as accurately as possible, because the accuracy of the calibration depends on them.

If the strain gage is directly shunted, then in contrast to the method described in 6.2, all influences affecting the indication are included, such as for example, the resistance of the connecting cable, the gain of the amplifier and the sensitivity of the indicating instrument.

If the ratio is formed between the calculated calibrated value ϵ^* and the indicated measurement ϵ_i , then the correction factor K_c is obtained:

$$\frac{\epsilon^*}{\epsilon_i} = K_c \quad (6.3-10)$$

ϵ_i multiplied with K_c gives the calibrated value ϵ^* which is numerically the same as the strain ϵ^*

$$\epsilon_i \cdot K_c = \epsilon^* = \epsilon \quad (6.3-11)$$

A more elegant method can be used if bridge amplifiers with adjustable gain are used, see section 6.1. These enable the indication to be made numerically the same as the calibration value ϵ^* , so that a correction calculation is no longer needed.

6.4 Calibration with a calibration unit

Whereas the method described in 6.3 is largely independent of the resistor values of the strain gages used and of the shunt resistances (they must only be accurately known), calibration units are designed for operation with certain standard resistance values, e.g. 120 Ω and 350 Ω . The nominal resistances of the calibration unit and the strain gage must correspond so that cable effects are properly acquired and eliminated. The calibration unit is always inserted into the circuit in place of the strain gage or the transducer, see Fig. 6.4-1, and is replaced after calibration by the strain gage or transducer.



Fig. 6.4-1: Arrangement of the calibration unit within the measurement equipment.
 a) calibration unit
 b) measuring amplifier
 c) indicating instrument

Calibration units operate using various techniques. The unit illustrated in Fig. 6.4-2 operates according to the shunt method described in section 6.4-3. Fig. 6.4-3 shows the basic circuit diagram.

With the accurately dimensioned shunt resistors which are built into the calibration unit, it is possible to produce both positive and negative bridge unbalances of various magnitudes. The different levels for bridge unbalance are printed on the switch scale in mV/V. The relationship between the bridge unbalance V_o/V_s which is given in mV/V and the strain ϵ is given by the equivalence $1 \text{ mV/V} \cong 2000 \mu\text{m/m}$ at $k = 2.0$, see section 6.2.

The bridge circuit in the calibration unit can be switched to half or full bridge configurations as required. The shunt resistances are each connected in parallel to only one bridge arm; a negative indication is produced parallel to R_1 and a positive one parallel to R_2 . However, quarter bridges, a circuit configuration which is used very often in experimental stress analysis, can also be calibrated just as easily. In this case the strain gage connecting cable is connected to terminals 1 and 2 on the calibration unit. Calibration is, however, only possible in the negative direction.



Fig. 6.4-2: Calibration Unit K 3602, incorporating the “shunt calibration” system.

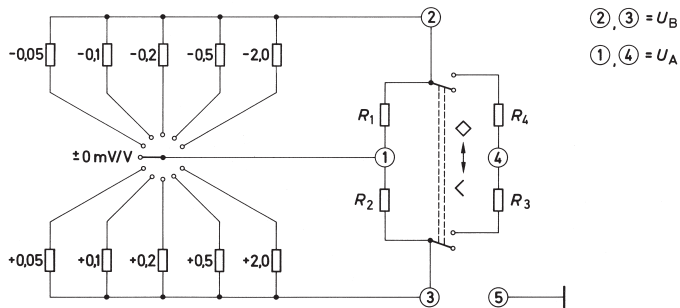


Fig. 6.4-3: Principal circuit diagram of a calibration unit based on the shunt method.

If the actual gage factors of the strain gages used deviate from the approximate value of 2, then corrections are necessary. The various methods of correcting the calibration and correcting the measurement are described in section 6.5.



Fig. 6.4-4: Calibration Unit K 3607

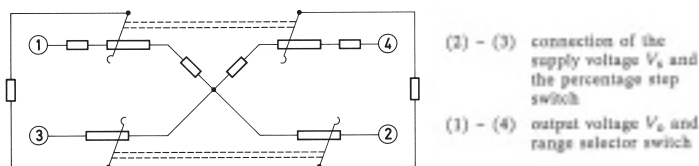


Fig. 6.4-5: Principal circuit diagram of the K 3607 Calibration Unit.

A different principle is used in the K 3607, which is illustrated in Fig. 6.4-4. It contains a high precision star network of resistors which provides simulation of the bridge unbalance from transducers with strain gage full bridge circuits. Measurement equipment can be calibrated with the calibration unit without the transducer being subjected to the measured quantity. It is designed for a bridge resistance of 350Ω , corresponding to the standard bridge resistance in commercially available transducers. The unit can also be used for checking the linearity of the measurement equipment using five different range settings for the calibration signal, which are then subdivided into 10% steps. The extremely low self-capacitance and self-inductance of the integral precision resistors enable the calibration unit to achieve a maximum measurement uncertainty of 0.025%.

In principle, longer connecting leads between the strain gage and the measuring amplifier should be included in the calibration in order to include the effects of the cable resistance and capacitance. With appropriate measuring amplifiers the calibration unit can also be operated in 6-wire circuits, see section 7.3.2.

6.5 Taking account of gage factors with a value other than 2

On the data sheets enclosed with strain gages, the gage factor determined for the relevant production lot is given with its tolerance as a percentage. The actual gage factors may deviate by a few percent from the average value given in Table 3.3.1. The tolerances within a production lot are however significantly tighter and are usually between 0.5 and 1%. The tolerance applies for properly applied strain gages and apart from the low stray values for the gage factor itself, it contains the unavoidable influences of the application.

For the user it is important to calibrate the measurement equipment to the actual gage factor.

For bridge amplifiers *with* a gage factor selector this is initially set to the numerical value of 2 and the indicated value is adjusted with the sensitivity control either to

- the numerical value of the present calibration signal in $\mu\text{m}/\text{m}$
- or to the numerical value 2000 at a calibration signal of 1 mV/V.

Then the gage factor selector is set to the numerical value of the actual gage factor of the strain gage. The gage factor selector varies the gain in the ratio 2 : k , so that the calibration for the different gage factor is again correct.

For bridge amplifiers *without* a gage factor selector and for calibration units the calibration value ε^* is calculated as follows:

- a) if the calibration signal is present with the numerical value Z in $\mu\text{m}/\text{m}$:

$$\varepsilon^* = Z \cdot \frac{2}{k_{SG}} \quad (6.5-1)$$

- b) if the calibration signal is present as the bridge unbalance V_o/V_s in mV/V, the following is obtained:

$$\varepsilon^* = \frac{V_o}{V_s} \cdot 2000 \cdot \frac{2}{k_{SG}}, \text{ similarly in } \mu\text{m}/\text{m} \quad (6.5-2)$$

Example of a):

$$Z = 5000 \mu\text{m}$$

$$k_{SG} = 2.07$$

$$\varepsilon^* = 5000 \cdot \frac{2}{2.07} = 4830.9 \mu\text{m}/\text{m}$$

Example of b):

$$\frac{V_o}{V_s} = 0.5 \text{ mV}/\text{V}$$

$$k_{SG} = 2.06$$

$$\varepsilon^* = 0.5 \cdot 2000 \cdot \frac{2}{2.06} = 970.9 \mu\text{m}$$

The bridge amplifier's gain control is now adjusted so that the indicating instrument shows the calculated numerical value of ε^* .

With digital indicating instruments the value of 4831 would be set for example a) above and 971 would be set for example b) .

For an analog instrument with a scale divided into 100 subdivisions, the indicated value is set to 48.3 scale divisions in case a) and to 97.1 scale divisions for case b), where the 1/10th scale divisions must be estimated. Fractions of $\mu\text{m}/\text{m}$ should always be rounded to the nearest full number.

7 The reduction and elimination of measurement errors

Each measurement - irrespective of its type - is unavoidably bound with a measurement error. The task is placed on the person taking the measurement of keeping the error within acceptable limits using reasonable means. The extent to which measurement errors can be influenced depends on

- the measurement method
- the care and attention of the user
- knowledge of possible sources of error
- information on suitable countermeasures
- the effort required to eliminate or correct the error.

The extraordinary wide field of application for strain gage techniques brings with it a wide spectrum of possible sources of interference. A summary of possible sources of error and interfering influences is given in Table 7.0-1. Here, the elements included in the overall term “strain gage measuring point” are identified and explained.

Sources of error in the measuring amplifiers, auxiliary equipment, etc. are not dealt with in the following. An important method for the prevention of measurement errors, i.e. calibration, has already been discussed in section 6. Other sources of error, which are specific to the equipment, cannot be dealt with here on account of the wide variation in equipment; the reader is therefore referred to the appropriate operating instructions which contain the required information on the prevention of errors. Furthermore, the errors due to the equipment are usually of less significance provided there are no errors in operation.

The effects of a number of the interfering influences on strain gages mentioned in Table 7.0-1 have already been discussed in section 3. In that section recommendations were made on how the prevention, reduction and correction of the resulting errors could be carried out. The following sections describe these methods.

Possible error sources and interference effects	
Mounting	selection of the strain-gage type, fixing method, measuring point protection, quality of the mounting, soldering, insulation
Mechanical loading	shock, impact, compression, acceleration, fatigue loading
Temperature	level, change, rate of change, active period
Cable effects	resistance, capacitance and symmetry of cable, surge impedance, insulation, screening
Exceeding the permissible limits	extensibility, temperature range, permissible load cycles
Pneumatic and hydraulic effects	pressure, vacuum
Chemical effects	humidity, water, chemicals, gasses, bacteria
Radiating fields	neutron, gamma and X-ray radiation, electric and magnetic fields
Component properties	inhomogeneities, anisotropic conditions, rheological properties

Strain-gage measuring point consisting of			
Component material adhesive and welding properties	Strain-gage measuring grid material carrier material	Fixing agent organ. adhesive ceram. mounting agent, welded joint	Electrical connections joining leads, solder points, connection cable
		Electrical circuit quarter bridge half bridge diagonal bridge full bridge	Protective agent covering agent screening armoring

Table 7.0-1: Possible sources of error and interference effects on a strain gage measuring point.

7.1 Compensation of thermal output

Response to temperature only occurs if the temperature on the test object, the connecting cables and/or the measurement equipment varies during the measurement. "During the measurement" means between the recording of the reference value, i.e. the zero reading, and recording of the measurement in the loaded state. The cause of thermal output arising from the strain gage has already been described in section 3.3.4. In that section the principle and the limits for automatic temperature response compensation using temperature compensated strain gages were explained.

Another factor contributing to a measuring point's temperature response, which cannot always be neglected, is the electrical connections within the bridge circuit. This appears particularly if the strain gages are connected with one another or to the amplifiers using long cables. Methods of providing compensation in the circuit are described in the following subsections.

The way in which a temperature response effect can occur in amplifiers is only mentioned here. The questions of whether it appears, and to what extent, can be answered by reference to the technical data on the unit.

As already stated at the beginning of this section, there is no response to temperature at constant temperature. However, with objects subject to a volume expansion a draft from an open window or a briefly opened door is sufficient to completely muddle a measurement, although there are only slight temperature differences present. In this case it is not so much the temperature response that is the problem as stress in the object resulting from non-uniform cooling. This causes corresponding strains which are acquired and indicated by the strain gage. Although in such cases the strain gage measurements are correct, their interpretation with regard to the measurement's objective is impossible. (See also section 8.4.7: Measurement of thermal stresses.) Here, it is better to correct the cause of the error.

Principally strain gages should be used which are temperature compensating for the appropriate thermal expansion coefficient of the test object's material. Where the temperature compensation of the strain gage is not sufficient for reasons outlined in section 3.3.4 or where a strain gage is not available to match the thermal expansion coefficient of the test object's material, the compensation methods offered by the Wheatstone bridge are used.

The bridge circuit's compensation principle is based on the fact that interference signals of the *same* sign, having an effect on *neighboring* arms of the bridge, contribute to the bridge unbalance with *opposite* signs. If they have the same amplitude, they fully compensate one another. The principle is clear if equation (7.1-1) is considered, which is derived from equation (5.2-7).

$$\varepsilon_0 = \frac{4}{k} \cdot \frac{V_0}{V_1} = +\varepsilon_1 - \varepsilon_2 + \varepsilon_3 - \varepsilon_4 \quad (7.1-1)$$

Here ε_0 is the indicated strain value, ε_1 to ε_4 are the strain signals supplied by arms 1 to 4 of the bridge.

Measurements on inhomogeneous materials, e.g. fiber reinforced synthetics, give problems with regard to thermal output. The carbon and the glass fibers have substantially smaller coefficients of thermal expansion than the bonding synthetics. Hence, there are different expansion coefficients in the longitudinal and transverse directions, in particular for parts with aligned fiber orientation, with all intermediate values in the directions between the two extremes. The values for the coefficients depend on the constituent materials and on the degree of filling. Temperature compensating strain gages cannot be produced for such materials. Temperature compensation using compensating strain gages is only satisfactory if they are applied under identical conditions to a part of the same material. A larger spread of values for the material characteristics than is usual with metals, and hence larger residual errors due to temperature response, must be taken into account.

7.1.1 Compensation for thermal output using a simple quarter bridge circuit.

In experimental stress analysis and in allied areas of application strain gages are used almost exclusively in the quarter bridge configuration, see section 5.2, Fig. 5.2-2a. Temperature compensating strain gages offer the only usable method of compensation for temperature response, see section 3.3.4. However, the temperature response of the connecting cables, i.e. the leads between the strain gage and the rest of the bridge circuit, still has an effect. The cause of this is the temperature dependence of the conductor material's electrical resistance. For copper the temperature coefficient of electrical resistance is about 0.4%/K, i.e. increasing resistance with rising temperature. For the materials usually used in the high temperature range, e.g. chrome-nickel alloys, platinum alloys, the changes in resistance due to temperature are significantly greater.

All changes of resistance occurring within the bridge circuit have an effect on the bridge unbalance. The bridge circuit cannot distinguish between resistance changes in the strain gage and those in the connecting leads, which are connected in series with the strain gage. This additional temperature response reduces the effectiveness of temperature compensating strain gages or nullifies their effect completely.

Fig. 7.1-1 shows a simple quarter bridge circuit. If the connection leads are heated, an indication occurs even when the measuring point itself remains mechanically and thermally unchanged. The indication is positive in arm 1 of the bridge; it would be negative in arm 2.

The extent of the temperature response caused by the leads is illustrated by an example below.

Example:

A copper lead of length 1 m, i.e. 0.5 m in each direction, having a cross-section of 0.15 mm² and connected in series with a 120 Ω strain gage causes a temperature response of 20 μm/m for a change in temperature of 10 K. With a 350 Ω strain gage the temperature response is only 7 μm/m, although the conditions are otherwise the same.

The simple quarter bridge circuit shown in Fig. 7.1-1 should therefore only be used with short leads and relatively constant temperature, as found for example under laboratory conditions. Longer leads, laid in the open, which are subject to sun and rain during a measurement, may cause significant measurement errors.

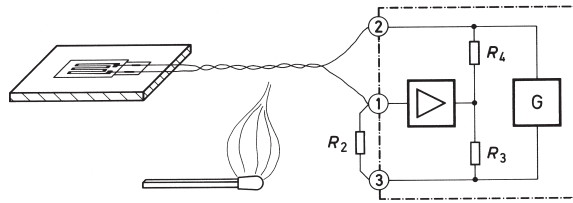


Fig. 7.1-1: Thermal output due to heating of the cable when using a simple quarter bridge circuit.

Calculation of the thermal output due to cable heating with leads which are connected in series with the strain gage in the same arm of the bridge.

ϵ_{ia} = thermal output of a measuring point due to cable heating

α_{RL} = temperature coefficient of resistance for the cable conductor material

$$\alpha_{ca} = 0.004 \frac{\Omega}{\Omega \cdot K}$$

Q = conductivity of the conductor material $q_{ca} = 0.018 \frac{\Omega \cdot \text{mm}^2}{\text{m}}$

$\Delta \vartheta$ = temperature change

R_L = cable resistance

ΔR_L = change of cable resistance

R_{SG} = resistance of the strain gage

k = gage factor

l = length of conductor

A = conductor cross-sectional area

$$\epsilon_{ia} = \frac{1}{k} \cdot \frac{\Delta R_L}{R_{SG} + R_L} \quad (7.1-2)$$

$$R_L = \rho \cdot \frac{l}{A}; \quad l \text{ in m} \quad A \text{ in mm}^2 \quad (7.1-3)$$

$$\Delta R_L = R_L \cdot \alpha_{RL} \cdot \Delta \vartheta = \rho \cdot \frac{l}{A} \cdot \alpha_{RL} \cdot \Delta \vartheta \quad (7.1-4)$$

$$\epsilon_{ia} = \frac{\rho \cdot l/A \cdot \alpha_{RL} \cdot \Delta \vartheta}{k (R_{SG} + \rho \cdot l/A)} \cdot 10^6 \text{ in } \mu\text{m/m} \quad (7.1-5)$$

7.1.2 Thermal output of a quarter bridge in a three-wire configuration

The explanations of the Wheatstone bridge principle in section 5 clearly show that resistance changes of the same sign occurring in neighboring arms of the bridge reduce the bridge unbalance and cancel one another if they are of the same magnitude.

This feature of the bridge circuit is used in various ways for the compensation of interference effects and for the compensation of temperature response.

Using the three-wire circuit it is possible to wire the leads responsible for the temperature response in neighboring arms of the bridge. This is achieved by accessing the electrical potential of the bridge output voltage directly on the strain gage using a third wire which is connected to the measuring instrument; hence the name “three-wire circuit”.

In Fig. 7.1-2 the three-wire circuit (b) is compared with the simple quarter bridge circuit (a).

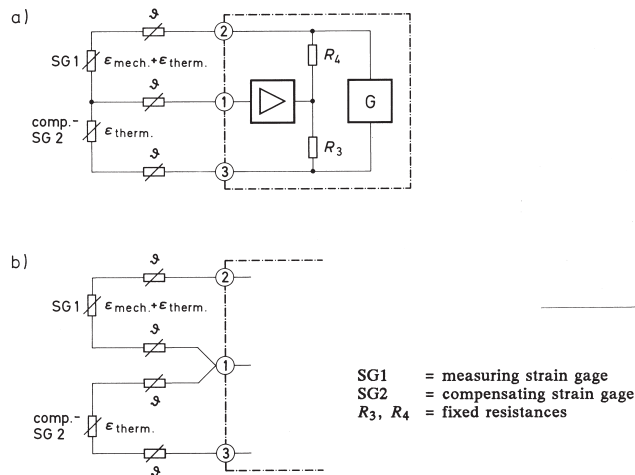


Fig. 7.1-2: Comparison of two-wire and three-wire configurations of the quarter bridge circuit.
 a) two-wire configuration, outward and return wires in series with the strain gage
 b) three-wire configuration, outward wire in series with the strain gage, return wire in series with the bridge completion resistor R_2

\mathcal{G} symbol for the temperature dependent cable resistance

For full compensation the outward and return leads must have identical physical data, i.e. length, cross-section, temperature coefficient, and they must experience the same temperature variations throughout their total length (conductors in the same sleeve, e.g. three-wire cable). Important: Cores having the same outward appearance may have different temperature coefficients if they do not originate from the same manufacturer. The 3rd (potential) wire is passed to the very high impedance amplifier input; its internal resistance and variations in its internal resistance therefore produce no interference effects on the measurement.

The three-wire circuit should be used for direct voltage bridge circuits and with leads of a few meters in length where carrier frequency supply is used. With long lengths of lead and where the supply is high frequency, e.g. 5 kHz carrier frequency, unsymmetrical capacitances can cause problems which are detectable at the CF measuring amplifier's modulation indicator, see section 7.4.

7.1.3 Temperature compensation of a quarter bridge with compensating strain gages.

Very good compensation for thermal expansion is obtained with quarter bridge configurations through the application of compensating strain gages.

The compensating strain gage differs from the measuring, i.e. active, strain gage only by its function in the measurement circuit. Otherwise it must have the same physical characteristics as the measuring strain gage. It should therefore originate from the same strain gage package and the same production lot. Although not essential, it is practical to use temperature compensated strain gages for the measuring and compensating gages, especially if the requirements mentioned below cannot be satisfied. Other requirements are:

The compensating strain gage must be applied to an unloaded point on the test object and must then experience the same temperature variations both with respect to time and amplitude as the measuring strain gage. It is often difficult or almost impossible to find such a point on the test object. The compensating strain gage can then be applied to a piece of the same material of which the test object is composed, e.g. a piece of sheet metal or a small block, which is then brought into thermal contact with the test object. The thermal contact can be produced by simple, unaided mechanical contact, by partial adhesion, or by mechanical fixing in a corner or on an edge using screws or spot welding. There must be no mechanical loading transferred from the test object to the compensating piece and it must not distort, for example due to residual stresses, under the effects of temperature. It must also be rigid enough so that it does not start to oscillate under vibration. This type of inherent behavior would cause measurement errors.

The thermal capacity, i.e. volume, of the compensating piece should be small enough to enable its temperature to closely follow that of the measurement object during temperature variations. It is only after temperature equilibrium has been reached that the full compensation is again obtained. With a small radius of curvature at the measuring point reference should be made to section 3.3.4 and care should be taken to ensure correct correspondence between the measurement object and the compensating piece.

The measuring and compensating strain gages are wired as a Wheatstone half-bridge, see section 5.2 and Fig. 5.2-2b, with R_1 as measuring strain gage and R_2 as compensating strain gage, see Fig. 7.1-3. This is a quarter bridge circuit from the measurement point of view, but it is a half bridge with regard to the circuit. The difference in function should be noted! The type of circuit shown in a) is used if the compensating strain gage can be positioned in close proximity to the measuring strain gage. The circuit in b) is found in applications where the compensating strain gage is mounted remote from the measuring strain gage. It is also used if a number of measuring strain gages are operated with a common compensating strain gage, e.g. via a multipoint scanner.

The effects of the connecting leads on the thermal output are compensated if the conditions required for the three-wire circuit outlined in section 7.1.2 are maintained.

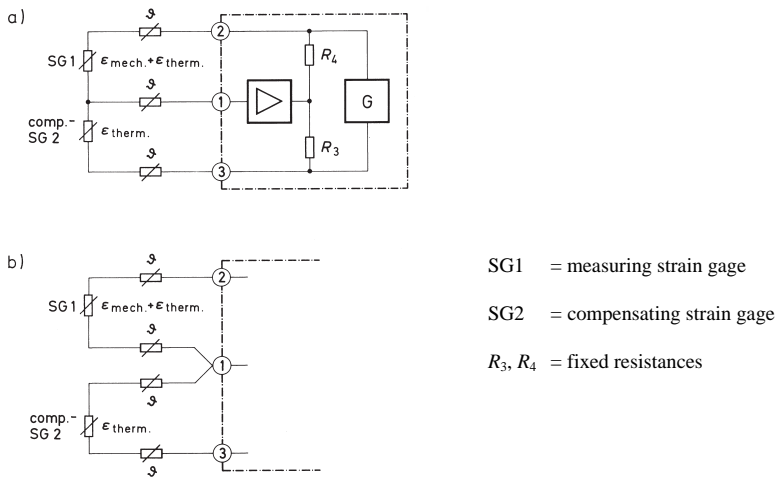


Fig. 7.1-3: Circuit with compensating strain gage
 a) and b) alternative methods of connection

The compensation for thermal expansion is here explained, based on an example.

Strain gage 1 supplies as strain signal ϵ_1 the sum of the mechanical strain ϵ_{mech} and the thermal strain ϵ_{therm} . The compensation strain gage 2 supplies as strain signal 2 only the thermal strain ϵ_{therm} of the compensation piece.

$$\epsilon_i = (\underbrace{\epsilon_{mech} + \epsilon_{therm}}_{\epsilon_1}) - (\underbrace{\epsilon_{therm}}_{\epsilon_2})$$

The arms R_3 and R_4 of the bridge are replaced by fixed resistors. Their contribution to the total signal ϵ_i in equation (7.1-1) is zero, so that the expression can be shortened to

$$\epsilon_i = \epsilon_1 - \epsilon_2 \tag{7.1-6}$$

The indicated measured value alone ϵ_i therefore corresponds to the strain ϵ_{mech} due to the mechanical loading.

With the proper use of compensating strain gages the unavoidable residual thermal output from temperature compensated strain gages is also corrected, see Figures 3.3-10 and 3.3-11.

7.1.4 Compensation of thermal output with the double quarter or diagonal bridge

The term “double quarter bridge” identifies the functional characteristics of the circuit shown in Fig. 7.1-4 better than the term “diagonal bridge”. With regard to the measurement, each of the halves of the bridge, 2-1-3 and 2-4-3, consists of a quarter bridge with a completion resistor as in Fig. 7.1-4a or alternatively they may consist of a quarter bridge with a compensation strain gage as in Fig. 7.1-4b. From the point of view of the circuit a full bridge is formed, but they should not be functionally confused.

To compensate for the thermal output caused by the connecting leads the three-wire circuit of section 7.1.2 is used in Fig. 7.1-4a and in Fig. 7.1-4b the compensation circuit of section 7.1.3 is used.

Where fixed resistors are used for R_2 and R_4 the measured value ϵ_i is formed as follows

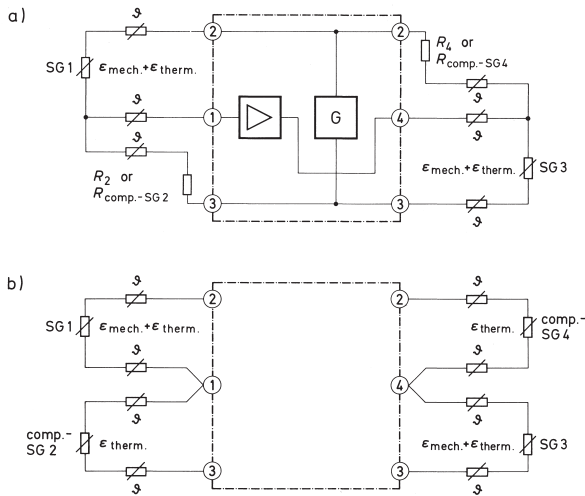
$$\epsilon_i = \underbrace{(\epsilon_{\text{mech1}} + \epsilon_{\text{therm1}})}_{\epsilon_1} - \underbrace{\text{ZERO}}_{\epsilon_2} + \underbrace{(\epsilon_{\text{mech3}} + \epsilon_{\text{therm3}})}_{\epsilon_3} - \underbrace{\text{ZERO}}_{\epsilon_4}$$

The circuit provides the sum of the mechanical strains ϵ_1 plus ϵ_3 . The thermal strains must be canceled out by using temperature compensating strain gages, taking into account the conditions applicable for their proper application, see sections 7.1.1 and 7.1.2. When using compensating strain gages for R_2 and R_4 the total strain then becomes

$$\epsilon_i = \underbrace{(\epsilon_{\text{mech1}} + \epsilon_{\text{therm1}})}_{\epsilon_1} - \underbrace{(\epsilon_{\text{therm2}})}_{\epsilon_2} + \underbrace{(\epsilon_{\text{mech3}} + \epsilon_{\text{therm3}})}_{\epsilon_3} - \underbrace{(\epsilon_{\text{therm4}})}_{\epsilon_4}$$

If the requirements described in section 7.1.3 are maintained, then very good temperature compensation is achieved.

The double quarter bridge is relatively seldom used.



SG1 and SG2 are measuring strain gages
 R1 and R4 are completion resistors or compensating strain gages

Fig. 7.1-4: Double quarter or diagonal bridge
 a) in a three-wire circuit
 b) with compensating strain gages

7.1.5 Compensation for thermal output using the half bridge circuit

Compensation for thermal output using the half bridge circuit is carried out in exactly the same manner as with compensating strain gages. The same requirements must be fulfilled. This method differs from that using compensating strain gages only in that the strain gage in arm 2 of the bridge must not be applied to a point which is free of mechanical loading, but instead contributes to the measurement of the mechanical strain. All the other conditions mentioned for the compensating strain gage also apply here. In the circuit diagrams shown in Figs. 7.1-3a and b the compensating strain gage R₂ is replaced by a measuring strain gage.

The measured value, the indicated strain ε_i, is formed according to the following expression

$$\epsilon_i = (\underbrace{\epsilon_{mech1} + \epsilon_{therm1}}_{\epsilon_1}) - (\underbrace{\epsilon_{mech2} + \epsilon_{therm2}}_{\epsilon_2})$$

The thermal strains ε_{therm 1} and ε_{therm 2} compensate one another if the requirements are satisfied. For opposite signs, the mechanical strains add and they subtract for the like signs:

$$\begin{aligned}\epsilon_i &= (+\epsilon_{\text{mech1}}) - (-\epsilon_{\text{mech2}}) = \epsilon_{\text{mech1}} + \epsilon_{\text{mech2}} \cdot \\ \epsilon_i &= (+\epsilon_{\text{mech1}}) - (+\epsilon_{\text{mech2}}) = \epsilon_{\text{mech1}} - \epsilon_{\text{mech2}} \cdot\end{aligned}$$

Therefore, the half bridge circuit is only used if the proportions of the strains ϵ_1 and ϵ_2 within the total signal ϵ_i are known in both magnitude and sign, e.g. with pure normal loading or pure bending load of a measurement object with symmetrical cross-section, see section 8.

In compensating the thermal output effects of the connecting leads care should be taken to ensure symmetry in the length, electrical resistance, temperature coefficient of leads 2 and 3 and to ensure that they experience the same temperature variations, see also sections 7.1.1 and 7.1.2.

7.1.6 Compensation for thermal output with the full bridge circuit

The full bridge circuit of Fig. 7.1-5 is mainly used in transducers and related measurement techniques. In this type of circuit all four arms of the bridge are occupied by measuring strain gages which are arranged in close proximity to one another. Therefore, the connecting leads, which are internal to the bridge and which produce an unwanted contribution to the thermal output, are very short and the error they produce is very small. If very high accuracy is required, these connections should correspond as closely as possible in both cross-section and length.

The thermal strain of the measurement object affects all four strain gages in the same manner, producing very good temperature compensation. The measurement signal ϵ_i consists of the arithmetic sum of the four measured strains ϵ_1 to ϵ_4 :

$$\epsilon_i = \epsilon_1 - \epsilon_2 + \epsilon_3 - \epsilon_4 \cdot$$

If the measurement object is subject to uneven temperature variations, e.g. due to single-sided thermal radiation, then an attempt should be made to provide thermal equilibrium by encapsulation in thermally insulating material, screening from thermal radiation or other suitable methods.

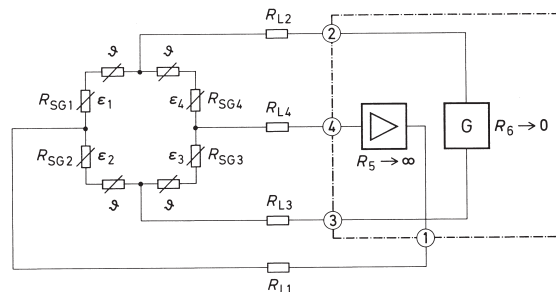


Fig. 7.1-5: Full bridge circuit

The bridge output leads (signal leads) shown in Fig. 7.1- 5, having lead resistances R_{L1} and R_{L4} have no influence on the thermal output nor on the measurement signal. The two bridge supply leads with lead resistances R_{L2} and R_{L3} also do not have any influence on the thermal output; section 7.2 deals with their influence on the measurement signal and the measured value.

In stress analysis the full bridge circuit can only be used if the strain distribution on the four individual strain gages is known exactly with respect to their sign and with respect to their ratios to one another, e.g. for a bending beam with symmetrical bending cross-section and for tension and compression bars, see section 8. The quarter bridge circuit must be used for all cases where the strain distribution is unknown.

7.2 The influence of lead resistances

The resistance of the connecting leads between the strain gage and the corner points of the bridge circuit (i.e. bridge connecting points 1 and 4 in the following circuit diagrams) can produce such a large bridge unbalance with asymmetrical circuits (simple quarter bridges, double quarter bridges or diagonal bridges), that they can no longer be corrected with the adjustment device (R compensation) on the connected measuring amplifier. The amplifier is almost fully driven or even overdriven.

In these cases the resistance of the adjacent completion resistor (R_2 for a quarter bridge, R_2 and R_4 for the double quarter bridge) must be increased appropriately. Very stable metal film resistors are the only ones suitable as completion resistors.

A second effect of the lead resistance, i.e. on the calibration, has already been mentioned in section 6: the resistance of the connecting leads reduces the measured value provided by the strain gage. It has been described how special calibration methods can eliminate this error (section 6.3). If there are sufficient precision shunt resistors available, shunt calibration is sometimes the most reliable method of reducing measurement errors. If multipoint techniques are used, then shunt calibration also enables the allocation of the strain gage to the switch position on the scanner to be checked. If calibration cannot be undertaken, then the effects due to the cables must be corrected. The following assumes constant supply voltage.

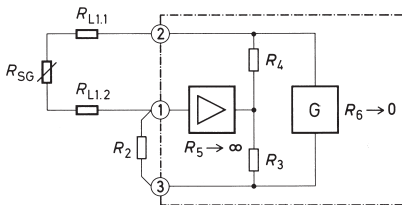
In the circuit diagrams the connections between the individual elements in the circuit are taken to have zero resistance. In reality this assumption depends on whether the cable is short and whether its resistance is at least two or three orders of magnitude smaller than that of the strain gage and the bridge circuit, so enabling it to be neglected. However, for long connecting cables this assumption is no longer valid. With the use of thin cable cores or leads in a material of high relative resistivity, e. g. in the high temperature range, even short sections of cable can produce significant measurement errors.

Sections 7.2.1 to 7.2.6 contain the equations for calculating the corrections to the measurements for the various circuits. Section 7.2.7 contains the equations for error correction using the gage factor selector on the amplifier.

For the influence of contact resistance in slip-ring techniques see section 8.4.4.1.

7.2.1 Simple quarter bridge circuit

The manner in which the resistance of the connecting leads reduces the strain gage signal is explained here based on a simple quarter bridge circuit, see Fig. 7.2-1. Together with the connecting leads the strain gage forms arm 1 of the bridge; the fixed resistors R_2 , R_3 , R_4 complete the bridge circuit.



- R_{SG} measuring strain gage
- $R_{L1,1}$, $R_{L1,2}$ resistances of the connecting leads between the strain gage and the rest of the bridge circuit
- R_2 to R_4 completion resistors
- R_5 input resistance of the measuring amplifier
- R_4 output resistance of the constant voltage generator G

Fig. 7.2-1: Influence of cable resistances for the simple quarter bridge circuit

The resistance of arm 1 of the bridge is formed from the individual resistances of the strain gage R_{SG} , the outward lead $R_{L1,1}$ and the return lead $R_{L1,2}$. For strain measurements with strain gages it is assumed that the bridge unbalance is a measure of the strain as in equation (5.2-9):

$$\frac{V_2}{V_1} = \frac{1}{4} \left(\frac{\Delta R}{R} \right)_{\infty} \quad (7.2-1)$$

The relative change of resistance of the strain gage is proportional to the strain:

$$\frac{\Delta R_{SG}}{R_{SG}} = \epsilon \cdot k, \quad (7.2-2)$$

In the case shown in Fig. 7.2-1 the bridge circuit “sees” the change in resistance ΔR of the strain gage relative to the total resistance of arm 1 of the bridge, i.e. a smaller relative change of resistance:

$$\frac{\Delta R_{SG}}{R_{L1,1} + R_{SG} + R_{L1,2}} < \epsilon \cdot k. \quad (7.2-3)$$

Therefore the measured signal is too small.

An example here provides an impression of the order of magnitude for the influence of the cable resistance on the measurement result.

Example:

A cable of length 100 m (2 cores each 100 m) with a core cross-section of 0.5 mm² copper in a quarter bridge circuit, i.e. cable resistances in series with the strain gage resistance, causes a measurement error of

-5.8% with a strain gage resistance of 120 Ω

- 1.8% with a strain gage resistance of 350 Ω
- 1.2% with a strain gage resistance of 600 Ω

With a core cross-section of 0.14 mm² the measurement error reaches

- 17.5% with a 120 Ω strain gage
- 6.8% with a 350 Ω strain gage
- 3.7% with a 600 Ω strain gage

The erroneous result can be easily corrected with the aid of the diagram in Fig. 7.2-2 according to the relationship

$$\epsilon = \epsilon_i \frac{100 \%}{\text{res. indication \%}} \tag{7.2-4}$$

Here ϵ is the correct value and ϵ_i is the indicated (wrong) value. The percentage of the residual indication or the loss in the signal (error) can be taken from the diagram.

Two examples are shown in Fig. 7.2-2 to explain of the use of the diagram.

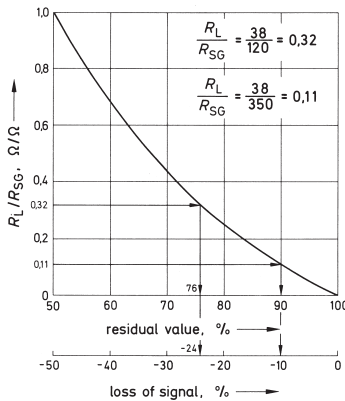


Fig. 7.2-2: Diagram for determination of the residual indication and the loss of signal as the result of cable resistance.

Firstly, the ratio R_L/R_{SG} is formed and the figure is found on the ordinate scale. From this point a line is traced horizontally to the curve and then a vertical line is traced downwards to the abscissa. Here the percentage of the residual indication can be read off and placed in the denominator in equation (7.2-4).

The indicated, uncorrected measurement value always applies as ϵ_i and for R_L the total cable resistance in series with the strain gage within the arm of the bridge. The accuracy of the correction mainly depends on the accuracy with which the cable resistances are measured.

With longer lengths of connecting cable it is possible that the total resistance $R_{SG} + R_{L1.1} + R_{L1.2}$ of bridge arm 1 is so large that the adjustment offered by the measuring amplifier is

no longer sufficient for compensation of the zero point. The completion resistor R_2 must then be matched. Increasing R_2 to the total resistance R_1 has no detrimental effect on the measurement result.

It is also possible to correct the measurement value ϵ_i by computer. For the simple quarter bridge circuit the following equation applies

$$\epsilon = \epsilon_i \frac{R_{L1,1} + R_{SG} + R_{L1,2}}{R_{SG}} \quad (7.2-5)$$

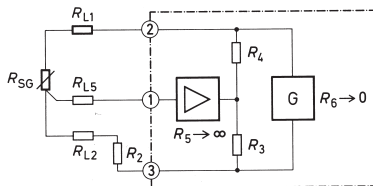
In Fig. 7.2-1 the resistances to be included in the correction are shown in heavy type. For both correction methods the resistance values of the leads to be considered and of the strain gage must be known, the former by measurement and the latter can be taken from the data sheet enclosed in the strain gage packing.

7.2.2 Quarter bridge in a three-wire circuit

With the quarter bridge in a three-wire circuit, see Fig. 7.2-3, only the outward lead is in series with the strain gage. Consequently, only the resistance R_{L1} affects the strain gage's measuring signal. The correction equation is

$$\epsilon = \epsilon_i \frac{R_{SG} + R_{L1}}{R_{SG}} \quad (7.2-6)$$

The values of the resistors shown in heavy print in Fig. 7.2.3 should be substituted into the correction equation.



Definitions as in Fig. 7.2-1.

Fig. 7.2-3: Influence of the cable resistance for the quarter bridge circuit with a three-wire strain gage connection.

The return lead with R_{L2} is located in the passive bridge arm R_2 and therefore has no influence on the measurement result.

The resistance R_{L5} of the signal lead can be neglected if the input resistance of the amplifier, R_5 , is at least one thousand times the strain gage resistance. Modern amplifiers fulfill this requirement.

The error correction can also be carried out with the aid of the diagram in Fig. 7.2-2.

7.2.3 Quarter bridge with compensating strain gage

Fig. 7.2-4 shows two variations of a quarter bridge circuit with compensating strain gages:

- measuring strain gage and compensating strain gage in a close configuration. The corresponding correction equation is equation (7.2-6),
- measuring strain gage and compensating strain gage in a separated configuration. Equation (7.2-5) is the corresponding correction equation.

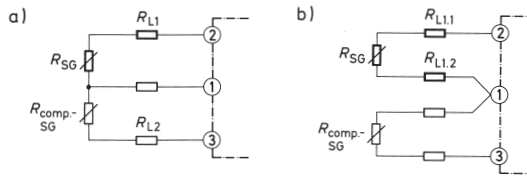


Fig. 7.2-4: Quarter bridge circuit with compensating strain gage
 a) measuring strain gage and compensating strain gage in a close configuration,
 b) measuring strain gage and compensating strain gage in a separated configuration.
 The resistances to be considered for error correction are shown in heavy print.

Circuit a) is used if the compensating strain gage is positioned in close proximity to the measuring strain gage. Circuit b) is used if a larger distance separates the measuring and compensating strain gages. It is also generally used in multipoint measuring equipment if the same compensating strain gage is consecutively switched to a number of measuring strain gages.

For both circuits the error correction can also be carried out using the diagram in Fig. 7.2-1.

7.2.4 Double quarter or diagonal bridge

Two variations of the double quarter bridge circuit are shown in Fig. 7.2-5:

- double quarter bridge circuit with the measuring strain gages SG 1 and SG 3 each in a three-wire circuit with the completion resistances R_2 and R_4 . The corresponding correction equation is:

$$\epsilon_1 + \epsilon_2 = \epsilon_1 \frac{R_{L2} + R_{SG11} + R_{SG3} + R_{L2}}{R_{SG1} + R_{SG3}} \quad (7.2-7)$$

If compensating strain gages in an adjacent arrangement are used in place of the fixed resistances (similar to Fig. 7.2-4a), then the same correction formula applies.

- If the compensating strain gage is in a separated arrangement (similar to Fig. 7.2-4b), then the correction equation is:

$$\epsilon_1 + \epsilon_3 = \epsilon_1 \frac{R_{L11} + R_{SG1} + R_{L12} + R_{L31} + R_{SG3} + R_{L32}}{R_{SG1} + R_{SG3}} \quad (7.2-8)$$

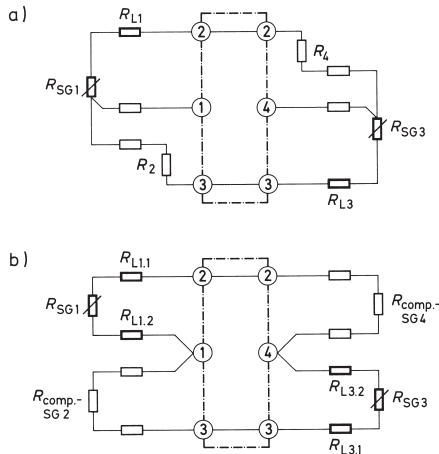


Fig. 7.2-5: Double quarter or diagonal bridge circuit
 a) double quarter bridge in a three-wire circuit
 b) double quarter bridge with separate positioning of the compensating strain gage

7.2.5 Half bridge circuit

The half bridge circuit in Fig. 7.2-6 contains two measuring strain gages; it therefore differs from the quarter bridge circuit in Fig. 7.2-4.

Two variations are again shown in Fig. 7.2-6. In a) the situation is shown where the strain gages are closely positioned adjacent to one another. The corresponding correction formula is:

$$\epsilon_1 - \epsilon_2 = \epsilon_1 \frac{R_{L1} + R_{SG1} + R_{SG2} + R_{L2}}{R_{SG1} + R_{SG2}} \quad (7.2-9)$$

In b) the case is shown where the two strain gages are separated from one another by some distance. Here the correction formula is:

$$\epsilon_1 - \epsilon_2 = \epsilon_1 \frac{R_{L1,1} + R_{SG1} + R_{L1,2} + R_{L1,3} + R_{GL2} + R_{L2,3}}{R_{SG1} + R_{SG2}} \tag{7.2-10}$$

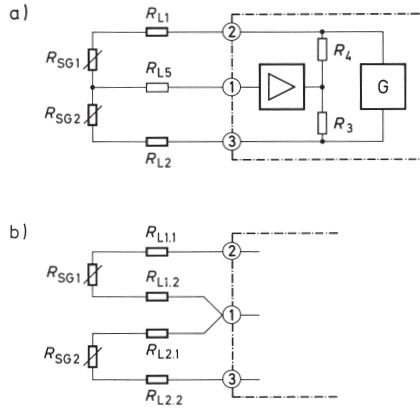


Fig. 7.2-6: Half bridge circuit
 a) strain gages in a close adjacent arrangement
 b) arrangement of strain gages with some distance between them.

7.2.6 Full bridge circuit

On account of its favorable characteristics - large measurement signal, automatic compensation of interference effects - the full bridge circuit is the arrangement preferred for use in transducer construction. Its advantages bring special benefits if the internal bridge wiring is short and symmetrical.

If this is the case, the resistance of the connecting wires is so small that it can be neglected and therefore requires no special consideration. Instead the resistance of the connecting cable between the measuring amplifier and the transducer should be taken into account, i.e. the two cores for the bridge supply with their resistances R_{L2} and R_{L3} , see Fig. 7.2-7. As in all the previous examples, the resistances in the signal leads 1 and 4 do not reduce the signal.

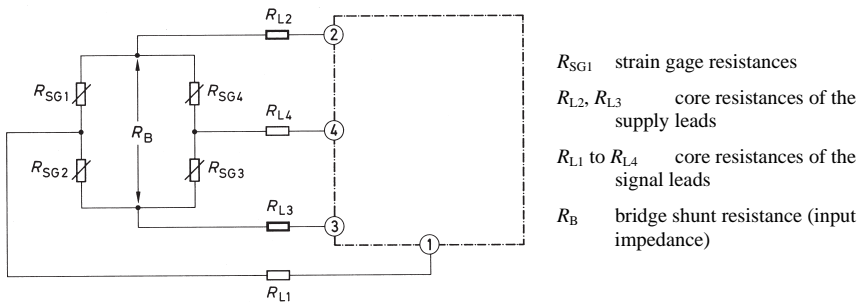


Fig. 7.2-7: Full bridge circuit

The correction equation is:

$$\epsilon_1 - \epsilon_2 + \epsilon_3 - \epsilon_4 = \epsilon_1 \frac{R_{L2} + R_B + R_{L3}}{R_B} \quad (7.2-11)$$

R_B identifies the bridge shunt resistance (input resistance).

$$R_B = \frac{(R_{SG1} + R_{SG2}) \cdot (R_{SG3} + R_{SG4})}{R_{SG1} + R_{SG2} + R_{SG3} + R_{SG4}} \quad (7.2-12)$$

If all the strain gage resistances are the same as one another, which can be assumed, then the bridge input resistance is the same as the strain gage resistance.

For measurements with transducers in a full bridge circuit the calibration method described in section 6.4 using a calibration unit should be regarded as being the most simple method which is also often the best method.

7.2.7 Error correction using the gage factor selector

There is another method of eliminating the effects of cable resistance if the measuring amplifier that is used has a gage factor selection switch, see sections 6.1 and 6.5.

The loss of signal that occurs due to the cable resistance can be considered as a reduction in the gage factor of the strain gage. If the gage factor selector is adjusted to the value of the reduced gage factor k^* , then the gain of the measuring amplifier is increased correspondingly, so that the indicated strain value is again correct. The following formulae for the calculation of the apparent gage factor k^* apply for the various circuits as follows:

Simple quarter bridge circuit as in Fig. 7.2-1:

$$k^* = k \cdot \frac{R_{SG}}{R_{L11} + R_{SG} + R_{L12}} \quad (7.2-13)$$

Quarter bridge in a three-wire circuit as in Fig. 7.2-3:

$$k' = k \cdot \frac{R_{B0}}{R_{B0} + R_{L1}} \quad (7.2-14)$$

Quarter bridge with compensating strain gage as in Fig. 7.2-4:

For case a) equation 7.2-14 applies,
for case b) equation 7.2-13 applies.

Double quarter or diagonal bridge as in Fig. 7.2-5:

For case a) equation 7.2-14 applies,
for case b) equation 7.2-13 applies.
It is assumed that both arms 1 and 3 of the bridge are occupied with identical components.

Half bridge circuit as in Fig. 7.2-6:

For case a) equation 7.2-14 applies,
for case b) equation 7.2-13 applies.
It is also assumed here that both arms 1 and 2 are occupied with identical components.

Full bridge circuit as in Fig. 7.2-7:

$$k' = k \cdot \frac{R_B}{R_{L2} + R_B + R_{L3}} \quad (7.2-15)$$

The bridge input resistance R_B should be measured or calculated according to equation (7.2-12).

7.3 Eliminating cable effects with special circuits in the measuring amplifier

Whereas the methods described in sections 7.1 and 7.2 are primarily concerned with the compensation of interference effects, here the design of equipment is described which from the outset avoids the occurrence of errors due to the cable connections. In [5-2] the operational principles of such a device are explained based on the circuit diagram. In the following section an extract from the quoted publication is reproduced with the kind permission of the author.

7.3.1 HBM bridge (citation from [5-2])*

As long ago as 1976 the author proposed a circuit [7-1] which was also based on the Wheatstone bridge but which avoided its error-producing drawbacks almost completely.

* The patented circuits are now used in commercially available equipment under the designation "Kreuzer Circuit" and "Extended Kreuzer Circuit"

Fig. 7.3-1 shows its principle. The bridge supply voltage V_s is no longer fed directly to the strain gages but simply acts as a reference voltage for amplifiers A2 and A3. These amplifiers correct their output voltages until the voltages picked off via the sensing leads to

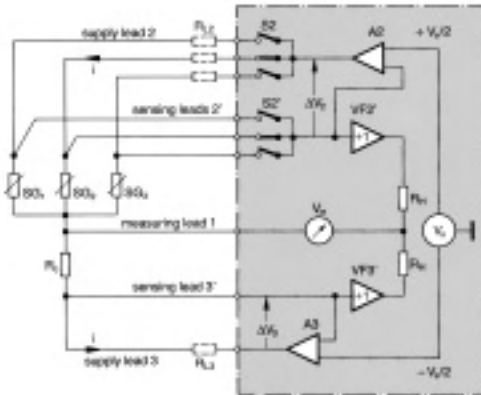


Fig. 7.3-1 Quarter-bridge circuit for almost error-free connection of single strain gages with completion resistor R_c close to the measuring point

the measuring points and fed back via the unity-gain amplifiers VF2' and VF3' are equal to the voltages $+V_s/2$ and $-V_s/2$. The voltage drops ΔV_2 and ΔV_3 on the supply leads and the supply switches S2 are therefore eliminated; the output voltages of amplifiers A2 and A3 exceed voltages $+V_s/2$ and $-V_s/2$ by the amount of the voltage drops ΔV_2 and ΔV_3 . Therefore, the precise bridge supply voltage is available at the measuring points.

Due to the extremely high input impedances of the amplifiers and unity-gain amplifiers VF2' and VF3', the sensing leads carry practically no current so their resistance and the resistance of the switches S2' can cause no voltage drops, and therefore no measuring errors. Since the internal half-bridge (resistor R_H), which makes the external half-bridge into a full bridge, is connected to the voltages fed back from the measuring points via the unity-gain amplifiers VF2' and VF3', the external and internal half-bridges are at precisely the same voltages, even when the voltage regulation of amplifiers A2 and A3 leaves small residual errors. By using modern operational amplifier circuits, the unity-gain amplifiers can be made so precise that their error is small enough to be neglected.

Thus, zero and sensitivity errors are almost completely eliminated. The circuit is suitable for DC and carrier-frequency operation. With the latter, an even greater precision is achieved because the small offset and temperature drift of the amplifiers have no effect. Another advantage of the circuit shown in Fig. 7.3-1 is that only two leads and two switches are needed for each additional strain gage connected.

On the other hand, the circuit requires the complementary resistor R_c to be placed close to the strain gages because voltage drops on the connection leads between the strain gages and the resistor are not balanced out. Also the direct metallic connection of the strain gages means that, should one of the gages ground, the readings of the whole group can become incorrect.

Fig. 7.3-2 shows an expanded version of the circuit in Fig. 7.3-1 which enables single strain gages to be connected over long distances up to 1000 m and the completion resistor can even be incorporated in the measuring unit [7-2]. Compared with the circuit in Fig. 7.3-1, the expanded circuit incorporates two additional unity-gain amplifiers VF1 and VF4 and a differential amplifier DA. The voltage drop ΔV_1 , caused by the supply current in the supply lead 4 and switch S4, i.e. the connection between the strain gage and the completion resistor R_C is tapped off from the unity-gain amplifiers VF1 and VF4 and halved exactly by the resistors R_D which provides equal proportions for the two arms of the external half-bridge. This eliminates the effect of the voltage drop V_1 on the zero. Since the voltage V_1 is fed to the bridge voltage generator via the differential amplifier DA, and the bridge supply voltage V_s there is increased by the amount V_1 , the sum of the voltages present directly at the strain gages and supplementary resistor is always a constant V_{ref} . Therefore, the voltage drops V_1 and V_2 have no adverse effect on the measuring sensitivity. Since the circuit in Fig. 7.3-2 switches the strain gage on and off completely, the grounding of one strain gage will not affect the others.

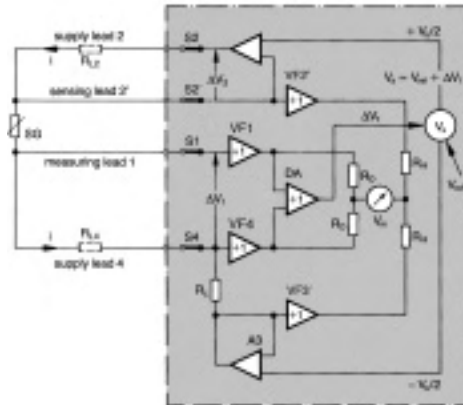


Fig. 7.3-2 Quarter-bridge circuit for almost error-free connection of single strain gages with completion resistor R_C remote from the measuring point

Fig. 7.3-3 shows in a more detailed form of the circuit in Fig. 7.3-2 the connection technique used by HBM for full, half and quarter bridges. It is possible to supplement individual strain gages with physically separate compensation strain gages, e.g. as shown for measuring point M2 in Fig. 7.3-3, or to extend single strain gages to a half bridge by means of the internal completion resistor $R_{C\text{int}}$ or a common external supplementary resistor $R_{C\text{ext}}$. When a carrier frequency is used, i.e. using a sinusoidal alternating voltage as the bridge supply voltage, the internal half bridge R_H and also the resistance divider R_D if necessary, can be made into an inductive divider, which effects a substantial reduction in the measuring error with half and quarter bridge circuits because inductive dividers can be made with substantially greater temperature stability and, particularly, long-term stability than resistance dividers.

End of the citation.

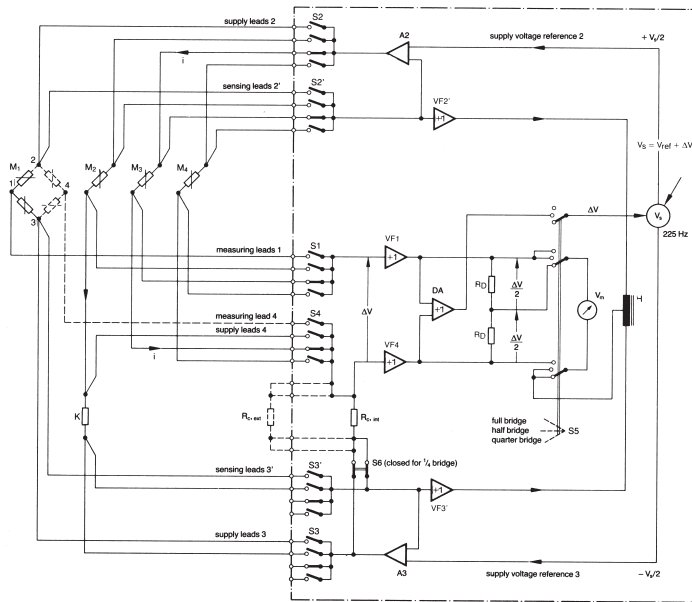


Fig. 7.3-3 HBM bridge circuit for the error-free connection of quarter, half and full bridges

7.3.2 The six-wire circuit

The six-wire circuit operates on similar principles as the Kreuzer circuit. It is however restricted to the connection of full bridge strain gage circuits. Fig. 7.3-4 shows the principle.

An adjustable voltage generator G provides the voltage V_G for the supply of the transducer fitted with full bridge strain gage circuit. As a consequence of the voltage drop arising due to the supply current I_B through the cable resistances R_{L2} and R_{L3} of the supply leads, the transducer receives the lower supply voltage V_s . The two sensing leads 6 and 7 return the voltage V_s to the comparator which compares it with a reference voltage V_{ref} . The reference voltage V_{ref} is equal to the required bridge supply voltage. The cable resistances R_{L6} and R_{L7} of the sensing leads do not have any detrimental effect because no current flows through them. If V_s deviates from V_{ref} , then the generator, controlled by the comparator, increases its voltage V_G until the sensing leads signal that V_s is the same as V_{ref} . The required voltage is then present across the transducer.

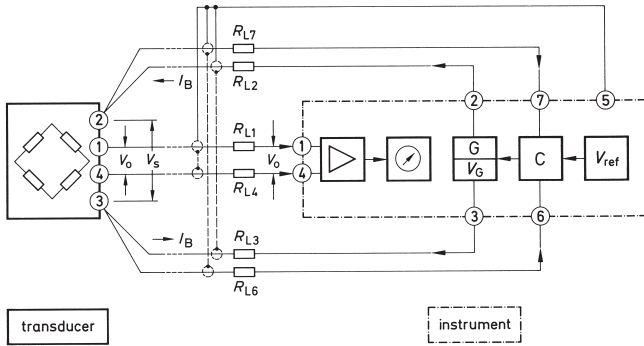


Fig. 7.3-4: Principle of the six-wire circuit.

The adjustment of the generator voltage can also be carried out manually as well as automatically. Automatic control has the big advantage in that changes in the resistances of the supply leads during a measurement, e.g. due to the temperature coefficient of the copper during temperature variations, are always immediately corrected. The measurement signal V_0 therefore corresponds to the measured value at any point in time. The resistances of the signal leads R_{L1} and R_{L4} also do not have any effect here, because the measuring amplifier also does take any current.

7.4 The influence of cable capacitances

The cores of a cable form capacitors between one another. Their capacitance depends on the length of the cores, the distance between them, their cross-section, their dielectric (insulation) and the temperature. This applies equally to separate wired leads.

Fig. 7.4-1 shows the circuit of a full strain gage bridge to which a screened cable is connected. The Wheatstone bridge circuit is formed by the resistances R_1 to R_4 . The capacitors C_1 to C_4 , C_9 and C_{10} are formed between the cores 1 to 4 of the connection cable. With screened cable the capacitances C_5 to C_8 are also formed.

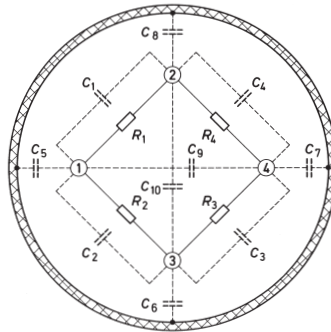


Fig. 7.4-1: Capacitances occurring in the screened connecting cable of a Wheatstone bridge circuit between the cable cores and between the cores and the screen.

The cable capacitances may occur as sources of error in two different ways:

- a) Capacitive unsymmetry in the bridge circuit can lead to overdriving of the measuring amplifier and therefore to erroneous measurement results. Capacitive overdriving is only possible with carrier frequency systems. Section 7.4.1 describes how this may be counteracted.
- b) With the resistances the cable capacitances form RC networks which produce a change of phase with dynamic signals. With direct voltage systems and with low frequency carrier frequency systems amplitude errors can occur if the demodulation control does not operate synchronously to the phase-shifted carrier frequency arriving at the amplifier. Countermeasures are explained in Section 7.4.2.

Both of these effects arise mainly with long sections of cable, but they may also be apparent in unfavorable cases with wrong equipment settings even with short leads. In any case it is advisable to use low capacitance cable of high quality and to avoid unnecessarily long cables.

7.4.1 Capacitive unsymmetry

Fig. 7.4-2 shows only a part of the cable capacitances contained in Fig. 7.4-1. These are the capacitances C_1 to C_4 . They are each located parallel to the bridge resistances R_1 to R_4 , forming a capacitive bridge in parallel to the resistive bridge.

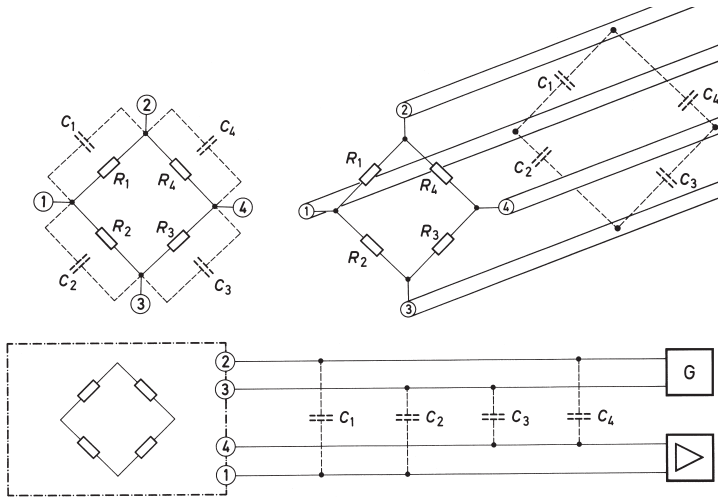


Fig. 7.4-2: The resistive bridge and the parallel capacitive bridge formed by the cable capacitances which is shown in three different ways.

For alternating voltage supply (carrier frequency operation) each capacitance behaves as a frequency dependent impedance. The capacitive impedance X_c , the reactive impedance, of a capacitor depends on its capacitance C and the frequency f of the alternating voltage:

$$X_c = \frac{1}{\omega C} = \frac{1}{2\pi \cdot f \cdot C} \quad (7.4-1)$$

Provided the four capacitances are equally large, the capacitive bridge is balanced. However if differences in capacitance occur, i.e. capacitive unsymmetry, the capacitive bridge becomes unbalanced and therefore a bridge output voltage occurs which is not determined by the measured variable. The capacitive output voltage is phase-shifted by 90° compared to the resistive output voltage. The following amplifier amplifies both of the resistive and capacitive bridge output voltages.

The demodulation, which depends on the phase, provided by the carrier frequency measuring amplifier ensures that only the signal originating from the resistive bridge unbalance, and not the capacitive unbalance, is amplified and passed to the indicating instruments. So far so good, but if with a high capacitive bridge unbalance the amplifier may be driven to a significant extent or even fully driven. If resistive bridge unbalance then occurs, the amplifier may be overdriven, i.e. the amplifier output voltage is no longer proportional to the resistive bridge unbalance and the indication is erroneous. Measuring amplifiers are fitted with an additional overdrive indicator to show when the amplifier is operating in the overdriven state. This only gives information on the total degree of overload on the amplifier without any indication of the cause. The deflection on the overload indicator can be brought to a minimum with the aid of the capacitance compensator on carrier frequency amplifiers ("C compensation"): The bridge is then capacitively balanced. If a residual indi-

ation remains then it is probably caused by a resistive bridge unbalance. Details can be taken from the operating instructions relevant to the measuring amplifier.

It should also be noted that there are carrier frequency amplifiers which do not possess any C compensation and which do not need any due to their special design. These are used in systems with low signal resolution.

How do capacitive unsymmetries arise?

In Fig. 7.4-3 the circuits usually encountered in strain gage technology are shown with the effective capacitances.

With the full bridge circuit, Fig. 7.4-3a, the geometrical arrangement of the cable cores must correspond with the corner points of the bridge circuit. If two adjacent cores are interchanged, then capacitive unsymmetry arises giving the problems previously outlined.

The core-core capacitance for measurement cable is between about 70 and 150 pF/m depending on its construction. HBM measurement cables exhibit good capacitive symmetry; even with long cable lengths usually no systematic trends occur. (The resistive unsymmetry is almost insignificant, i.e. the difference in resistance between the individual cores.) Difficulties in compensation when testing for capacitive symmetry during fault finding may indicate wiring faults in plugs or connections. The test is carried out with capacitance measuring equipment whose frequency should if possible be between 1,000 to 10,000 Hz.

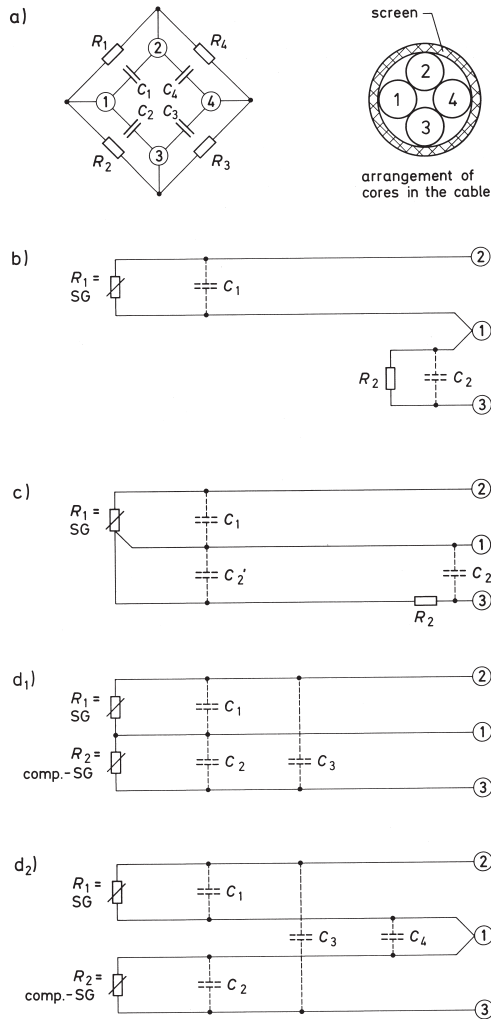


Fig. 7.4-3: Representation of the cable capacitances for the various methods of connecting strain gages

- a) The capacitances between cores 1 and 2 (C_1) and between cores 1 and 3 (C_2) must be equal in size. A difference of 100 to 200 pF can be tolerated, irrespective of the cable length.
- b) The capacitances between cores 4 and 2 (C_4) and between cores 4 and 3 (C_3) must also be equal to within 100 to 200 pF.

If the capacitance values for a) and b) are different, it does not matter. It is important that there is symmetry within each of the bridge halves 2-1-3 and 2-4-3. If an unsymmetry arises which exceeds the tolerance mentioned, it can be compensated with supplementary

capacitors. It should be first ensured that there are no wiring faults. The capacitors may be connected at the start or at the end of the cable.

Drastic capacitive unsymmetry occurs with the *simple quarter bridge* configuration, Fig. 7.4-3b, if the strain gage (R_1) is connected with long leads and the completion resistor (R_2) is connected with short leads in the vicinity of the measuring amplifier. C_1 is then substantially greater than C_2 . If the capacitance compensation of the measuring amplifier is not sufficient to balance out the unsymmetry, a capacitor of suitable size can be wired to the connections 1 and 3.

Principally the unsymmetrical methods of configuration, i.e. quarter and double quarter bridges, are the most unfavorable with regard to their susceptibility to errors. The *quarter bridge in a three-wire configuration*, Fig. 7.4-1c, compensates the measuring point thermal output due to the leads, but does not compensate the capacitive unsymmetries. Leads 1 and 3 are wired together at the strain gage and are therefore at the same potential. As a result of this short circuit the capacitance C_2 is ineffective. If symmetrical balancing with a capacitor is required, it must be wired at the amplifier from connection 1 to connection 3.

The *quarter bridge with compensating strain gage*, Fig. 7.4-3d₁, is a better solution even if a completion resistor is used instead of the compensating strain gage. The equally long leads 1, 2 and 3 ensure symmetry of the two capacitances C_1 and C_2 . C_3 has no effect; the two lines 2 and 3 are almost short circuited by the extremely low internal impedance of the bridge supply.

The variation in 7.4-3 d₂ does not differ in its capacitive characteristics from that shown in d₁. This is also the case if a measuring strain gage is used instead of a compensating strain gage. A *half bridge circuit* is then obtained.

With the *double quarter bridge* the capacitive unsymmetry doubles compared to the simple quarter bridge and compared to the quarter bridge in a three-wire configuration.

7.4.2 Phase rotation

In section 4.2.3.2 the advantages were pointed out of using screened cable for the connection of the strain gage or transducer to the measuring amplifier. Careful earthing of the copper braid screening guards against the effects of electric fields, including the unwanted “line hum” and induced effects from the 50 Hz power supply network.

Thus there arise, in addition to those discussed in section 7.4.1, the capacitances C_5 to C_8 between the cable cores and the screen, as well as the diagonally acting capacitances C_9 and C_{10} in the four-core cable. This is shown in Fig. 7.4-4.

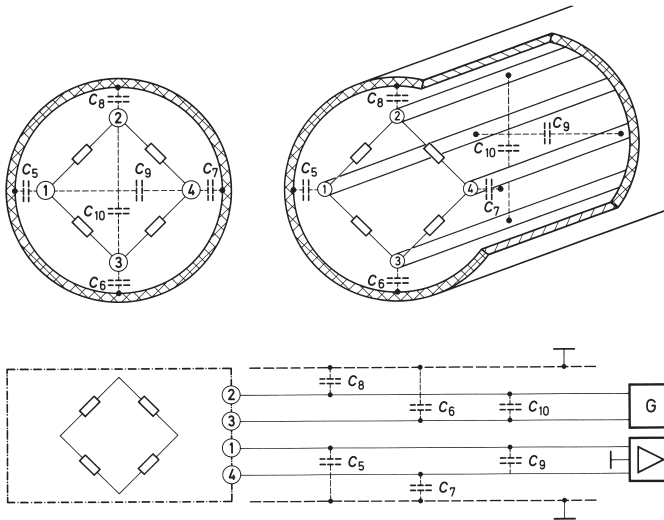


Fig. 7.4-4: Cable capacitances which contribute to the phase rotation in the measurement signal.

The capacitors between the bridge supply cores 2, 3 and the screen, together with the interacting capacitances C_6 , C_8 and C_{10} , only appear as an additional load on the supply when it is an alternating voltage supply and they have no detrimental effects on the measurement.

In contrast the capacitances C_5 , C_7 and C_9 form an RC network through the measuring leads 1 and 4 together with the bridge internal resistance of the transducer. A phase shift between the measurement signal on the transducer's output and the input of the measuring amplifier occurs due to the network's time constant τ and the frequency f of the supply voltage (or the frequency of the measurement signal with a direct voltage supply).

$$\tau = R \cdot C \quad (7.4-2)$$

$$\varphi = \frac{R \cdot C}{f} \cdot 2\pi \quad (7.4-3)$$

With direct voltage supply this is only of interest if a number of signals must be acquired in parallel and synchronously.

With carrier frequency amplifiers the demodulator must convert the amplitude modulated transducer signal into a rectified output signal. Therefore the switching voltage taken from the generator, i.e. the oscillator, for the demodulator must have the same phase relationship as the transducer signal on the demodulator input. The matching is carried out purely empirically with the aid of a second RC network in the measuring amplifier whose time constant is adjustable; thus the switching voltage's phase relationship can be aligned with that of the transducer signal. The simple adjustment that is necessary is described in the operating instructions under the heading "Reference phase adjustment".

The reference phase adjustment for the prevention of measurement errors is used in the same manner and with the same effectiveness in all the other circuit configurations described in section 7.

7.5 Correction of the transverse sensitivity of a strain gage

The term “transverse sensitivity” means that a strain gage does not only react, producing a change in resistance, to strains in its measurement grid's longitudinal direction, but also to transverse strains. The definition of transverse sensitivity and its causes are described in section 3.3.3. Fortunately, the transverse sensitivity of modern foil strain gages is very small. In the diagrams in Figs. 3.3-7a and b the transverse sensitivity is given for a number of normal linear strain gages and strain gage rosettes. For the most popular types this is ± 0.005 ($\pm 0.5\%$), but a special type achieves the ideal value 0 and with the remaining types the transverse sensitivity is in the region of 0.01 (1%). Therefore in most cases correction of the measurement can be waived [7-3] without incurring severe errors unless extremely large transverse strains affect the strain gage or extraordinarily high measurement accuracy is required. Correction is only worthwhile in these cases. In transducer design the transverse sensitivity is of secondary importance, because the transducer is calibrated in its final state. It is only with multicomponent transducers that the transverse sensitivity of the strain gage may contribute to “crosstalk”, but even here the strain gage is only partly responsible.

Note:

Multicomponent transducers are those which, for example, can measure forces in different axial directions independently of one another. If for example, a force acting on the X axis affects the measurement system for the Y axis in an undesired manner, the effect is known as “cross talk”, a term which is taken from a similar effect in electro-acoustics.

In the following sections, formulae for the correction of measurements are given. Theoretical dissertations with the derivation of the formulae can be found in [7-4, 7-5].

Before dealing with the corrections themselves, the method of determining the gage factor (see section 3.3.1) must be considered again. Strain gages are calibrated (see [2-1]) in the uniaxial stress field of a steel beam according to an internationally accepted method. A uniaxial stress condition produces a biaxial strain field. The two principal strain directions are aligned in the longitudinal direction, $\varepsilon_1 = \varepsilon_l$, and in the transverse direction, $\varepsilon_2 = \varepsilon_t$. The relationship of the two strains to one another is expressed by Poisson's Ratio (see sections 2.2.4 and 2.3.3). Poisson's Ratio for the calibrating beam is designated ν_0 ; for steel calibrating beams it is

$$\nu_0 = \frac{\varepsilon_t}{\varepsilon_l} = 0.285 .$$

For calibration the strain gage is mounted with its longitudinal axis in the direction of the longitudinal strain on the calibration beam. By definition the strain gage's gage factor is obtained from the calibration:

$$k = \frac{\Delta R/R_0}{\epsilon_1} \quad (7.5-1)$$

The transverse strain ϵ_t , acting on the strain gage has not been considered. This has historical reasons. It is obvious that with a strain gage that has a certain strain sensitivity in its transverse direction, the transverse strain ϵ_t of the calibrating beam will give a change in resistance:

$$\frac{\Delta R}{R} = k_1 \cdot \epsilon_1 + k_q \cdot \epsilon_t \quad (7.5-2)$$

The transverse sensitivity (q) is defined as the quotient between the k-factor in measuring grid direction (k_1) and the k cross transverse (k_q).

$$q = \frac{k_q}{k_1} \quad (7.5-3)$$

This value is printed on the DMS packaging and forms the basis for the following correction calculations. The k-factors k_1 and k_q do not correspond to the k-factors given on the packaging.

Using (7.5-3) and

$$\epsilon_t = -\nu_0 \cdot \epsilon_1 \quad (7.5-4)$$

This gives

$$\frac{\Delta R}{R} = k_1 \cdot \epsilon_1 - k_1 \cdot q \cdot \nu_0 \cdot \epsilon_1 \quad (7.5-5)$$

ν_0 is the Poisson ratio of the calibration bar; for HBM strain gauges $\nu_0=0.285$.

7.5.1 Corrections for individual measuring grids

The strain gage that is applied on any material changes the resistance to the outgoing signal as follows:

$$\left(\frac{\Delta R}{R} \right)_{mess} = k_1 \cdot \epsilon_1 + k_q \cdot \epsilon_t \quad (7.5-6)$$

The strain in measuring grid direction would be the same for the experiment and the calibration. The relative error is expressed as

$$f = \frac{\left(\frac{\Delta R}{R} \right)_{mess} - \left(\frac{\Delta R}{R} \right)}{\left(\frac{\Delta R}{R} \right)} \quad (7.5-7)$$

Through replacement this gives

$$f = \frac{(k_1 \cdot \varepsilon_1 + k_1 \cdot \varepsilon_t \cdot q) - (k_1 \cdot \varepsilon_1 - k_1 \cdot q \cdot \nu_0 \cdot \varepsilon_1)}{(k_1 \cdot \varepsilon_1 - k_1 \cdot q \cdot \nu_0 \cdot \varepsilon_1)} \quad (7.5-8)$$

This expression can be easily simplified:

$$f = \frac{(\varepsilon_1 + \varepsilon_t \cdot q) - (\varepsilon_1 - q \cdot \nu_0 \cdot \varepsilon_1)}{(\varepsilon_1 - q \cdot \nu_0 \cdot \varepsilon_1)} \quad (7.5-9)$$

$$f = \frac{\varepsilon_t \cdot q + q \cdot \nu_0 \cdot \varepsilon_1}{\varepsilon_1 - q \cdot \nu_0 \cdot \varepsilon_1} \quad (7.5-10)$$

$$f = \frac{\varepsilon_t \cdot q}{\varepsilon_1(1 - q \cdot \nu_0)} + \frac{q \cdot \nu_0 \cdot \varepsilon_1}{(1 - q \cdot \nu_0)} \quad (7.5-11)$$

$$f = \frac{\varepsilon_t \cdot q}{\varepsilon_1(1 - q \cdot \nu_0)} + \frac{q \cdot \nu_0}{(1 - q \cdot \nu_0)} \quad (7.5-12)$$

$$f = \frac{q}{1 - q \cdot \nu_0} \left(\frac{\varepsilon_t}{\varepsilon_1} + \nu_0 \right) \quad (7.5-13)$$

It can be seen that the error caused by the transverse strain is always critical if either the quotient of transverse and longitudinal strain or the transverse sensitivity of the strain gage is very large. With a single axis stress state, no error will occur as long as the Poisson ratio corresponds to the calibration conditions.

The following calculation corrects the error leading to the actual strain ε .

$$f = \frac{\varepsilon_{\text{mess}} - \varepsilon}{\varepsilon} \rightarrow \varepsilon = \frac{\varepsilon_{\text{mess}}}{1 + f} \quad (7.5-14)$$

$\varepsilon_{\text{mess}}$ = the value displayed on the measuring amplifier, that is the actual strain measured.

Example 1:

T-rosette XY13-3/350 with traverse sensitivity $q = 0.2\% = 0.002$

Bonded on aluminium: Poisson ratio $\nu_{Al} = 0.33$

The Poisson ratio of the calibration bar is $\nu_0 = 0.285$

Load: uniaxial stress status

Measured strain in voltage direction is: $\varepsilon_{\text{mess}} = 1000 \mu\text{m}$

This gives the traverse strain (not to be confused with the traverse sensitivity of a strain gage):

$$\varepsilon_t = -\nu_{Al} \cdot \varepsilon_1 = -330 \mu\text{m} / \text{m}$$

For a strain gage with a measuring grid lying in the voltage direction, this results in an error of -0.009% when the parameters in equation (7.5-13) are replaced. This error is very small and can certainly be disregarded.

If a strain gage is displaced by 90 degrees in the voltage direction, an error of -0.5% occurs in the calculation as ε_t and ε_l must be exchanged here.

Solution:

The correct strain is produced by using the error in equation (7.5-14):

in the voltage direction:

$$\varepsilon_1 = \frac{\varepsilon_{mess}}{1+f} = \frac{1000\mu m/m}{1-0.00009} = 1000.98\mu m/m$$

90° to the voltage direction:

$$\varepsilon_1 = \frac{\nu - \varepsilon_{mess}}{1+f} = \frac{330\mu m/m}{1-0.005} = 331.66\mu m/m$$

The diagram in Fig. 7.5-1 shows eleven different $\varepsilon_t/\varepsilon_l$ ratios as parameters and covers transverse sensitivity factors of $q = +0.03$ to -0.03 . Intermediate values can be found by interpolation.

The application of the diagram assumes that the ratio of strains $\varepsilon_t/\varepsilon_l$ is known. In the uniaxial stress field, $\varepsilon_t/\varepsilon_l$ in the main directions is

$$\frac{\varepsilon_t}{\varepsilon_l} = -1 \cdot \nu \quad (7.5-15)$$

The Poisson's ratios of different materials can be found in the Table 2.3-2.

Three examples are given to explain the diagram.

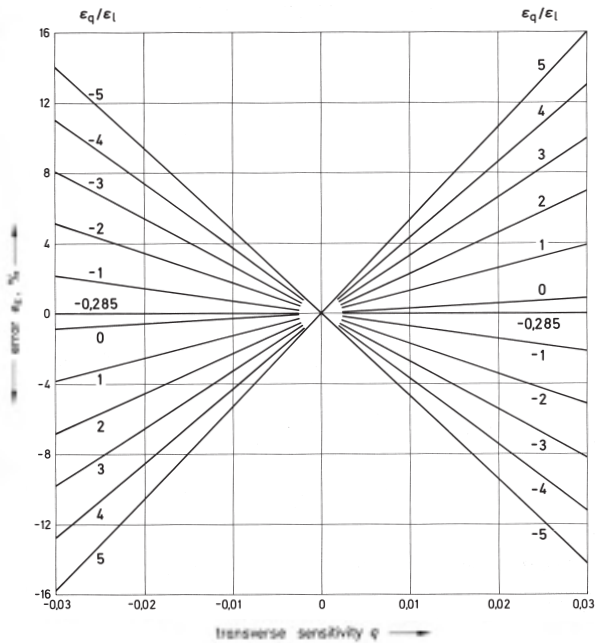


Fig. 7.5-1: Diagram for finding the measurement error due to a strain gage's transverse sensitivity.

Example 2:

$q = -0.01$;

uniaxial stress field = biaxial strain field;

component material: aluminum, $\nu = 0.33$;

principle strain 1 was measured, $\varepsilon_1 = \varepsilon_l$.

The measurement error due to the strain gage's transverse sensitivity q is required.

Note:

The strains are indexed in different ways. The indices 1 and 2 ($\varepsilon_1, \varepsilon_2$) designate the principal directions, i.e. the perpendicular (orthogonal) directions, in which the extreme values occur *on the measurement object*.

The indices 1 and q ($\varepsilon_1, \varepsilon_q$) also refer to the perpendicular strains corresponding to their direction of action *to the strain gage*.

At some other places the indices x and y ($\varepsilon_x, \varepsilon_y$) appear. They refer to the directions x and y of a *randomly aligned axial system*. The directions x and y may be different from the principal directions 1 and 2 and from the strain gage directions l and t.

Solution:

First of all the ratio $\varepsilon_i/\varepsilon_1$ is formed:

$$\frac{\varepsilon_i}{\varepsilon_1} = -1 \cdot \nu = -0.33 .$$

There is no parametric curve on the diagram for the value -0.33. The value is found by interpolation. The point lies so close to the zero error axis, i.e. the horizontal center line of the diagram, that a graphical evaluation is almost impossible. The error is about +0.07% and is therefore negligible.

Example 3:

Data as in Example 1, but the error is now required which occurs if the transverse strain ε_2 of the object is measured with the strain gage. In this case $\varepsilon_2 = \varepsilon_1$.

Solution:

$$\frac{\varepsilon_i}{\varepsilon_1} = \frac{\varepsilon_1}{\varepsilon_2} = -\frac{1}{\nu} = -\frac{1}{0.33} = -3 .$$

In the diagram the parametric curve -3 is followed until it crosses with the vertical abscissa coordinate $q = -0.01$. From there one crosses horizontally to the left to read off the result from the error scale. Intermediate values are obtained by interpolation.

Result:

$$e_{\varepsilon_1} = e_{\varepsilon_2} = +2.8 \%$$

Example 4:

$q = -0.015$;

biaxial strain field; $\varepsilon_1/\varepsilon_2 = \varepsilon_1/\varepsilon_1 = 5:1$;

measurement in the direction $\varepsilon_1/\varepsilon_2$

$\varepsilon_i = \varepsilon_1 = 1:5 = +0.2$

Error $e_{\varepsilon_1}/e_{\varepsilon_2} = +1.2\%$

An equally simple method of error correction is provided by the diagram in Fig. 7.5-2. It is used in a similar manner to the error diagram. The correct strain value ε is obtained by multiplying the indicated strain value ε_i with the correction factor C taken from the diagram:

$$\varepsilon = \varepsilon_i \cdot C . \quad (7.5-16)$$

No correction is required for the 1st example.

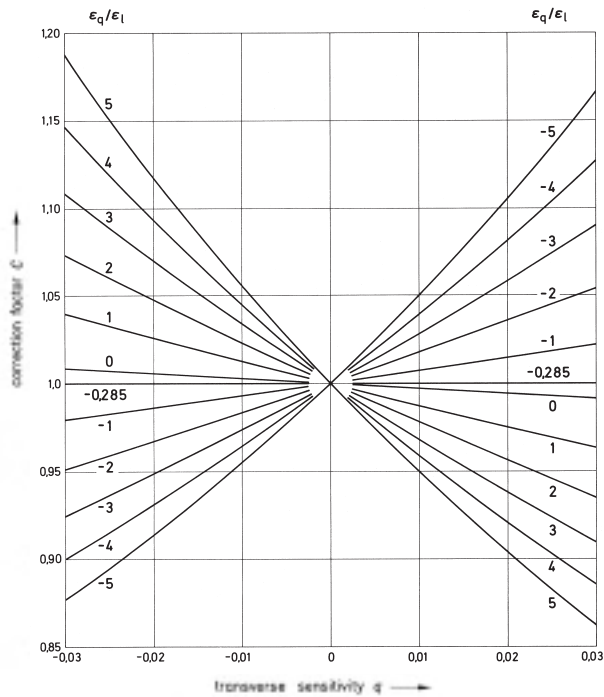


Fig. 7.5-2: Diagram for determination of the correction factor C for correcting the measurements obtained with a strain gage which is sensitive to transverse strain.

Example 3 gives $C = 0.974$

$$\varepsilon_1 = \varepsilon + e = 100\% + 2.8\% = 102.8\%$$

$$\varepsilon = \varepsilon_1 \cdot C = 102.8\% \cdot 0.974 = 100.1\%$$

Range of error: +0.1%

Example 4 gives $C = 0.9991$

$$\varepsilon_1 = 100\% + 1.2\% = 101.2\%$$

$$\varepsilon = \varepsilon_1 \cdot C = 101.2\% \cdot 0.9991 = 100.2\%$$

Range of error: +0.2%

For the error computation and correction previously described the ratio $\varepsilon_t/\varepsilon_l$ must be known. For example, this is relevant for uniaxial stress conditions with a known Poisson's ratio and with pure torsional loading of a shaft ($\varepsilon_1 = -\varepsilon_2$). In all other cases the strains in the direction of the measurement grid and transverse to it must be measured, e.g. with X rosettes (see section 3.2.2.2).

7.5.2 Correction for strain gage rosettes

For foil strain gages the transverse sensitivity of geometrically identical measurement grids is dependent to a slight extent on the direction which the axis of the measurement grid has in relation to the grain of the foil. For X rosettes with the measurement grids arranged $0^\circ/90^\circ$ the grid axes are arranged at $\pm 45^\circ$ during manufacture and therefore have the same transverse sensitivity. For three-Part rosettes of the $0^\circ/45^\circ/90^\circ$ and of the $0^\circ/60^\circ/120^\circ$ types this matching can only be achieved approximately. However, the differences are so slight that for practical purposes they can be taken as being equal. In the diagram in Fig. 3.3.7b only one value is therefore given.

7.5.2.1 X rosettes $0^\circ/90^\circ$

X rosettes with two measurement grid axes arranged at 90° to one another (see section 3.2.2.2) are usually used for strain measurements in biaxial strain fields with known principal directions. The grid axes 1 and 2 are mounted to correspond with the principal axes ε_1 and ε_2 . The principle stresses σ_1 and σ_2 can be calculated from the measurements of ε_1 and ε_2 (see section 8.2.1).

The following correction calculation applies, however, not only to arrangements of strain gages in the principal directions, but it also applies for any direction of the coordinate system within the strain field. The indexing of the strain is now represented with x and y instead of 1 and 2 ($\varepsilon_x, \varepsilon_y$ instead of $\varepsilon_1, \varepsilon_2$). For any orientation of the 90° coordinate system for the measuring grids the correct strains ε_x and ε_y can be calculated from the indicated, i.e. measured, strain values ε_{xi} and ε_{yi} .

$$\varepsilon_x = \frac{1 - \nu_0 \cdot q}{1 - q^2} (\varepsilon_{xi} - q \cdot \varepsilon_{yi}) = (1 - \nu_0 \cdot q) (\varepsilon_{xi} - q \cdot \varepsilon_{yi}) \quad (7.5-17)$$

$$\varepsilon_y = \frac{1 - \nu_0 \cdot q}{1 - q^2} (\varepsilon_{yi} - q \cdot \varepsilon_{xi}) = (1 - \nu_0 \cdot q) (\varepsilon_{yi} - q \cdot \varepsilon_{xi}) \quad (7.5-18)$$

The approximate forms for equations (7.5-7) and (7.5-8) are sufficiently accurate for practical purposes, because $1 - q^2$ is greater than 0.999 even for $q = 0.03$.

Alternatively, the diagram in Fig. 7.5-2 can be used for calculation of the correction. First the ratio of the transverse to longitudinal strain must be calculated for each of the two strain gages; this is

$$\frac{\varepsilon_{yi}}{\varepsilon_{xi}} \quad \text{for the strain gage in the x direction,}$$

$$\frac{\varepsilon_{xi}}{\varepsilon_{yi}} \quad \text{for the strain gage in the y direction}$$

Then the relevant value for q is found in the diagram, a line is followed vertically upwards until the strain ratio $\varepsilon_i/\varepsilon_1$ (or the intermediate value) appropriate for the rosette measuring grid is met and then a horizontal line is followed left to the ordinate scale where the correction factor C_x or C_y can be read off.

$$\epsilon_x = C_x \cdot \epsilon_{xi}, \quad (7.5-19)$$

$$\epsilon_y = C_y \cdot \epsilon_{yi}. \quad (7.5-20)$$

The two methods are explained based on an example and their results are compared.

Example:

X rosette $0^\circ/90^\circ$,

$q = 0.03$

$\nu_0 = 0.285$

Measurements: $\epsilon_{xi} = + 1280 \mu\text{m/m}$
 $\epsilon_{yi} = + 750 \mu\text{m/m}$

Substituting in equations (7.5-7) and (7.5-8):

$$\epsilon_x = (1 - 0.285 \cdot 0.03) \cdot (1280 - 0.03 \cdot 750) = 1247 \mu\text{m/m}$$

$$\epsilon_y = (1 - 0.285 \cdot 0.03) \cdot (750 - 0.03 \cdot 1280) = 706 \mu\text{m/m}$$

The following results are obtained using the correction diagram in Fig. 7.5-2:

$$\frac{\epsilon_{yi}}{\epsilon_{xi}} = \frac{750}{1280} = 0.59 \approx 0.6 \quad \text{for the x measuring grid,}$$

$$\frac{\epsilon_{xi}}{\epsilon_{yi}} = \frac{1280}{750} = 1.61 \approx 1.7 \quad \text{for the y measuring grid,}$$

$$C_x = 0.977; \quad C_y = 0.945.$$

Therefore

$$\epsilon_x = C_x \cdot \epsilon_{xi} = 0.977 \cdot 1280 = 1250 \mu\text{m},$$

$$\epsilon_y = C_y \cdot \epsilon_{yi} = 0.945 \cdot 750 = 708 \mu\text{m}$$

7.5.2.2 Rosettes

If the directions of the principal axes are unknown, three independent measurements are required for complete determination of the strains or stress conditions. The usual rosette shapes are described in section 3.2.2.2. The rosettes with $0^\circ/45^\circ/90^\circ$ and $0^\circ/60^\circ/120^\circ$ angular intervals between their measuring grids come into consideration here. They are equally suitable, but require different formulae for correction for the transverse sensitivity. (The methods for calculation of the principal strains and principal stresses together with their directions are described in section 8.2.2.)

R rosettes $0^\circ/45^\circ/90^\circ$

The measurements from the 0° and the 90° measurement grids should be corrected in the same manner as the $0^\circ/90^\circ$ X rosette. Equations (7.5-7) and (7.5-8) apply in the form (7.5-11) and (7.5-13).

Similarly the diagram in Fig. 7.5-2 can be used for the determination of the correction factors.

The middle 45° measuring grid needs a different correction equation. For the sake of simplicity all three equations are listed below, but the divisor $1 - q^2$ has been ignored.

$$\epsilon_{0^\circ} = 1 - \nu_0 \cdot q(\epsilon_{0^\circ i} - q \cdot \epsilon_{90^\circ i}) \quad (7.5-21)$$

$$\epsilon_{45^\circ} = 1 - \nu_0 \cdot q[\epsilon_{45^\circ i} - q(\epsilon_{0^\circ i} + \epsilon_{90^\circ i} - \epsilon_{45^\circ i})] \quad (7.5-22)$$

$$\epsilon_{90^\circ} = 1 - \nu_0 \cdot q(\epsilon_{90^\circ i} - q \cdot \epsilon_{0^\circ i}) \quad (7.5-23)$$

The index “i” always stands for the indicated strain value; $\epsilon_{0^\circ i}$ is the indicated, i.e. measured, strain value of the measuring grid in the 0° direction, etc.

ϵ_{0° , ϵ_{45° , ϵ_{90° , are the corrected strain values in the 0° , the 45° and the 90° directions.

R rosettes $0^\circ/60^\circ/120^\circ$

The correction of the measurements of the 0° , 60° and the 120° measuring grids is made in a similar manner as above, but according to the equations given below. Here also the divisor $1 - q^2$ has been left out.

$$\epsilon_{0^\circ} = 1 - \nu_0 \cdot q \left[\left(1 + \frac{q}{3} \right) \cdot \epsilon_{0^\circ i} - \frac{2}{3} q (\epsilon_{60^\circ i} + \epsilon_{120^\circ i}) \right] \quad (7.5-24)$$

$$\epsilon_{60^\circ} = 1 - \nu_0 \cdot q \left[\left(1 + \frac{q}{3} \right) \cdot \epsilon_{60^\circ i} - \frac{2}{3} q (\epsilon_{120^\circ i} + \epsilon_{0^\circ i}) \right] \quad (7.5-25)$$

$$\epsilon_{120^\circ} = 1 - \nu_0 \cdot q \left[\left(1 + \frac{q}{3} \right) \cdot \epsilon_{120^\circ i} - \frac{2}{3} q (\epsilon_{0^\circ i} + \epsilon_{60^\circ i}) \right] \quad (7.5-26)$$

8. Hooke's Law for the Determination of Material Stresses from Strain Measurements

In the elastic deformation range of materials the methods of calculating the material stresses from the measured strains are based on Hooke's Law. In its simplest form Hooke's Law is

$$\sigma = \epsilon \cdot E \quad (8.0-1)$$

σ = material stress (see section 2.2.1)

ϵ = strain (see section 2.1)

E = modulus of elasticity, i.e. Young's modulus, (see section 2.3.1)

This version of Hooke's Law only applies to the uniaxial stress state; biaxial and multiaxial stress states require extended versions (see section 2.2.4 and the following sections).

In this connection the reader is referred to an important factor:

With strain measurements only the difference can be determined between an initial output condition and a condition which occurs later. The initial condition may be a load-free condition, but it may also be a condition with significant pre-loading, for example due to the object's own weight as with a bridge.

Pre-hading or also residual stress conditions (see section 2.2.3) can only be measured if interference with the object is allowed, e.g. making a small drill hole (see section 8.3).

8.1 The uniaxial stress state

The simplest case of the uniaxial stress state occurs with tension and compression bars. The maximum of the tension or compression stresses acts in the direction in which the force acts. In all other directions the stresses are smaller and follow the relationship

$$\sigma = f(\varphi) = \frac{1}{2} \sigma_{\max} (1 + \cos 2\varphi) . \quad (8.1-1)$$

φ = angle between the active direction of force, i.e. the principal direction, and the direction under consideration.

In Fig. 8.1-1 this relationship is represented in a polar diagram for the tension bar.

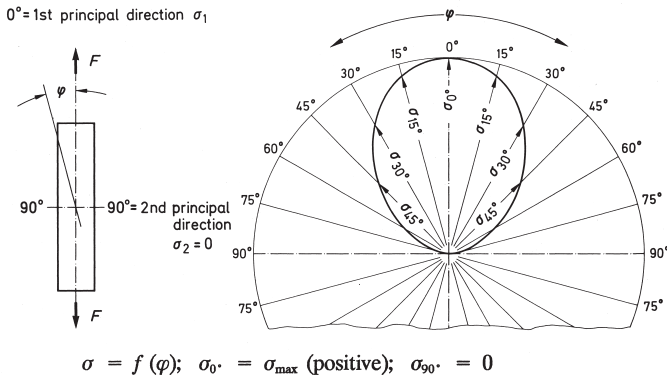


Fig. 8.1-1: Stress distribution on the tension bar

Fig. 8.1-2 shows the relationship (8.1-1) for the compression bar.

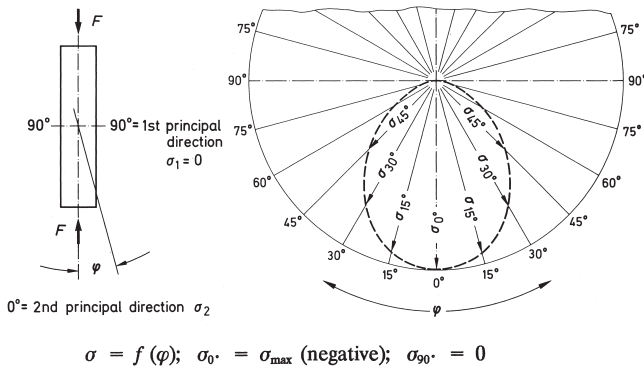


Fig. 8.1-2: Stress distribution on the compression bar

Note:

Both principal directions are always perpendicular to one another. Principal direction 1 is always that with the algebraically larger numerical value; therefore there is a change in the indexing of the tension and compression bars.

If the strain distribution is regarded in a similar manner as with the stress distribution, a *bi-axial strain* state is found despite the *uniaxial stress* state.

There are two defined directions, one in the active direction of the force (0°) and the other perpendicular to it (90°).

Starting from the principal strain $\epsilon_0 = \epsilon_1$, the strains ϵ_φ , which occur at the angle

$0^\circ < \varphi < 90^\circ$ to the x direction, can be calculated according to the relationship:

$$\epsilon = f(\varphi) = \frac{1}{2} \epsilon_1 [1 - \nu + \cos 2\varphi (1 + \nu)] \tag{8.1-2}$$

The ratio of the two principal strains is expressed by the transverse strain factor m or its reciprocal, Poisson's ratio ν , (see section 2.3.3):

$$\epsilon_2 = -\nu \cdot \epsilon_1 \tag{8.1-3}$$

In Figs. 8.1-3 and 8.1-4 the relationship (8.1-2) is shown for a tension bar, resp. a compression bar.

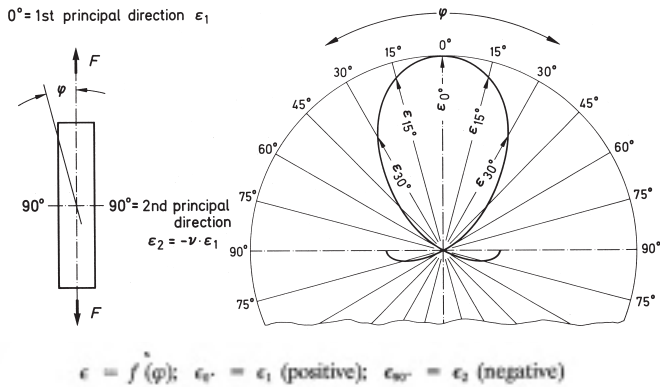


Fig. 8.1-3: Strain distribution on the tension bar

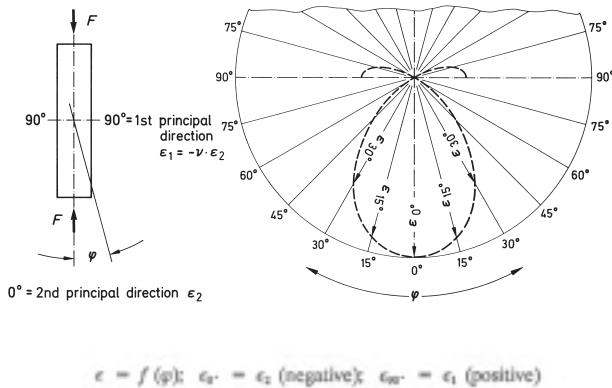


Fig. 8.1-4: Strain distribution on the compression bar

Note:

The diagrams in Figs. 8.1-3 and 8.1-4 are drawn for a material with a Poisson's ratio $\nu = 0.3$. In this case the strain becomes zero at an angle $\varphi = 61^\circ 20'$, i.e. the zero crossover between the positive and the negative strain regions is in this direction.

The difference, shown in the diagrams, between the stress distribution and the strain distribution in dependence of the active direction of the force leads to an extremely important conclusion:

The material stress σ should be calculated from the measured strain only according to Hooke's Law for the uniaxial stress state as in equation (8.0-1), if the strain ε was measured in the active direction of the force (the 0° direction in Figs. 8.1-3 and 8.1-4).

In the transverse direction (90° direction) there is *no material stress present* despite the measurable strain (transverse contraction, transverse dilation).

Therefore, for reliable results the active direction of the force must be known and the strain must be measured in this direction. If this direction is unknown or only known approximately, then the measurements and their evaluation should be carried out with the biaxial stress state with *unknown* principal directions as in section 8.2.2.

8.2 The biaxial stress state

In problems in experimental analysis the uniaxial stress state is more the exception rather than the rule. The biaxial stress state is met far more often and its determination should not be undertaken with the simple method used for the uniaxial stress state; this would lead to significant errors (see section 8. 1).

For a plane stress condition the extreme normal stresses σ_1 and σ_2 occur in the perpendicular directions 1 and 2. The stresses σ_1 and σ_2 are termed the principal stresses and similarly the directions 1 and 2 are the principal directions of the stress state. If the principal normal stresses and their active directions are known, then the biaxial stress condition is unambiguously defined.

Known principal directions of stress are found, for example, on the surface of a round cylindrical vessel under internal pressure, on a shaft loaded with pure torsion and in an area away from the edges on a bent plate.

With other objects and with the simultaneous action of different variables, such as normal force and bending or torsion and bending, etc. the principal directions must be assumed to be unknown.

8.2.1 The biaxial stress state with known principal directions

The relationship between stresses and strains in the biaxial stress state and the interaction of the longitudinal and transverse stresses is explained step by step in an example. The initial condition of the object in the example is an unloaded quadratic surface element as shown in Fig. 8.2-1a.

This surface element is then loaded with an even tensile force F_1 acting over the whole surface of the element in the direction 1-1, see Fig. 8.2-1b. The material stress σ_1 occurs in the active direction of the force as well as the longitudinal strain ϵ_1 . In the transverse direction the material stress $\sigma_2 = 0$ (uniaxial stress state) and the transverse strain ϵ_2 is negative, i.e. transverse contraction.

If in addition to this uniaxially loaded surface element a second tensile force F_2 acts in the direction 2-2 perpendicular to the 1-1 direction, the two stresses σ_1 and σ_2 are superimposed producing a reactive effect on the existing strain condition, see Fig. 8.2-1c. In the direction 2-2 a strain ϵ_2 occurs which is superimposed on the transverse contraction of the loading condition in b (even exceeding it in the example). As a consequence of the loading in the 2-2 direction, in the 1-1 direction a transverse contraction arises which is superimposed on the existing strain from the loading condition in b, thus reducing it. Due to the superimposition of the strain and transverse contraction from the two loads in the principal directions 1 and 2, the simple linear relationship between stress and strain as formulated by Hooke's Law for the uniaxial stress condition is lost. Equation (8.0-1) can no longer be applied, because it does not take into account the effects of transverse strain, (see the note on page 221). Therefore the determination of the biaxial stress condition from a single strain measurement is not possible. Both of the principal strains ϵ_1 and ϵ_2 occurring in the principal directions 1 and 2 must be measured separately.

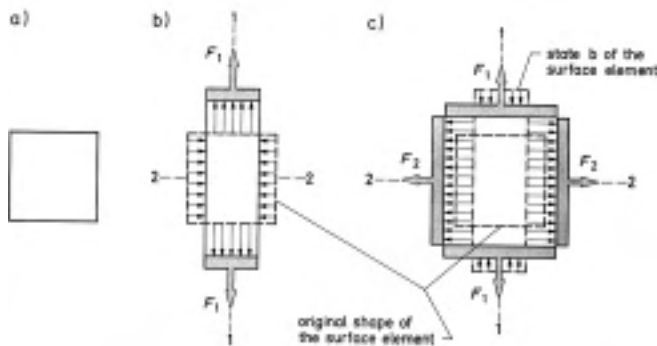


Fig. 8.2-1: Biaxial stress state illustrating the resulting strain state

- a) unloaded surface element
- b) surface element loaded in direction 1
- c) surface element loaded in directions 1 and 2

The principal normal stresses σ_1 and σ_2 of the biaxial stress state are calculated according to the extended version of Hooke's Law from the measured principal strains ϵ_1 and ϵ_2 , the material's modulus of elasticity E and Poisson's ratio ν for the material:

$$\sigma_1 = \frac{E}{1-\nu^2}(\epsilon_1 + \nu \cdot \epsilon_2) \quad (8.2-1)$$

$$\sigma_2 = \frac{E}{1-\nu^2}(\epsilon_2 + \nu \cdot \epsilon_1) \quad (8.2-2)$$

It is assumed that the stress σ_3 in the principal direction 3 (perpendicular to the surface) is equal to zero.

Equations (8.2-1) and (5.2-2) should be used as a basis for the evaluation of measurements, even if $\epsilon_2 = 0$!

Note:

In the given example the two principal normal stresses σ_1 and σ_2 are positive and of similar size. It is possible that the two stresses are very different in size or that they even have different signs, giving a strain condition which is substantially more complicated. It may happen that a negative stress is present in one direction despite a positive strain and vice versa.

An example for an object whose surface is subject to a biaxial stress state with known principal directions is shown in Fig. 8.2-2.

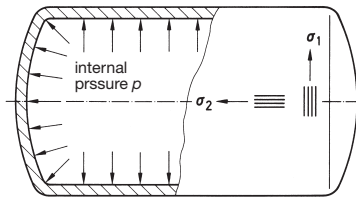


Fig. 8.2-2: A vessel with a round cylindrical cross-section which is loaded with an internal pressure

On the external surface of the cylindrical vessel there exists a biaxial stress state. Its principal direction 1, σ_1 , runs tangentially (in the circumferential direction) and the principal direction 2, σ_2 , is aligned in the axial direction. The two principal stresses σ_1 and σ_2 are calculated from the measured principal strains ϵ_1 and ϵ_2 according to the formulae (8.2-1) and (8.2-2).

Another example, about a shaft under torsional loading, is described in section 8.4.4.

Even with these types of loading conditions which appear straightforward, the measurement engineer should always apply a healthy measure of skepticism, because additional normal and/or bending loading, which may not be externally apparent, can easily convert the expected state with known principal directions into one with unknown principal directions. Then the formulae given in section 8.2.2 should be applied.

To simplify mounting procedures, X rosettes as described in section 3.2.2.2 and as shown in Fig. 3.2-9a are suitable for measurements in the biaxial stress field with known principal directions. The axes of the two measuring grids must be mounted in alignment with the axes of the principal normal stresses (principal strain directions).

8.2.2 The biaxial stress state with unknown principal directions

For objects of complex shape, with the superimposition of different types of loading (normal, bending or torsional loadings) or for points of inhomogeneity (e.g. changes in cross-sectional area), prediction of the principal directions of the stress state is generally not possible. Analysis according to the methods described in section 8.2.1 cannot therefore be carried out.

In each case where the directions of the principal stresses are not clearly defined, the stress analysis must be carried out according to the methods described below [8-1].

Fig. 8.2-3 and 8.2-4 show a shell type supporting structure as an example of a complex shaped object. The stress analysis using strain gages was undertaken on the model shown in Fig. 8.2-3 [8-2]. Fig. 8.2-4 shows the finished full-scale structure.

The objective here is also to determine the principal normal stresses σ_1 and σ_2 and their directions.

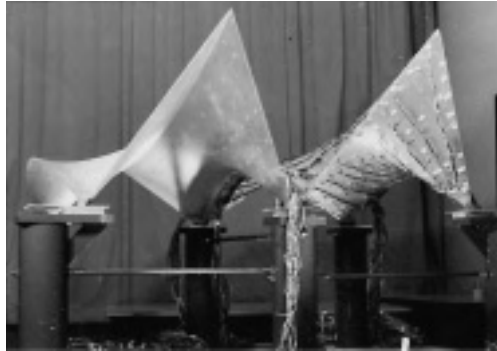


Fig. 8.2-3: Example of an object with unknown directions of principal stresses (from [8-2]) - a plastic model of a concrete-shell roof for investigation by stress analysis using strain gages



Fig. 8.2-4: Full-scale finished structure of the model in Fig. 8.2-3 (from [8-2])

Here it is necessary to measure the strain in three different directions for each measuring point. These directions, which do not correspond to the principal directions, are usually labeled with the letters a, b and c and the strains measured in these directions are indexed ϵ_a , ϵ_b and ϵ_c . It is important that the sequence of the axes of the measuring grids a, b and c is in the mathematically positive direction of rotation, i.e. anticlockwise with a plan view of the measuring object, because the formulae (8.2-3) to (8.2-7) for the calculation of the principal normal stresses and their directions are based on this direction of rotation. In order to avoid confusion the appropriate measuring grid connections on HBM rosettes are labeled with the letters a, b and c.

Principally these three strains can be measured in any direction. However, two systems have emerged in practice for which evaluation is made according to the corresponding formulae. The special strain gages, the R rosettes, which are available for this purpose, each have three measuring grids on a common carrier. They are described in section 3.2.2.2.

8.2.2.1 Measurements with the 0°/45°/90° rosette

Fig. 3.2-9b shows some examples of possible measuring grid arrangements with the group of 0°/45°/90° rosettes.

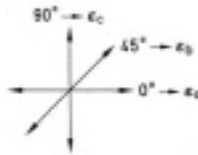


Fig. 8.2-5: Allocations of the strains ϵ_a , ϵ_b and ϵ_c to the angular directions 0°, 45° and 90°

The calculation of the principal normal stresses σ_1 , σ_2 is made according to the relationship

$$\sigma_{1,2} = \frac{E}{1-\nu} \cdot \frac{\epsilon_a + \epsilon_c}{2} \pm \frac{E}{\sqrt{2}(1+\nu)} \cdot \sqrt{(\epsilon_a - \epsilon_b)^2 + (\epsilon_c - \epsilon_b)^2} \quad (8.2-3)$$

8.2.2.2 Measurements with the 0°/60°/120° rosette

Fig. 3.2-9c shows some examples of possible measuring grid arrangements within the group of 0°/60°/120° rosettes.

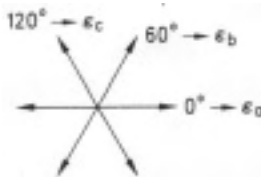


Fig. 8.2-6: Allocation of the strains ϵ_a , ϵ_b and ϵ_c to the angular directions 0°, 60° and 120°.

According to this type of measuring grid arrangement of the rosette, the calculation of the principal normal stresses σ_1 and σ_2 is made according to the equation

$$\sigma_{1,2} = \frac{E}{1-\nu} \cdot \frac{\epsilon_a + \epsilon_b + \epsilon_c}{3} \pm \frac{E}{1+\nu} \cdot \sqrt{\left(\frac{2\epsilon_a - \epsilon_b - \epsilon_c}{3}\right)^2 + \frac{1}{3}(\epsilon_b - \epsilon_c)^2} \quad (8.2-4)$$

8.2.2.3 The determination of the principal directions

The principal directions are the directions in which the principal normal stresses σ_1 and σ_2 occur as calculated using the equations (8.2-3) and (8.2-4). (They are identical with the principal strain directions ϵ_1 and ϵ_2 .) They can be determined using geometrical relationships from the strains ϵ_a , ϵ_b and ϵ_c measured with the R rosette.

The aim of the following treatment is to provide the practical engineer with a convenient and reliable method. The theoretical aspects of Mohr's Stress Circle, which form the basis of this treatment, are described in the specialist literature [8-1] and they are not dealt with here.

First a tangent of an auxiliary angle ψ is calculated:

for the $0^\circ/45^\circ/90^\circ$ rosette according to the formula

$$\tan \psi = \frac{2\epsilon_b - \epsilon_a - \epsilon_c}{\epsilon_a - \epsilon_c} \quad \left| \quad \frac{N}{D} \right. \quad (8.2-5)$$

for the $0^\circ/60^\circ/120^\circ$ rosette according to the formula

$$\tan \psi = \frac{\sqrt{3}(\epsilon_b - \epsilon_c)}{2\epsilon_a - \epsilon_b - \epsilon_c} \quad \left| \quad \frac{N}{D} \right. \quad (8.2-6)$$

Note:

The tangent of an angle in the right-angled triangle is the ration of the opposite side (numerator N) to the adjacent side (denominator D):

$$\tan \psi = \frac{\text{opposite side}}{\text{adjacent side}} = \frac{N}{D} \quad (8.2-7)$$

Fig. 8.2-7 shows that the angle ψ may be in four different quadrants in the circular arc depending on the signs of the opposite and adjacent sides.

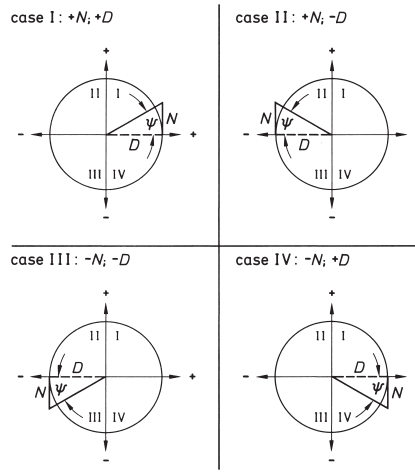


Fig. 8.2-7: Diagrams for finding the quadrants relating to the angle ψ

The ambiguity relating to the tangent makes it necessary to determine the signs of the numerator (N) and the denominator (D) before carrying out the final calculation of the two quotients (8.2-5) and (8.3-6). They are important because they alone determine the quadrant of the circular arc in which the angle ψ is located. This unambiguous location is essential for the determination of the principal directions 1 and 2.

From the numerical value of the tangent the size of the angle should then be found, either from a table or using a computer:

$$\psi = \arctan [\quad] \tag{8.2-8}$$

Then the angle ϕ should be determined. This is carried out using the scheme shown in Fig. 8.2-8.

N	$\geq 0 (+)$	$> 0 (+)$	$\leq 0 (-)$	$< 0 (-)$
D	$> 0 (+)$	$\leq 0 (-)$	$< 0 (-)$	$\geq 0 (+)$
corresponding quadrant	I	II	III	IV
$\phi =$	$\frac{1}{2} \cdot (0^\circ + \psi)$	$\frac{1}{2} \cdot (180^\circ - \psi)$	$\frac{1}{2} \cdot (180^\circ + \psi)$	$\frac{1}{2} \cdot (360^\circ - \psi)$

Fig. 8.2-8: Scheme for finding the angle ϕ

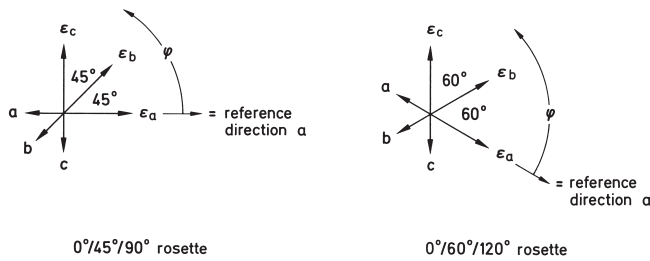


Fig. 8.2-9: Finding the principal direction 1
 a) for the 0°/45°/90° rosette
 b) for the 0°/60°/120° rosette

The angle φ , found in this manner, should be applied from the axis of the reference measuring grid a in the mathematically positive direction (anticlockwise, see Fig. 8.2-9). The axis a forms one side of the angle φ , the other side gives the principal direction 1 (direction of the principal normal stress σ_1 , which is identical to direction of the principal strain ϵ_1). The point of the angle is located at the intersection of the axes of the measuring grids.

The principal direction 2 (σ_2, ϵ_2) has the angle $\varphi + 90^\circ$.

8.2.2.4 Other ways of determining the principal normal stresses and their directions

- A) There are programmable pocket calculators which solve the rosette equations after input of the values for ϵ_a , ϵ_b and ϵ_c .
- B) During extensive testing programs the signals from the individual measuring grids are interrogated manually or automatically by multipoint scanning equipment, amplified either sequentially or in parallel and passed through interfaces to the host computer equipment which carries out the evaluation and any processing.

8.2.3 Mohr's Stress Circle

The feature of the principal directions 1 and 2 of a plane stress state is that in these directions the principal normal stresses σ_1 and σ_2 take on their greatest and smallest values, whereas the shear stresses τ become zero. In all the other directions the normal stresses lie between these extreme values and the shear stresses take on finite values.

Fig. 8.2-10a shows a section of a biaxially stressed surface with the directions of the principal stresses σ_1 and σ_2 . Within this surface an element is shown whose coordinates x and y are rotated by the angle φ to the principal axes. The stresses occurring on the element can be calculated according to the relationships:

$$\sigma_x = \frac{\sigma_1 + \sigma_2}{2} + \frac{\sigma_1 - \sigma_2}{2} \cdot \cos 2\varphi, \quad (8.2-9)$$

$$\sigma_y = \frac{\sigma_1 + \sigma_2}{2} - \frac{\sigma_1 - \sigma_2}{2} \cdot \cos 2\varphi, \quad (8.2-10)$$

$$\tau_{xy} = \tau_{yx} = \frac{\sigma_1 - \sigma_2}{2} \cdot \sin 2\varphi. \quad (8.2-11)$$

τ_{xy} and τ_{yx} are always the same size; Fig. 8.2-10b shows the rules governing their signs.

The principal normal stresses σ_1 and σ_2 and their directions should be calculated according to the methods described in sections 8.2.1 and 8.2.2.

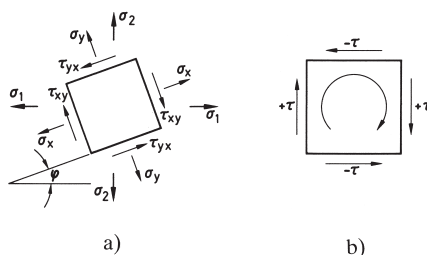


Fig. 8.2-10: Biaxial stress state

- a. stresses on a surface element whose coordinates x and y are rotated by the angle φ with respect to the principal directions 1 and 2
- b. rules for the signs of shear stresses τ (set by declaration)

The biaxial stress state can be unambiguously described by two methods:

1. by stating the principal normal stresses σ_1 , σ_2 and their directions,
2. by stating the normal stresses σ_x , σ_y and the shear stresses τ_{xy} , τ_{yx} .

The first solution is produced by the methods described in sections 8.2.1 and 8.2.2 and the second method is produced from Mohr's circle. The second method is chosen if the stresses are to refer to a predetermined coordinate system on the component.

Mohr's circle is represented in an orthogonal σ - τ coordinate system, see Fig. 8.2-11a.

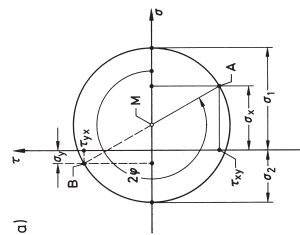
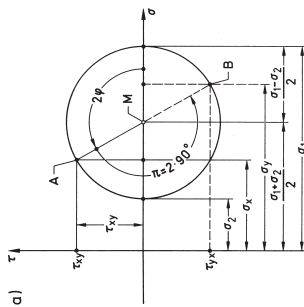
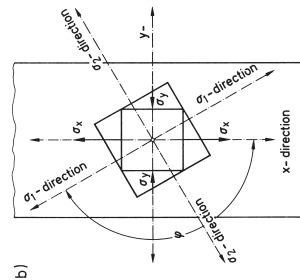
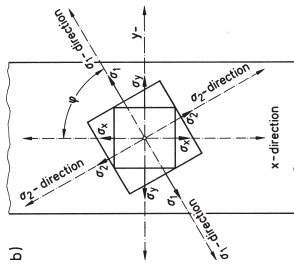
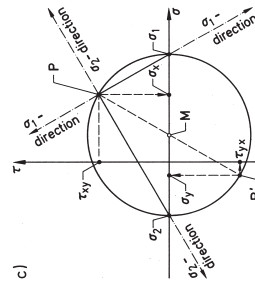
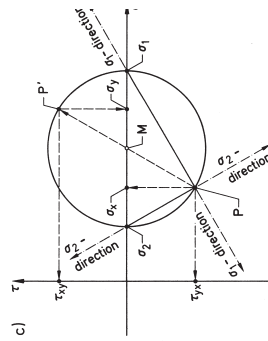


Fig. 8.2-11: Mohr's Stress Circle, 1st example

a) construction b) stresses in the component c) pole construction

Fig. 8.2-11: Mohr's Stress Circle, 2nd example

Both axes should be scaled using the same scale in N/mm². Then the principal stresses σ_1 and σ_2 , calculated from the strain measurements according to the equations in sections 8.2.1 or 8.2.2, are recorded with their correct sign on the σ axis. A circle is drawn around the center point M ; M lies on the σ axis at the point $(\sigma_1 + \sigma_2)/2$, its radius is $(\sigma_1 - \sigma_2)/2$. The circle cuts the points σ_1 and σ_2 .

In Mohr's circle all angles appear with double their value. The angle included between the principal direction 1 and the σ axis (see Fig. 8.2-11b) should therefore be recorded with the amount 2ϕ starting from the σ axis in the mathematically positive direction (anticlockwise); its first leg is formed by the axis and its second leg cuts the circle at point A. The second leg of the angle $2\phi + 2 \cdot 90^\circ$ (shown broken) corresponds to the σ_y direction; it cuts the circle at point B. Points A and B are projected onto the σ axis and the values for σ_x and σ_y are read off. When projected onto the τ axis, points A and B give the values for the shear stresses τ_{xy} and τ_{yx} .

In Fig. 8.2-11b the surface elements, drawn within one another, are lined up with the principal directions 1 and 2 and to the object coordinates x and y .

An alternative method is the pole construction of Mohr's circle. This is shown in Fig. 8.2-11c.

The pole construction is an alternative method for determination of the stresses σ_x , σ_y , τ_{xy} and τ_{yx} . The pole construction in Fig. 8.2-11c is also based on the object situation shown in Fig. 8.2-11b.

The Mohr's circle should be drawn as above in the orthogonal σ - τ coordinate system from the calculated principal stresses σ_1 and σ_2 , as in Fig. 8.2-11c. The rest of the procedure is different from the previously described method.

The *directions* of the σ - τ coordinates are regarded as corresponding to the component's reference coordinate system and in the example the axis τ of the diagram is parallel to the component's x axis and the σ axis is parallel to the component's y axis. Then the σ_1 *direction* is transferred as a straight line onto the circle, so that it intersects the circle at point σ_1 . In the same manner the σ_2 *direction* is transferred so that it intersects the circle at point σ_2 . The intersection point P of the two lines must be located on the circle; it is the pole of the Mohr's circle. By projecting the pole onto the axes, σ_x and τ_{xy} are obtained. A straight line is then drawn from the pole P through the center point M, cutting the circle on the opposite side; the point P' is obtained. The values for σ_y and τ_{yx} are obtained by the projection of P' onto the σ and τ axes.

In Fig. 8.2-11 σ_1 and σ_2 are both positive. In the example in Fig. 8.2-12 σ_1 is positive and σ_2 is negative.

8.3 Determination of residual stresses according to the drill-hole method

Residual stresses in the surface of components can only be determined with strain gages if the existing stress condition is disturbed by mechanical interference. The requirement of keeping the disturbance as small as possible is a positive factor in using the drill-hole technique. The drill-hole rosette shown in section 3.2.2.3, Fig. 3.2-14 requires a small drill-hole, having both diameter and depth only 1.5 mm. Hence the method can be regarded as being almost non-destructive.

The following should be observed when drilling the hole: center punching is not permitted, because the residual stress condition in the region of the rosette will be affected. Therefore, the RY 61 Drill-Hole Rosette illustrated in Fig. 8.3-1 is fitted with a drilling bush which,

together with an auxiliary device, ensures correct centering of the drill. The drill must be perfectly sharp otherwise additional residual stresses are produced which affect the measurement result.

The drill-hole causes an interruption of the flow of force in the component surface, leading to relaxation of the material surrounding the drill-hole.

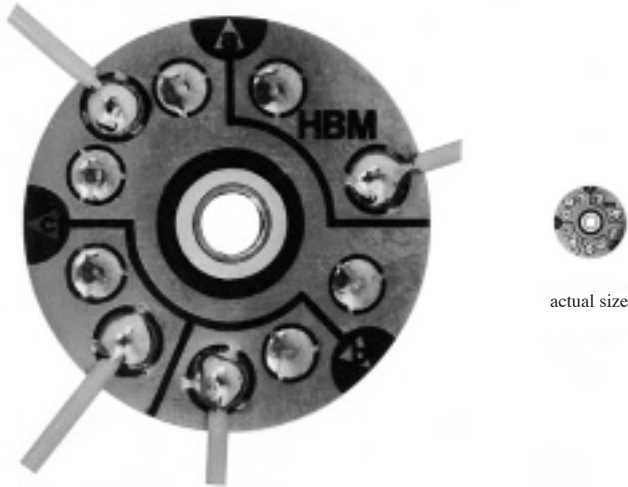


Fig. 8.3-1: RY 61 Drill-Hole Rosette

The stress condition which was previously present can be calculated from this relaxation measured with the strain gage. It is assumed that a biaxial stress state with unknown principal directions exists and so the relaxation is measured in three different directions.

A comprehensive description of the method is given in the articles [3-6] and [3-7]. There the derivation of the formulae for evaluation of the measurement results is also given. The following equations assume strain measurements made in the $0^\circ/45^\circ/90^\circ$ directions; they are taken from [3-7] and [8-3].

Before drilling the reference values ϵ_R are measured on the measurement grids a, b and c. After drilling the changed values ϵ_D are measured. The difference is the required relaxation strain $\Delta\epsilon$

$$\Delta\epsilon = \epsilon_D - \epsilon_R \quad (8.3-1)$$

In order to differentiate between the measured values, they are indexed with the corresponding measuring grid designations, i.e. $\Delta\epsilon_a$, $\Delta\epsilon_b$ and $\Delta\epsilon_c$. On HBM rosettes the designations of the measuring grid can be found on the measuring grid connections, see Figs. 8.3-1 and 8.3-2.

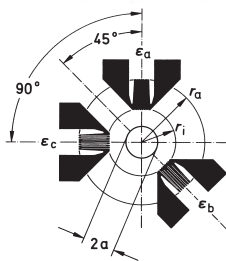


Fig. 8.3-2: Dimensions of the RY 61 Drill-hole Rosette

From the three measurements $\Delta\epsilon_a$, $\Delta\epsilon_b$ and $\Delta\epsilon_c$ the biaxial stress state which prevailed before the drilling was made into the surface can be unambiguously determined. The stress condition is found if the principal normal stresses σ_1 and σ_2 , together with their directions, are known.

$$\sigma_{1,2} = -\frac{E}{4A}(\Delta\epsilon_a + \Delta\epsilon_c) \pm \frac{E}{4B} \sqrt{(\Delta\epsilon_c - \Delta\epsilon_a)^2 + (\Delta\epsilon_a + \Delta\epsilon_c - \Delta\epsilon_b)^2} \quad (8.3-2)$$

E = modulus of elasticity of the measurement object material.

A and B are constants, which can be determined in the following manner:

$$A = \frac{a^2(1+\nu)}{2r_o \cdot r_i}; \quad (8.3-3)$$

$$B = \frac{2a^2}{r_o \cdot r_i} \cdot \left[1 - \frac{a^2(1+\nu)(r_o^2 + r_o \cdot r_i + r_i^2)}{4r_o^2 \cdot r_i^2} \right]. \quad (8.3-4)$$

ν = Poisson's ratio for the measurement object material

r_o = external radius of the measurement grid

r_i = internal radius of the measurement grid

a = radius of the drill hole

} see fig. 8.3-2

The directions of the principal stresses must be determined according to the scheme given in section 8.2.2.3 for the 0°/45°/90° rosette.

The following treatment applies with the figures for the RY 61 Drill-Hole Rosette:

r_o = 3.3 mm,

r_i = 1.8 mm,

a = 0.75 mm.

The values are obtained with using these figures:

$$A = 0.04735(1 + \nu)$$

$$B = 0.1894 - 0.01515(1 + \nu).$$

The evaluation is simplified if equation (8.3-2) is written in the form

$$\sigma_{1,2} = -A'(\Delta\epsilon_a + \Delta\epsilon_c) \pm B' \sqrt{(\Delta\epsilon_a + \Delta\epsilon_c - 2\Delta\epsilon_b)^2 + (\Delta\epsilon_c - \Delta\epsilon_a)^2} \quad (8.3-5)$$

Where

$$A' = \frac{E}{4A} = \frac{E}{0.1894(1 + \nu)} \quad (8.3-6)$$

$$B' = \frac{E}{4B} = \frac{E}{0.7576 - 0.0606(1 + \nu)} \quad (8.3-7)$$

Note:

For steel with $E = 206000 \text{ N/mm}^2$ and $\nu = 0.28$:

$$A^* = 849720 \text{ N/mm}^2$$

$$B^* = 302930 \text{ N/mm}^2$$

For aluminum alloy with $E = 70600 \text{ N/mm}^2$ and $\nu = 0.33$:

$$A^* = 280270 \text{ N/mm}^2$$

$$B^* = 104280 \text{ N/mm}^2$$

8.4 Strain measurements and stress analysis for various loading cases

The elementary loading cases “normal” (tensile, compressive loading), “bending” and “torsion” occur very seldom, if at all, in a pure form. Usually the loading cases are superimposed to some extent whether this is desired or not. In the following subsections the options for the determination of pure or combined loadings are discussed. The arrangements of the strain gages on the object and within the Wheatstone bridge play a significant role here.

Special attention should be paid to the sign of the measured strains.

Explanation of the formula symbols used in section 8.4 where they are not otherwise given in the text and references to sections with additional information are given below.

SG 1 ... SG 4 = temperature compensated strain gages (3.3.4.1) for compensation for thermal expansion (7.1)

E = modulus of elasticity (2.3.1)

F = force

G = shear modulus (2.3.2)

$R_1 \dots R_4$ = position of the resistances within the bridge circuit (5)

R_C = completion resistances for making up the bridge circuit (5.2)

ε_i = indicated strain value

ε_b = bending strain

ε_n = normal strain (tensile or compressive)

ν = Poisson's ration (2.3.3)

σ = material stress (2.2.1)

σ_b = bending stress

σ_l = stress in the longitudinal direction of the measurement object

σ_n = normal stress (2.2.1)

σ_u = stress on the upper side of the measurement object

σ_{lo} = stress on the underside side of the measurement object

ω = angular frequency

8.4.1 Measurement on a tension/compression bar

With a tension bar the positive longitudinal strain ε_l occurs in the active direction of the force, i.e. the longitudinal direction; in the transverse direction the negative transverse strain, i.e. transverse contraction, ε_t occurs. With a compression bar the longitudinal strain is negative and the transverse strain is positive.

The following relationship applies for the longitudinal strain ε_l

$$\varepsilon_l = \frac{F}{A \cdot E} \quad (8.4-1)$$

With a pure normal force $\varepsilon_l = \varepsilon_n$.

For the transverse strain ε_t

$$\varepsilon_t = -\nu \cdot \varepsilon_l = -\nu \frac{F}{A \cdot E} \quad (8.4-2)$$

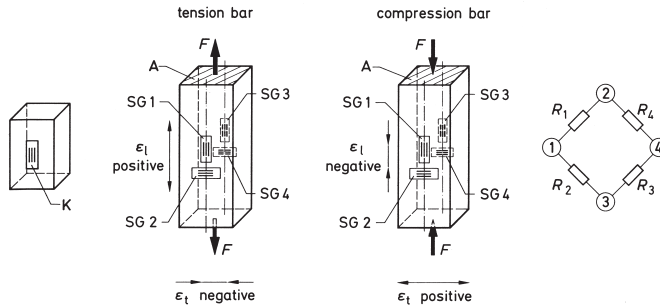
The normal stress σ_n is given by the following relationships

$$\sigma_n = \frac{F}{A} \quad (8.4-3)$$

or

$$\sigma_n = \epsilon_n \cdot E, \tag{8.4-4}$$

The arrangement of the strain gages on the tension/compression bars and in the bridge circuit is shown in Fig. 8.4-1. Depending on circumstances not all bridge arms need be occupied with strain gages. The characteristics, advantages and disadvantages of the various types of circuit are shown in Table 8.4-1.



K = compensating strain gage on a mechanically unloaded part (see section 7.1-3)

Fig. 8.4-1: Arrangement of the strain gages on the tension/compression bar and in the bridge circuit

Bridge arm	R_1	R_2	R_3	R_4	Result	Notes
Bridge equation	$\epsilon_1 - \epsilon_2 + \epsilon_3 - \epsilon_4 = \epsilon_i$					1
Simple quarter bridge	SG1	R_C	R_C	R_C	$\epsilon_i = \epsilon_1$	2
Quarter bridge with comp. strain gage	SG1	K	R_C	R_C	$\epsilon_i = \epsilon_1$	3
Half bridge	SG1	SG2	R_C	R_C	$\epsilon_i = \epsilon_1 + \epsilon_q = (1 + \nu) \cdot \epsilon_1$	4
Diagonal bridge	SG1	R_C	SG3	R_C	$\epsilon_i = 2 \cdot \epsilon_1$	5
Diagonal bridge with 2 comp. strain gages	SG1	K	SG3	K	$\epsilon_i = 2 \cdot \epsilon_1$	6
Full bridge	SG1	SG2	SG3	SG4	$\epsilon_i = 2(\epsilon_1 + \epsilon_q) = 2(1 + \nu)\epsilon_1$	7

Table 8.4-1: Circuits that could be used for the tension/compression bar with their results. See Fig. 8.4-1 for an explanation of the symbols

Notes on table 8.4-1:

1. Attention should be given to the change of sign in the equation and to the sign of the strains!
2. Superimposed bending strains occur in the result.

Thermal strains must be eliminated with temperature compensated strain gages, otherwise they occur as an error in the measurement result.

$$\sigma_1 = \sigma_s + \sigma_b = \epsilon_1 \cdot E \quad (8.4-5)$$

3. The compensation of the thermal strain with the compensating strain gage is also obtained if the thermal expansion coefficient of the component material deviates from the standard value of the temperature compensated strain gage or if the compensation range of the strain gage is exceeded. Otherwise the situation is as in 2.
4. Superimposed bending strains occur in the result. Thermal strains are very well compensated.

$$\sigma_1 = \sigma_s + \sigma_b = \frac{\epsilon_1 \cdot E}{1 + \nu} \quad (8.4-6)$$

5. With mirror-imaged bar cross-sections superimposed bending strains are compensated. Thermal strains must be eliminated with temperature compensated strain gages, otherwise they occur as errors in the measurement result.

$$\sigma_s = \frac{1}{2} \epsilon_1 \cdot E \quad (8.4-7)$$

6. With regard to the compensation of the thermal strain, see Note 3. Otherwise the procedure is as in Note 5.
7. With a mirror-imaged cross-section superimposed bending strains are compensated. Thermal strains are very well compensated. Interference effects through internal bridge connections are largely suppressed. This is very well suited to the measurement of normal force.

$$\sigma_b = \frac{\epsilon_1 \cdot E}{2(1 + \nu)} \quad (8.4-8)$$

$$F = \frac{\epsilon_1 \cdot E}{2(1 + \nu)} \cdot A \quad (8.4-9)$$

Note:

The strain gages must be aligned in the directions of the principal axes to avoid errors (see also section 8.1). A directional error of 5° (which is really extremely large) in the uniaxial stress field produces an error of -1% in the principal direction 1 and an error of -3.3% in the principal direction 2 (traverse), both being calculated for $\nu = 0.3$. An X rosette which is twisted by 5° would give a total error of -1.54% with a half or full bridge circuit.

Apart from the normal loading, various disturbances affect the tension bar, such as bending, torsion and heat. Depending on the objective of the measurements, it may be desirable to eliminate the superimposed bending strains (e.g. for force measurements) or alternatively to also measure them (e.g. for the determination of the maximum values of stress). The various types of Wheatstone bridge circuit, however, can only be used for bars with mirror image cross-sections. For measurements on asymmetrical cross-sections, see section 8.4.3.

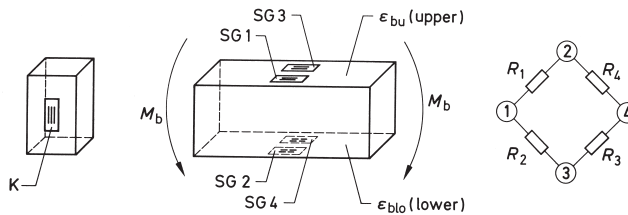
The influence of torsion as a disturbance can be largely suppressed by the arrangement of the strain gage close to or symmetrically to the center axis. The determination of the maximum loading occurring due to superimposition can only be made using the method for determination of the biaxial stress state with unknown principal directions (see section 8.2.2 and 8.4.5).

8.4.2 Measurements on a bending beam

Bending produces a positive strain on one side of the bent beam and a negative strain on the opposite side. With mirror-imaged cross-sections the positive and negative strains have the same magnitude. It is therefore possible to use the features offered by the Wheatstone bridge for the addition of the strain signals or for compensation of the disturbances.

Normal loading, torsion and thermal strain can occur as disturbances.

Fig. 8.4-2 shows the arrangement of the strain gages on the bending beam. As with the tension bar (section 8.4.1) all four arms of the bridge need not be occupied with strain gages. The characteristics of the various types of circuit are listed in Table 8.4-2.



K = compensating strain gage on a mechanically unloaded part (see section 7.1-3)

Fig. 8.4-2 Arrangement of the strain gages on the bending beam and in the bridge circuit

The strain gages must point with their axes in the principal directions of stress. If the principal directions are unknown (e.g. with superimposed torsion) and the principal stresses are to be determined, then the procedure used is as described in section 8.2.2 or 8.4.5.

Bridge arm	R_1	R_2	R_3	R_4	Result	Notes
Bridge equation	$\varepsilon_1 - \varepsilon_2 + \varepsilon_3 - \varepsilon_4 = \varepsilon_i$					1
Simple quarter bridge	SG1	R_C	R_C	R_C	$\varepsilon_i = \varepsilon_{bu}$	2
	SG2	R_C	R_C	R_C	$\varepsilon_i = \varepsilon_{blo}$	
Quarter bridge with comp. strain gage	SG1	K	R_C	R_C	$\varepsilon_i = \varepsilon_{bu}$	3
	SG2	K	R_C	R_C	$\varepsilon_i = \varepsilon_{blo}$	
Half bridge	SG1	SG2	R_C	R_C	$\varepsilon_i = 2\varepsilon_b$	4
Diagonal bridge	SG1	R_C	SG3	R_C	$\varepsilon_i = 2\varepsilon_{bu}$	5
	SG2	R_C	SG4	R_C	$\varepsilon_i = 2\varepsilon_{blo}$	
Diagonal bridge with 2 comp. strain gages	SG1	K	SG3	K	$\varepsilon_i = 2\varepsilon_{bu}$	6
	SG2	K	SG4	K	$\varepsilon_i = 2\varepsilon_{blo}$	
Full bridge	SG1	SG2	SG3	SG4	$\varepsilon_i = 4\varepsilon_b$	7

Table 8.4-2: Circuits which can be used on the bending beam with a mirror-imaged cross-section
See Fig. 8.4-2 for an explanation of the symbols.

Notes on Table 8.4-2:

1. Attention should be given to the change of sign in the equation and to the sign of the strains!
2. Superimposed bending strains occur in the result.

Thermal strains must be eliminated with temperature compensated strain gages, otherwise they occur as an error in the measurement result.

$$\sigma = \sigma_b + \sigma_{\theta} = \varepsilon_i \cdot E. \quad (8.4-10)$$

3. Compensation of the thermal strain using the compensating strain gage is also obtained if the thermal expansion coefficient of the component material deviates from the standard value of the temperature compensated strain gage or if the compensation range of the strain gage is exceeded. Otherwise the situation is as in 2.
4. Superimposed normal strains are compensated. Thermal strains are compensated to a high degree.

$$\sigma_b = \frac{1}{2} \varepsilon_i \cdot E. \quad (8.4-11)$$

The active bending moment M_b can be calculated according to the equation

$$M_b = \sigma_b \cdot S. \quad (8.4-12)$$

The figure for the section modulus S which is dependent on the cross-section of the beam can be taken from specialist literature. The formulae for the calculation of S for some frequently occurring cross-sectional shapes are listed in Table 8.4-3.

- Superimposed normal strains occur in the result. Thermal strains must be eliminated with temperature compensated strain gages, otherwise they occur as errors in the measurement result.

$$\sigma = \alpha_b + \alpha_t = \frac{1}{2} \epsilon_t \cdot E. \tag{8.4-13}$$

- Compensation of the thermal strain using the compensating strain gage is also obtained if a suitable temperature compensated strain gage is not available or its compensating range is inadequate. Otherwise, the notes in 5 apply.
- With a mirror-imaged cross-section, normal strains are compensated. Thermal strains are compensated to a high degree. Interference effects through internal bridge connections are largely suppressed. This is very suitable for the measurement of bending moments and bending forces where the length of leverage is known.

$$\alpha_b = \frac{1}{4} \epsilon_t \cdot E. \tag{8.4-14}$$

The effective bending moment M_b can be calculated according to the equation (8.4-12).

See note 4 and Table 8.4-3 for the calculation of S .

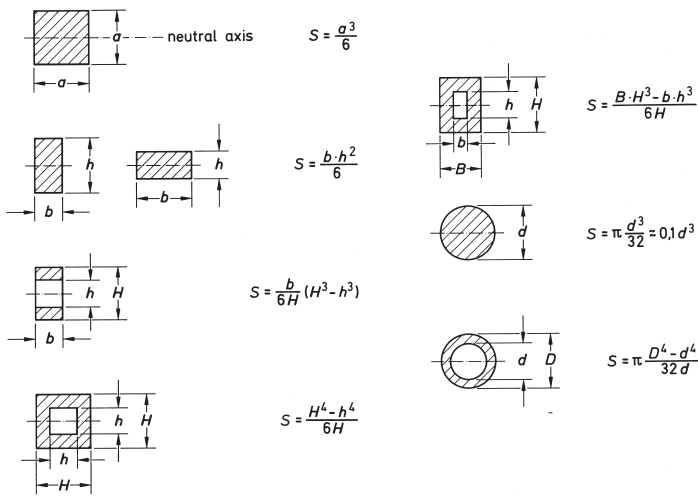


Table 8.4-3: Bending section moduli for some frequently occurring cross-sectional shapes

8.4.3 Symmetrical and asymmetrical cross-sectional beams loaded with both an axial force and a bending moment

In sections 8.4.1 and 8.4.2 it has already been described how the normal strains and the bending strains can be determined and with which circuit the sums of the normal and bending strains for symmetrical cross-sections can be found. With asymmetrical cross-sections the bending strains on opposite sides have different values. They can therefore only be determined with separate measurements. With simultaneous superimposition of normal strains and bending strains the bending and normal portions of the strains can no longer be separated using tricks in the circuitry. Here only graphical or computed solutions are possible. Both methods of solution are explained using two examples.

Bending strains on oppositely located sides always have opposite signs. Despite this it may occur that the measured strains possess the same sign. This happens when the superimposed normal strain is greater than the bending strain (see Fig. 8.4-3).

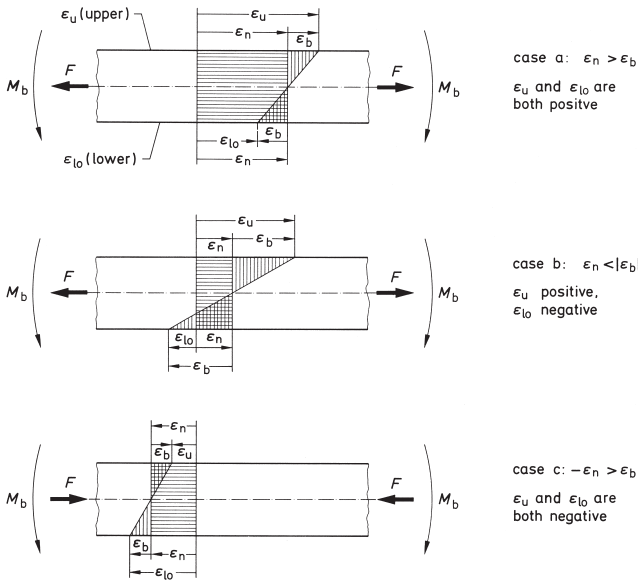


Fig. 8.4-3: Example of the strain distribution in an object with superimposed normal and bending loads

The following examples are based on measurements on a model. The cross-sectional areas A of the two beams are equal; their cross-sectional shapes are square in Example 1 and T-shaped in Example 2. The normal loads and the bending moments are also equal.

Example 1:

Beam with square cross-section. The example applies for all mirror imaged cross-sectional shapes.

Measurements:

The strains ϵ_u and ϵ_{lo} should be measured separately.

Measurement results:

$$\epsilon_u = 900 \mu\text{m/m},$$

$$\epsilon_{lo} = 1140 \mu\text{m/m}.$$

A: Computed solution

Test sample of Al-Cu-Mg 1, $E = 72100 \text{ N/mm}^2$.

From the two measured strains ϵ_u and ϵ_{lo} the stresses can be calculated as

$$\sigma_u = \epsilon_u \cdot E = 900 \cdot 10^{-6} \cdot 72100 = 64.9 \text{ N/mm}^2,$$

$$\sigma_{lo} = \epsilon_{lo} \cdot E = -1140 \cdot 10^{-6} \cdot 72100 = -82.2 \text{ N/mm}^2.$$

The strain components are:

$$\begin{aligned} \epsilon_n &= \frac{1}{2} (\epsilon_u + \epsilon_{lo}) \\ &= \frac{1}{2} (900 - 1140) = -120 \mu\text{m/m}, \end{aligned}$$

$$\begin{aligned} \epsilon_b &= \pm \frac{1}{2} (\epsilon_u - \epsilon_{lo}) \\ &= \pm \frac{1}{2} (900 + 1140) = \pm 1020 \mu\text{m/m}. \end{aligned}$$

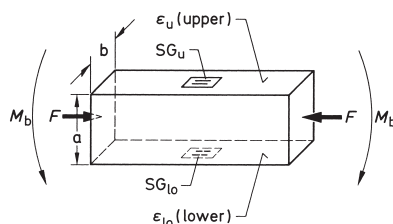


Fig. 8.4-4: Sketch for Example 1

B: Graphical solution

The contour of the test specimen in the region of the strain measurement is drawn to a suitable scale, i.e. either enlarged or reduced, on a page of millimeter-squared paper and a ϵ scale is drawn close to it, see Fig. 8.4-5a.

The gravitational axis passes through the centers of gravity of the cross-sectional areas; with mirror-imaged cross-sections it is identical to the center axis.

The measured strain values ϵ_u and ϵ_{lo} are entered on the scale and projected onto the corresponding edges of the sketch of the object. The two points are then joined with a straight line. The intersection point N of this line with the line ϵ_0 gives the distance d of the neutral axis to the lower edge of the test sample; this can be measured from the sketch, see Fig. 8.4-5a.

The hatched fields to the right and left of the line ϵ_u indicate the strain distribution over the cross-section of the test specimen; the positive strains are on the right, the negative strains on the left, see Fig. 8.4-5b.

The intersection point with the line between ϵ_u and ϵ_{l0} is marked on the gravitational axis and this point is projected onto the ϵ scale. The magnitude of the normal strain created by a normal force F can be read off here; it is $-120 \mu\text{m}/\text{m}$ in the example, see Fig. 8.4-5c.

The bending strains, which have the same magnitude but opposite signs, correspond to the sections

$$\overline{\epsilon_{\pm\epsilon_u}} = \epsilon_{bu} = 900 - (-120) = 1020 \mu\text{m}/\text{m} \text{ and}$$

$$\overline{\epsilon_{\pm\epsilon_{l0}}} = \epsilon_{bl0} = -1140 - (-120) = -1020 \mu\text{m}/\text{m}$$

The accuracy of the graphical solution depends on the drawing accuracy.

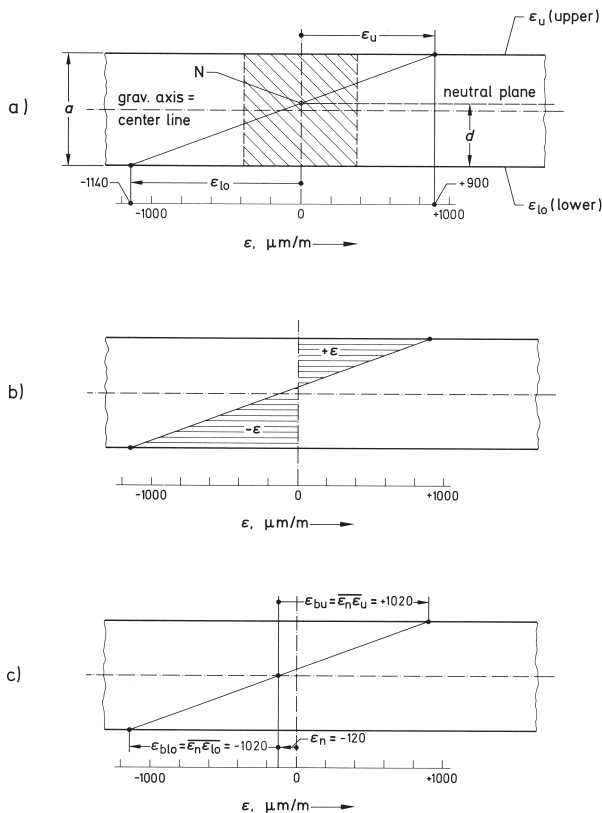


Fig. 8.4-5: Graphical solution to Example 1

Example 2:

Beam with T-shaped cross-section. (The principle used to give a solution to this problem can also be used for other cross-sectional shapes.)

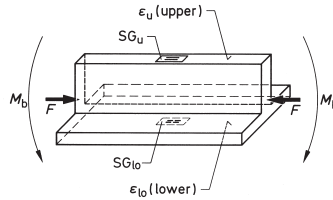


Fig. 8.4-6: Sketch for Example 2

Measurement object material: Al-Cu-Mg 1; $E = 72100 \text{ N/mm}^2$

Measurements:

The strains ϵ_u and ϵ_{lo} should be measured separately.

Measurement results:

$$\epsilon_u = +490 \text{ } \mu\text{m/m,}$$

$$\epsilon_{lo} = -400 \text{ } \mu\text{m/m}$$

A: Calculated solution

From the two measured strains ϵ_u and ϵ_{lo} the boundary stresses can be calculated as

$$\sigma_u = \epsilon_u \cdot E = 490 \cdot 10^{-6} \cdot 72100 = 35.3 \text{ N/mm}^2,$$

$$\sigma_{lo} = \epsilon_{lo} \cdot E = -400 \cdot 10^{-6} \cdot 72100 = -28.8 \text{ N/mm}^2.$$

To determine the strain components by calculation the distance h_{cg} to the center of gravity is required (see Fig. 8.4-7). It is listed in tables for standard profiles; for other shapes of profile the formulae for the calculation can be found in specialist literature. For the profile in Example 2:

$$h_{cg} = \frac{1}{2} \cdot \frac{a \cdot H^2 + b \cdot c^2}{a \cdot H + b \cdot c}. \quad (8.4-15)$$

With the dimensions of the model according to Fig. 8.4-7 the distance h_{cg} is

$$h_{cg} = \frac{1}{2} \cdot \frac{2.5 \cdot 15^2 + 12.5 \cdot 2^2}{2.5 \cdot 15 + 12.5 \cdot 2} = 4.9 \text{ mm.}$$

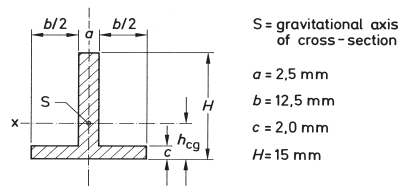


Fig. 8.4-7: Sketch of the T cross-section

The normal strain ϵ_n is calculated according to the relationship

$$\epsilon_n = \epsilon_{l0} + e \cdot \frac{\epsilon_u - \epsilon_{l0}}{H} \quad (8.3-16)$$

For Example 2 this gives:

$$\epsilon_n = -400 + 4,9 \cdot \frac{490 - (-400)}{15} = 4,9 \cdot \frac{890}{15} - 400 = -109 \text{ } \mu\text{m/m}$$

The normal force F_n is

$$F_n = \epsilon_n \cdot E \cdot A = -109 \cdot 10^{-6} \cdot 72100 \text{ N/mm}^2 \cdot 64 \text{ mm}^2 = 503 \text{ N} \quad (8.4-17)$$

For asymmetrical cross-sections the bending strains have different amplitudes. They are

$$\begin{aligned} \epsilon_{l0} &= \epsilon_0 - \epsilon_n = -400 - (-109) = -291 \text{ } \mu\text{m/m} \\ \epsilon_{u0} &= \epsilon_u - \epsilon_n = -490 - (-109) = +381 \text{ } \mu\text{m/m} \end{aligned}$$

B: Graphical solution

The method of solution is similar to that for symmetrical cross-sections. The contours of the test object are first drawn out on a page of millimeter paper, alongside an ϵ scale, see Fig. 8.4-8a.

In the sketch the gravitational axis is drawn at a distance h_{cg} from the base; it is a line which joins the centers of gravity of the cross-sectional surfaces.

The measured strain values ϵ_u and ϵ_{l0} are entered on the scale, they are then projected onto the appropriate boundary lines on the sketch of the object and the two points are joined with a straight line. The intersecting point N of this line with the ϵ_0 line gives the distance d of the neutral bending plane to the lower edge of the test object; it can be measured from the sketch, see Fig. 8.4-8a.

The shaded areas to the right and left of the ϵ_0 line show the strain distribution over the cross-section of the test object; the positive strains are on the right, the negative strains on the left, see Fig. 8.4-8b.

On the gravitational axis the point of intersection with the line between ϵ_u and ϵ_{lo} is marked and this point is then projected onto the ϵ scale, see Fig. 8.4-8c. There the magnitude of the normal strain ϵ_u can be read off, i.e. $-110\mu\text{m/m}$ in Example 2.

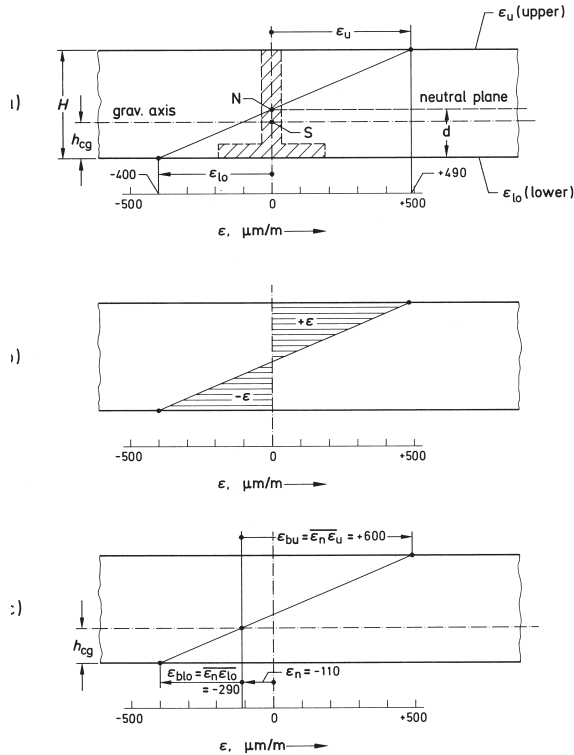


Fig. 8.4-8: Graphical solution to Example 2

The bending strains correspond to the sections

$$\overline{\epsilon}_{bu} = \epsilon_{bu} = 600 \mu\text{m/m}$$

$$\overline{\epsilon}_{bl} = \epsilon_{bl} = -290 \mu\text{m/m}$$

Here also, the drawing accuracy has a direct bearing on the accuracy of the result and it depends on the choice of scale.

8.4.4 Measurements on a shaft under torsion (twisted shaft)

A measurement on a twisted shaft can have a number of objectives:

1. The determination of the normal and the shear stresses for stability considerations.
2. The determination of the effective torsion moment M_t from which the transmitted power P can be calculated for a rotating shaft.
3. The determination of the shear deformation angle γ or of the twist angle φ .

For 1.

A shaft loaded with torsion is subject to a biaxial stress state. The principal normal stresses occur at an angle of $\pm 45^\circ$ to the cylindrical planes (lines running parallel to the longitudinal axis of the shaft). The strains produced by the normal stresses can be measured with strain gages. The X rosettes shown in Fig. 3.2-9a are very suitable for this purpose, particularly the V shape with the measuring grid axes at $\pm 45^\circ$ to the axis of symmetry. The measuring grid axes must correspond to the principal stress directions, see Fig. 8.4-9.

Note:

A correct result will only be given by a correct measurement. The axes of the measuring grids must correspond to the principle stress directions. Deviations by the angle α give an error e of

$$e = (\cos 2\alpha - 1) \cdot 100\% \quad (8.4-18)$$

If a strain gage is mounted with a directional error of $\alpha = 5^\circ$, the measured value will be 1.6% too small. With half and full bridge configurations, if the other strain gages are correctly oriented, then the error is reduced to -0.8% for the half bridge configuration and to -0.4% for the full bridge configuration. It should be noted, however, that with unsymmetrical arrangements of strain gages larger errors can occur due to improper compensation of any existing normal and bending strains.

Suitable configurations are the half and full bridge circuits. With the transmission of measurement signals from rotating shafts through slip-rings the full bridge circuit must be used, because otherwise changing contact resistances within the bridge circuit can cause significant measurement errors. With the full bridge circuit the contact resistances in supply leads 2 and 3 are in series with the bridge resistance and in the measurement leads 1 and 4 they are in series with the amplifier input impedance. In both cases their effects shrink to insignificant proportions, provided the slip-rings and brushes are of good quality (see section 8.4.4.1).

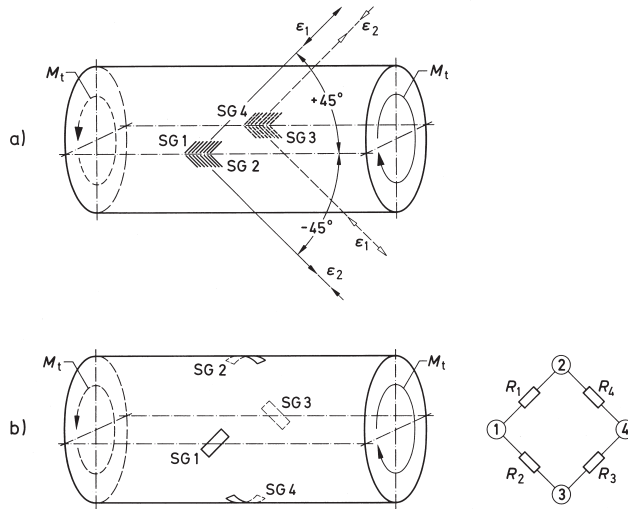


Fig. 8.4-9: Torsion shaft with strain gages mounted in the principal strain directions ϵ_1 and ϵ_2 and their positions in the bridge circuit

- a) with the application of special X rosettes
 b) with the application of single strain gages

The full bridge configuration is also the best in compensating interference signals from superimposed normal and bending loading, if the strain gages are applied as shown in Fig. 8.4-9a and b.

The principal normal stresses σ_1 and σ_2 can be calculated from the measured strains ϵ_1 and ϵ_2 according to the formulae (8.2-1) and (8.2-2) for the biaxial stress state with known principal directions; they are given again below:

$$\sigma_1 = \frac{E}{1-\nu^2}(\epsilon_1 + \nu \cdot \epsilon_2), \quad (8.2-1)$$

$$\sigma_2 = \frac{E}{1-\nu^2}(\epsilon_2 + \nu \cdot \epsilon_1). \quad (8.2-2)$$

The following applies to the twisted shaft:

$$|\epsilon_1| = |\epsilon_2|, \quad (8.4-19)$$

$$\epsilon_2 = -\epsilon_1, \quad (8.4-20)$$

If the strain gages are wired as a half bridge in the bridge arms 1 and 2, then a change of sign occurs for ϵ_2 , see section 5 and equations (5.2-5) and (5.2-7). The indicated strain value ϵ_i then becomes

$$\epsilon_1 = \epsilon_1 - (-\epsilon_2) = |\epsilon_1| + |\epsilon_2| = 2\epsilon \quad (8.4-21)$$

A corresponding result is obtained for the full bridge circuit.

Hence there is a change of sign in the expression within brackets in the following equation compared to equations (8.2-1) and (8.2-2).

For the half bridge circuit:

$$\sigma_{1,2} = \pm \frac{1}{2} \cdot \frac{E}{1-\nu^2} \cdot (1-\nu) \cdot \epsilon_1 \quad (8.4-22)$$

For the full bridge circuit:

$$\sigma_{1,2} = \pm \frac{1}{4} \cdot \frac{E}{1-\nu^2} \cdot (1-\nu) \cdot \epsilon_1 \quad (8.4-23)$$

The shear stress τ increases from $\tau = 0$ at the center to the maximum value τ_{\max} at the circumference.

$$\begin{aligned} \tau_{\max} &= 2\epsilon_{45^\circ} \cdot G \\ &= \epsilon_1 \cdot G \text{ for the half bridge circuit,} \\ &= \frac{1}{2} \epsilon_1 \cdot G \text{ for the full bridge circuit} \end{aligned} \quad (8.4-24)$$

ϵ_i = indicated strain value for the full and half bridge circuits

G = shear modulus (see section 2.3.2, equation 2.3-2)

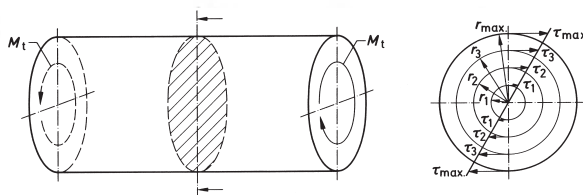


Fig. 8.4-10: Distribution of the torsion stress over the cross-section of a twisted shaft

For 2.

The torsional moment M_t can be calculated from the shear stress τ_{\max} , which is determined according to equation (8.4-24), and from the polar section modulus S_p of the shaft as follows:

$$M_t = \tau_{\max} \cdot S_p = 2\epsilon_{45^\circ} \cdot G \cdot S_p \quad (8.4-25)$$

For the half bridge circuit:

$$M_t = \epsilon_t \cdot G \cdot S_p \quad (8.4-26)$$

For the full bridge circuit:

$$M_t = \frac{1}{2} \epsilon_t \cdot G \cdot S_p \quad (8.4-27)$$

With τ and G in N/cm^2 and S_p in cm^3 M_t is given in Ncm .

The polar section modulus S_p is dependent on the cross-sectional shape of the twisted shaft. Formulae for its calculation are given in the appropriate literature. For a cylindrical shaft the following applies:

$$S_p = \frac{\pi \cdot d^3}{16} \approx 0.2d^3. \quad (8.4-28)$$

The power P transferred from the rotating shaft is calculated as

$$P = \omega \cdot M_t = \frac{2\pi \cdot n}{60} \cdot M_t = 0.105 \cdot n \cdot M_t = \frac{n \cdot M_t}{9.55}. \quad (8.4-29)$$

With M_t in Nm and the speed n in min^{-1} , P is obtained in $\text{Nm}/\text{s} = \text{W}$.

See section 8.4.4.1 regarding the transfer of the measuring signal from rotating shafts.

For 3.

Fig. 8.4-11 shows the shear deformation angle γ and the angle of twist φ on the twisted shaft.

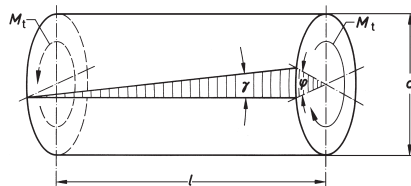


Fig. 8.4-11: Shear deformation angle γ and angle of twist φ

The shear deformation angle γ is calculated as

$$\gamma = \frac{r_{\max}}{G} \quad (8.4-30)$$

and the angle of twist φ as

$$\varphi = 2 \cdot \frac{l}{d} \cdot \gamma = 4\epsilon_{45} \cdot \frac{l}{d}; \quad (8.4-31)$$

for the half bridge

$$\varphi = 2\epsilon_1 \cdot \frac{l}{d}; \quad (8.4-32)$$

for the full bridge

$$\varphi = \epsilon_1 \cdot \frac{l}{d}. \quad (8.4-33)$$

8.4.4.1 Transferring the measuring signal from rotating shafts

There are various methods of transferring the measuring signal from rotating shafts.

For a slow rate of rotation with only a few revolutions of the measuring object, a cable that winds and unwinds provides the simplest solution. It is applicable to all types of circuit (also to the quarter bridge configuration, but with the restrictions mentioned in sections 7.1.1 and 7.2.1).

A second method is the transfer of the bridge supply voltage and the measuring signal using sets of slip rings. Only high quality versions are suitable due to the requirements for extremely low contact resistance between the slip ring and the brush. Low wear at high speeds and very low thermal voltages are also demanded.

HBM supplies this type of equipment as slip ring assemblies for fitting to rotating shafts of various sizes with two sets of brushes for separate mounting. The set contains five slip rings; four for connection of the strain gages and the fifth providing a ground connection with the rotating shaft to prevent interference. Slip ring assemblies for mounting on the free end of a shaft can be supplied with six or 12 slip rings (Fig. 8.4-12). The data sheets give information on the permissible speed and other technical details.

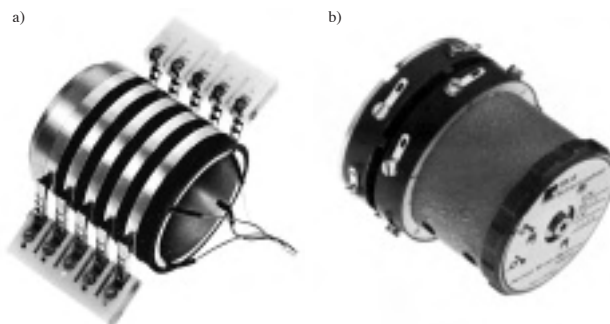


Fig. 8.4-12: Slip ring assemblies

- a) SK5, Slipring Assembly with 2 sets of SK5/ZB Brushes
- b) SK6, Slipring Assembly

Despite better contact materials a certain amount of variation of the contact resistance (contact noise) is unavoidable with slip ring transmitters. HBM states a contact resistance between the slip ring and the brush of $40\text{ m}\Omega$ with variations of $<2\text{ m}\Omega$. Whereas the contact resistance itself is relatively unimportant, variations in its value are reproduced in the measuring signal. If the resistance of a $120\ \Omega$ strain gage at a strain of $1000\ \mu\text{m/m}$ changes by about $240\ \text{m}\Omega$, then a variation in the measuring signal of about $1.7\% = 17\ \mu\text{m/m}$ occurs through two sliprings when a quarter bridge is used. The constant part of the contact resistance of $2 \times 40\ \text{m}\Omega$ causes an apparent reduction in sensitivity in the strain gage of only 0.06% .

The relationships are significantly more favorable if a half bridge circuit is connected. Here the contact resistances are in series with the half bridge resistance. Hence with a $120\ \Omega$ strain gage an apparent loss in sensitivity of only 0.03% occurs due to the drop in the supply voltage at the contact points; with higher strain gage resistances this is less still. The contact resistance of the third slip ring and of the signal path has no influence on the measurement.

On account of its advantages regarding the compensation of interference effects, the full bridge should be used where possible. Examples for the application of slip ring transmission in strain gage measurements are described in [8-7, 8-8].

With substantially overdimensioned components only slight strain values are produced. Hence there is the risk that the measuring signals will be masked to some extent due to the noise voltages and other interference signals. Here the mounting of the amplifier or a pre-amplifier on the rotating part and the transfer of the amplified signal via slip rings is one method to be considered, see Fig. 8.4-13.

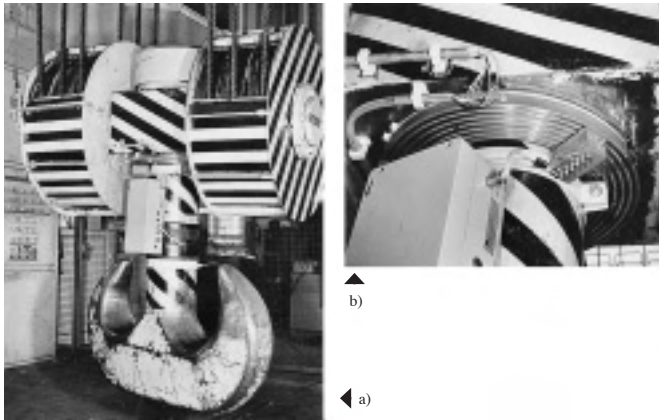


Fig. 8.4-13: Example of the fitting of an amplifier to a moving part and the transfer of the amplified measuring signal via sliprings (photographs taken from [8-9])

- a) full view of a 120 t crane hook with mounted strain gages and industrial measuring amplifier
- b) close-up of the sliprings and brushes for transfer of the supply voltage, the amplified measuring signal and a control signal.

With non-contact transmission of measuring signals, there are significant advantages in minimizing the number wearing parts and in providing substantial immunity against interference. Depending on the design of the system the supply of the strain gage circuit can be obtained from rotating batteries or from non-contact, inductive transfer of electrical energy.

Decoupling of the frequency modulated measuring signal can be carried out capacitively or inductively, depending on the application. The conversion of the pulse frequency into a direct voltage proportional to the measured value is undertaken in peripheral units. Fig. 8.4-14 shows examples of two types of non-contact measurement transmitters.



Fig. 8.4-14: Non-contact measurement transmitters
 a) system for shaft-mounting with battery container and measurement transmitter with peripheral receiver preamplifier
 b) rotating transmitter for mounting on the end of a shaft

The progression from torque measurement to power measurement requires only slight additional complexity to determine the rotational speed. Apart from the tachogenerator, which provides a voltage proportional to the speed, noncontact optical or magnetic systems for measuring the speed should be considered. Examples of the latter are shown in Fig. 8.4-15.

By multiplying the voltage proportional to the torque with that which is proportional to the speed in a multiplying amplifier, a signal proportional to speed is obtained.



Fig. 8.4-15: Transducer systems for the non-contact acquisition of the speed of rotating parts

8.4.5 Measurement on a twisted shaft with superimposed axial force and bending moment

There are two different objectives:

1. the determination of the separate loading components,
2. the determination of the maximum material stress.

Both are possible, but require different applications of strain gages.

For 1.

Each loading component should be measured separately. If the components are to be measured simultaneously because their dynamic interrelationships are important, then a channel is required for each of the components. The measuring signals may, e.g. be synchronously recorded with a multichannel recorder.

Torsion with superimposed axial loading.

The separate measurement of each loading component requires:

strain gages mounted according to section 8.4.4, Fig. 8.4-9 for the measurement of the torsion,

strain gages mounted according to section 5.4.1, Fig. 8.4-1 for the measurement of axial loading.

This type of measurement problem arises, for example, in ships' propeller shafts. It has been found from experience that rather small strains are involved and therefore the full bridge circuit should be used. It ensures the best suppression of disturbances.

Torsion with superimposed bending

Also in this case both components can be measured in a similar manner.

The measurement of torsion again requires strain gages mounted as shown in section 8.4.4, Fig. 8.4-9.

The bending component can be measured with strain gages mounted according to section 8.4.2, Fig. 8.4-2; however, the direction of the bending moment and the bending plane must be known. If the direction of the bending plane is unknown, then it can be found with investigatory measurements with axially positioned separate strain gages at 90° over the circumference or by the use of an auxiliary procedure. This includes the brittle coating method [8-4], the birefringence coating method and special ceramic coatings. The latter require a stoving temperature of 550°C .

For 2.

The resultant stresses in an object loaded with different components can only be determined according to the analytical procedure for a biaxial stress state with unknown principal directions as in section 8.2.2.

For torsion with superimposed axial loading the location of the measurement is unimportant, because both loads act uniformly over the cross-section. This is not the case for tor-

sion with superimposed bending. The bending load passes through the cross-section from a positive maximum to a negative maximum. The points of maximum loading can be found if the direction of the bending plane is known. Measurements at a number of points at 90° over the circumference or by the use of one of the above mentioned auxiliary methods can be made.

8.4.6 Measurements on a shear beam

It has been shown how shear stresses appear in conjunction with a torque in a twisted shaft. They may also arise in a shear beam with a bending moment. This is illustrated with an example in Fig. 8.4-16.

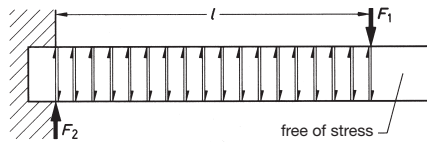


Fig. 8.4-16: Formation of shear stresses in a cantilever beam

The beam which is clamped on one end (cantilever beam) is loaded with a force F_1 at a distance l . The equal reactive force F_2 acts in the opposite direction. A force couple is produced as shown in Fig. 2.2-2. The fact that the points of application of the forces are separated by a large distance is of no significance for the shear stresses which arise. Shear stresses arise in each cross-sectional plane between the points of application. The normal stresses σ_1 and σ_2 which arise in conjunction with the shear stresses τ run - as with the twisted shaft - at an angle of 45° to the shear plane, see Fig. 8.4-17a. Also the force F multiplied by the distance l forms a bending moment; the bending stresses thus produced are superimposed on the normal stresses. Therefore the angular value of $\pm 45^\circ$ is only exact at the level of the neutral zone, where the bending stresses are zero. The coordinate system is rotated toward the boundaries so that the boundary stresses, which are pure bending stresses, run parallel to the boundaries, see Fig. 8.4-17b. Therefore it is important to mount the strain gage as close as possible to the neutral plane:

The shear stresses τ and the shear deformation angle γ cannot be measured with strain gages; however, both can be calculated from the strains measured at 45° . The following relationship applies

$$\epsilon_{45^\circ} = \frac{\tau}{2G} = \frac{1}{2}\gamma \quad (8.4-34)$$

This results in:

$$\begin{aligned} \tau_{max} &= \gamma \cdot G = 2\epsilon_{45^\circ} \cdot G \\ &= \epsilon_1 \cdot G \text{ for the half bridge circuit,} \\ &= \frac{1}{2} \epsilon_1 \cdot G \text{ for the full bridge circuit.} \end{aligned} \quad (8.4-35)$$

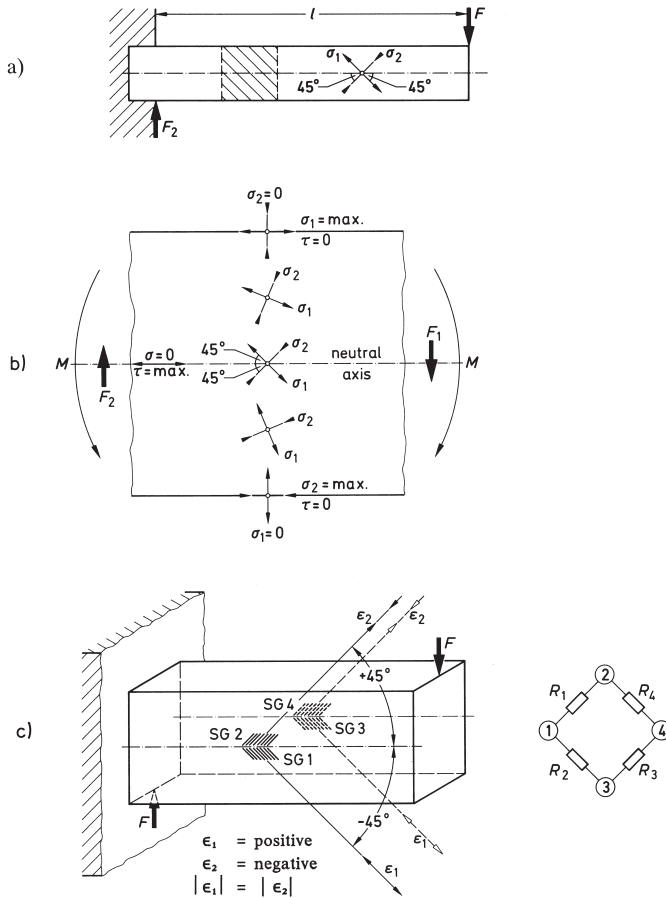


Fig. 8.4-17: Stress and strain conditions in the shear beam
 a) directions of the principal normal stresses σ_1 and σ_2 in the level of the neutral plane
 b) directions of the principal normal stresses σ_1 and σ_2 and the shear stresses τ along the cross-sectional level for superimposed shear and bending loads
 c) arrangement of the strain gages for the measurement of the strain maxima ϵ_{45° and the strain gages as they appear in the bridge circuit

$$\gamma = 2\epsilon_{45^\circ} \quad (8.4-36)$$

The shear stress distribution over the cross-section is non-linear. For a rectangular cross-section the distribution is approximately as shown in Fig. 8.4-18.

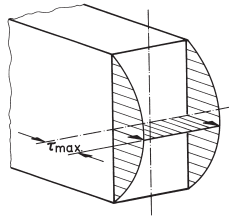


Fig. 8.4-18: Shear stress distribution in a rectangular cross-section

The superimposed bending strains/bending stresses can be determined according to the method described in section 8.4.2. In addition the strain gage arrangement described in that section is required.

The force F can also be determined from the measured strain ε_{45° . The following relationship applies:

$$F = \frac{2\varepsilon_{45^\circ} \cdot G \cdot A}{c_A} \quad (8.4-37)$$

which is derived from

$$\tau_{\max} = \frac{F}{A} \cdot c_A = \gamma \cdot G = 2\varepsilon_{45^\circ} \cdot G \quad (8.4-38)$$

The shape factor c_A depends on the cross-sectional shape of the beam. For rectangular cross-sections with $b/h \leq 1/2$, $c_A = 3/2$; for a circular cross-section $c_A = 4/3$ and for an annular shaped cross-section $c_A = 2$. For other cross-sectional shapes c_A can be calculated from the formulae given in specialist literature.

If the shear beam is used exclusively to measure the force, then it is recommended that a profile is used that has a maximum bending section modulus for a minimum of cross-sectional area, e.g. an I shape. Compared to a rectangular shape its advantages are:

- the ε_{45° strains become larger,
- the bending stresses become smaller,
- the shear stress distribution in the region of the strain gage becomes more uniform,
- the measuring signal becomes independent of the application point of the force (in contrast to the bending beam).

Fig. 8.4-19 shows an example. The variant b) with a fold-back arm enables the point of application for the force to be moved beyond the measuring point.

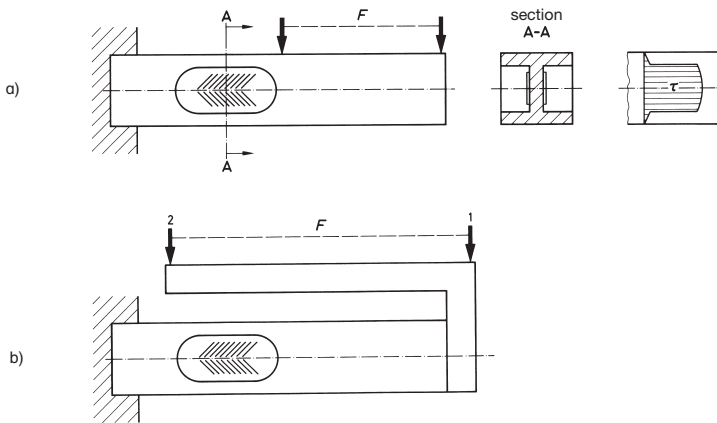


Fig. 8.4-19: I-shape section for the measurement of force and shear stress distribution in the beam

The arrangement of the strain gages is made as in Fig. 8.4-17c using a full bridge circuit. The correspondence of the measuring signal ε_i to the force F is found by calibration with a force of known size.

8.4.7 Measurement of thermal stresses

Thermal stresses arise in components if the expansion or contraction caused by temperature changes is forcibly restricted or prevented. Thermal stresses are normal material stresses. A typical example of an object in which thermal stresses appear on a larger scale are the endless welded rails on railway tracks. An example explains how thermal stresses occur.

A steel tube of length $l = 2$ is heated from 15°C to 35°C , i.e. $\Delta\vartheta = 20\text{K}$. The linear expansion coefficient of steel is $\alpha = 12 \cdot 10^{-6} \text{ m}/(\text{m} \cdot \text{K})$. Therefore the change in length Δl can be calculated as

$$\Delta l = l \cdot \alpha \cdot \Delta\vartheta = 2\text{m} \cdot 12 \cdot 10^{-6} \frac{\text{m}}{\text{m}} \cdot 20\text{K} = 480 \cdot 10^{-6} \text{m} = 480 \mu\text{m}.$$

When referred to a length of 1 m this gives a strain of

$$\varepsilon = \frac{\Delta l}{l} = \frac{480 \mu\text{m}}{2\text{m}} = 240 \mu\text{m}/\text{m}.$$

In order to compensate this strain a force is required that presses the tube back to its original shape. Hence a longitudinal stress (negative in this case) arises in the tube. The same stress occurs if the tube is held fixed in its original length by external stresses. The longitudinal stress can be calculated as

$$\sigma = \varepsilon \cdot E = -240 \mu\text{m}/\text{m} \cdot 206 \text{ kN}/\text{mm}^2 \approx -50 \text{ N}/\text{mm}^2.$$

The resulting compression force F is dependent on the cross-sectional area A of the tube. For a tube with an external diameter of 50 mm and a wall thickness of 3 mm, the cross-sectional area can be calculated from the mean diameter D multiplied by the wall thickness s

$$A = (D - s) \cdot \pi \cdot s = (50 - 3) \cdot \pi \cdot 3 = 443 \text{ mm}^2.$$

$$F = \sigma \cdot A = -50 \text{ N/mm}^2 \cdot 443 \text{ mm}^2 = -22150 \text{ N}.$$

The example shows that relatively small temperature changes can produce significant stresses and forces.

The arrangement of the strain gages on the measurement object depends on the aim of the measurements. For bar-shaped objects information is given in sections 8.4.1 to 8.4.3 and for objects with a large area, in section 8.2.2. Temperature compensated strain gages should be preferred. A simultaneous temperature measurement [8-5, 8-6] often provides useful additional information in many cases.

The problem is now; how can restricted strains be measured with strain gages? The following section describes a number of methods, whose effectiveness depends on the conditions affecting the measurement object.

The special problems during the determination of the thermal stresses using strain gages on epoxy resin models are described in [8-10].

8.4.7.1 Comparison of measurements on a free and on a restrained object

A comparative measurement is only possible if the component to be investigated can be relieved of loading either before or after the load measurement and if it can be subjected to a reference measurement in the same temperature range. In this manner errors due to thermal output can be found and eliminated. The method is explained using an example of a model test.

An aluminum tube which is unrestricted in its thermal expansion has two strain gages mounted on opposite sides and in addition has one type Pt 100 resistive temperature sensor for temperature measurement. The strain gages are wired as a 2/4 or diagonal bridge for doubling the measured value ε_1 and for providing compensation of possible bending. With the double quarter bridge circuit $\varepsilon_1 = \frac{1}{2} \varepsilon_i$.

The tube is heated from room temperature to 45°C. The measurement result $\varepsilon = \frac{1}{2} \varepsilon_1 = -100 \mu\text{m/m}$ arises due to the mismatching of the strain gages to the thermal expansion coefficient of the aluminum tube (thermal output), Fig. 8.4-20a.

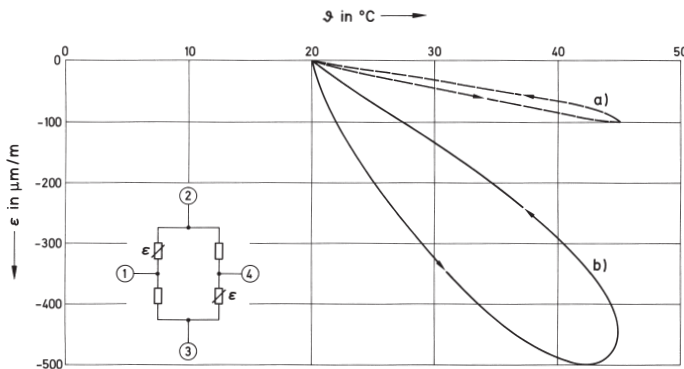


Fig. 8.4-20: Result of a model test for the determination of thermal stresses
 a) signal for the freely expanding tube (reference measurement),
 b) signal for the restrained tube (load measurement).
 For the double bridge circuit the relationship $\epsilon = \frac{1}{2} \epsilon_i$ applies

After cooling, the tube is clamped at both ends in a strong vice, preventing the thermal expansion of the tube. On reheating, a measurement result of $\epsilon = \frac{1}{2} \epsilon_i = -500 \mu\text{m}/\text{m}$ (load measurement) is obtained, although the length of the tube is held constant, see Fig. 8.4-20b.

The difference of $-400 \mu\text{m}/\text{m}$ corresponds to the restricted thermal strain. (The large hysteresis loop is caused by the non-uniform cooling of the tube in the stressed state. Due to the large mass of the clamping elements, the ends of the tube cool down significantly faster than the middle of the tube where the temperature is measured. Whereas the temperature is indicated for just one point, the indicated strain is determined by the strain integral over the length of the tube.)

An error of 20% would arise without this reference measurement.

8.4.7.2 Measurement with a compensating piece

The simplest method of compensating for the error due to thermal output is that where a separate piece of the component material is used as a compensating piece. With measurements on railway lines this may be another unstressed piece of rail. This type of compensation for thermal output is described in section 7.1. The advantage is that the correct result is obtained with only one measurement and the reference measurement is not needed.

8.4.7.3 Separate or later determination of the thermal output

If it is not possible to carry out the reference measurement on the actual object, it can be made on a separate piece of the same component material. However, then the relationship of the strain measurement to temperature is required, i.e. the temperature must be measured on the comparison piece and on the measurement object close to the strain gage.

If it is acceptable, the strain gage and all the material underneath it can be separated from the measurement object after the load measurement, similar to the method shown in Fig.

3.2- 10. The strain gage must not be damaged in the cutting process. The reference measurement (measurement of thermal output) can then be undertaken later as previously mentioned.

Depending on whether monoaxial or biaxial thermal stresses are expected, linear strain gages or R rosettes must be used. The evaluation of the measurements is made according to sections 8.1 and 8.2.2

9 Measurement accuracy

As supplied strain gages are a finished product but they are not a measurement instrument. This apparently contradictory statement results from the fact that the strain gage is only capable of being used for measurements after being mounted by the user. In this respect the accuracy specifications given by the manufacturer are linked to the relevant conditions for the strain gage. Therefore, in order that the user can obtain good measurement results, information on possible sources of error is given in the appropriate sections of this book and compensation or correction methods are described.

It is well known from the field of transducers that strain gages are able to supply extraordinarily accurate measurement results. Load cells for use with equipment subject to official calibration head this field with a permissible error of less than 0.02%. The time constant for the nominal sensitivity is better than $1 \cdot 10^4$ /year. This extreme accuracy can only be achieved with transducers and can only be maintained where the measuring point is hermetically encapsulated. The latest designs of precision force transducers for the international comparison of standard force measuring equipment have brought a substantial increase in accuracy [9-1].

Under the conditions relevant to experimental stress analysis and similar fields of application the measurement accuracy that can be achieved reduces rapidly to conventional values in the percentage region. However, it should not be overlooked that all the links within the chain of measurement equipment, including the measurement object, contribute to the measurement error.

One only has to think of electrical unsymmetries in the bridge circuit, mechanical unsymmetries in the measurement object (e.g. due to production tolerances, distortion of the cross-section due to loading, anisotropy of the elastic characteristics), directional errors of the strain gage, etc.

Careful consideration of the errors involved should therefore accompany each measurement: before the measurement - to find large sources of error and, if possible, to correct them; and after the measurement - to obtain a definite impression of the order of the remaining, probable measurement error.

A new philosophy is replacing the term "measurement error" in but a few exceptions by the term "measurement uncertainty". A more detailed treatment of the topic discussed in this section can be found in [9-2].

9.1 Causes of measurement errors

Each measurement result is affected by error if there are inadequacies

- in the measurement object
- in the measuring instruments (including the display of the measurement)
- in the measurement method
- due to environmental influences
- due to personal influences of the observer
- due to time changes of all the above mentioned sources of error.

Each measurement deviates by a certain amount from the true value of the measured variable due to these influences. A measurement result itself is insufficient if a statement regarding the degree of errors contained in it cannot be made. Limits must be stated within which the true value of the measured variable lies.

A grouping can be made as follows:

- a) large errors
- b) random deviations
- c) systematic deviations

Considering a):

Large errors occur for example due to

- the choice of an unsuitable measurement or evaluation method,
- incorrect application of the transducer (e.g. improper mounting),
- errors in the circuit,
- incorrect operation of the measurement instrument,
- logging errors,
- neglecting a source of error.

There is no possibility of correcting large errors. They are either detected before it is too late and eliminated or they are transferred completely to the measurement result. Sometimes it can be seen from an improbable result that a large error has crept in. However, sometimes “improbable” results are correct and the expectations were wrong.

Considering b):

Random deviations occur due to influences whose presence depends on coincidence. Included here are all changes occurring during the measurement which are not measured and on which no influence can be exerted:

- the measurement object (ageing)
- the environment (temperature, humidity, air pressure, electrical and magnetic fields, radiation).
- the loading equipment (friction, wear, play in the lever mechanism),
- the instruments (ageing, alteration of the operating voltage, environmental influences),
- the observer (fatigue, impairment due to external influences).

The various influences cannot be separated and do not follow any recognizable law. Random deviations vary unequally in magnitude and sign (\pm). They can only be evaluated by repeating the measurement a number of times.

Considering c):

Systematic deviations are mainly caused by

- imperfections in the measurement object,
- imperfections in the measurement method,
- imperfections in the measuring instruments,

but the following should also be taken in account

- influences of the environment,
- characteristics of the observer.

Systematic deviations have a certain magnitude and a certain sign (either + or -). They can be principally evaluated by comparative measurements with instruments or methods using high accuracy. A known systematic deviation may be caused by the measurement principle used (e.g. by connection of a transducer with non-linear characteristics to a measuring amplifier with a linear characteristic). The correction K has the opposite sign to the deviation.

9.2 Calculating the degree of random deviation in a measurement series

Using statistics the random deviations can be numerically estimated and the estimation becomes more reliable, the greater the number of measurements that are carried out, i.e. limits can be stated outside of which the measurement is unreliable.

9.2.1 Test requirements

The test requirements have an influence on the distribution of the measurements. There is a difference between two limiting cases for the practical test requirements:

Repetitive conditions

An observer repeats the measurement with the same measuring instrument under the same operating conditions. Systematic errors cannot be detected under repetitive conditions.

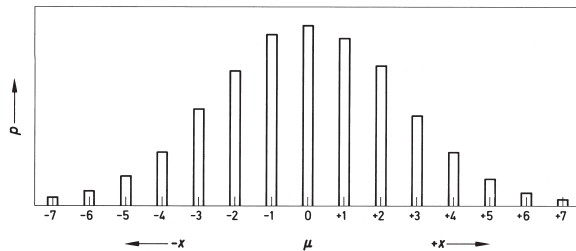
Comparative conditions

Different observers carry out the measurements in different laboratories using different measurement instruments of the same type. In this case the standard deviation is usually greater than under repetitive conditions.

9.2.1.1 The Gaussian distribution

A Gaussian normal distribution of the variable under investigation is assumed for the statistical evaluation of a measurement. The Gaussian distribution can be expected wherever the distribution of the measured variable is purely random; no preselection or other methods should be used which may give a one-sided displacement or preference to one section of the distribution. This means that all measurements must be repeated, but under comparative conditions.

From a large number of separate measurements (e.g. 1000) obtained in this way the arithmetical mean is calculated according to equation (9.2-1), section 9.2.2. The difference to the mean is computed for each separate measurement. It is found that a large number of individual measurements is situated exactly at the mean, that another large number lies close to the mean and that decreasing numbers have increasingly large positive and negative deviations from the mean.



x = deviation from the mean μ (expected value)
 p = number of measurements within each group

Fig. 9.2-1: Histogram of the distribution of the deviations for a series of measurements

If the numbers p found for each difference value are entered into a histogram (column diagram), then a characteristic distribution is obtained, Fig. 9.2-1.

Under ideal conditions and with an infinitely finely divided representation, a normal distribution is obtained which is named the Gaussian distribution after its founder, see Fig. 9.2-2.

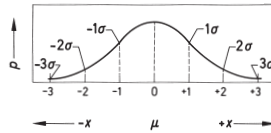


Fig. 9.2-2: Frequency distribution p of the Gaussian distribution

In the Gaussian distribution the contents of the sections of area under the curve correspond to the proportions of the individual values in the total number of measurements, i.e. the total population.

The points of inflection in the curve bounding the area are identified in Fig. 9.2-2 with -1σ and $+1\sigma$. The section σ on the abscissa (in Fig. 9.2-2 $1\sigma = 1x$) is defined as the standard deviation of the total population.

With the normal distribution (Gaussian distribution) of the measured variable and with 1000 independent individual values the following values are obtained:

683 in the region $x \pm 1\sigma$ (68.3%),
 954 in the region $x \pm 2\sigma$ (95.4%),
 997 in the region $x \pm 3\sigma$ (99.7%).

The percentage figures correspond to the equivalent confidence levels $(1 - \alpha)$.

In production quality control in industry a confidence level $(1 - \alpha)$ of 95% is being increasingly applied and in some fields even 99%.

With 1000 independent single values

950 fall in the range $x \pm 1.96 \sigma$, $1 - \alpha = 95\%$,
 990 fall in the range $x \pm 2.58 \sigma$, $1 - \alpha = 99\%$.

If the spread of a measured variable is only slight, a narrow curve is obtained as in Fig. 9.2-3a and with a large spread a broad curve is obtained as in Fig. 9.2-3b.

It can be seen from the figure for σ whether a measured variable has a small or large spread of values.

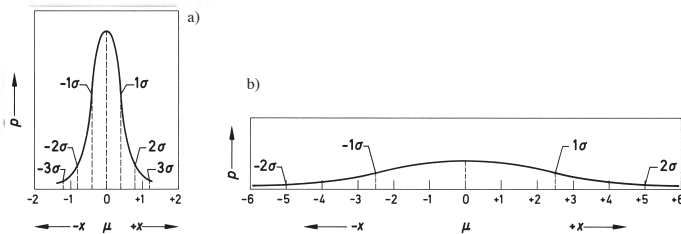


Fig. 9.2-3: Frequency distribution p in a Gaussian diagram
 a) with low spread of the measured variable ($\sigma = 0.4x$)
 b) with a large spread of the measured variable ($\sigma = 2.5x$)

In practice it is not possible to repeat each measurement 1000 times. Therefore, instead of the standard deviation σ of the total population, an estimated value for σ , the standard deviation s , is calculated from a smaller number of measurements using the equation (9.2-2), section 9.2.3. The larger the number of individual measurements taken, then the closer is s to the value of σ .

9.2.2 Arithmetical mean

If in a series of measurements n single values $x_1 \dots x_i \dots x_n$, all independent from one another, are measured under repetitive or comparative conditions, then the arithmetic mean of these n single values is usually taken as the result, i.e. the mean value \bar{x} (pronounced “x bar”).

$$\bar{x} = \frac{1}{n} \sum_{i=1}^n x_i = \frac{x_1 + x_2 + \dots + x_n}{n} \tag{9.2-1}$$

\bar{x} is an estimated value for the expected value μ .

9.2.3 (Empirical) standard deviation s and coefficient of variance v

The most important computational variable for the numerical evaluation of the random distribution of n single values in a series of measurements about its mean \bar{x} is the square deviation of the single observations; this is termed the (empirical) standard deviation s :

$$s = \sqrt{\frac{1}{n-1} \sum_{i=1}^n (x_i - \bar{x})^2} = \sqrt{\frac{(x_1 - \bar{x})^2 + \dots + (x_n - \bar{x})^2}{n-1}} \tag{9.2-2}$$

The (empirical) standard deviation s is an estimated value for the standard deviation σ (see section 9.3).

Instead of the (empirical) standard deviation s , the (empirical) coefficient of variance v is also used; v is also expressed in %. For $x \neq 0$ the following applies:

$$v = \frac{s}{|\bar{x}|} = \frac{100 s}{|\bar{x}|} \% \quad (9.2-3)$$

The coefficient of variance was formerly known as the “relative standard deviation s_r ”.

9.2.4 Confidence limits and confidence range for the expected value μ

It should not be assumed that the mean \bar{x} is equal to the expected value μ or the true value x_t . However, it is possible to state an interval about the mean \bar{x} , corrected for systematic deviations, which covers the expected value with a specified probability $(1 - \alpha)$. The limits of this interval are called *confidence limits* for the expected value and the interval itself is termed the *confidence range* for the expected value; they are assigned to the *confidence level* $(1 - \alpha)$. The chosen confidence level must be stated. The confidence limits which lie symmetrically about the mean for the expected value μ can be calculated as

$$\bar{x} + \frac{t}{\sqrt{n}} \cdot s \quad (\text{upper confidence limit}) \quad (9.2-4)$$

$$\bar{x} - \frac{t}{\sqrt{n}} \cdot s \quad (\text{lower confidence limit}) \quad (9.2-5)$$

The factor t (t distribution according to Student) depends on the chosen confidence level $(1 - \alpha)$. In Table 9.2-1 the figures are summarized with extracts for various confidence levels.

Number of individual values, n	Values for t and t/\sqrt{n} (rounded off)					
	Confidence level $(1 - \alpha)$					
	68.3%		95%		99%	
	t	t/\sqrt{n}	t	t/\sqrt{n}	t	t/\sqrt{n}
2	1.84	1.30	12.7	8.98	63.7	45.0
3	1.32	0.76	4.3	2.48	9.9	5.7
4	1.20	0.60	3.2	1.59	5.8	2.9
5	1.15	0.51	2.8	1.24	4.6	2.1
6	1.11	0.45	2.6	1.05	4.0	1.7
8	1.08	0.38	2.4	0.84	3.5	1.2
10	1.06	0.34	2.3	0.71	3.3	1.0
20	1.03	0.23	2.1	0.48	2.9	0.6
200	1.00	0.07	1.97	0.14	2.6	0.2

Table 9.2-1: Extracts of values for t and t/\sqrt{n} for various values of the confidence level $(1 - \alpha)$

The rise in t , which extends beyond the sensible physical limits, shows that for small values of n and particularly for high confidence levels, that with only two measurements no real statistical statement can be made if s or σ is not known from earlier observations.

On the other hand it is not worth choosing the number of measurements to be too large. Generally, n should not be larger than 10, since the desired reduction in the confidence

limit is no longer in proportion to the degree of effort involved. It is better to reduce the standard deviation s by careful measurement and by selection of a reliable measurement technique. However, if possible, the measurement process should be repeated 4 or 5 times, because the measurement uncertainty is obtained with sufficient reliability with reasonable effort.

9.2.5 Measurement uncertainty u

The measurement result from a series of measurements is the mean value \bar{x} , corrected for the known systematic deviations and based on an interval in which the true value of the measured variable is located. The measurement uncertainty is defined as the interval between the corrected mean value and the upper or the lower interval limit. Note: the complete width of the interval between the upper and lower limits should *not* be termed the measurement uncertainty [9-2].

The measurement uncertainty u has two components:

- the random component u_r for the random deviations,
- the systematic component u_s for the unknown systematic deviations.

The equation

$$u_r = \frac{t}{\sqrt{n}} \cdot s \quad (9.2-6)$$

applies for a series of measurements under repetitive conditions with unknown repetitive standard deviation σ_r .

The systematic component u_s can generally only be estimated based on adequate experimental experience (or using reliable data from the manufacturer).

The following should be noted regarding the manufacturer's data:

All measuring devices have systematic deviations, which vary in their size depending on unavoidable irregularities in production from sample to sample. It would be far too expensive to find the actual deviation of each individual device by comparison with a standard. It is sufficient to give limits within which the greatest deviations lie above and below the desired value. With high quality devices the technical data is listed in the data sheets and stated with their limits. The manufacturer only checks whether the deviations are within the guaranteed limits. In this respect the figures are not absolute limits.

The fact should be noted that the deviations can affect the variables through addition or multiplication; they can in addition possess different signs and may compensate one another to a greater or lesser extent. It is therefore recommended that an estimated value for the systematic component u_s of the measurement uncertainty is determined for the systematic deviations which cannot be individually found. The geometrical sum of all single values a_i is a possible way of achieving this.

$$u_s = \pm \sqrt{a_1^2 + a_2^2 + \dots + a_n^2} \quad (9.2-7)$$

The measuring uncertainty u is obtained by the linear addition of both u_z and u_s components:

$$u = u_z + u_s. \quad (9.2-8)$$

If the two components are approximately of equal size, then u can also be found using a geometrical summation:

$$u = \sqrt{u_z^2 + u_s^2}. \quad (9.2-9)$$

9.2.6 Measurement result

The result y of a measurement is composed of:

- the arithmetic mean \bar{x} of a series of measurements,
- the correction K for the systematic deviations obtained,
- the measurement uncertainty u
- the statement of the chosen confidence level $(1 - \alpha)$

$$y = \bar{x} + K \pm u \text{ for } (1 - \alpha) = \dots\%. \quad (9.2-10)$$

Note:

The details in section 9 are based on [9-2]. The passages have been taken which are relevant for strain measurements using strain gages. Further information can be obtained from the standard.

10 Literature

- [1-1] Hooke, Robert: De potentia restitutiva. London 1678.
- [1-2] Wheatstone, Charles: An Account of several new Instruments and Processes for determining the Constants of a Voltaic Circuit. Philosophical Transactions of the Royal Society of London, 1843.
- [1-3] Thomson, William: On the Electro-dynamic Qualities of Metals. Philosophical Transactions of the Royal Society of London, 1856.
- [1-4] Tatnall, F.G.: Tatnall on Testing. American Society for Metals, Metals Park, Ohio, USA, 1966.
- [1-5] USA Patent No. 2 292 549, Title: Material Testing Apparatus, date filed: 23rd February 1940, date issued: 11th August 1942.
- [1-6] British Patent No. 728,606, Title: Electric Resistance Devices, date filed: 28th August 1952, date issued: 20th April 1955.
- [1-7] Ort, W.: Eine neue Technologie zur Herstellung von Dünnschicht-Dehnungsmeßstreifen für den Aufnehmerbau. Messtechnische Briefe 13 (1977) No. 1, pp 7-11. Hottinger Baldwin Messtechnik GmbH, Darmstadt.
- [1-8] Bray, A., and P. Valabrega: The strain sensitivity of Nichrome Films prepared by vacuum deposition. Presentation at 2me Conference D'Analyse des Contraintes, Paris 1962
- [1-9] Bray, A., and M. Plassa: The strain sensitivity of Ge and Cr-Si Thin-Films deposited under Vacuum. Presentation at IMEKO Conference, Stockholm 1964.
- [1-10] Watanabe, O. and K. Shioda: Meßtechnische Eigenschaften von Dünnschicht-Halbleiter-Dehnungsmeßstreifen. Materialprüfung 9 (1967) No. 6, pp 223-227.
- [1-11] Schulz, M.: Einsatz kapazitiver Dehnungsmeßstreifen für statische Messungen bei hohen Temperaturen. VDI-Berichte No. 313 (1978), pp 317-322. VDI-Verlag GmbH, Düsseldorf.
- [1-12] Schulz, M.: Statische Dehnungsmessung bei 500°C über 10720 Stunden zur Bestimmung von Materialkonstanten. VDI-Berichte No. 439 (1982), pp 155-159, VDI-Verlag GmbH, Düsseldorf.

- [1-13] Fortmann, M.: Hochtemperatur-Dehnungsmessungen mit dem neuen kapazitiven Meßgeber von Interatom. VDI-Berichte No. 514 (1984), pp 45-48, VDI-Verlag GmbH, Düsseldorf
- [1-14] Böhm, W., P. Hofstötter and N. Rasche: Laboruntersuchungen zum Langzeitverhalten kapazitiver Dehnungsmeßstreifen CERL-Planer und Interatom bei Temperaturen bis 550°C. VDI-Berichte No. 552 (1985), pp 97-111. VDI-Verlag GmbH, Düsseldorf
- [1-15] Procter, E.: High temperature creep strain measurements using a capacitance type strain gauge. VDI-Berichte No. 514 (1984) pp 101-107
- [1-16] Tatnall, F.G.: Development of the Scratch Gage. *Experimental Mechanics*, June 1969, pp 27N-34N.
- [1-17] Bertodo, R.: Development of High-temperature Strain Gauges, *Proceedings of the Institution of Mechanical Engineers*, Vol. 173 (1959) No. 23, pp 605-616, London
- [1-18] Greger, G.: Zur Herstellung von Siliziumkristallen nach dem Czochralsky-Verfahren. *Z. f. angew. Physic* (1961) No. 1, pp 47-51.
- [1-19] Anon.: Silicon Semiconductor Strain Gauges. *Magazine Direct Current*, Sept. 1962, pp 235-237.
- [2-1] VDI/VDE-Richtlinie 2653, Page 1: Dehnungsmeßstreifen mit metallischem Meßgitter. Kenngrößen und Prüfbedingungen. August 1974, Beuth-Vertrieb GmbH, Berlin and Cologne.
- [2-2] Wolfstieg, U.: Stand und Möglichkeit der röntgenographischen Spannungsanalyse. VDI-Berichte No. 313, 1978, pp 217-226. VDI-Verlag GmbH, Düsseldorf.
- [2-3] Law on units in measurement of 2.7.1969. *Bundesgesetzblatt, Teil I* (1969) No. 55, pp 709-712.
- [2-4] Ausführungsverordnung zum Gesetz über Einheiten im Meßwesen vom 26.6.1970. *Bundesgesetzblatt Teil I* (1970) No. 62, pp 981-991.
- [2-5] Winter, F.W.: Die neuen Einheiten im Meßwesen. 2nd Editn. (1974). Girardet paperback No. 10, Essen.
- [2-6] Peiter, A.: Eigenspannungen I. Art, Ermittlung und Bewertung. Michael Tritsch-Verlag, Düsseldorf, 1966.
- [2-7] Rappe, H.-A.: Messung von Schweiß eigenspannungen mit Dehnungsmeßstreifen. *Messtechnische Briefe* 9 (1973) No. 2, pp 31-37. Hottinger Baldwin Messtechnik GmbH, Darmstadt.
- [2-8] DIN 50125: Prüfen metallischer Werkstoffe. Zugproben. Richtlinien für die Herstellung. (March 1986). Beuth-Vertrieb GmbH, Berlin 30

- [3-1] Hoffmann, K.: Über die Ermittlung von Kenngrößen metallischer Dehnungsmeßstreifen (DMS). ATM. Archiv für technisches Messen V 1372-3 (February 1976), pp 65-68.
- [3-2] Müller, R.K.: Der Einfluß der Meßlänge auf die Ergebnisse bei Dehnungsmessungen an Beton. "Beton" 14 (1964) No. 5, pp 205-208. Beton-Verlag GmbH, Düsseldorf-Oberkassel. Reprint in Messtechnische Briefe 2 (1966) No. 3, pp 37-41. Hottinger Baldwin Messtechnik GmbH, Darmstadt.
- [3-3] Stein, P.K.: Measurement Engineering, Vol. II, 2nd Edition, Chapter 21: Gage length effects. Stein Engineering Services, Inc. Phoenix AZ, USA.
- [3-4] Hirt, M.: Dehnungsmessungen am Zahnfuß von geradeverzahnten Stahl-Stirnrädern. Messtechnische Briefe 10 (1974) No. 2, pp 33-38. Hottinger Baldwin Messtechnik GmbH, Darmstadt.
- [3-5] Wolf, H., and W. Böhm: Das Ringkern-Verfahren zur Messung von Eigenspannungen und seine Anwendung bei Turbinen und Generatorwellen. Arch. für Eisenhüttenwesen, 42nd yr. No.3 (March 1971) pp 195-200. Verlag Stahleisen m.b.H., Düsseldorf.
- [3-6] Birkenfeld, W.: Messen von Eigenspannungen mittels Dehnungsmeßstreifen. Messtechnische Briefe 4 (1968) No. 3, pp 37-42, Hottinger Baldwin Messtechnik GmbH, Darmstadt.
- [3-7] Keil, St.: Zur Eigenspannungsermittlung mit DMS-Bohrlochrosetten. Messtechnische Briefe 11 (1975) No. 3, pp 53-58. Hottinger Baldwin Messtechnik GmbH, Darmstadt.
- [3-8] Amberg, C., and N. Czaika: Über das langzeitige Drift- und Kriechverhalten gekapselter, aufschweißbarer Dehnungsmeßstreifen mit Cr-Meßdraht bei Temperaturen bis 320°C. VDI-Berichte No. 399 (1981), pp 105-111. VDI-Verlag GmbH, Düsseldorf.
- [3-9] Böhm, W., and N. Rasche: Bestimmung von DMS-Eigenschaften bei höheren Temperaturen mit einer rechnergesteuerten Prüfungseinrichtung. VDI-Berichte No. 366 (1980), pp 51-53. VDI-Verlag GmbH, Düsseldorf.
- [3-10] Böhm, W.: Hinweise zur Anwendung des 2fachen Aufschweißens von EATON-Hochtemperatur Dehnungsmeßstreifen zur Voruntersuchung von DMS-Eigenschaften. VDI-Berichte No. 480 (1983), pp 167-169. VDI-Verlag GmbH, Düsseldorf.
- [3-11] Gentsch, A.: Probleme der Bestimmung statischer Beanspruchung mit Hilfe der Dehnungsmeßtechnik bei hohen Temperaturen. Maschinentechnik 12 (1963) No. 9, pp 474-480. VEB-Verlag Technik, E. Berlin.
- [3-12] Wolf, H., and H.-D. Schlichting: Zur Messung statischer Beanspruchungen großer Bauteile bei hohen Temperaturen mit Dehnungsmeßstreifen. ATM Blatt V 132.12 (12.1967). Verlag R. Oldenbourg, Munich.

- [3-13] Ludewig, H.: Schwingungsmessungen an Turbinenschaufeln von Abgasturbo-ladern mit Hochtemperatur-Dehnungsmeßstreifen. Messtechnische Briefe No. 1 (1969), pp 8-11. Hottinger Baldwin Messtechnik GmbH, Darmstadt.
- [3-14] Amberg, C., and N. Czaika: Zur Vorherbestimmung und Reproduzierbarkeit des Nullpunkttemperaturganges aufschweißbarer DMS bis 320°C bzw. 600°C. VDI-Berichte No. 480, 1983, pp 145-150. VDI-Verlag GmbH, Düsseldorf.
- [3-15] Felgner, K., and K. Hoffmann: Das Verhalten von induktiven Wegaufnehmern und von DMS bei tiefen Temperaturen (-196°C). Messtechnische Briefe 3 (1965), pp 2- 4. Hottinger Baldwin Messtechnik GmbH, Darmstadt.
- [3-16] Rohrbach, Chr., and E. Knublauch: Dehnungsmessungen mit Meßstreifen bei hohen Temperaturen. Materialprüfung 10 (1968) No. 4, pp 105 -115.
- [3-17] Böhm, W., P. Hofstötter, N. Rasche and J. Weichsel: Praktischer Einsatz gekapselter Hochtemperatur-Dehnungsmeßstreifen bis 315°C. VGB Kraftwerkstechnik 61 (1981), No. 6, pp 502-509.
- [3-18] Hofstötter, P., and J. Weichsel: Einsatz einer Klemmvorrichtung zur Kalibrierung von Hochtemperatur-Dehnungsmeßstreifen. Technische Überwachung 21 (1980) No. 4, pp 147-150. VDI-Verlag, Düsseldorf.
- [3-19] Hofstötter, P.: Calibration of High-temperature Strain Gages with the Aid of a Clamping Device. Experimental Mechanics Vol. 22 (1982), pp 223-225
- [3-20] Anderko, K, D. Keibach and E. Wacker: Wärmespannungsmessungen an einem Aluminium-Kolben für einen mittelgroßen Dieselmotor mit Hilfe von Dehnungsmeßstreifen. MTZ Motortechnische Zeitschrift 28 (1967). Franckh'sche Verlagshandlung, Stuttgart.
- [3-21] Fukamichi, K., Kimura, H. M., Masumoto, T. and Gambino, R.J.: Strain Gauge Characteristics of Ni-Base Amorphous Alloys. IEEE Transactions on Mag-netics. Vol. Mag.-16, No. 5 (1980) pp 907-909.
- [3-22] Tsen-tai Wu, Liang-cheng Ma, and Lin-bao Zhao: Development of Tempera-ture-compensated Resistance Strain Gages for Use to 700°C. Experimental Mechanics (1981) pp 117-123.
- [3-23] Andreae, G., and G. Niessen: Über die Ursache des Driftens von Hochtempe-ratur-Dehnungsmeßstreifen, insbesondere solcher mit PtW-Leiter. Material-prüfung 24 (1982) No. 12, pp 431-436.
- [3-24] Dorsey, J.: Semiconductor Strain Gage Handbook, company publication BLH-Electronics, Inc. Waltham MA, USA.
- [3-25] Hoffmann, K.: Der Temperaturgang von Dehnungsmeßstreifen und die Besei-tigung seines Anteils an Meßergebnissen. TZ f. prakt. Metallbearbeitung 56th yr. (1962) No. 11, pp 639-644. Techn. Verlag G. Grossmann GmbH, Stuttgart-Vaihingen.

- [3-26] Hoffmann, K.: Ursachen temperaturabhängiger Nullpunkts- und Empfindlichkeitsänderungen bei Dehnungsmeßstreifen-Aufnehmern. VDI-Berichte No. 137 (1970) pp 23-27. VDI-Verlag GmbH, Düsseldorf.
- [3-27] Stein, P.K.: Measurement engineering, Vol. II, 2nd Edition, Chapter 22: Effect of Temperature. Stein Engineering Services, Inc. Phoenix AZ, USA.
- [3-28] Andreae, G.: Über das Verhalten von Dehnungsmeßstreifen bei großen Dehnungen. Materialprüfung 13 (1981) No. 4, pp 117-123.
- [3-29] Hoffmann, K.: Zum Linearitätsfehler bei Dehnungsmessungen mit Dehnungsmeßstreifen im Hochdehnungsbereich. Messtechnische Briefe 12 (1976) No. 3, pp 53-57. Hottinger Baldwin Messtechnik GmbH, Darmstadt.
- [3-30] Kern, W.F.: Über Verformungsmessungen an Kraftfahrzeugreifen mittels spezieller Dehnungsgeber. ATZ, Automobiltechnische Zeitschrift, 63rd yr. No. 2 (1961), pp 33-41, Franckh'sche Verlagshandlung, Stuttgart.
- [3-31] Oi, K.: Transient Response of Bonded Strain Gages, Experimental Mechanics Sept. 1986, pp 463-469.
- [3-32] Bagaria, W.J., and W.M. Sharpe jr.: Temperature and Rise-Time Effects on Dynamic Strain Measurements. Paper No. 2309 A of the 1974 SESA Spring Meeting, Detroit/Mich., published in International Aerospace Abstracts, Technical Information Service, American Institute of Aeronautics and Astronautics, Inc., New York.
- [3-33] Rohrbach, Chr., and N. Czaika: Über das Dauerschwingverhalten von Dehnungsmeßstreifen. Materialprüfung 3 (1981) No. 4, pp 125-136.
- [3-34] Müller, R.K.: Ein Beitrag zur Dehnungsmessung an Kunstharzmodellen. Habilitationsschrift Stuttgart 1964.
- [3-35] Rohrbach, Chr., and N. Czaika: Deutung des Mechanismus des Dehnungsmeßstreifens und seiner wichtigsten Eigenschaften an Hand eines Modells. Materialprüfung 1 (1959) No. 4, pp 121-131. Deutscher Verband f. Materialprüfung (DVM), Düsseldorf.
- [3-36] Andreae, G.: Zur Genauigkeit von Dehnungsmeßstreifen. Materialprüfung 12 (1970) No. 3, pp 87-92.
- [3-37] Andreae, G.: Über den Einfluß hydrostatischen Drucks auf Dehnungsmeßstreifen. Materialprüfung 16 (1974) No. 4, pp 98-102.
- [3-38] Hoffmann, K., D. Jost and St. Keil: Experimentelle Untersuchung des Einflusses hydrostatischen Drucks auf Dehnungsmeßstreifen-Applikationen und die Ermittlung von Korrekturwerten. VDI-Berichte No. 313 (1978), pp 553-558. VDI-Verlag GmbH, Düsseldorf.
- [3-39] Anon.: DMS messen den Impuls bei der weichen Landung von Surveyor I auf dem Mond. Messtechnische Briefe, No. 1 (1967), p 19, Hottinger Baldwin Messtechnik GmbH, Darmstadt

- [3-40] Caris, R.F.: Strain Gages in Hard Vacuum, Proceedings of Western Regional Strain Gage Committee, Spring Meeting 1968, pp 29-35,
- [3-41] Telinde, J.: Strain Gages in Cryogenics and Hard Vacuum. Proceedings of Western Regional Strain Gage Committee, Spring Meeting 1968, pp 45-54.
- [3-42] Krevitt, R.: A Compilation of Literature on Radiation Effects. Proceedings of Western Regional Strain Gage Committee, Fall Meeting 1967, pp 65-68.
- [3-43] Gunn, J.: Investigation of Strain Gages in Strong Magnetic Fields. Proceedings of Western Regional Strain Gage Committee, Fall Meeting 1966, pp 37-40.
- [3-44] Armand, G., and J. Laujoulade: Mesures des Contraintes par jauges a fil resistance en présence de champ magnétique. *Analyse des Contraintes*, Vol. IV (1961) Nos. 1 and 2.
- [3-45] Vigness, J.: Magnetostrictive Effects in Wire Strain Gages. Proceedings of the Society for Experimental Stress Analysis, Vol XIV (1957) No. 2.
- [3-46] Strauss, H.E.: Method for Measuring of Magnetostriction Corrected for Initial Domain Distribution and Its Application to Nickel and Iron. *J. Appl. Phys.*, Vol. 29 (1958) No. 2
- [3-47] Takahi, H., and T. Tsuji: A Note on the Magnetoresistance Effect of Strain Gage Wire. *J.Phys. Soc. Japan*, Vol. 13 (1958), pp 1406.
- [3-48] Stein, P. K.: Representative Magnetic Field Strengths. *Strain Gage Readings 1* (1958) No. 4, pp 24. Verlag Stein Engineering Services, Phoenix AZ, USA.
- [3-49] Bickle, L.W.: The Response of Strain Gages to Longitudinally Sweeping Strain Pulses, *Experimental Mechanics*, August 1970, pp 333-337.
- [3-50] Andreae, G., and G. Niessen: Über Möglichkeiten und Grenzen der Hochtemperatur-Dehnungsmeßstreifen mit Platin-Wolfram-Leiter. Teil I: Zur Ursache des Driftens und zum Kriechverhalten. *Materialprüfung 27* (1985) No. 11, pp 344-346.
- [3-51] Hoffmann, K.: Zur Herstellung moderner Folien-Dehnungsmeßstreifen und den dabei gegebenen Korrekturmöglichkeiten für Kriechen und Querempfindlichkeit. *Messtechnische Briefe 22* (1986) No. 2, pp 41-46. Hottinger Baldwin Messtechnik GmbH, Darmstadt.
- [3-52] Glücklich, D.: Die Versteifung von Kunststoffmodellen durch elektrische Dehnungsmeßstreifen. Reports from Institut für Modellstatik at University of Stuttgart, No. 4, 1975.
- [4-1] Hoffmann, K.: Practical hints for the application of strain gauges, Technical Note VD 84005e, Hottinger Baldwin Messtechnik GmbH, Darmstadt.
- [4-2] Michel, M.: *Adhäsion und Klebetechnik*. Carl Hanser Verlag, Munich (1969)

- [4-3] Mittrop, F.: Das Kleben als Befestigungsverfahren für Dehnungsmeßstreifen. In „Haus der Technik e.V. Essen Vortragsveröffentlichungen“ No. 31 (1965), pp 15-27
- [4-4] Anon.: A Megohmeter Circuit for SR-4 Strain Indicators. BLH Measurement Topics Vol. 4, No. 2, June 1966, p 6
- [5-1] Kreuzer, M.: Linearitäts- und Empfindlichkeitsfehler beim Messen mit Einzeldehnungsmeßstreifen bei spannungsgespeisten und stromgespeisten Schaltungen. Messtechnische Briefe 19 (1983) No. 2, pp 37-42. Hottinger Baldwin Messtechnik GmbH, Darmstadt.
- [5-2] Kreuzer, M.: Vergleichende Betrachtung verschiedener Schaltungsarten für das Messen mit Dehnungsmeßstreifen. Messtechnische Briefe 19 (1983) No. 3, pp 63-68. Hottinger Baldwin Messtechnik GmbH, Darmstadt.
- [5-3] Kreuzer, M.: Messungen mit Dehnungsmeßstreifen ohne schaltungstechnischen Nullabgleich. VDI-Berichte No. 509 (1984), pp 159-162. VDI-Verlag GmbH, Düsseldorf.
- [5-4] Kreuzer, M.: Praktische Bedeutung der effektiven Dehnung für die Schaltungstechnik von Dehnungsmeßgeräten. VDI-Berichte No. 514 (1984), pp 121-127. VDI-Verlag GmbH, Düsseldorf.
- [5-5] Heringhaus, E.: Trägerfrequenz- und Gleichspannungs-Meßverstärker für das Messen mechanischer Größen - ein Systemvergleich aus anwendungstechnischer Sicht.
- Teil 1: Arbeitsweisen und Vergleich charakteristischer Eigenschaften. Messtechnische Briefe 18 (1982) No.2, pp 42-49.
- Teil 2: Verhalten gegenüber externen Störeinflüssen und praktische Auswahlhilfen. Messtechnische Briefe 18 (1982) No.3, pp 70-73, Hottinger Baldwin Messtechnik GmbH, Darmstadt.
- [6-1] VDI/VDE-Richtlinie 2600, Blatt 3: Metrologie (Meßtechnik), Gerätetechnische Begriffe (November 1973) Beuth-Vertrieb GmbH, Berlin and Cologne.
- [7-1] Kreuzer, M.: Eine Vielstellenmeßanlage mit FET-Schaltern. Messtechnische Briefe 12 (1976) pp 4-9 und pp 35-41. Hottinger Baldwin Messtechnik GmbH, Darmstadt.
- [7-2] Kreuzer, M.: Elektrische Vielstellen-Meßeinrichtung; German Patent DE 3238 482 (1983).
- [7-3] Meyer, M.L.: On the measurement of transverse sensitivity of strain gauges. Strain, Vol. 9 (1973) No. 1, pp 26-28, London.
- [7-4] Baumberger, R., and F. Hines: Practical Reduction Formulas for Use on Bonded Wire Strain Gages in Two-Dimensional Stress Fields. Experimental Stress Analysis, Vol II No. 1 (1944), pp 113-127.

- [7-5] Measurements Group: Errors due to Transverse Sensitivity in Strain Gages. *Experimental Techniques* 1983 No. 1, pp 30-35.
- [8-1] Keil, St.: Stress calculation from measured strains in the elastic deformation range. *Reports in Applied Measurement*, Vol.3 (1987), No.2, pp 56-62. Hottinger Baldwin Messtechnik GmbH, Darmstadt.
- [8-2] Müller, R.K.: Modellstatische Untersuchungen von Schalentragwerken. Report from Institut für Modellstatik at University of Stuttgart, No. 2, 1973.
- [8-3] Technical Data Sheet D 24.32.0e, Hottinger Baldwin Messtechnik GmbH, Darmstadt.
- [8-4] Spangenberg, D.: Grundlagen und Anwendung des Reißlackverfahrens zur Spannungsanalyse. *Techn. Überwachung* 12 (1971) No. 3, pp 80-84.
- [8-5] Lindorf, H.: Technische Temperaturmessungen. Verlag W. Girardet, Essen. 3rd Edition 1968.
- [8-6] Winter, F.W.: Technische Wärmelehre. Verlag W. Girardet, Essen. 7th Edition 1970.
- [8-7] Maute, D. and U. Stöckle: Kraft- und Drehmomentmessungen am Antriebssystem eines Wehrsegments der Staustufe Iffezheim. *Messtechnische Briefe* 19 (1983) No. 1, pp 1-6. Hottinger Baldwin Messtechnik GmbH, Darmstadt.
- [8-8] Grünbaum, P.: Drehmomentmessung an Nockenwellen von Dieselmotoren. *Messtechnische Briefe* 21 (1985) No.2, pp 39-46. Hottinger Baldwin Messtechnik GmbH, Darmstadt.
- [8-9] Kranz, E.: Gewichtsbestimmungen von 5-MVA- bis 100-MVA-Transformatoren mit Hilfe von Dehnungsmeßstreifen an einem 120-t-Brückenkran. *Messtechnische Briefe* 18 (1982) No.1, pp 7-10. Hottinger Baldwin Messtechnik GmbH, Darmstadt.
- [8-10] Haas, E.: Ermittlung von Wärmespannungen mit Dehnungsmeßstreifen an Epoxydharz-Modellen. No. 6, 1977, Report from Institut für Modellstatik at University of Stuttgart.
- [9-1] Hellwig, R.: Precision force transducer for international comparison measurements on force standard machines, *Reports in Applied Measurement*, Vol.3 (1987) No.1, pp 17-22. Hottinger Baldwin Messtechnik GmbH, Darmstadt.
- [9-2] DIN 1319: Grundbegriffe der Meßtechnik, Blatt 3; Begriffe für die Messunsicherheit und für die Beurteilung von Meßgeräten und Meßeinrichtungen. Edition August 1983: Beuth-Verlag GmbH, Berlin 30.

11 Index

- Adhesive 82, 83, 92, 108
- Alternating voltage supply 134
- Applications 36
- Areas of application 7, 36
- Arithmetic mean 39, 239
- Axial direction 14
- Axial force 212, 226

- Bending moment 209, 212
- Biaxial stress 45
- Biaxial stress state 192
- Biomechanics 7, 36
- Bridge circuit 126
- Bridge completion resistors 130
- Bridge excitation 126, 133

- Cable capacitances 172
- Calibration 135
- Calibration signal 139, 140
- Calibration unit 144
- Capacitive strain gages 52
- Capacitive unsymmetry 173
- Carrier frequency method 133
- Cleaning agents 112
- Combined loads 212
- Compensating strain gage 154, 164, 177
- Compensation of thermal output 151
- Compression bar 206
- Confidence limits 240
- Connecting leads 116
- Connection methods 115
- Continuous vibration characteristics 71
- Correction of transverse sensitivity 179
- Covering agents 123
- Covering methods 121
- Creep 80
- Cut-off frequency 74

- Dependence of sensitivity on temperature 67
- Dependence of the gage factor on temperature 68
- Determination of residual stresses 202
- Diagonal bridge 131, 157, 176

Direct voltage supply 133
Double quarter 131, 164
Double quarter bridge 157, 164, 177
Dynamic strain 42
Dynamic strain measurement 70

Effects of temperature 51, 90
Eisler, Paul 6
Electrical continuity 118
Electrical loading 79
Electrical resistance 50
Elementary loading cases 205
Environmental influences 90
Error correction 167

Fluxing agents 114
Foil strain gage 6
Free-grid strain gages 49
Full bridge 131
Full bridge circuit 159, 166, 175

Gage factor 146
Gage factor for metal strain gages 53
Gage factor for semiconductor strain gages 54
Gage factor k 53
Gaussian distribution 237

Half bridge 130
Half bridge circuit 158, 165, 177
HBM bridge 168
High-strain strain gages 69
High-temperature strain gages 49, 50
Hole-drilling method 47
Homogeneous field of strain 38
Hooke, Robert 1
Hooke's Law 189
Humidity 90
Hydrostatic pressure 91
Hysteresis 87, 92

Inhomogeneous materials 152
Inhomogeneous strain field 40
Insulation resistance 91, 119, 120
Introduction 1
Ionizing radiation 99

Kelvin, Lord 2
Kreuzer Circuit 168

Lead material 116
Lead resistances 160

- Length of measuring grid 37, 40
- Length of the measuring grid 75
- Linear strain gages 37
- Longitudinal strain 193

- Magnetic fields 116
- Magnetic fields 104
- Material stress 1
- Measurement equipment 135
- Measurement of dynamic strain 70
- Measurement result 242
- Measurement system 15
- Measuring amplifier 137
- Measuring amplifiers 133
- Measuring chain 135
- Measuring residual stress 46
- Mechanical hysteresis 87
- Mechanical strain 16
- Mechanical strain gages 11
- Mechanical stress 21
- Metal strain gages 2
- Methods of testing 118
- Model measurement techniques 36
- Modulus of elasticity 26
- Mohr's Stress Circle 199
- Mounting materials 108, 112
- Mounting strain gages 108
- Multiple strain gages 42

- Normal force 206

- Parameters 52
- Phase rotation 177
- Planar stress state 25
- Principal directions 190, 192, 197, 199
- Principal normal stresses 193, 197, 199
- Principal stresses 195
- Protection of the measuring point 120
- Protective materials 121

- Quarter bridge configuration 130, 152, 161, 164, 177
- R rosettes 37, 45

- Reduction and elimination of measurement errors 149
- Residual stress 24
- Ring-core method 46
- Rosettes 42, 44, 187
- Ruge, Arthur Claude 3

- Selection criteria 34
- Semiconductor strain gage 7

Shear modulus 28
Shear stresses 227
Shock wave 74
Shunt calibration 141
Simmons, Edward E. 3
Six-wire circuit 171
Smith, C.S. 7
Solder terminals 115
Soldering agents 113, 114
Soldering devices 113
Standard deviation 239
Static elongation 69
Storage 107
Strain 17
Strain gage applications 34
Strain gage chains 36, 37, 42
Strain gage design 6
Strain gage parameters 36
Strain gage resistance 50
Strain gage rosettes 186
Stress analysis 1, 36
Stress gradients 42
Stress in a notch 40

Tatnall, Francis 6
Technical data 52
Temperature compensated strain gages 61
Temperature compensating strain gages 151
Temperature response 59
Tension bar 206
Test requirements 236
Thermal drift 67
Thermal expansion 31, 62
Thermal output 151
Thermal stresses 230
Thermal voltages 133
Thin-film strain gages 8
Thomson, William 2
Three-dimensional stress state 25
Three-wire circuit 154, 163, 177
Transducer construction 36
Transferring the measuring signal from rotating shafts 222
Transverse sensitivity 56
Triaxial stress state 25
Types of strain gages 37

Uniaxial stress state 189
Useful temperature range 51

Vacuum conditions 96
Vapor-deposited strain gages 8

Visual inspection 118
Voltage supply 127

Weldable strain gages 49, 50
Wheatstone, Sir Charles 126
Wound-wire technique 6

X rosettes 37, 45, 186, 194

Zero referenced measurements 90

List of Tables

Table 2.3-1:	Young's modulus for some materials	28
Table 2.3-2:	Poisson's ratio for some materials	30
Table 2.3-3:	Average thermal expansion coefficients for various materials for different temperature ranges between 20° and ϑ °C in $10^{-6} \frac{m}{m} \cdot \frac{1}{K}$	31
Table 3.0-1:	Chart for the analysis of conditions which must be fulfilled by a strain gage measurement point.....	35
Table 3.3-1:	Average gage factors for strain gages with various measuring grid alloys.	54
Table 3.4-1:	The strain gage/adhesive combinations which were investigated for pressure sensitivity.....	94
Table 3.4-2:	The influence of hydrostatic pressure on the tested strain gage bonds in $\mu\text{m}/\text{m}$ per 100 bar, also showing the standard deviation s . Valid for the pressure range under investigation, i.e. 0 to 500 bar.	95
Table 3.4-3:	Gas release rates for various materials in a vacuum (from [3-41]).	98
Table 3.4-4:	Critical radiation dose for some synthetic materials.....	102
Table: 3.4-5:	Resistance of parts of a strain gage measuring point to gamma radiation.....	104
Table 3.4-6:	Zero-point displacement of strain gages in a static magnetic field (from 3-44)...	106
Table 3.4-7:	Flux density, i.e. intensity, of magnetic fields (from [3-48]).	107
Table 4.2-2:	Examples of soft solders.....	114
Table 4.2-3:	The most important cable and lead insulating materials and some of their technical data	117
Table 7.0-1:	Possible sources of error and interference effects on a strain gage measuring point.	150
Table 8.4-1:	Circuits that could be used for the tension/compression bar with their results. ...	207
Table 8.4-2:	Circuits which can be used on the bending beam with a mirror-imaged cross-section.....	210
Table 8.4-3:	Bending section moduli for some frequently occurring cross-sectional shapes... 211	
Table 9.2-1:	Extracts of values for t and t/\sqrt{n} for various values of the confidence level $(1 - \alpha)$	240